



HAL
open science

Silent chromatin dynamics upon major metabolic transitions

Micol Guidi

► **To cite this version:**

Micol Guidi. Silent chromatin dynamics upon major metabolic transitions. Cellular Biology. Université Pierre et Marie Curie - Paris VI, 2015. English. NNT : 2015PA066609 . tel-01668453

HAL Id: tel-01668453

<https://theses.hal.science/tel-01668453>

Submitted on 20 Dec 2017

HAL is a multi-disciplinary open access archive for the deposit and dissemination of scientific research documents, whether they are published or not. The documents may come from teaching and research institutions in France or abroad, or from public or private research centers.

L'archive ouverte pluridisciplinaire **HAL**, est destinée au dépôt et à la diffusion de documents scientifiques de niveau recherche, publiés ou non, émanant des établissements d'enseignement et de recherche français ou étrangers, des laboratoires publics ou privés.

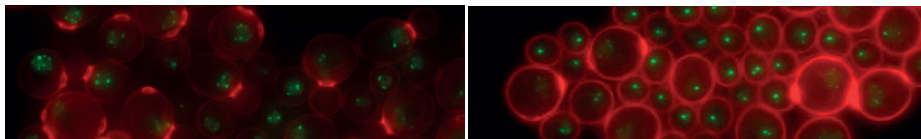
Université Pierre et Marie Curie

Ecole doctorale Complexité du vivant – ED515

Thèse de doctorat de Biologie cellulaire et Génétique

Par **Micol GUIDI**

Silent chromatin dynamics upon major metabolic transitions



Dirigée par Angela TADDEI

UMR3664 CNRS / Institut Curie / UPMC

Equipe Compartimentation et Dynamique des fonctions nucléaires

Présentée et soutenue publiquement le 18 Decembre 2015

Devant un jury composé de :

Dr. Paola Fabrizio	Rapporteur
Dr. Saadi Khochbin	Rapporteur
Pr. Susan Gasser	Examineur
Dr. Teresa Teixeira	Examineur
Dr. Angela Taddei	Directeur de thèse

Acknowledgments

I would like to sincerely thank to all the members of my thesis jury, whose work inspired me during these years and who kindly accepted my invitation to evaluate my work and to participate to my thesis dissertation. In particular to Paola Fabrizio, for the useful exchanges we had in Lyon and for accepting to review my manuscript on nuclear dynamics; to Saadi Khochbin, for the interesting discussion we had in front of my poster, for his kindness and for taking some time to read and evaluate my manuscript; to Susan Gasser, for flying to Paris to participate to my thesis defence; to Teresa Texeira, who followed my work since the beginning, for her presence and her suggestions during these years.

I would like to thank all the members of my PhD thesis committee, for their useful advises: Genevieve Almouzni, Valerie Borde, Vincent Galy, Manolis Papamichos, Nathalie Dostatni, Jean Pierre Quivi and Teresa Texeira.

I would like to thank to my thesis director, Angela Taddei, for many reasons. First, for accepting me in her lab, although my CV was quite far from both nuclear dynamics and budding yeast, thus giving me the opportunity to work in the international and dynamic environment of the Institut Curie. Second, because she was an inspiring and open-mind boss: thanks for teaching me the importance of being rigorous and critical on anything but especially for letting me free to follow my interests, lose myself and make mistakes. I learnt so so much in these years! Third, I would like to thank to the person Angela, for her big hug when I announced that I was pregnant, for her spontaneous and fundamental help for my “survival” in Paris.

I would like to thank to Myriam, because she taught me about microscopy and yeast genetics from scratch, repeating things one, five, hundreds of times, until they were really clear; for all the time that she fixed the microscope, for her support at any time, her suggestions.. and yes, also because she used to bring Seb’s delicious cakes to the lab! And to Sebastian, who also participated to our crazy discussions on the link between glucose signalling and telomere clusters: sincerely thanks!

I would like to thank to all the other present and past members of our lab, for creating a nice and friendly atmosphere. In particular, to Isabelle, for her unique and supportive look, for her loving care, and for giving me the name of the best osteopath in Paris! To Judith, who was extremely nice, especially during my pregnancy, for all her useful presents and personal suggestions. To Antoine, for the fun, the “coffee and speculations”, the sustain and the music after 7pm in the lab: ahhh, le bonheur! To Cyrille, to Michael, to Patricia, to Chloe, to Antonin, to “my student” Sheldon, to Clementine, to Karine: thanks a lot for your presence during this PhD adventure. To Dominique and Marion for their important help with administration papers. To our collaborators, Romain Koszul, Martial Marbouty, Axel Cournac and Julien Mozziconacci, for their contribution to the paper that we published together.

I would like to sincerely thank to a person who was essential for me during these last 5 years, Ivaylo, the former PhD student in our lab. For letting me enter in his world, listening to my monologues, pushing me to walk and to discover Paris, and helping me with everything one could imagine!

To Cedric, for taking care of me, helping me with my headaches, listening to my outburst, and for having shown me the real French life-style.

To all the other people who made my days in this unit, with a smile or a nice word: Petra, Paolo, Elisabetta, Fabiana, Federico, Anne, Sara, Tanguy, Raphaele, Hose?, Lisa, Suraya, Claire, Anifa, Bruno and many others.

I would like to thank to my friend Beppe, for the magic moments that we spent together, from the fires of the 14th of July on the “peniche” to the crazy nights in Paris.

For his hugs, his eyes, his smile that I will never forget.

I would like to thank to all the people who shared nice and less nice moments with me in this amazing city, or who supported me from Italy, thanks to you all.

I would like to thank to my family: to my mother, to my father and to my brothers, for their support and for letting me know that they are always there for me.

Finally, I would like to thank to my new little family. To the best men I could ever find, who made me smile everyday, left his Italian life to follow me here in Paris, and became a super father! And to my little Lorenzo, for his enthusiasm, for his love, and because his big smile early in the morning gives me the strength to start each day with a positive thought, no matter what.

A Beppe

Table of contents

Preamble	5
Introduction	7
1. The 3D architecture of the eukaryotic nucleus	7
1.1 Generalities: the concept of chromatin	7
1.1.1 Different types of chromatin	11
1.2 Chromatin organization within the eukaryotic nucleus	14
1.2.1 Genome organization in relation with nuclear structures	15
- Nuclear structures in metazoan	16
- <i>S. cerevisiae</i> versus metazoan	18
1.2.2 The organization of chromosomes in the nuclear space	19
1.2.3 Long-range pairing mediated by repetitive sequences	24
1.2.4 Impact of nuclear organization on genome function	25
- When a different chromatin organization leads to an advantage: nocturnal lifestyle and inverted nuclear organization	26
- When the 3D nuclear organization is disrupted: laminopathies and cancer	27
1.3 Telomere clustering in budding yeast: a model for silent chromatin domains	29
1.3.1 Telomeres and subtelomeres: structure and function	29
1.3.2 Telomeric silent chromatin and the SIR complex	32
Sir2: gene silencing through histone deacetylation	33
Sir3: specificity, spreading and clustering	34
Sir4: scaffolding and anchoring roles	36
1.3.3 Model for SIR spreading and telomere foci formation	38
- Functional role of telomere clustering	40
2. Impact of the external environment on nuclear organization	42
2.1 Generalities	42
2.2 Spatiotemporal reorganization of metazoan 3D nuclear architecture	43
2.2.1 Chromatin architecture dynamics during differentiation and development	44
2.3 Can the environment directly affect the chromatin structure?	47
2.3.1 NAD ⁺ and the regulation of sirtuins	49
2.3.2 Acetyl-CoA and the regulation of histone (de)acetylation	51
2.4 The yeast response to the external environment	54
2.4.1 Gene expression changes in response to different nutrients	55
The “make-accumulate-consume (ethanol) strategy	55
Yeast metabolic cycles in chemostat	55
Growth curve in glucose based liquid medium (batch culture)	56
2.4.2 Concept of “differentiation” in yeast	57
Yeast differentiation within a colony	58
Yeast differentiation in liquid cultures	59
Sporulation as another way to differentiate	60
2.4.3 The quiescent state	61

Different ways to induce quiescence lead to different quiescent cells	62
What is the hallmark of quiescent cells?	63
Chromatin changes linked to quiescent state in yeast	65
2.4.4 How long a cell can be quiescent? The chronological life span	66
Aging in yeast: chronological life span versus replicative life span	66
External factors known to have an impact on yeast CLS	67
Aim of the thesis	71
Results	72
Result part I: Spatial reorganization of telomeres in long-lived quiescent cells	72
Additional files	88
Result part II: Quiescent-specific telomere hyper-cluster is a Mec1/Rad53-dependent programmed event	94
-Telomere hyperclustering is a programmed event	95
-Rad53 checkpoint kinase activity is important for telomere cluster commitment	97
- SP hyperclusters are Mec1 and Rad53 dependent	98
- Rph1 inactivation through the Mec1/Rad53 checkpoint pathway renders cells competent to form telomere hyperclusters	99
- Conclusions	101
- Additional material and methods	101
Result part III: Memory of the hypercluster	102
- The “memory effect”	105
- Conclusions	107
- Additional material and methods	108
Result part IV: Sir2 increased activity counteracts telomere clustering and CLS in long-lived quiescent cells	110
-The “adenine effect” on telomere clustering	110
-The adenine effect is Sir2-dependent	112
- Sir2 has an “anti-clustering” activity	113
- Sir2 role in WT post diauxic shift clustering	114
- SP telomere clustering requires Sir3 and Sir4 but not Sir2	115
- Link between medium composition, Sir2 activity, nuclear architecture and CLS	116
- Conclusions	117
- Additional material and methods	118
Discussion	120
Massive telomere organization upon carbon source exhaustion	120
Physiological relevance of telomere hypercluster formation	120
-Quiescent specific telomere hyperclusters are the result of a programmed event starting upon cellular respiration	120
- Do telomere hyperclusters occur also in the wild?	121
- Role of asymmetric post DS cell division in the commitment process	123
- Link between mitochondrial activity and nuclear organization: the H2O2/Mec1/Rad53/Rph1 pathway commits cells to the hypercluster formation	124
Mechanisms	126
-H3K36me3 involvement in telomere clustering	126
- SIRs involvement on the formation of telomere hyperclusters	127
- Other possible mechanisms leading to the increased telomere	

grouping	129
- Mechanisms leading to telomeres detachment from the nuclear periphery	130
- Best protocol to study mechanisms connected to telomere hyperclusters in long lived quiescence	131
- The two-faced role of Sir2 on telomere clustering	131
Possible function of telomere hyperclusters	133
- Link with similar chromatin organization in other organisms?	136
References	137
List of the major abbreviations used in this manuscript	157

Preamble

Multicellular organisms are composed of organs and tissues with specific functions. Each tissue is an organized structure composed of different kinds of cells (from Latin *cellula*, small room). Within each of these cells many distinct types of reactions can occur simultaneously, thanks to a conserved architecture that permits to subdivide the cellular space, providing optimal conditions for metabolic reactions and thus increasing the cellular efficiency. One of these organelles is the nucleus, which stores the majority of the genetic information of the cell, the deoxyribonucleic acid (DNA) molecules. Interestingly, even though almost all the cells of an organism share the same DNA content, not all genes are simultaneously expressed within a cell. How this can happen? We now know that gene expression is influenced by external or environmental factors that switch genes on and off. Moreover, during the last years it became evident that the tri-dimensional architecture of the nucleus has a profound effect on the gene expression. Researchers now aim to understand how nuclear functions are influenced by nuclear constraints.

As “nature makes nothing incomplete, and nothing in vain” (Aristotle 300 BC), I wanted to understand why the eukaryotic nucleus is so well organized and how this organization is achieved, and I decided to approach these complex questions by starting from a simple point of view.

The “cell theory” (XIX century by T. Schwann, M. J. Schleiden and R. Virchow) states that all organisms are composed of at least one cell, and all cells originate from pre-existing ones: *Omnis cellula e cellula*. Vital functions, whether in bacteria, yeast and multicellular organisms, take place within cells. However, only eukaryotic cells have a real nucleus (from Greek, *eu* = well formed, *kernel* = nucleus). I thus chose to work with a eukaryotic organism composed of a single cell, the budding yeast *Saccharomyces cerevisiae*, to study the functional link between the external environment and the internal organization of the nucleus.

Budding yeast is able to adapt to adverse conditions by switching between different gene expression programs and is an excellent model system for testing the functional role of nuclear organization. As a unicellular organism, any genetic manipulation or stress

directly affects *S. cerevisiae*'s nucleus and can be easily visualized. On the other hand, yeast cells are “social” organisms that form populations and colonies, which are thought to strongly affect the vital functions of a single cell.

In this manuscript, I will first introduce the general features of nuclear organization in the eukaryotic cell, with particular focus on the nuclear architecture and functions in budding yeast. Next I will discuss the impact of external factors on nuclear organization and genome functions, and I will focus on the budding yeast response to changes in the external environment.

In the following section, I will present my work on nuclear dynamics in response to changes in the nutrient availability in *S. cerevisiae*.

Next I will discuss the possible mechanisms leading to the environment-dependent changes in the nuclear architecture that we have found in yeast, proposing few experimental procedures that could help gain some insight into these processes. Finally I will discuss the hypothetical functions of the specific nuclear re-organization that occurs in quiescent yeast cells able to sustain long-term starvation.

Introduction

1. 3D architecture of the eukaryotic nucleus

1.1 Generalities: the concept of chromatin

The most obvious organelle found in eukaryotic cells is the nucleus, which is enclosed by the nuclear envelope and communicates with the cytosol via numerous pore complexes. Each nucleus contains the majority of the organism's hereditary information under the form of a double helical molecule of deoxyribonucleic acid, DNA. However, a small portion of the DNA in eukaryotic cells is found outside of the nucleus, within other organelles specialized in the generation of energy in the form of adenosine triphosphate (ATP), the mitochondria. Impressively, each cell of our organism contains about 2.3 m of DNA divided in 46 chromosomes and stored in a nuclear volume of 10 microns in diameter.

How can such a long DNA fiber fit in a nucleus of microscopic scale?

Thanks to several decades of research (summarized in Figure 1) we now know that the DNA is extremely packed and folded into a structure that we now call "chromatin" (from the greek word *chroma* – colour – because of its affinity for basic colorants, Flemmling 1882). Chromatin is a dynamic but highly organized DNA-protein complex that occupies the nuclear volume forming sub-compartments that are thought to facilitate particular nuclear functions. This concept is conserved from yeast to men (Lemaitre and Bickmore, 2015; Pombo and Dillon, 2015; Taddei and Gasser, 2012).

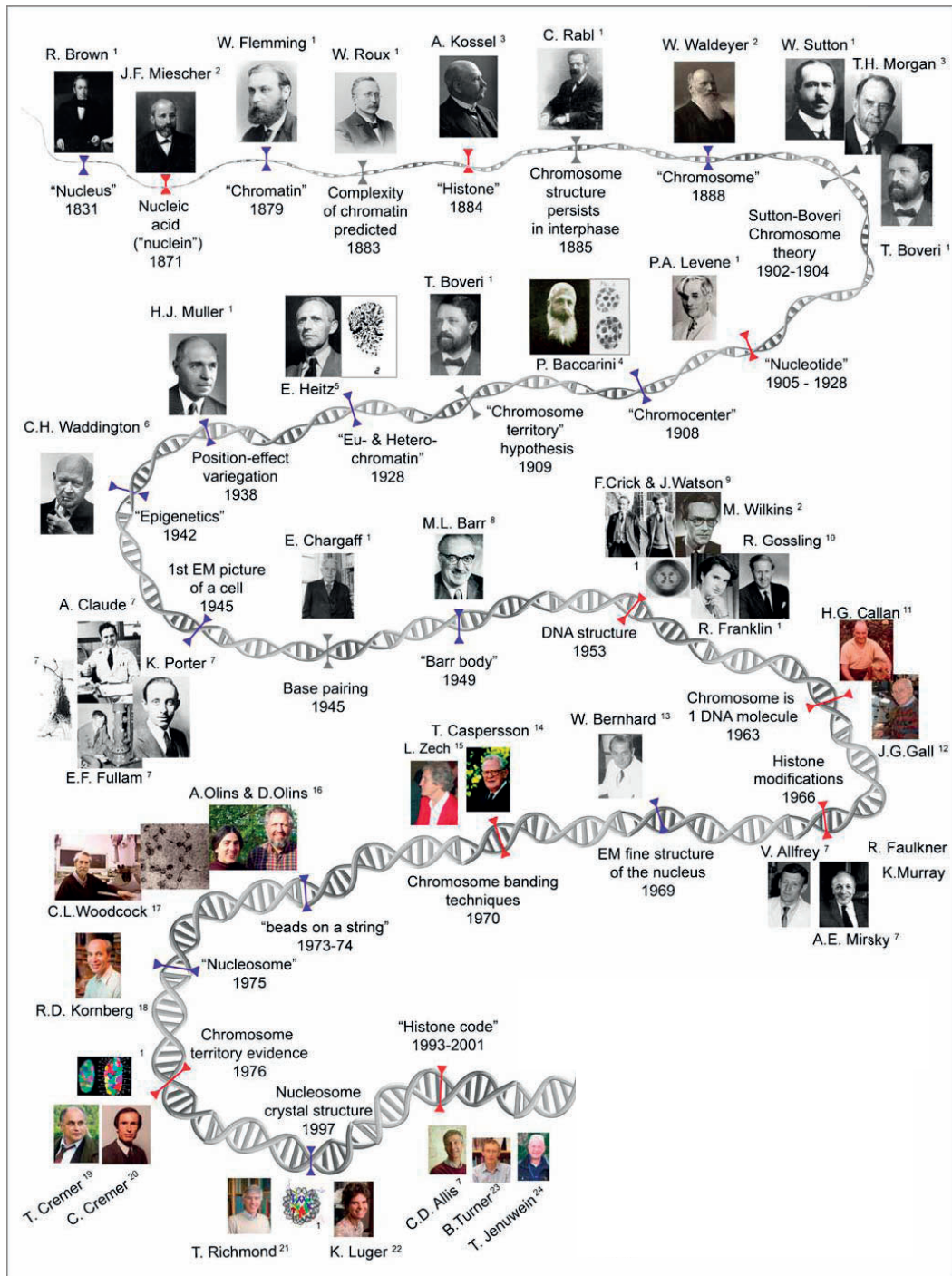


Figure 1: Timeline compilation landmark discoveries and concepts (grey) on molecular (red) and cellular (blue) aspects of chromatin, from the discovery of the cell nucleus to the hypothesis of a “histone code”. Adapted from (Jost et al., 2012)

The fundamental unit of chromatin is the nucleosome, whose “core” is composed of 147 base pairs of DNA wrapped in two turns around a protein complex - the histone octamer (Figure 2). Nucleosomes also include linker DNA and, in most instances, a

linker histone (Cutter and Hayes, 2015; Izzo et al., 2008). Almost 20 years ago, Luger and colleagues published the first crystal structure of the nucleosome core particle at 2.8Å resolution (Luger et al., 1997), which appears relatively invariant from yeast to metazoan (White et al., 2001). (White et al., 2001). In this structure, the positively charged histone core proteins associate tightly with the negatively charged molecule of DNA. Histone's N- and C- termini or “tails” are flexible and have important regulatory functions as they are subjected to post translational modifications (PTMs) (Strahl and Allis, 2000) that can either alter the local chromatin structures or serve as a docking surface for trans-acting factors (Maze et al., 2014). The first evidences that histones could be modified came from the sixties, when acetyl and methyl groups were found on histones (Allfrey et al., 1964; Phillips, 1963). However at that time researchers did not fully understand the physiological roles of PTMs. So far, several histone PTMs have been identified, including acetylation -and more generally acylation (Rousseaux and Khochbin, 2015)-, methylation, phosphorylation, ubiquitination, SUMOylation and others recently discovered modifications whose functions are still under intense investigations (Zhao and Garcia, 2015).

Besides the canonical histones H3, H4, H2A and H2.B, other specific histones, with different sequences and timing of expression have been found *in vivo*. These so called “histone variants” have been shown to play important roles during mitosis, transcription, genome repair, differentiation and development (Govin and Khochbin, 2013; Gurard-Levin and Almouzni, 2014; Maze et al., 2014; Melters et al., 2015).

As mentioned above, nucleosome cores are linked to each other by linker DNA. Under conditions of low ionic strength, they form long chains that, when visualized by an electron microscope (EM), have the appearance of a “string of beads”, a structure also called the 11 nm fiber (Olins and Olins, 1974). The packaging of DNA into nucleosomes shortens the fiber’s length about sevenfold. *In vitro* studies suggest that chromatin is further coiled into a shorter and thicker fiber of 30 nm, but due to the scarce evidences of the existence of this structure *in vivo*, this organization is still under debate (Bednar et al., 1998; Luger et al., 2012; Tremethick, 2007). The combination of heterogeneous DNA sequences, linker DNA, histone compositions and modifications makes native nucleosomal arrays highly versatile. In order to perform X-ray and EM analysis on uniform chromatin, researchers have developed *in vitro* reconstitution systems generating extremely well-defined and regularly spaced nucleosomal arrays, where the condensed chromatin fiber has a diameter of around 30 nm. Studies of these reconstituted

chromatin fibers led to the proposal of two main structural models, named (i) the one-start solenoid model –in which nucleosomes are arranged linearly in a solenoid-type helix with a bent linker DNA- and (ii) the two-start cross-linker model – where nucleosome zig-zag back and forth connected by a relatively straight linker DNA. (Dorigo et al., 2004; Li and Zhu, 2015; Robinson et al., 2006). Recent works provided a more detailed view of this structure (Li and Zhu, 2015). However, how much these results from *in vitro* studies mirror the structure of the 30 nm chromatin fiber *in vivo* is questionable (Li and Zhu, 2015). Recently, a new HiC-based method in which chromatin fragmentation is performed by micrococcal nuclease digestion (microC) was developed to analyse short-range nucleosomal interactions *in vivo* (Hsieh et al., 2015). Interestingly, while Hsieh and colleagues did not find evidence for the existence of a 30 nm fiber structure, they observed a pattern of short-range interactions consistent with the zig zag motif, thus supporting the possibility that this motif may exist *in vivo* (Hsieh et al., 2015).

The 30 nm fiber is then thought to acquire additional higher levels of compaction forming structures that eventually lead to the highest level of chromatin condensation: the metaphase chromosomes.

How the genome folds is crucial for the regulation of gene expression. For example, distal control DNA elements, such as enhancers, can be several hundred kilobases or even megabases far away from their target genes, but due to the folding of the genome, they come in close proximity to their target elements and exert their functions (Shlyueva et al., 2014). Moreover, chromatin influences also inter chromosomal interactions. Together with its role in compaction of the genome, chromatin facilitates cell division, preserves the genome integrity and regulates gene activity by controlling the access of genomic elements to specific factors (Melters et al., 2015). This regulation can occur at each level of compaction, from nucleosomes up to chromatin domains.

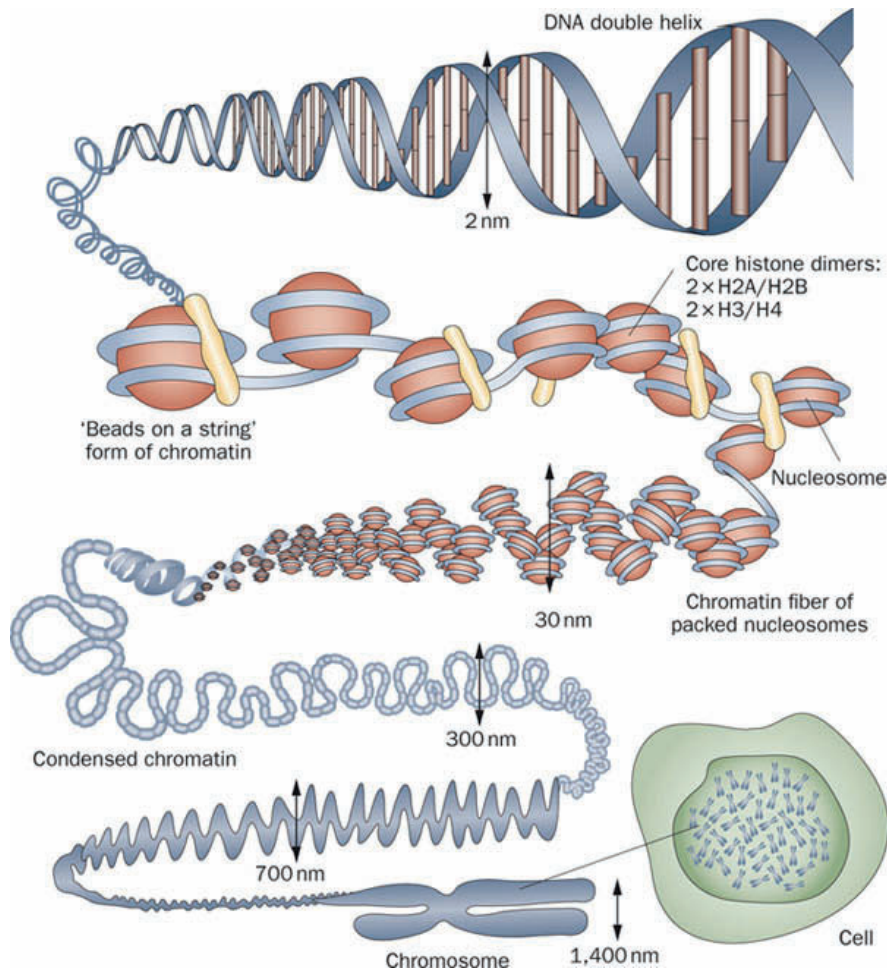


Figure 2: Schematic representation of different levels of chromatin compaction.

The double stranded DNA is wrapped around histones forming the smallest structural component of chromatin, the nucleosome. Multiple nucleosome cores are linked together via linker DNA in a linear fashion producing the 11 nm fiber, also known as “beads on a string”. Additionally, nucleosomes interact between themselves with the help of protein scaffold forming complex 3D structures that will finally lead to the formation of metaphase chromosomes. Adapted from (Tonna et al., 2010)

1.1.1 Different types of chromatin

At the beginning of the XX century, classical cytological studies identified two distinct types of chromatin, termed “heterochromatin” and “euchromatin” by Emil Heitz in 1928. Heitz hypothesized that the lightly stained structure that decondensed during interphase – euchromatin- was “genically active” while the structure staining intensely and

remaining compacted during the progression through the whole cell cycle – heterochromatin- was “genically passive” (Jost et al., 2012).

With the subsequent improvements in staining methods and the development of the electron microscopy, it became apparent that heterochromatin could be subdivided into two subtypes, named constitutive and facultative (Trojer and Reinberg, 2007). The term “constitutive heterochromatin” is usually associated with repetitive sequences – for long time considered “junk DNA” (Palazzo and Gregory, 2014)- and is particularly important for genome integrity. This kind of chromatin is normally localized at the nuclear periphery, where it concentrates factors and favours inter-chromosome interaction, thus contributing to the organization of the nuclear space (Meister and Taddei, 2013). Due to its essential functions, constitutive heterochromatin organization is well conserved and does not vary much between different species. On the other hand, the term “facultative heterochromatin” was indicative of a dynamic structure assuming closed and silenced or opened and transcriptionally active forms depending on the influence of several factors, and associated with processes such as cell differentiation and morphogenesis (Trojer and Reinberg, 2007).

Each chromatin type is characterized by specific “marks”, namely the combinations of post translational modifications of histone tails and the enrichment of specific proteins. Already 15 years ago, Strahl and Allis proposed the existence of a “histone code” read by other proteins to induce distinct downstream events (Strahl and Allis, 2000).

Thanks to the investigation of chromatin landscapes in metazoan through genome-wide studies, we now know that the myriad of chromatin proteins and possible interactions among them can lead to the formation of several chromatin types (Ciabrelli and Cavalli, 2015; van Steensel, 2011). The precise number of chromatin types varies among the studies, depending on the parameters used, such as the algorithm, the resolution and other criteria. For example, a systematic study conducted in cultured *Drosophila* cells by the Van Steensel’s lab describes five principal chromatin types, and named each of them with a different colour (Filion et al., 2010). In this study, yellow and red chromatins mark the most transcriptionally active genes, blue chromatin is associated with genes involved in the regulation of developmental processes, black chromatin cover tissue specific repressed genes and finally green chromatin occupies repetitive sequences. However, the general idea is that metazoan nuclei show an active chromatin environment, sometimes

further subdivided, together with three major types of repressive chromatin (Ciabrelli and Cavalli, 2015; Padeken and Heun, 2014).

Active chromatin

Active chromatin represents a highly accessible environment (measured by DNase I sensitivity) and is the most heterogeneous chromatin type. It displays binding sites for many chromatin factors and is adorned by a myriad of histone modifications, such as methylation of histone 3 lysine 4 (H3K4), lysine 36 (H3K36) and lysine 79 (H3K79) and acetylation of multiple lysine residues on both H3 and H4 N-terminal tails (Ciabrelli and Cavalli, 2015).

Constitutive heterochromatin

This chromatin type corresponds to the original definition of regions that maintain their condensed state regardless the cellular context. In metazoan, this type of chromatin is usually found contiguous to centromeres and is also defined “pericentric heterochromatin”. Depending on the species it can also be found in other genomic regions. It is highly enriched in tandem repeats, satellite DNA and silencer transposable elements, and contains few genes that are often essential for viability. Marks of constitutive heterochromatin are the presence of H4K20 trimethylation (H4K20me₃), H3K9 di and tri-methylation (H3K9me₂ H3K9me₃) as well as the enrichment in heterochromatin protein 1a (HP1) (Ciabrelli and Cavalli, 2015).

Polycomb chromatin

This major type of repressive chromatin has been defined as “polycomb-repressed chromatin” as it contains polycomb group genes (PcG) (Lewis, 1978). Polycomb chromatin is responsible for the silencing of a big portion of the metazoan genomes. The classical mark of this chromatin is the trimethylation of H3K27 (Ciabrelli and Cavalli, 2015).

Null chromatin

This last “obscure” chromatin type shows a lack of specific enrichments for the histone modification tested, and is associated with proteins found also in other repressive chromatin types, with a strong enrichment for lamins (see chapter 1.2.1). Indeed, null chromatin is likely to represent the major flavour of chromatin to be localized both at the nuclear periphery and around the nucleoli (see paragraph 1.2.1 for definition) in metazoan. Null chromatin has been described in *Drosophila* and mammals (Ciabrelli and Cavalli, 2015), but a structure resembling null chromatin was also found in *C. elegans*, in

this case with an enrichment in H3K9 mono-di and tri methylation marks (Liu et al., 2011).

In summary, chromatin is a highly dynamic and complex structure that allows the compaction of the DNA molecule. Enrichments of specific proteins and histone marks characterize the different types of chromatin and influence gene expression.

As its spatial organization is of fundamental importance both for genome compaction and functions, below I will describe how chromatin is organized within the eukaryotic nucleus.

1.2 Chromatin organization within the eukaryotic nucleus

The traditional view of the nucleus as a simple container of chromatin is now abandoned thanks to improved imaging and molecular biology techniques. It is now clear that, similarly to the cell, this organelle is composed of different sub-compartments associated with specific functions. Intriguingly, contrary to cellular organelles, nuclear sub-compartments are not delimited by any physical barrier. The mechanisms by which they are formed as well as their roles in regulating genome functions are still not completely understood and constitute an area of intense investigation.

The way chromatin is folded within the nucleus depends mainly on two fundamental factors: (i) polymer physics –which impose some restrictions to the possible architectural conformations, and (ii) specific biochemical interactions, which lead to a) local compaction (described above), b) long range interactions and c) allow anchoring to nuclear scaffolds (van Steensel, 2011) (Figure 3).

In this chapter, I will first introduce the most important nuclear structures that influence the chromatin organization. Then I will discuss the similarities and differences between the nuclear architecture of metazoans and *S. cerevisiae*. Finally, I will describe the long-range interactions occurring at the chromosome level and between DNA repeats.

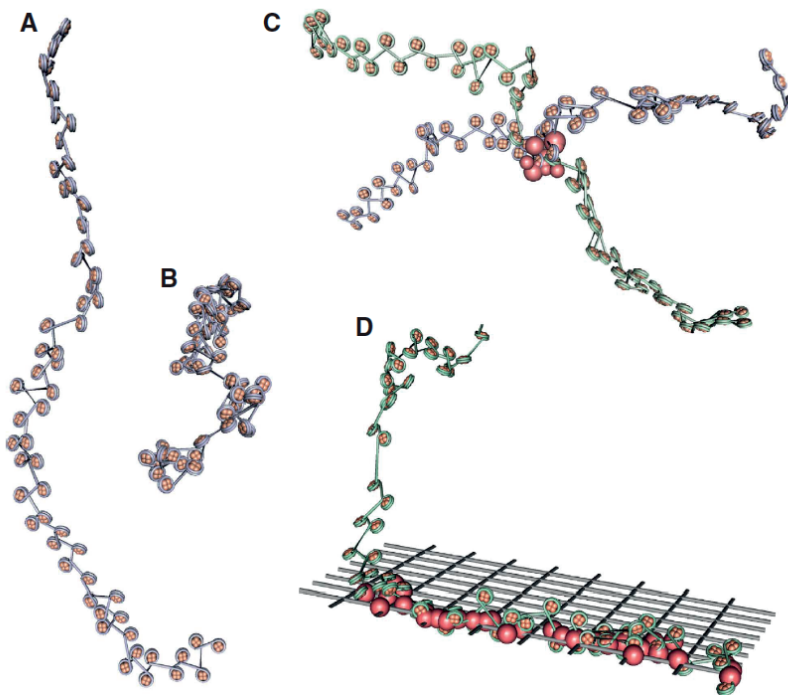


Figure 3: principles of 3D organization of chromatin. A and B: 3D computer simulations of a nucleosome fiber consisting of 60 nucleosomes with different bending of the linker DNA. The fiber is highly flexible and can adopt many different configurations and become extended (A) or compacted (B). These configurations are influenced by the DNA sequence but also by histone modifications or variants. C: Long-range contacts between distant loci that physically interact in the nuclear space, often held together by a specific protein complex. These contacts could be between chromatin fragments belonging to the same chromosome, such as in the case of enhancer-promoter interactions, or between DNA loci found in different chromosomes, such as chromocenters in mouse or telomere clusters in budding yeast. D: Anchoring of specific genomic segments to fixed nuclear landmarks such as the nuclear lamina (depicted by the grey lattice). Red spheres in C and D depict hypothetical anchoring proteins or protein complexes. Adapted from (van Steensel, 2011).

1.2.1 Genome organization in relation with nuclear structures.

Eukaryotic genomes observed at low resolution show an organization in sub-compartments due to contacts with several nuclear structures, mainly i) the nuclear envelope, ii) the nuclear pore complexes and iii) the nucleolus.

While single players involved in the mechanisms of this nuclear architecture are specific for each organism, the global scenario is conserved from yeast to men.

Nuclear structures in metazoan

The nuclear envelope and its lamina

The mammalian nuclear envelope is composed of the outer nuclear membrane (ONM) – which is in continuity with the endoplasmic reticulum (ER) found in the cytoplasm-, a perinuclear space (PNS) and the inner nuclear membrane (INM), and is pierced by nuclear pore complexes. Associated with the nuclear face of the INM is found the nuclear lamina, composed of proteins members of the family of the A-type and B-type lamins. The nuclear lamina, which is coupled to elements of the cytoskeleton through the linker of the nucleoskeleton and cytoskeleton (LINC complex), is important to maintain the structural integrity of the nuclear envelope and provides anchoring sites for chromatin and regulatory proteins (Burke and Stewart, 2013). Lamins and nuclear envelope transmembrane proteins can bind to chromatin components such as heterochromatin protein 1 (HP1) and histones, thus regulating chromosome positions and genome functions. The development of the DamID (DNA adenine methyltransferase identification) technique (Greil et al., 2006) allowed the identification of DNA sequences that interact with the nuclear lamina, defined as lamin-associated domains (LADs), mainly containing transcriptionally inactive heterochromatin (Bickmore and van Steensel, 2013).

Pore complexes

Nuclear pores are channels formed by nucleoporin proteins that perforate the nuclear envelope. They are composed of a central transport channel, two rings –one cytoplasmic and the other nuclear, and eight proteins connecting the nuclear and cytoplasmic rings. Nuclear pore channels (NPCs) allow the passage of molecules up to 40 kDa between cytoplasm and nucleus by passive diffusion. Larger molecules are transported thanks to specific receptors (Ma et al., 2012). In addition to their transport function, NPC complexes have been shown to have a role in the regulation of gene expression, mitosis, chromatin organization and DNA repair (Lemaitre and Bickmore, 2015).

Chromatin regions found close to NPCs differs from that of the rest of the nuclear periphery and form heterochromatin exclusion zones (HEZs). Thus, despite their proximity, nuclear pores and nuclear lamina constitute two distinct compartments with very different roles in the regulation of genome functions (Lemaitre and Bickmore, 2015).

Nucleolus

The third nuclear structure involved in the 3D organization of chromatin is the nucleolus, where rRNA synthesis and preribosome assembly occur. Nucleoli are dense structures visible by electron microscopy. They form around rRNA genes that are transcribed, processed and packaged into preribosomes.

Chromatin zones associated with this subcompartment are named nucleolus-associated domains (NADs). Similarly to LADs, NADs have GC-poor and gene poor content (Nemeth et al., 2010; van Koningsbruggen et al., 2010).

Other substructures, also associated to specific functions, are found within the metazoan nucleus, such as Cajal bodies, PML bodies, Gems or Paraspeckles,.

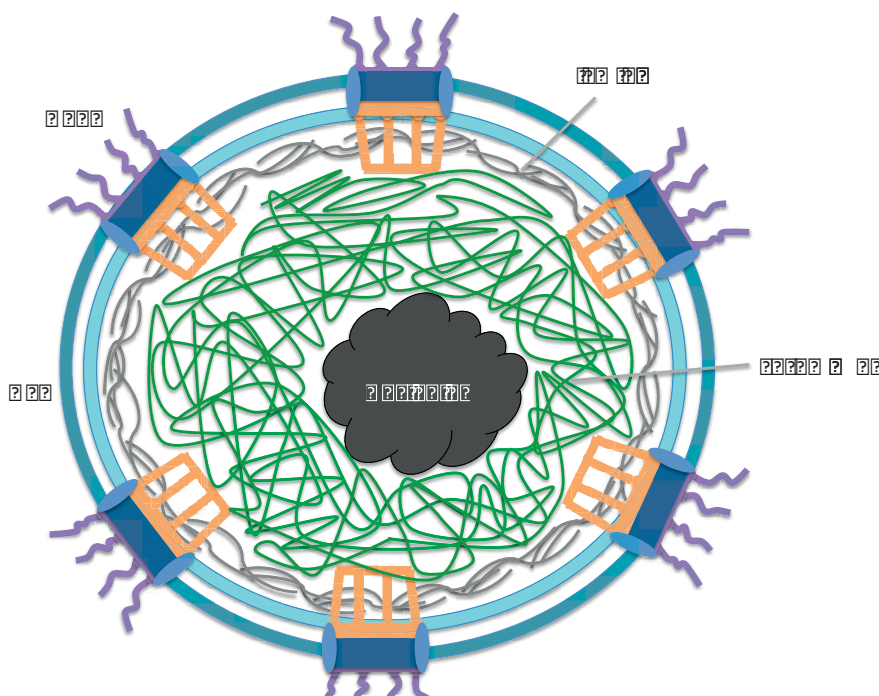


Figure 4: Schematic representation of the main nuclear structures in metazoans. NPC=Nuclear pore complex, NE= nuclear envelope. Chromatin is represented in green.

S. cerevisiae versus metazoan

As previously mentioned, the basic principles of nuclear organization are conserved from yeast to humans. Accordingly, the three dimensional architecture of the budding yeast genome is strongly influenced by chromatin interactions with structural elements of the nucleus, namely NE, NPC and nucleolus and by the biophysical properties of long-range chromatin dynamics (Mekhail and Moazed, 2010; Zimmer and Fabre, 2011). Several DNA-based compartments, such as the nucleolus, telomere foci, tRNA genes clusters, replication foci and sites of DNA repair, are found. On the other hand, the nucleus of *S. cerevisiae* presents some differences compared to the ones of other multicellular organisms (Taddei and Gasser, 2012).

To start with, the budding yeast nucleus is definitively smaller than the metazoan's ones, as it has a diameter of less than 2 μm . It contains 16 chromosomes, which are anchored to the nuclear periphery for the whole interphase through centromeres-spindle pole body (SPB) interactions. This physical constraint leads to the clustering of centromeres and consequently strongly orients all the chromosomes. Chromosome extremities also tend to localize at the nuclear periphery, forming an average of 3 to 5 telomere clusters per haploid cell (see below). The SPB position follows the site of new bud emergence. Still associated with the nuclear periphery but opposite to the SPB is the nucleolus, a "ribosome factory" generates around a single rDNA locus on chromosome XII containing approximately 200 tandem copies of a 9.1 kb repeat. The 9.1 kb repeat leads to a single transcription unit (45S), encoding the 28S, 5.8S, and 18S rRNAs (Taddei and Gasser, 2012).

The condensed and darkly stained chromatin (heterochromatin) found in metazoan is not visualized in budding yeast, but perinuclear clusters of telomeric silent chromatin are present (Taddei and Gasser, 2012). Indeed, TG repeats found at yeast telomeres generate repressive chromatin structures that spread several kilobases from the chromosomal ends (Gottschling et al., 1990). This phenomenon is called telomere position effect (TPE) (Grunstein and Gasser, 2013) and is analogue to the position variegation effect (PEV) (Elgin and Reuter, 2013) spreading from satellite-containing centromeres in other species. However, budding yeast does not contain any RNA interference machinery and the TPE phenomenon depends on a trimeric protein complex, named the silent information regulator (SIR) complex (see paragraph 1.3.1).

Importantly, the *S. cerevisiae* genome contains very few repetitive sequences and does not show simple satellite repeat DNA at centromeres, what in many other organisms constitutes the centric heterochromatin. Not surprisingly, budding yeast also lacks the heterochromatin associated histone mark H3 K9 methylation and the major ligand recognizing this modification: heterochromatin protein 1, HP1 (Taddei et al., 2010).

Moreover, the yeast genome does not contain canonical linker histones H1 and H5, but it encodes for a H1-related protein named Hho1 that is not a core component of chromatin but can bind nucleosomal linker DNA only in rare cases (Taddei and Gasser, 2012).

Another feature of budding yeast is the lack of lamins, even though other structural proteins are associated with the nuclear envelope, some of which are orthologous of proteins involved in chromatin anchoring in metazoan. Moreover, budding yeast has a closed mitosis: this means that its nuclear envelope does not disassemble and reassemble during the cell cycle (Taddei and Gasser, 2012).

Finally, the *S. cerevisiae*'s nucleus lacks several subnuclear compartments such as Cajal and PML bodies, probably because of its reduced size. However, many of the activities coordinated within these compartments in metazoan are undertaken by the yeast nucleolus, which has a role in the biogenesis of small nuclear ribonucleic proteins (snRNPs) and by nuclear pores, which have been shown to play roles in double strand break processing (Nagai et al., 2008) and regulation of gene expression (Taddei et al., 2010).

1.2.2 The organization of chromosomes in the nuclear space

Each genome is divided in a specie-specific number of chromosomes. Individual chromosomes are folded into two kinds of compartments: open/active and closed/inactive (Figure 5). Closed compartments are preferentially found at the nuclear periphery or near the nucleolus as visualized by electron microscopy (Akhtar and Gasser, 2007), where they form heterochromatic regions; oppositely, open chromosome compartments compose the euchromatin regions occupying the majority of the nuclear volume.

Chromosomes are packaged and folded through different mechanisms to occupy distinct “territories” (Cremer et al., 1982; Cremer and Cremer, 2010). Interestingly, it has been

shown that each chromosome has a preferential position within the nucleus, correlated with its gene density (Boyle et al., 2001; Cremer et al., 2001; Croft et al., 1999). Indeed, gene-dense chromosomes tend to position in the nuclear interior while gene-poor chromosomes are mainly found next to the nuclear periphery (Bolzer et al., 2005) (Cremer et al., 2001; Kalhor et al., 2012; Kupper et al., 2007). However, the position of a given chromosome seems likely to be neither random nor fixed but rather probabilistic (Lemaitre and Bickmore, 2015).

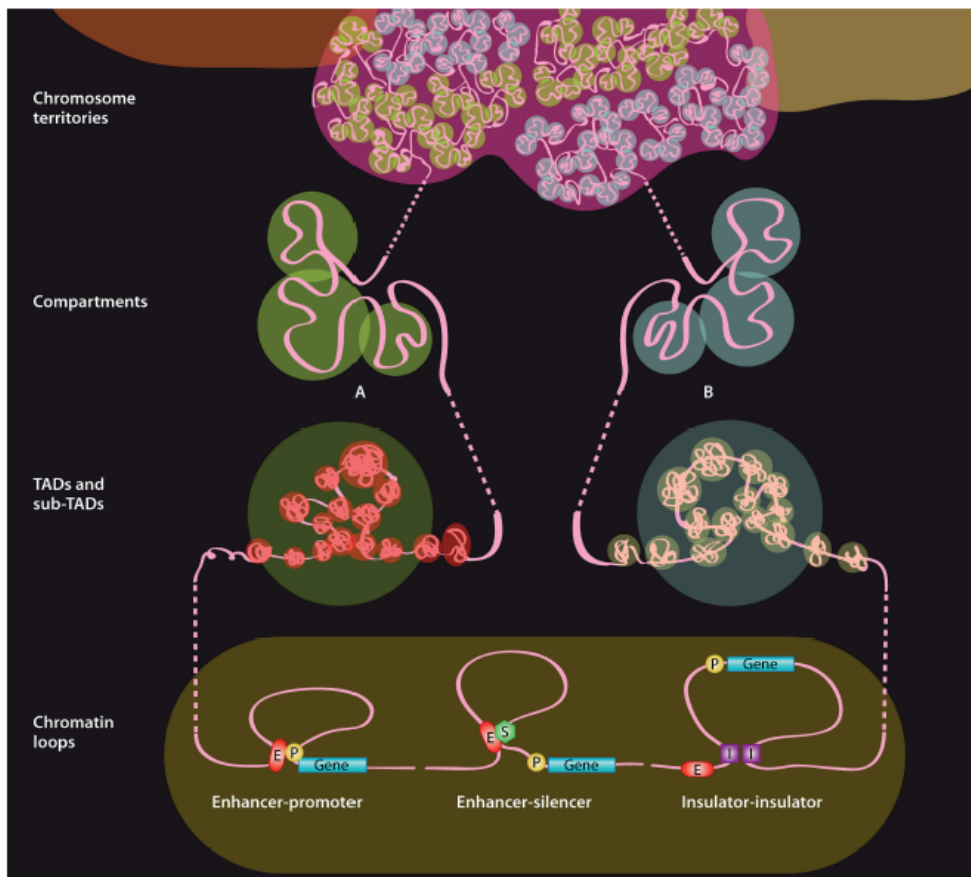


Figure 5: Chromatin organization across genomic scales. Four different levels of chromosome organization –chromosome territories, active and inactive compartments, TADS and sub-TADs and finally chromatin loops- are visualized, from low (bottom) to high (top) resolution (see text). The chromatin fiber is visualized in pink. Adapted from (Fraser et al., 2015).

All these levels of DNA packaging create contacts between different genomic regions that would be otherwise far away within the linear DNA fiber. This concept, that have been first proposed after genetic experiments (Bulger and Groudine, 1999; Ptashne and

Gann, 1997; Taddei et al., 2004), is now confirmed and refined thanks to the application of innovative visual techniques and molecular approaches (Figure 6).

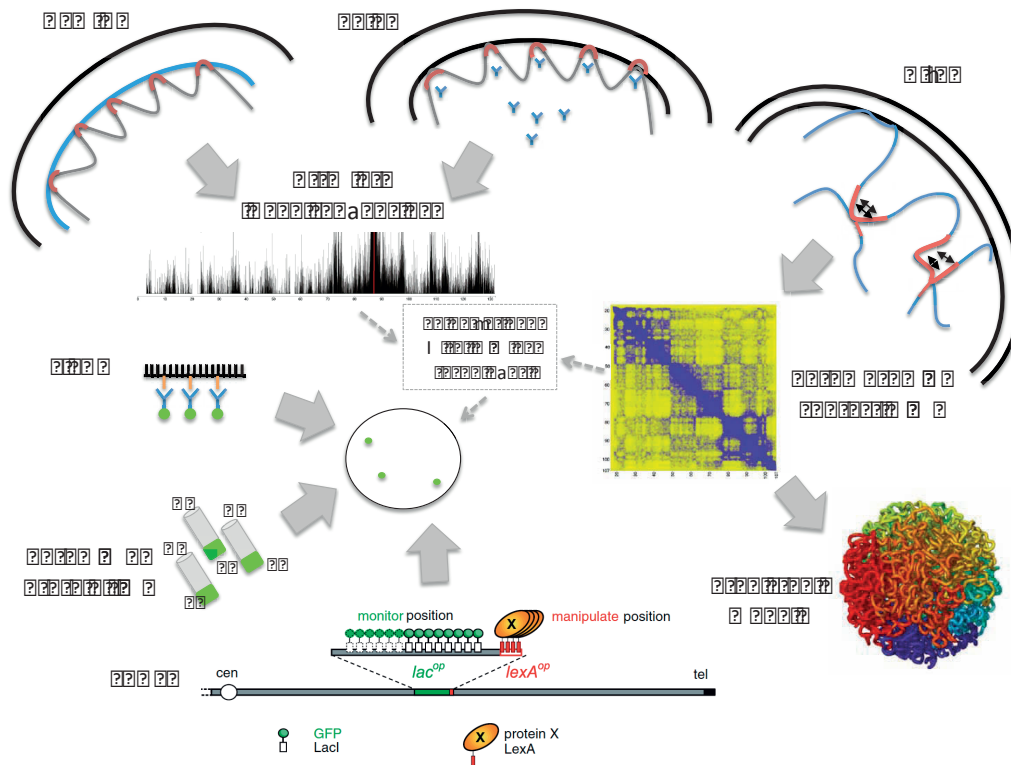


Figure 6: Different assays actually used to study nuclear architecture.

Chromatin organization, which has been studied for years combining genetic approaches with imaging techniques, can be now studied also through several new molecular assays.

Three main imaging techniques are shown on the left bottom corner. 1) FISH based techniques, to visualize specific DNA sequences within the nucleus, alone or in association with specific proteins (immuno-FISH). Sensitivity and resolution are the main limitations of these techniques. 2) *in vivo* fluorescent-tagged or *in vitro* photoactivable tag of chromatin proteins, visualized from low to high resolution depending on the microscope used (Lakadamyali and Cosma, 2015). In this case, it is important to test for genetic complementation by fusion protein, and the protein-DNA association needs to be confirmed by immuno-FISH. 3) Green fluorescent proteins (GFP) tagged repressor-operator system (FROS, bottom-center), to detect a specific locus by the binding of fluorescent protein to an array of sequences inserted at this locus. Importantly, when studying the localization of a locus with FROS one should keep in mind the impact of using this system (Loiodice et al., 2014).

Three main molecular assays are shown on the top. 1) DNA Adenine Methyltransferase Identification (DamID) method (left corner top), to map genomic interaction sites of a given protein *in vivo* (Greil et al., 2006). The Dam enzyme from bacteria is fused in frame with a protein of interest and any chromatin that comes in contact with this protein will be methylated. 2) Chromatin immunoprecipitation (ChIP), to identify specific chromatin domains using antibodies that recognize and bind chromatin proteins/modifications. The DNA sequences identified by DamID and ChIP are isolated and processed. When possible, both the techniques should be

controlled by immuno-FISH. 3) HiC, a derivative of chromosome conformation capture technique (3C), to identify “all versus all” genomic interactions. 3C based methods involve the preparation of chromatin after mild formaldehyde crosslinking, followed by chromatin fragmentation (by sonication or digestion with restriction enzymes) and ligation of the DNA fragments obtained. The ligation products are then captured by a variety of approaches and amplified by PCR or sequencing using unbiased next-generation sequencing methods. Analysis of the sequences leads to the detection of genome-wide interacting regions that could lead to models of chromosomal positioning within the nucleus (de Wit and de Laat, 2012). Deep sequencing image, HiC map and predicted model adapted from (de Wit and de Laat, 2012). FROS drawing adapted from (Loiodice et al., 2014).

New insights into the 3D chromatin organization come from the development of the chromatin immunoprecipitation technique followed by deep sequencing (ChIP-seq) and by chromosome conformation capture (3C) based experiments, in particular the most recent HiC. ChIP-seq allows the production of a vast amount of genome wide data for several DNA binding factors and post-transcriptional histone modifications, while results produced by HiC are interpreted as “chromatin contacts” that generally correlate well with functional studies of regulatory elements at several loci. These contacts depend on the proximity of their DNA sequences, on the local folding of chromatin and on the long-range chromatin architecture, and are strongly influenced by the binding of several nuclear proteins (Pombo and Dillon, 2015). Nevertheless, it is important to note that 3C data have to be carefully interpreted taking into account few technical issues that could bias the result – such as the ligation and cutting efficiency (Pombo and Dillon, 2015)- and should ideally be complemented by microscopy approaches (see box 1). For example, Cryo-FISH analysis –a high resolution method where FISH is combined with ultrathin sectioning of cryoprotected cells- in human lymphocytes showed that chromosomes intermingle extensively and this could promote preferential rearrangements between specific chromosomes depending on their physical proximity (Branco et al., 2008). It has also been proposed that sequences at regions of intermingling are more prone to recombine than those at the interior of chromosome territories (Fraser et al., 2015).

Merged together, these genome-wide data support “looping models” for chromatin organization (Pombo and Dillon, 2015; Tolhuis et al., 2002).

	Imaging techniques	HiC (molecular technique)
Advantages	<ul style="list-style-type: none"> - The result is visualized as an image, which is easy to understand for expert and less expert people. - The localization of a given protein or DNA locus is determined in its context, thus in relation with other nuclear landmark chosen by the researcher. - Single cells are studied, and the result does not come from mixed populations but from selected ones. - Depending on the microscopy are used, the resolution could be very high (up to 20 nm with PALM/STORM super-resolution microscopy). 	<ul style="list-style-type: none"> - These methods allow genome-wide analysis. - High amount of data are produced with a single experiment. - The development of mathematical models that use HiC data allows the prediction of genome folding and permits to visualize the model.
Disadvantages	<ul style="list-style-type: none"> - Artefacts could occur, and controls need to be performed. - Fluorescent tags or insertion of bacterial operators could have secondary effects that should be controlled. - Several images should be taken and the results needs to be quantified and summarized by graphs or plots in order to provide different information. 	<ul style="list-style-type: none"> - The resolution can vary from 10 kb to 1 Mb. - Data needs to be sorted, processed, statistically analysed and the result is not easy to interpret. - The results are influenced by the cutting efficiency. - Imprecision of what exactly is measured: false positives could occur, in particular during the ligation step. - These methods are performed on population of cells and the results are an average of their nuclear organization (which could be far from reality if the population is highly heterogeneous)

Box1: main advantages and disadvantages of the main techniques used in the result section of this manuscript.

As both imaging and molecular techniques show positive and negative points, ideally the two methods should be performed in parallel.

In addition, 5C and HiC analyses showed that the genome is partitioned into megabase-scale Topologically Associated Domains (TADs), which have been proposed to represent regulatory units within which enhancers and promoters can interact (Dixon et al., 2012; Nora et al., 2012). These domains are separated by boundaries enriched for housekeeping genes and histone marks associated with enhancers and are conserved between cell types and across different species. To date, TADs have been found in drosophila (Sexton et al., 2012) and mammals (Pombo and Dillon, 2015). However, similar self associating features defined as chromosomally interacting domains (CIDs)

have been discovered in bacteria (Le et al., 2013), fission yeast (Mizuguchi et al., 2014) and recently also in budding yeast (Hsieh et al., 2015).

The functional importance of TADs is controversial. Given that TADs are largely static across different species and cell types, they are thought to organize the physical proximity between genes and their enhancers (de Laat and Duboule, 2013). However, considering their large size, it has been proposed that the organization of the genome into TADs unlikely creates functional domains (Pombo and Dillon, 2015). Nevertheless, a recent elegant work clearly showed that the destruction of TAD boundary elements leads to *de novo* enhancer-promoter interactions that can cause limb malformation, thus underlying the functional importance of TADs for orchestrating gene expression via the genome architecture (Lupianez et al., 2015).

Finally, the chromatin is further folded into tissue specific sub-TADs, which likely reflect the level and type of genome activities (Phillips-Cremins et al., 2013).

1.2.3 Long-range pairing mediated by repetitive sequences

The third element determining nuclear organization is composed by long-range interactions due to DNA repeats.

DNA repeat sequences, mainly found at centromeres and at telomeric regions, tend to cluster together and to localize close to the nuclear periphery, or near the nucleolus. In different organisms, this organization appears to favour specific functions: it allows the concentration of specific factors thus counteracting their dispersion elsewhere and promoting gene expression or silencing (Perrod and Gasser, 2003), (Figure 7). These subcompartments have also been proposed to serve as a sink or reservoir for specific factors, such as SIRs in budding yeast (Gotta et al., 1996; Kennedy et al., 1997; Marcand et al., 1996; Taddei et al., 2009).

Centromeric DNA repeats group together to form either chromocenters or foci of pericentric heterochromatin. These structures have been found in *Drosophila* (Wakimoto, 1998) and in mammals. They show deacetylated histones, trimethylation at H3K9 histone tails and enrichment of the Heterochromatic Protein 1 (HP1). Repetitive sequences at centromeres are also found in *S. pombe*, where these silent domains are enriched for the HP1 fission yeast homologue Swi6 (Haldar et al., 2011).

The genome of budding yeast contains DNA repeats only at telomeres and within the chromosome XII at the rDNA locus. Interestingly, both these two types of repeats are separated from the rest of the genome, and form distinct sub-compartments: telomere foci and the nucleolus, respectively.

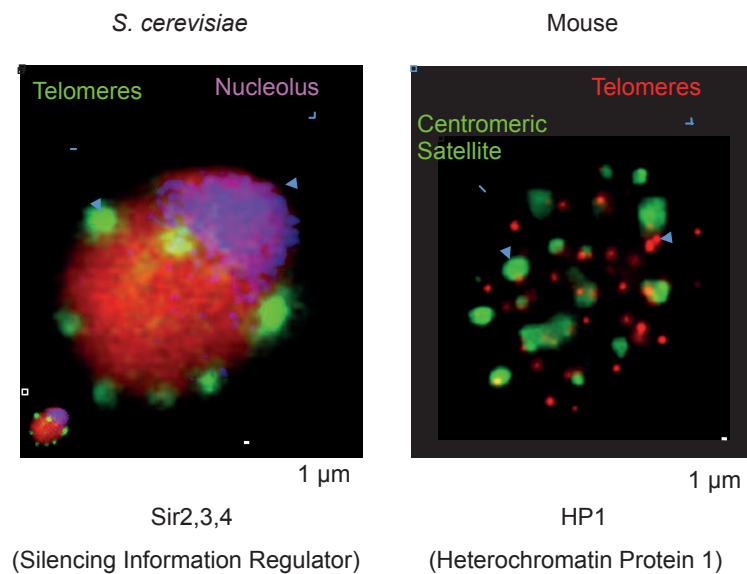


Figure 7: Conserved clustering of DNA repeats in foci enriched for silencing factors. Mechanisms promoting chromatin-mediated silencing show common features from yeast to metazoans (Perrod and Gasser, 2003). In budding yeast (left), telomeres group together and form few clusters localized close to the nuclear periphery and enriched in proteins of the SIR complex, Sir2, Sir3 and Sir4. *S. cerevisiae* nucleus is visualized with two different scales, the one in the corner allows comparison with the mouse nucleus on the right. Similarly, in mouse nuclei (right) centromere repeats, visualized in green by FiSH, cluster together in subcompartments enriched in Heterochromatin Protein 1 HP1. Mouse nucleus image adapted from (Taddei et al., 2001), *S. cerevisiae* nucleus image adapted from (Taddei and Gasser, 2012).

Telomere grouping is not a unique feature of *S. cerevisiae*. It is found also in other organisms, where it is associated with specific functions (Edward J. Louis, 2014).

As my PhD work is based on telomere clustering, this topic will be further discussed more in detail in paragraph 1.3.

1.2.4 Impact of the nuclear organization to genome function

Building silent compartments and keeping them at the nuclear periphery seems to obey a similar pattern in the majority of the experimental system studied, although fine details vary depending on the organism (Meister and Taddei, 2013).

However, up to now few cell types have been reported showing heterochromatin far from the nuclear periphery (Figure 8). Among them there are (i) the mouse round spermatid formed after meiosis, whose nuclei are characterized by the assembly of all pericentric regions into a unique large chromocenter (Govin et al., 2007), (ii) rod cells found in the retina of nocturnal animals, showing an “inverted” architecture (Solovei et al., 2009), (iii) mouse olfactory neuron nuclei, where heterochromatic foci localize in the center of the nucleus tethered to the NE only by a small amount of heterochromatin, (Clowney et al., 2012) and (iv) muscle nuclei located close to the synapsis (unpublished work from Alexandre Mejat laboratory). On the other hand, perturbation of the classical chromatin architecture is found in certain senescent cells (Corpet and Stucki, 2014) and in cancer cells -feature nowadays used to diagnoses different cancer phenotypes (Polak et al., 2015; Reddy and Feinberg, 2013). Finally, destruction of perinuclear organization leads to diseases known as laminopathies (see below) (Worman and Bonne, 2007).

When a different chromatin architecture leads to advantages: nocturnal lifestyle and inverted nuclear organization

Computer simulations indicate that nuclei in which chromatin is arranged in a concentric fashion according to gene density function as lenses able to channel the light more efficiently toward the light-sensing rod outer segments (Solovei et al., 2009). These results, together with the evident correlation between inverted nuclei and nocturnal lifestyle, strongly suggest that such 3D architecture favours nocturnal vision. Interestingly, Solovei and colleagues propose that the inverted pattern appeared very early in the evolution of mammals as an adaptation event in a group of nocturnal animals and that the conventional pattern was repeatedly reacquired in mammals that readopted a diurnal lifestyle (Solovei et al., 2009). This is in agreement with the idea that the conventional nuclear organization is the best rearrangement to increase the opportunity for “gene regulation through nuclear organization” (Sexton et al., 2007), while the

inverted pattern is likely to strongly reduce the diversity of chromosome neighbourhoods.

When the 3D nuclear organization is disrupted: laminopathies and cancer

I already mentioned that the nuclear envelope is an important player in the maintenance of the correct organization of the nucleus. In yeast and worms, interactions between chromatin and NE have been shown to regulate transcription, even if in mammals the function of this interaction is not as clear (Burke and Stewart, 2013). However, mutations in *LMNA* genes, responsible for the formation of the lamina, lead to nearly 30 different inherited diseases and anomalies known as laminopathies (Worman and Bonne, 2007). Laminopathies probably represent the strongest evidence that the association between chromatin and nuclear envelope is of fundamental importance for the proper genome function.

These pathologies are mainly split in 3 groups: i) diseases affecting the striated muscle such as dystrophies, ii) defects in white fat and skeletal homeostasis and iii) pathologies associated with premature aging. It is intriguingly how mutations in the same gene, which codify for the same ubiquitously expressed protein, could result in such a range of tissue-specific diseases (Burke and Stewart, 2013).

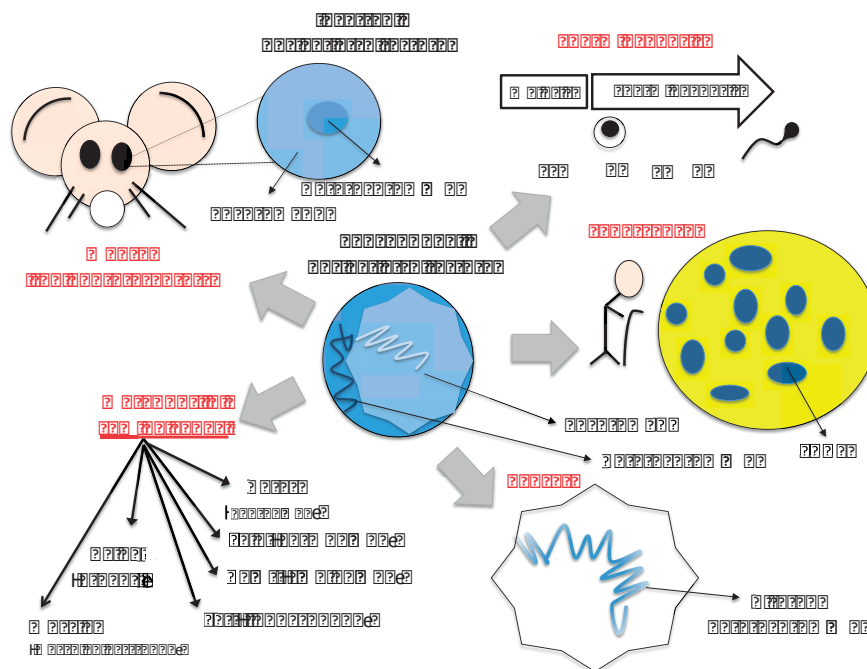


Figure 8: strong correlation between nuclear architecture and genome function.

In the majority of healthy cells, chromatin is highly organized within the nucleus, with the nuclear periphery enriched for heterochromatin and the nuclear interior mainly constituted of euchromatin, “conventional architecture”. During cell differentiation, the architecture of the nucleus changes still keeping its typical “conventional” organization. However, exceptions exist. One case is the dramatic chromatin reorganization occurring during mouse spermatogenesis (maturation of male haploid germ cells) (Rousseaux et al., 2008). Sc= spermatocytes; R= round spermatids; E= elongating spermatids; C= condensing and condensed spermatids. Adapted from (Govin et al., 2007) Another exception is constituted by nuclei of rod photoreceptors of nocturnal animals, which show an “inverted” nuclear organization, with heterochromatin found in the middle of the nucleus and euchromatin at the periphery (Solovei et al., 2009). In addition, punctate DNA foci named senescence associated heterochromatin foci (SAHF) can be visible in DAPI-staining during certain type of senescence (Corpet and Stucki, 2014). In cancer cells, heterochromatin organization is strongly altered and this characteristic is actually used in diagnostic ((Zink et al., 2004). Finally, genetic mutations in genes encoding for nuclear lamina lead to several diseases affecting different organs/tissue (laminopathies, see text).

To summarize, the 3D architecture of the nucleus is influenced by several factors, namely physical constrains, DNA sequence and specific interactions involving both DNA and proteins. The level of compaction of the chromatin fiber and its organization control both accessibility to protein complexes and their binding, thus having a profound effect on gene expression. However, up to now it is not clear whether nuclear architecture is a consequences or a determinant of genome functions.

1.3 Telomere clustering in budding yeast: a model for silent chromatin domains

Silent chromatin in *S. cerevisiae* shares many features of heterochromatin, such as the peripheral localization, the presence of hypoacetylated histones, the reduced accessibility to enzymes, the late replication timing and its propensity to associate in trans (Grunstein and Gasser, 2013).

Budding yeast silent chromatin depends of members of the SIR complex, namely Sir2, Sir3 and Sir4. SIR-dependent silencing was initially discovered at the homothallic mating

loci (*HM*), and successively found also at subtelomeric regions. Together with these two sites of silent chromatin, another repressive chromatin structure for polIII transcription is found in the nucleolus, where rDNA repeats are localized. However, Sir3 and Sir4 are not necessary for the silencing of the rDNA repeat. On the other hand, silencing and compaction in this subcompartment are Sir2 dependent (Taddei and Gasser, 2012).

As my PhD work is based on telomere clustering as a model for silent chromatin compartment, I will describe more in detail telomeric silent chromatin, with a particular focus on key players for its formation: the SIRs. But first, I will introduce telomeres from the molecular point of view.

1.3.1 Telomeres and subtelomeres: structure and function

Telomeres constitute the tip of chromosomes and their main function is to protect the stability of the genome by capping chromosome's extremities and avoiding their degradation or fusion (Kupiec, 2014). As telomeres constitute the ends of linear chromosomes, they contain DNA that resembles one half of a DNA double-stranded break (DSB). In yeast, DSB induces cell cycle arrest and can be processed either by homologous recombination (HR) or by non-homologous end joining (NHEJ). However, these structures distinguish between the natural chromosomal ends and unwanted double-stranded breaks (Dewar and Lydall, 2012). Finally, telomeres are also essential for the regulation of gene expression, the nuclear organization, gene recombination and proper mitotic and meiotic divisions (Kupiec, 2014).

Telomeric chromatin is not predominantly formed by nucleosomes but is rather composed by non-histone proteins and telomere components. At the molecular level, telomeres of *S. cerevisiae* consist of 250-300 bp of irregular tandem repeats with the consensus sequence TG1-3 in which no genes are encoded (Kupiec, 2014). However, telomeres are transcribed into specific transcripts, referred to as telomeric repeat-containing RNA (TERRA) that, in budding yeast, have been proposed to regulate telomere length (Luke et al., 2008).

The G-rich strand contains a 10-15 bp 3' overhang that is generated at the end of the S phase after completion of replication and functions as a template for the action of the

telomerase. Indeed, at each cell cycle, during replication, a specific addition of the 3'G-rich overhang is required to avoid telomere shortening and its dramatic consequences on cell ageing and death. G-tail addition is performed by a conserved ribonucleoprotein complex with reverse transcriptase activity named the telomerase complex (Kupiec, 2014). It is composed of a core, formed by the “even shorter telomeres” 2 (Est2) and the template Tlc1, plus two auxiliary subunits namely Est1 and Est3. G-tail formation also involves the Repressor Activator protein 1 (Rap1) –an essential yeast protein with several roles including telomere capping and nucleating silencing at the tips-, the heterotrimer CST (Cdc13, Stn1/Ten1) that binds the single-stranded G-rich overhang, the end-binding complex yKu heterodimer –which plays an essential role in telomere maintenance (Dewar and Lydall, 2012)-, the DNA damage repair MRX complex (Mre11/Rad50/Xrs2) (Marcomini and Gasser, 2015) and other proteins with unclear specific roles (Kupiec, 2014)

Rap1 binds the double stranded TG1-3 repeats through a double Myb-like domain. The number of repeats, and therefore of Rap1 molecules, for each telomere within the same nucleus is not homogeneous, and telomerase does not act on every telomere at each cell cycle (Teixeira et al., 2004). Telomere elongation events are likely to occur within clusters containing few telomeres and several telomerase molecules. The rate at which telomeres are elongated is dependent on their length, and the chance of being elongated is higher for short telomeres (Gallardo et al., 2011; Malyavko et al., 2014; Marcand et al., 1999; Teixeira et al., 2004). Rap1 establishes a negative feedback loop on telomere elongation through its C-terminus domain by recruiting Rif1 and Rif2 (RAP1-Interacting Factors), involved in telomere capping. At longer telomeres, increase of Rif1 and 2 counteracts the binding of Tel1 (ATM) (Hirano et al., 2009), which is required for telomerase recruitment. Moreover, the silencing factors Sir3 and Sir4 also bind Rap1 at its C-terminus (Figure 9). As a consequence, the competition between Sir4 and Rif1 balances telomerase activity and thus telomere length (Grunstein and Gasser, 2013) (Kueng et al., 2013). Several other regulatory pathways have been proposed to control telomerase action, but the complexity of telomere length homeostasis is still far from being completely understood (Malyavko et al., 2014).

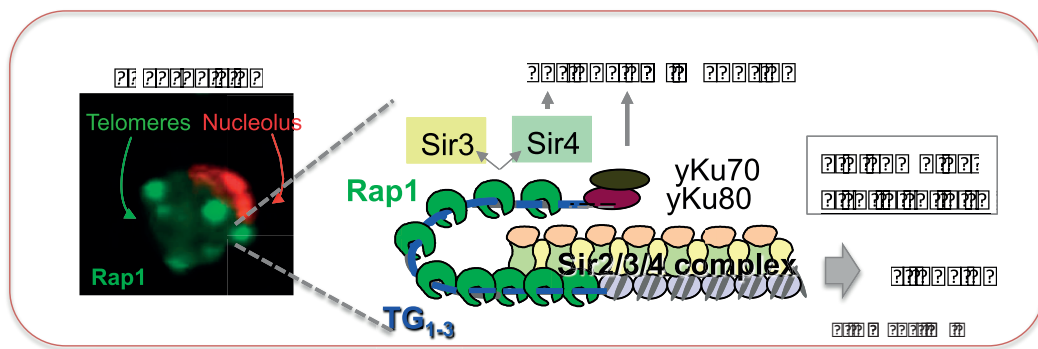


Figure 9: schematic representation of a telomere.

On the left, fluorescent image of a haploid budding yeast nucleus. Telomeres are visualized through Rap1-GFP tag (green), the nucleolus is visualized by Sik1-RFP tag (red). On the right, schematic draw of a telomere. Rap1 protein binds TG repeats at the tip of the telomere, and recruits Sir3 and Sir4. Sir4, together with the yKu complex and other proteins, contributes to telomere anchoring at the nuclear periphery. Sir4 also recruits Sir2, the NAD⁺ dependent histone deacetylase, thus allowing the formation of the SIR complex (Sir2-4). Sir2 deacetylates the neighbouring histone tails thus creating a docking surface for Sir3, and eventually leading to the spreading of the complex for 2-3 kb along the chromosome.

Contrary to telomeres, the structural definition of subtelomeres remains a challenge, since no clear barrier has been found to distinguish a subtelomere from a non-subtelomeric domain. Yet subtelomeres are normally described as large chromosomal regions in which few non-essential genes, separated by long AT-rich intergenic regions, are found (Edward J. Louis, 2014). Subtelomeric sequences are composed of X elements, subtelomeric repeats (STR) and long tandem Y' repeats which could origin from transposable elements (Fourel et al., 1999) and vary a lot between strains and species (Liti et al., 2009). These regions include both proto-silencer elements favouring SIR-mediated silencing and anti-silencing sequences referred to as subtelomeric anti-silencing regions (STARs) (Edward J. Louis, 2014;(Power et al., 2011). As mentioned before, budding yeast subtelomeric regions also harbour some non essential genes, which are involved in cell survival under unfavourable conditions, a characteristic that is found also in other microorganisms, for example in the human pathogen *Candida glabrata* (*EPA* genes) and in the *Plasmodium falciparum* (*var* genes, see paragraph 1.3.3) (Edward J. Louis, 2014; Verstrepen and Fink, 2009; Verstrepen et al., 2004).

Subtelomeric genes in *S. cerevisiae* can be roughly divided in three categories: (i) those involved in carbohydrate metabolism, such as the *MAL* gene family (ii) in adhesion, namely *FLO* family (Verstrepen et al., 2004) and (iii) gene families that are not yet fully

characterized, including *COS* genes possibly conferring resistance to salt stress and *PAU* genes which have a putative role in cell-wall remodelling (Edward J. Louis, 2014). Interestingly, subtelomeric gene content seems to reflect the lifestyle of the organism under study, as the degree of plasticity of these genomic regions allows organisms to rapidly adapt to their environment (see discussion chapter). Subtelomere proximal genes are often transcriptionally silenced in a position-dependent manner, referred to as Telomere Position Effect (TPE), which will be further discussed in the next paragraphs.

1.3.2 Telomeric silent chromatin and the SIR complex

Heterochromatic silencing, in yeast like in the other organisms, shows a substantial difference with the promoter-specific gene repression: the absence of sequence specificity in the repressor complex binding. However, this type of silencing is restricted to specific regions of the genome because the recruitment of silencing proteins relies on factors that bind the genome in a sequence specific manner (Kueng et al., 2013). This process, called “nucleation”, constitutes the first point of a three step molecular mechanism that eventually leads to gene silencing. In budding yeast, nucleation involves the recruitment of the SIR complex by multifunctional DNA-binding factors, namely ORC (Origin Recognition Complex), Abf1 (ARS-Binding Factor 1) and Rap1 (Repressor activator protein 1). These proteins recognize specific motifs clustered within short elements flanking the homothallic mating loci left and right (*HML* and *HMR*) defined as *E* (essential) and *I* (important) silencers, and (Rap1 only) the TG1-3 repeat tract at telomeres. Once nucleation is set up, the second step occurs: the SIR complex spreads along the chromosome until it stops (third step) because of boundary elements or insulators or because of the limiting amount of the SIR proteins themselves (Kueng et al., 2013). It has to be noted that Abf1 and Rap1, which are necessary for the nucleation step of gene silencing, function as transcription factors in other contexts (Kueng et al., 2013).

Although all the members of the SIR complex are essential for both establishment and maintenance of silent chromatin, each SIR has a different function. In the next paragraphs I will describe each of them in detail.

Sir2: gene silencing through histone deacetylation

Sir2 is a highly conserved class III NAD-dependent histone deacetylase (HDAC), essential for SIRs spreading and silencing (Moazed, 2001) and founding member of the evolutionally conserved longevity factor sirtuins (Wierman and Smith, 2014).

In budding yeast, together with Sir2, other 4 sirtuins are found, namely Hst1-4. However, Sir2 is the only sirtuin able to form a heterodimer with Sir4; Sir2-Sir4 complex is quite stable and has been shown to increase Sir2 ability to deacetylate the H4K16 substrate (Kueng et al., 2013). Its enzymatic activity at telomeres is counteracted by Sas2, which acetylates the same lysine 16 of the H4 histone tail (Suka et al., 2002).

Sir2 is the enzymatic member of both the SIR complex -found at telomeres and mating type loci- and the RENT' complex- found at the rDNA. At telomeres, Sir2-dependent deacetylation of H4K16 –together with its fundamental role in silencing- has been proposed to antagonize replicative ageing (Dang et al., 2009). Finally, as transcription of TERRA has been associated with telomere shortening thus with senescence, SIR mediated silencing at telomeres appears important for telomere homeostasis (Maicher et al., 2012).

At the rDNA, Sir2 controls recombination between the repeats, thus reducing the locus instability and the number of extrachromosomal rDNA circles (ERCs), both thought to affect the aging process (replicative lifespan) (Longo et al., 2012).

Given that the Sir2 protein is limiting for silencing, its amount in one or the other complex has been shown to strongly condition TPE and rDNA repeat stability (Kennedy et al., 1997; Salvi et al., 2013; Smith et al., 1998).

As mentioned before, Sir2 is also the founding member of the sirtuins, a family of NAD⁺ dependent deacetylases highly conserved from bacteria to man (Wierman and Smith, 2014). Sirtuins can deacetylate both histones and nonhistone substrates, such as cytoplasmic proteins (Lin et al., 2009; Yu and Auwerx, 2009). In the enzymatic reaction, while the target lysine side chain is deacetylated, a molecule of NAD⁺ is cleaved into nicotinamide (NAM) (Landry et al., 2000) and O-acetyl-ADP-ribose (Tanny and Moazed, 2001). Consistently, variations in NAD⁺ levels modulate Sir2 enzymatic activity while NAM inhibits Sir2 activity both *in vitro* and *in vivo* (Belenky et al., 2007; Bitterman et al., 2002; McClure et al., 2012). The other product resulting from this reaction, named O-acetyl-ADP-ribose (O-AADPR), has been proposed to act as a second messenger that

could protect cells against ROS in *S. cerevisiae* (Tong and Denu, 2010) and to regulate SIRs spreading mainly enhancing Sir3 loading activity to nucleosomes (see below). However, direct binding of O-AADPR has been detected only for Sir2, suggesting that this molecule could possibly lead to a conformational change of the complex.

Given their sensitivity to the NAD⁺ metabolite for their catalytic activity, sirtuins are able to translate different metabolic states into global cellular changes.

Both in yeast and in other organisms (i.e. worms, flies, mice and humans) sirtuins are implicated in the regulation of the aging process and for this reason they are subject of intense investigation. However, Sir2 function on yeast lifespan is a complex matter and will be further discussed in the second chapter of this manuscript, paragraph 2.3.4. A schematic representation of the Sir2 protein is shown in Figure 10.

Sir3: specificity, spreading and clustering

Within the members of the SIR complex, Sir3 is the one that ensures the specific binding of deacetylated histones and is important for the spreading of silent chromatin along the chromosome (Oppikofer et al., 2013a) and for the clustering of telomeres (Ruault et al., 2011).

The *SIR3* gene arose from the whole-genome duplication of the *Saccharomyces* lineage and shares several features with its paralog *ORC1*. The resulting protein is composed of an N-terminal bromo-adjacent homology domain (BAH domain, aa 1-214) that binds nucleosomes, a central AAA+ ATP-ase like domain (AAA aa 532-834) that has an interaction domain both with nucleosomes and with the Sir4 protein, and a C-terminal domain, winged helix-turn-helix (xH, aa 840-978) that mediates homodimerization (Kueng et al., 2013), (see Figure 10).

Sir3 is thought to be able to bind nucleosomes in more than one conformation (Norris and Boeke, 2010; Oppikofer et al., 2013a), and this characteristic is thought to be important for the proper formation of silent chromatin. It has indeed been proposed that Sir3 binding to nucleosomes needs to be “just right”, such as in the “Goldilocks principle”: Sir3p should be at the right place and in the good conformation to get a correct affinity to chromatin. This appears to happen thanks to several factors, such as the balance between BAH and C-terminal domains, electrostatic repulsions between Sir3 and DNA and the H3K79me3 mark, catalyzed by Dot1, counteracting Sir3 binding. On the other hand, when Sir3 binds the DNA too strongly, it is counterproductive for telomeric silencing (Norris and Boeke, 2010).

Overexpression of Sir3 leads to the formation of a “hypercluster” of telomeres that localize far from the nuclear periphery (Ruault et al., 2011).

As mentioned above, the Sir3 BAH domain primarily mediates the selective binding of the protein to unmodified nucleosomes, in particular not acetylated at histone H4K16 and not methylated at H3K79 (Armache et al., 2011), even though the central AAA domain, which is sensitive to the methylation of H3K79, contributes to this selectivity (Ehrentraut et al., 2011). Sir3 N-terminal BAH domain is essential for SIRs spreading. When overexpressed, this domain is not only able to spread along nucleosomes but also promotes the spreading of intact SIR complexes as well (Connelly et al., 2006; Gotta et al., 1998). On the other hand, while the BAH domain is crucial for repression in the context of the intact protein, it is not able to mediate silencing on its own (Armache et al., 2011; Kueng et al., 2013). The N-terminal domain of Sir3 is subjected to acetylation by Nat1, a subunit of the N-term acetylase NatA. Mutations of the acetyl-acceptor residue at Sir3 compromise gene silencing (Ruault et al., 2011; Wang et al., 2004) probably because it destabilizes the BAH-nucleosome interface (Arnaudo et al., 2013; Yang et al., 2013).

The central part of Sir3 is important for its recruitment at the sites of repression, and for Sir3 interaction both with Rap1 and Sir4. The Sir3 AAA domain is catalytically dead due to its inability to bind and hydrolyse ATP. However, this domain could be important to bind nucleotides once assembled in the SIR complex or loaded into chromatin. Moreover, it has been proposed that Sir3, through its AAA domain, could bind the byproduct of Sir2's deacetylase activity O-AADPR (Liou et al., 2005; Martino et al., 2009). Interestingly, the *in vitro* addition of this small molecule to purified Sir2-3-4 and nucleosomes leads to the formation of filaments visible with electron microscope (EM) (Liou et al., 2005). Moreover, addition of O-AADPR to SIR complexes purified from baculovirus-infected cells increases the SIRs affinity for trinucleosomes. Finally, O-AADPR addition to Sir3 alone also increases Sir3p affinity for nucleosomes, even if the effect is less striking than with the complete complex (Martino et al., 2009). However, it has been shown that telomeric silencing can occur also in absence of O-AADPR, as fusion of the NAD⁺ independent deacetylase Hos3 proteins to Sir3 silences as well as Sir3-Sir2 fusion protein (Chou et al 2008).

Taken together these data suggest that, even though O-AADPR *per se* is not absolutely required for silencing, at telomeric regions -where Sir3 is incorporated within the SIR complex- O-AADPR may increase Sir3 affinity for chromatin thus promoting silencing.

Finally, the C-terminal part of Sir3 is both necessary and sufficient for Sir3 dimerization. This xH-mediated homodimerization is essential for silencing, as its loss has been shown to impair Sir3 loading onto nucleosomes *in vitro* and eliminates silencing at telomeres and *HM* loci *in vivo* (Oppikofer et al., 2013b).

Sir4: scaffolding and anchoring roles

The Sir4 protein has several fundamental roles in telomeric silent chromatin formation, as it anchors the whole SIR complex to the nuclear envelope through its interactions with Esc1 and Yku, it functions as a scaffold and it is required for the nucleation step (Kueng et al., 2013; Oppikofer et al., 2013a). Moreover, it is involved in telomere homeostasis by inhibiting telomere-telomere fusions and by regulating telomere length (Marcand et al., 1997; Marcand et al., 2008).

Sir4 has high affinity for both DNA and chromatin, even though this affinity is not very specific, and does interact with several partners (Martino et al., 2009).

Sir4 extreme C-terminal domain is important for Sir4 scaffolding and anchoring functions. Indeed, it mediates homodimerization and binding with other factors namely Sir3, Yku and Rap1. Upstream from this it contains binding sites for Sir2 (SID domain) and for the enhancer of silent chromatin Esc1 (PAD domain). The C-terminal half domain can also bind Ubp10, which is the enzyme that deubiquitylates H2BK123. This modification counteracts methylation at H3K4 and H3K79 (marks for active chromatin) thus contributing to the formation of a more closed chromatin structure (Kueng et al., 2013)

The N-terminal domain, which is essential for TPE, allows Sir4 binding to the DNA with high but not specific affinity (Martino et al., 2009). However, as Sir4 is mainly found in a stable dimer with Sir2, the heterodimer binds preferentially nucleosomes with H4K16 acetylated tails, likely because of Sir2 affinity for H4K16 acetylated substrates. The N domain also binds Yku80 and is important for interaction with Sir1, which is found at *HM* sites but not at telomeres (Kueng et al., 2013). A schematic representation of the Sir4 protein is found in Figure 10.

Interestingly, all the SIRs can be post-translational modified.

Sir4 and Sir2 PTM have effects on nuclear architecture. In particular, SUMOylation of Sir4 promotes telomere perinuclear binding (Ferreira et al., 2011), while SUMOylation of Sir2 has been recently reported to unbalance Sir2 localization between telomeres and nucleolus by compromising the formation of the Sir2-Sir4 heterodimer (Hannan et al., 2015). The Sir3 protein is subjected to PTM in response to the external environment, and subsequent effects in spreading, silencing and aging have been reported (Ai et al., 2002; Ray et al., 2003; Stone and Pillus, 1996). I will develop furthermore this topic in the “Discussion” chapter.

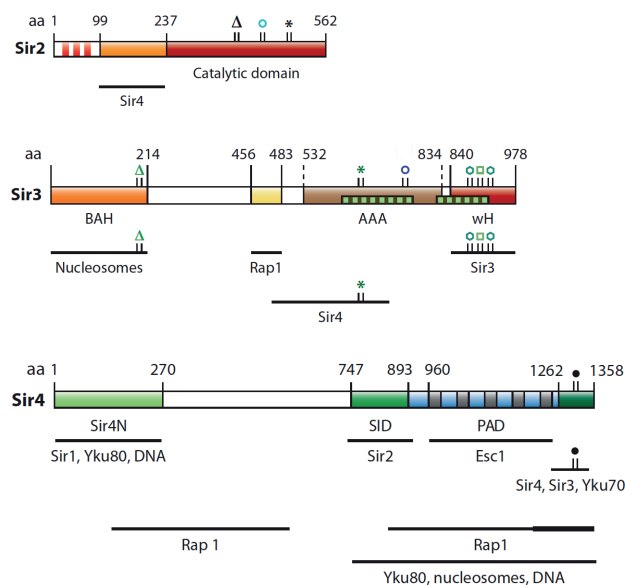


Figure 10: schematic structures of the members of the SIR complex.

The numbering refers to the primary sequence of the protein. Top: schematic structure of Sir2 with its main protein-protein interaction domains. N terminus (red/white dashes); Sir4-interacting domain (orange); catalytic domain (dark red). Mutations that disrupt catalytic activity: N345A, triangle; H364A, cyan open circle. Mutation that disrupt trimer formation: P394L, asterisk. Center: Schematic representation of Sir3 protein with its important domains, protein-protein interactions and mutations: BAH domain (orange) and mutation D205N (green triangle); Rap1 binding site (yellow); AAA domain (brown) with mutations that interfere with Sir4 binding (K657A/K660A; dark green asterisks) and a mutation that enhances chromatin interaction (L738P; blue circle); wH domain (dark red) with mutations interfering with dimerization (L861A/V909A; teal hexamers); and mutations that makes mating SIR1-dependent (P898R; green square). CHD1 and CHD2, the two chromatin binding domains in the C terminus, are shown in olive and brown dash boxes.

Bottom: Schematic representation of Sir4 protein with its important protein-protein interaction domains as follow: Sir4N (olive); Sir2-interacting domain (SID, green); partitioning-and-anchoring domain (PAD; blue-grey); coiled-coil domain (dark green). Closed circle represent the mutations disrupting Sir3-Sir4 interaction. The C terminus – essential but probably not sufficient

for Rap1 interaction - is shown in a fat line within the full Rap1-interaction domain. Adapted from (Kueng et al., 2013)

1.3.3 Model for SIR spreading and telomere foci formation

It has been proposed that telomere clusters are the consequence of non-specific events governed only by some structural constraints namely chromosome structure, SPB attachment and nuclear crowding (Therizols et al., 2010; Wong et al., 2012; Zimmer and Fabre, 2011). However, a more recent analysis taking into account both microscopy data and mathematic models indicates that random encounter does not account for the dynamics of telomere foci observed *in vivo*, and suggests that telomere clustering is more likely generated by a random dynamics of aggregation-dissociation (Hoze et al., 2013).

In agreement with this hypothesis, telomere clustering has been proposed to be involved in a positive feed back loop that links concentration of silencing proteins with perinuclear localization and gene silencing (Figure 11) (Meister and Taddei, 2013). As I previously discussed, the formation of silent chromatin depends on nucleation, spreading and stop of the SIR complex. The sequential assembly model for SIR-mediated repression suggests that Sir4, through its interactions with both the TG repeats bound protein Rap1 and with Ku, Mps3 and Esc1 proteins found at the nuclear membrane, brings telomeres at the nuclear periphery (Kueng et al., 2013; Taddei and Gasser, 2012). Here Sir4 is mainly found associated with Sir2, which has high affinity for acetylated histones. Several recent evidences suggest that H4K16ac helps recruiting the Sir2-Sir4 complex (Kueng et al., 2013). Once there, Sir2 can deacetylate the acetylated histones, and is likely to trigger a conformational change in either a SIR protein or the SIR complex in a way that could reinforce its association with chromatin. Sir3, which has affinity for unmodified histones, binds the new deacetylated histones and, through its interaction with Sir4, leads to the spreading of the complex along the chromosome (Kueng et al., 2013). In wild type conditions, the SIR complex spreads over 2 to 3 kb in a Sir3 dosage dependent manner (Renauld et al., 1993). This spreading is thought to favour the 3D organization of telomeres in 3-5 foci mainly localized at the nuclear periphery and enriched for Rap1 and SIR proteins (Gotta et al., 1996; Meister and Taddei, 2013). In line

with this hypothesis, when Sir3 is not limiting it can spread till 10-15 kb from the telomeric end -if not blocked by a boundary (Hecht et al., 1996; Radman-Livaja et al., 2011). This induces a stronger and more stable silencing and a drastic increase in telomere grouping (Ruault et al., 2011). Interestingly, telomere clustering can occur also in absence of silencing. Indeed, the overexpression of a non acetylatable form of Sir3 (sir3-A2Q), defective for silencing, leads to the formation of a “hypercluster” in the center of the nucleus independently of the other members of the complex Sir2 and Sir4 (Ruault et al., 2011). These data, together with *in vitro* evidences that Sir3-Sir3 interactions could promote trans-interactions between Sir3-bound regions (Georgel et al., 2001; McBryant et al., 2008), strongly argue that Sir3 is the main player in the process of telomere clustering.

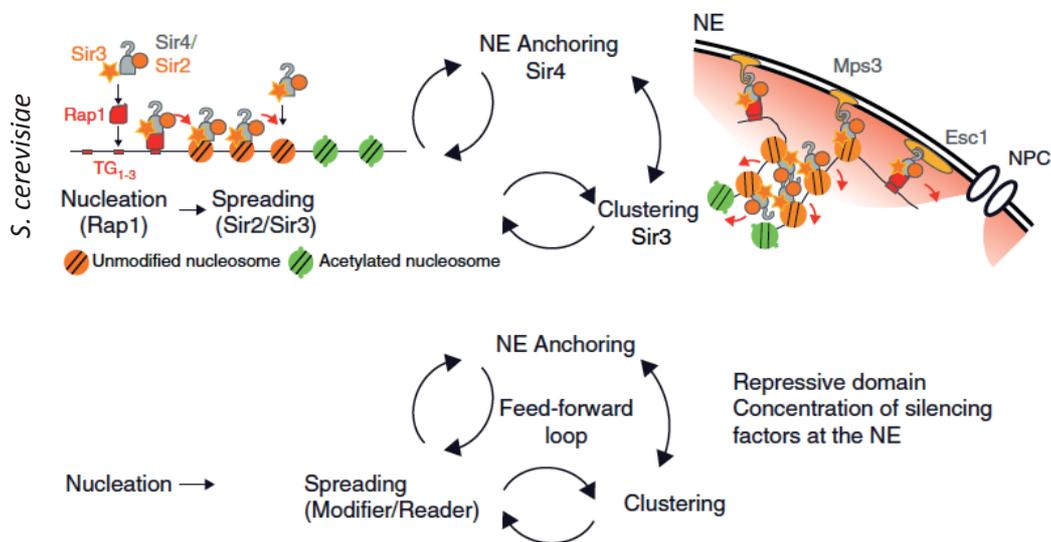


Figure 11: Feed-back loop model for concentrating silencing factors at the nuclear periphery.

Yeast telomeres are bound by Rap1, which achieves silent chromatin nucleation recruiting the members of the Sir complex Sir4 and Sir3. Sir4 form a heterodimer with the histone deacetylase Sir2. The Sir2 and Sir3 dependent spreading of the complex lead to the deacetylation of neighbour nucleosomes and silencing of proximally localized genes. Sir4 mediates telomere anchoring to the nuclear periphery by interacting with yKu and with the Mps3 and Esc1 proteins found at the nuclear membrane. Sir4 dependent anchoring favours both SIRs spreading and telomere clustering; at the same time, Sir3 mediated telomere clustering favours Sir2-dependent histone deacetylation (thus gene silencing) and telomere localization.

Bottom: model of positive feed-back loop to concentrate silencing factors close to the nuclear periphery. In different model organisms, anchoring to the nuclear periphery and clustering of silent chromatin increase the local concentration of heterochromatin factors spreading along the chromatin fiber. This in turn reinforces both anchoring and clustering. Entry into this feed-forward loop requires a nucleation event achieved by specific DNA proteins (*in red*). Adapted from (Meister and Taddei, 2013)

As telomere clustering regulates silencing at the subtelomeric regions, which in yeast harbour genes linked to adaptive responses, it is tempting to speculate that telomere organization could be affected by changes in the external environment. In support of this hypothesis, it has been recently proposed that telomere clustering and homeostasis is influenced by sphingolipid metabolism, as abnormalities in this process cause downregulation of expression levels of genes involved in telomere organization (Ikeda et al., 2015).

Functional role of telomere clustering

Telomere clustering is not only found in budding yeast (Palladino et al., 1993) but also in other microorganisms, such as fission yeast (Funabiki et al., 1993), *Trypanosoma brucei* (Weiden et al., 1991) and *Plasmodium falciparum* (Freitas-Junior et al., 2000). Actually, in all these organisms subtelomeric regions host specific genes crucial for the organism's virulence and/or survival (Edward J. Louis, 2014;).

P. falciparum constitutes an interesting example illustrating the key role of nuclear organization driven by telomere clustering for the organism survival. The malaria parasite is able to evade the host immune system attack by constantly changing the composition of the antigenic proteins expressed at the surface of the erythrocyte that they infect. These proteins are encoded by the *var* genes, which are mainly localized at subtelomeric regions. As mentioned before, telomeres of *P. falciparum* associate in clusters, which are localized near the nuclear periphery in asexual blood-stage parasites or in bouquet-like configuration near one pole of the elongated nuclei in sexual parasite forms. These subcompartments create alignment of *var* genes in heterologous chromosomes; this alignment is thought to facilitate gene conversion thus promoting the diversity of antigenic and adhesive phenotypes (Freitas-Junior et al., 2000).

In budding yeast, Sir3 has been shown to bind nucleosomal arrays in a stable and stoichiometric complex together with Sir2 and Sir4 (Martino et al., 2009). Knowing that Sir proteins are limiting for gene silencing, one of the most obvious effect of telomere clustering is the concentration of silencing factors that creates an environment hostile for RNA polIII dependent gene transcription (Andrulis et al., 1998; Maillet et al., 1996).

Moreover, it has been proved that the presence of these subcompartments specialized in silencing functions prevents the promiscuous binding of SIRs elsewhere in the genome (Marcand et al., 1996). Indeed, by eliminating telomere anchoring without deleting SIR factors, it has been shown that SIRs dispersion induces global changes in gene expression, with promiscuously repressed transcription at non-telomeric genes (Maillet et al., 2001; Taddei et al., 2009). Finally, perinuclear tethering of telomeres have been shown to contribute to genome stability as it favours a proper telomerase control and suppresses recombination among telomere repeats (Ferreira et al., 2011; Schober et al., 2009).

To summarize, budding yeast telomeres, whose homeostasis is fundamental for the stability of the whole genome, are clustered together in 3-5 foci localized close to the nuclear envelope. This subnuclear organization appears important for genome function, as it allows the concentration of silencing proteins (SIRs) at subtelomeric regions, hence promoting telomere grouping and localized gene silencing (TPE).

2. Impact of the external environment on nuclear organization

2.1 Generalities

Although the causal relationship between genome architecture and function is not clear yet, the fact that the nuclear organization reflects genome function is widely accepted (Fraser and Bickmore, 2007; Sexton and Cavalli, 2015; Shchuka et al., 2015; Taddei and Gasser, 2012; Taddei et al., 2004). On the other hand, cell functions can change upon time; if properly stimulated, cells undergo differentiation and acquire new characteristics (Figure 12).

The cell differentiation process, which is based on a defined gene expression program, appears strictly linked to the external environment in which the cell is placed (Das and Zouani, 2014) and leads to a global reorganization of nuclear architecture (Dixon et al., 2015; Giadrossi et al., 2007; Solovei et al., 2013).

Moreover, not only physiological changes but also different kinds of stress have been shown to strongly affect human's behaviour. Both clinical researches and works from animal models provide evidences that stressful experiences, either during the perinatal period or adulthood, do affect DNA methylation (Blaze and Roth, 2015). A highly discussed yet controversial concept is whether the effects of strong stresses, such as the holocaust drama, can be epigenetically inherited (Kellermann, 2013). However, to our knowledge, whether these physiological changes do affect chromatin architecture has not been studied yet.

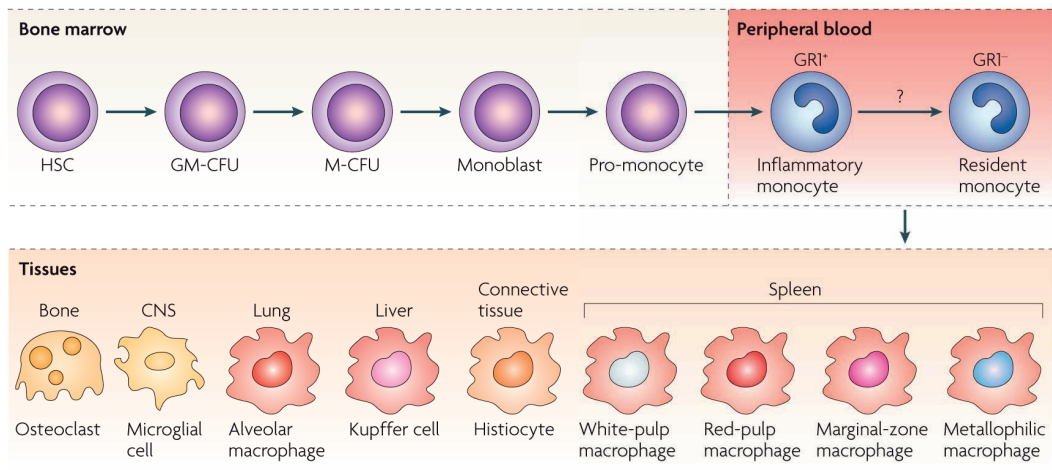


Figure 12: The environment impacts on cell morphology and function: the HSC differentiation into macrophage example.

Haematopoietic stem cells localized within the bone marrow are subjected to stimulating factors and will become monocytes that enter the bloodstream. Next, they will migrate to different tissues and replenish tissue-specific macrophages, each of them showing specific morphologies reflecting cell function. Adapted from (Mosser and Edwards, 2008).

To summarize, it appears clear that the external environment plays a key role in defining both cell and organism identity and can strongly influence genome function.

In this second part of the introduction, I will first report recent evidences that the 3D organization of genomes changes during metazoan development; then I will discuss the impact of the amount/limitation of certain nutrients for proper chromatin function; finally I will introduce the budding yeast response to unfavourable external environment, focusing on yeast cell survival during a specific stage of their life defined as quiescence.

2.2 Spatiotemporal reorganization of metazoan 3D nuclear architecture

As mentioned before, metazoan genomes are subjected to drastic changes in gene expression upon development, differentiation, senescence and diseases and these events go along with a reshaping of the nuclear architecture. As expected, one of the key players

influencing genome organization is the nuclear envelope, whose interaction with chromatin has been shown to temporally change thus affecting nuclear 3D architecture (Joffe et al., 2010; Mattout et al., 2015; Peric-Hupkes et al., 2010; Solovei et al., 2013).

In this paragraph I will briefly describe few examples of drastic spatiotemporal nuclear architectural changes occurring in metazoan during life-time.

2.2.1. Chromatin architecture dynamics during differentiation and development

I already mentioned that multicellular organisms are composed of different typologies of cells, each one with specific morphology and function. All these cells, although sharing the same DNA, accomplish distinct patterns of gene expression. This is due to the differentiation process, during which the spatial distribution of chromatin domains drastically changes. Several research groups are now trying to solve whether nuclear organization is a cause or a result of differentiation.

In general, pluripotent genomes are less rigidly organized than differentiated states (Fisher and Fisher, 2011; Joffe et al., 2010; Mattout et al., 2015). Already several years ago, electron microscopy studies revealed that in concomitance with cell differentiation heterochromatic domains accumulated at the nuclear periphery (Figure 13) (Fawcett, 1966).

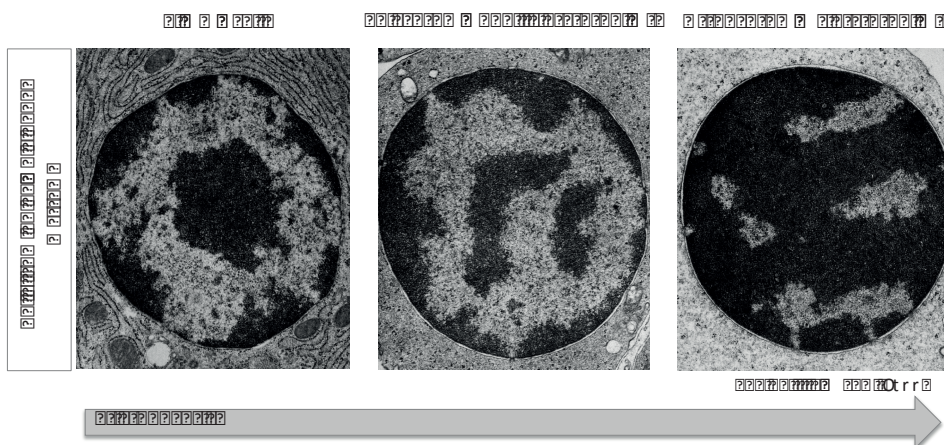


Figure 13: electron microscope images of guinea pig bone marrow cells upon differentiation.

Heterochromatin is visualized as dark stain. Adapted from (Fawcett, 1966).

Successively, an increasing number of studies demonstrated that the differentiation process implies genome-wide changes both in transcription (Efroni et al 2008) and in global chromatin architecture (Meshorer et al 2006), with genome wide dynamics of replication timing (Hiratani et al 2010), epigenetic modifications (Mattout et al 2011) and constitutive heterochromatin reorganization (Fussner et al 2011). Similarly, the inactivated X chromosome in mammalian female somatic cells becomes more compact as cells differentiate (Chow and Heard 2009).

Interestingly, during cellular differentiation and development heterochromatin is kept tethered to the nuclear envelope through two distinct mechanisms, which are sequentially coordinated (Figure 14) (Solovei et al., 2013). The first mechanism depends on the lamin B receptor (LBR), which is expressed until the lamin A/C appears and replaces it. Concordantly, rod cells of nocturnal animals, which exhibit an inverted nuclear organization (Solovei et al 2009), showed a cease of LBR expression after postembryonic day 14 (P14) without initiation of LamA/C expression (Figure 14). In agreement with that, the differentiation-dependent downregulation of LBR in mouse olfactory neurons correlates with the formation of particular heterochromatic foci containing exclusively olfactory receptor (*OR*) genes from different chromosomes (Clowney et al., 2012).

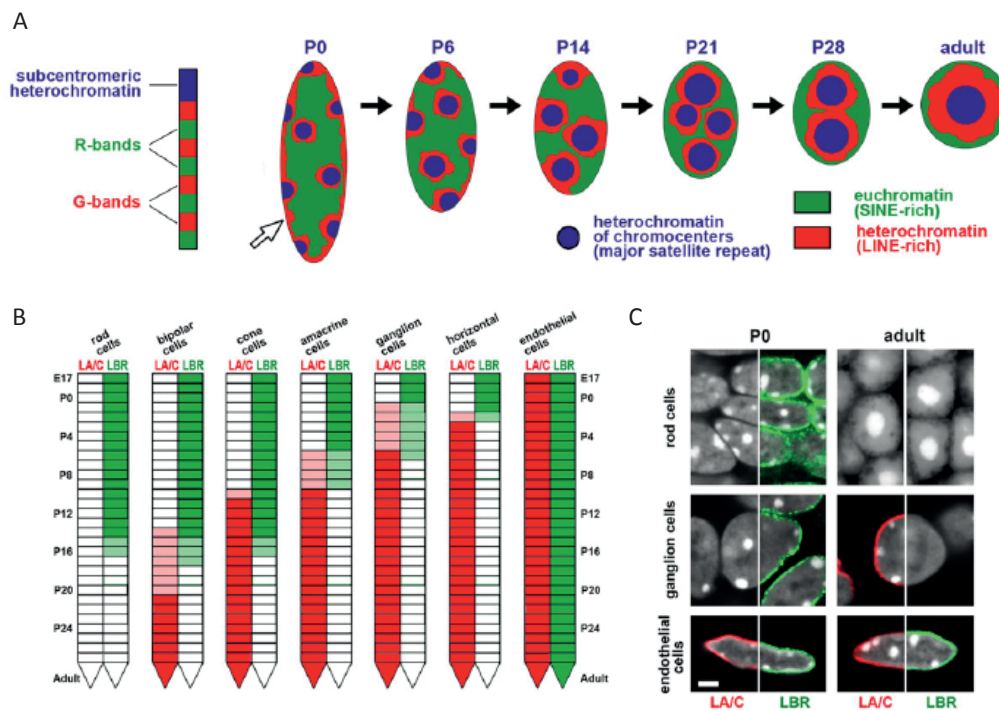


Figure 14: Chromatin architecture in cells from the mouse retina during differentiation.

A: The nuclear architecture of rod cells drastically changes during differentiation, passing from a conventional nuclear architecture, with the majority of chromocenters at the nuclear periphery together with a layer of heterochromatin, to an inverted chromatin organization, with euchromatin close to the nuclear envelope and heterochromatin in the interior part. B and C: temporal coordination in retinal cell types. Lamin A/C expression is shown in red and LBR expression in green. Cells expressing at least one of the lamins show the conventional nuclear architecture, while adult rod cells, which do not express LA/C nor LBR, present internal heterochromatin (DAPI staining). Adapted from (Solovei et al., 2013)

Another interesting case in which both cellular and nuclear architecture undergo extensive reorganization is constituted by the differentiation of progenitor spermatogenic cells –spermatogonia- into mature spermatozoa. Before being able to start their adventurous journey outside of their organism in order to fertilize the maternal egg, the haploid spermatids undergo striking chromatin reorganization and compaction, with stage-specific incorporation of specialized histone variants combined with histone post-translational modifications (Govin and Khochbin, 2013; Rathke et al., 2014). The specific chromatin packaging occurring within these nuclei should impact on sperm functions.

Finally, a particular global nuclear reorganization occurs in mouse during the passage between embryonic stem cells (ESC) to neural precursor cells (NPC) and post-mitotic neurons (PMN). In this case, pre-existing chromocenters found in ESC become dispersed in NPC to eventually become integrated into large heterochromatic foci in PMN (Aoto et al., 2006).

High-throughput studies have brought other information regarding genome architecture during differentiation (Gorkin et al., 2014; Hawkins et al., 2010; Peric-Hupkes et al., 2010; Phillips-Cremins et al., 2013; Xie et al., 2013). A recent paper presented genome-wide chromatin interaction maps in H1 human ES cells and in four H1-derived lineages (Dixon et al., 2015). Dynamic organization of chromatin during ES cells differentiation is observed at multiple hierarchical scales (Dixon et al., 2015).

To summarize, the nuclear architecture of each single cell is subjected to a programmed reorganization during the developmental process. These changes

can be more or less prominent depending on the cell type. In general, cell specialization correlates with increased heterochromatic regions.

2.3 Can the environment directly affect the chromatin structure?

Organisms must be able to rapidly react in response to changes in their environment. Recent works suggest that the regulation of gene expression in tune with the metabolic state is influenced by epigenetic marks that are sensitive to nutrients.

As I have previously discussed, the chromatin structure, which allows DNA hierarchical packaging, is highly dynamic and regulates the access of several factors to the genetic material in order to control DNA replication, repair and transcription. The level of chromatin accessibility is dependent on histone reversible covalent modifications, such as acetylation, methylation, phosphorylation, ubiquitylation, SUMOylation and poly-ADP – ribosylation, which strongly influence chromatin architecture. Interestingly, many of the enzymes performing these histone modifications employ essential metabolites for their functions. In particular, adenosine triphosphate (ATP) (Hardie, 2015), nicotinamide adenine dinucleotide (NAD⁺) (Canto and Auwerx, 2011; Kato and Lin, 2014), acetyl-Coenzyme A (acetyl-CoA) (Galdieri et al., 2014; Shi and Tu, 2015) and S-adenosylmethionine (SAM) (Nishikawa et al., 2015; Sadhu et al., 2013) and others are thought to be key metabolites linking chromatin and metabolism (Gut and Verdin, 2013). Emerging evidences indicate that fluctuating levels of these metabolites, which have been viewed as “gatekeepers of chromatin” (Kaochar and Tu, 2012), directly and rapidly influence gene activity (Gut and Verdin, 2013; Huang et al., 2015; Keating and El-Osta, 2015).

Below I will briefly discuss the impact of two metabolites particularly important for silent chromatin regulation through histone (de)acetylation, namely acetyl-CoA, which is used by histone acetyltransferases as acetyl donor, and NAD⁺, the cofactor of the class III histone deacetylases (HDAC) also known as sirtuins (Figure 15).

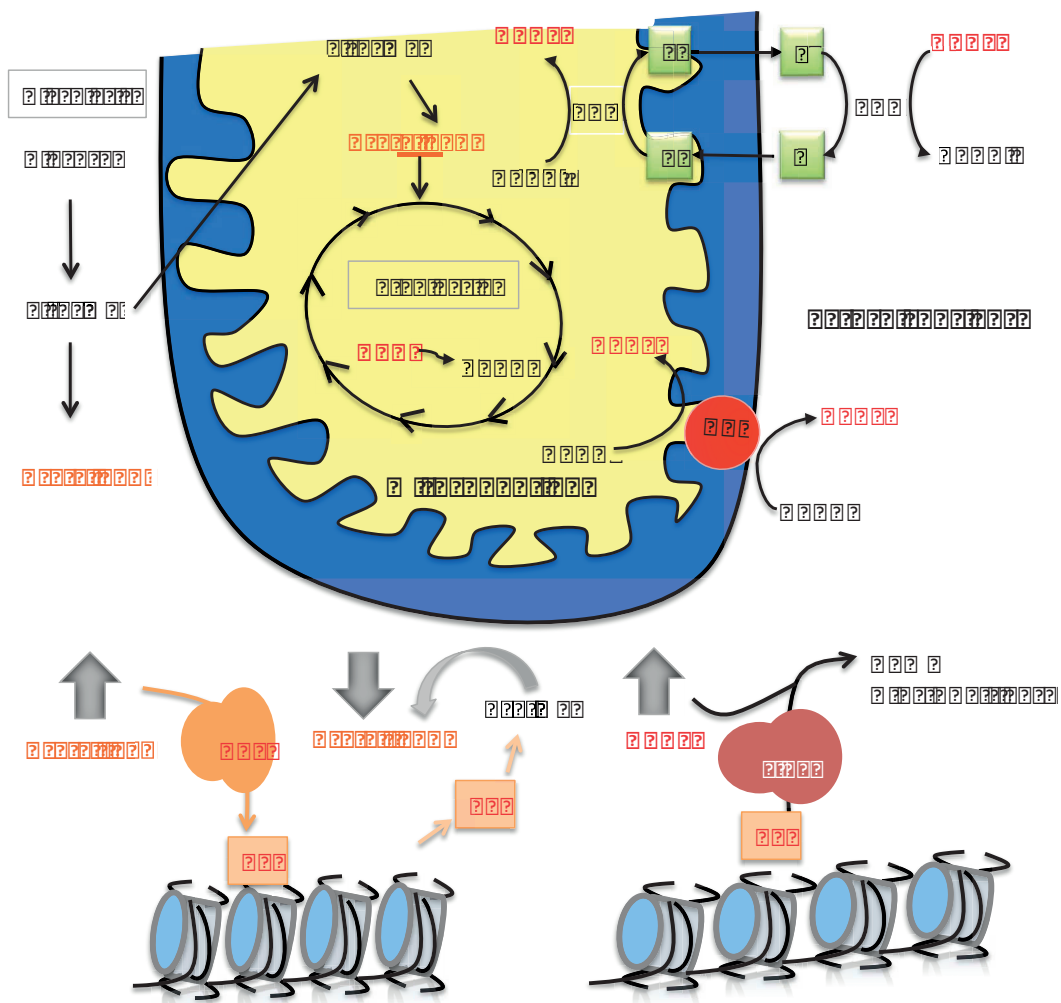


Figure 15: Metabolism links mitochondria and histone acetylation.

During fermentation, which occurs in the cytosol, each molecule of glucose eventually leads to the formation of two molecules of pyruvate. Pyruvate enters the mitochondria, where it is converted in Acetyl-CoA and successively fed into the Krebs Cycle. During each Krebs Cycle, NAD^+ is reduced in NADH. Mitochondrial NADH dehydrogenases (ND) re-oxidise NADH both from cytosolic and mitochondrial pools, thus leading to increase NAD^+ concentration. The ethanol-acetaldehyde shuttle system balances the NAD^+/NADH ratio between the cytosolic and mitochondrial pool, producing acetaldehyde (A) when NAD^+ levels are high within the mitochondria. Acetaldehyde diffuse to the cytosol and is reduced in ethanol (E) via alcohol dehydrogenase (ADH), resulting in an increase in cytosolic NAD^+ (Lin and Guarente, 2003). Increased NAD^+ levels enhance the enzymatic activity of sirtuins, thus inducing deacetylation of histones with the production of NAM and O-acetyl-ADP-ribose (O-AADPR). Glucose fermentation also leads to the formation of nucleocytoplasmic acetyl CoA, which can be used by histone acetylase enzymes (HAT) to acetylate histone tails. Acetylated histones can also store acetate in order to release it when needed for the production of acetyl-CoA (Galdieri et al., 2014).

2.3.1 NAD⁺/NADH ratio and the regulation of sirtuins

As I previously mentioned, HDACs are enzymes that deacetylate histone tails, thus promoting an increased condensation of the chromatin structure that correlates with repressed transcription. HDACs can be divided in two groups, based on their catalytic mechanism. HDACs belonging to the first group, composed of class I, II and IV, use activated water as the nucleophile to perform their enzymatic activity; on the other hand, class III HDACs, also known as sirtuins, needs nicotinamide adenine dinucleotide (NAD⁺) as a cofactor (Yang and Seto, 2008). Given that NAD⁺ is a key electron carrier in the oxidation of hydrocarbon fuels, sirtuins are evident candidates linking external environment and metabolism with chromatin regulation.

NAD⁺/NADH functions both as substrate and signalling molecule in key cellular processes, and aberrations on its metabolism have been linked to pathologies such as cancer, vitamin deficiency diseases (pellagra) and neurodegenerative diseases (Canto et al., 2015; Kato and Lin, 2014). NAD⁺ levels can change during physiological processes, for example declining NAD⁺ levels are a hallmark of senescence, while NAD⁺ increases in response to exercise or caloric restriction in mammals (Canto et al., 2015). In order to maintain a constant replenishment of NAD⁺ essential for cellular fitness, cells and organisms have developed complex interconnecting biosynthetic and signalling pathways that slightly change between species and are yet not completely known.

In budding yeast, NAD⁺ can be generated both via the tryptophan dependent *de novo* synthesis and via nicotinic acid (NA) / nicotinamide (Nam) / nicotinic riboside (NR) salvage pathways (Figure 16). During exponential growth on standard rich (YPD) media, which are enriched in niacin, yeast cells produce NAD⁺ predominantly via the NA/Nam salvage pathway. Moreover, yeast cells constantly release NR and retrieve it back, and this traffic between intracellular and extracellular compartments has been proposed to facilitate yeast cells response to metabolic stresses (Lu and Lin, 2010). Particular interest has grown around NR salvaging pathways for the maintenance of NAD⁺ homeostasis and cellular fitness (Belenky et al., 2007; Kato and Lin, 2014), possibly through Sir2 activity (Lu et al., 2009b).

NAD⁺ and its derivatives have been shown to be important for sirtuin regulation (Kato and Lin, 2014), and defects in NAD⁺ levels abolish Sir2 mediated silencing (Smith et al., 2000). Regulation of the clearance of Nam (Figure 16), a Sir2 inhibitor generated during

sirtuin-mediated deacetylation, has also effect on events downstream of Sir2, namely gene silencing and replicative lifespan (Gallo et al., 2004).

NAD⁺ is not only a co-substrate in sirtuin-mediated deacetylation; together with its reduced form NADH, it is an essential redox carrier, connecting metabolism of biomolecules to ATP synthesis (Lu and Lin, 2010). During both respiration and caloric restriction, the ratio NAD⁺/NADH within the mitochondria increases (Lin et al., 2004; Lin and Guarente, 2003). As NADH can function as a competitive inhibitor of Sir2 activity *in vitro* (Lin et al., 2004), it has been suggested that these two conditions enhance Sir2 activity. However, this model remains controversial, as NADH levels *in vivo* are probably too low to inhibit Sir2 activity. Nevertheless, it is possible that the intracellular compartmentalization of NAD⁺ could create high local NAD⁺/NADH ratio thereby promoting Sir2 activity *in vivo* (Kato and Lin, 2014). Indeed, cells contain two pools of NAD⁺, one cytosolic/nuclear and the other mitochondrial, which can modulate the activity of compartment-specific metabolic pathways such as glycolysis and TCA cycle or oxidative phosphorylation. As the mitochondrial inner membrane is impermeable to NAD⁺ and NADH, NADH shuttle system balances the NAD⁺/NADH ratio between the two subcompartments (Lu and Lin, 2010).

While speculating about the possible role of metabolic changes and Sir2 activity, it is important to underline that the most abundant expressed sirtuin in yeast is Hst2, which accounts for most of the intracellular NAD⁺-dependent deacetylase activity *in vitro* (Smith et al., 2000). Hst2, contrary to Sir2, is mainly localized in the cytoplasm (Perrod et al., 2001); still it can regulate subtelomeric *FLO* gene expression in a Sir3-dependent manner (Halme et al., 2004) and rDNA silencing (Perrod et al., 2001) and recombination (Lu and Lin, 2010; Perrod et al., 2001; Yang and Seto, 2008).

Finally, the NAD⁺ metabolism has also been linked to the phosphate-responding signalling *PHO* pathway, which monitors and responds to changes in the phosphate availability and interacts with other nutrient/stress sensing pathways. Indeed, activation of the *PHO* pathway seems to play important roles in the maintenance of the NAD⁺ pool (Lu and Lin, 2011).

It seems thus clear that, as the NAD⁺ metabolic pathway is dynamic and complex, it is quite difficult to determine the levels of the inter-convertible pyrimidine nucleotides.

However, it seems reasonable that pyridine nucleotides and their metabolites could be critical for the regulation of several mechanisms and could link external environment and chromatin organization.

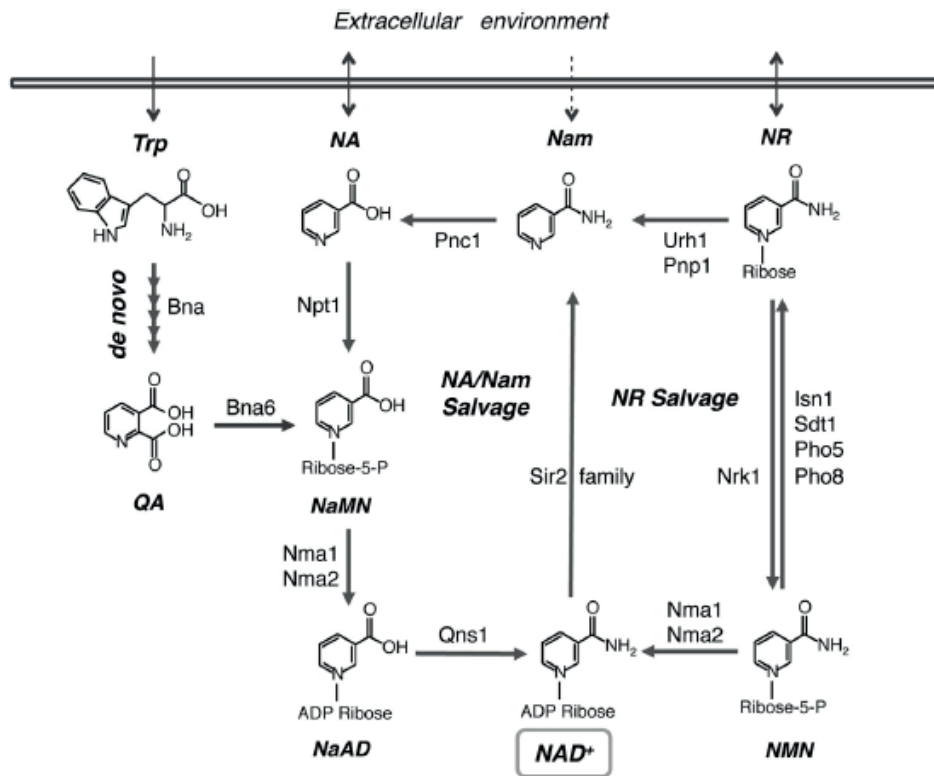


Figure 16: A: simplified scheme of NAD⁺ synthesis pathway in yeast.

S. cerevisiae can synthesize NAD⁺ both *de novo*, from tryptophan (Trp) and by salvaging pathways, in particular from nicotinic acid (NA), nicotinamide (Nam), quinolinic acid (QA) and nicotinamide riboside (NR). Cell can also salvage nicotinic acid riboside (NaR) by converting it to NA or NaMN (nicotinic acid mononucleotide), but for simplicity this pathway is not shown in this figure. NaAD, deamido NAD⁺. NMN, nicotinamide mononucleotide. NAD⁺ and its intermediates are italicized. Abbreviations of protein names catalysing each step are in bold. Adapted from (Kato and Lin, 2014).

2.3.2 Acetyl-CoA and the regulation of histone (de)acetylation

For several years, studies performed in carbon-rich media may have mask the contributions of acetyl-CoA in cellular regulation. However, most organisms and particular tissue microenvironments *in vivo* experience challenges in the nutrient

environment – i.e. carbon starvation or hypoxia- with the consequent limitation of acetyl-CoA availability.

Acetyl-CoA is produced by glycolysis as well as by other catabolic pathways and can be used as a substrate for the citric acid cycle (TCA), as a precursor in synthesis of fatty acid and steroid and in other anabolic pathways. Moreover this metabolite serves as a substrate for lysine acetyltransferases (KATs), including HATs (Figure 17). Thus acetyl-CoA not only shows a central position in metabolism but also has key roles in signalling, chromatin structure and gene transcription (Guarente, 2011). Fluctuations in the concentration of this metabolite depend on the external environment. Within the cell, acetyl-CoA is found at two different places: within mitochondria and in the nucleocytosolic compartment. In general, high levels of acetyl-CoA within the nucleocytosolic compartment are indicative of a “fed” state, and the cell normally proceeds to store the excess of carbohydrates as fat. Moreover, acetyl-CoA can be used for histone acetylation and activation of gene expression. On the other hand, under fasted or survival states, fatty acids are oxidized and acetyl-CoA is channelled into the mitochondria for synthesis of ATP and ketone bodies (Galdieri et al., 2014; Shi and Tu, 2015). Given that histones are so abundant, it has been proposed that they could “store” a substantial amount of acetate in order to liberate it when needed by deacetylation. Supporting this idea, there are strong evidences that acetate can be captured as a source of acetyl-CoA, which may promote growth and survival of certain tumours (Comerford et al., 2014; Huang et al., 2015). Moreover, acetate present on histones has also been proposed to be an intracellular pH regulator (McBrian et al., 2013).

During the last decade several works, most of which performed on budding yeast (Cai et al., 2011; Shi and Tu, 2014; Takahashi et al., 2006), have begun to provide evidences that many protein acetylations are modulated by acetyl-CoA availability (Galdieri et al., 2014). In stationary phase, both gene expression and histone acetylation are dramatically decreased (Gasch et al., 2000; McKnight et al., 2015; Mews et al., 2014). Interestingly, ChIP-seq analysis on yeast stationary phase cells upon exit from quiescence revealed that the initial burst of growth gene reactivation involves dramatic increases of histone acetylation, while histone methylation is static during quiescence exit (Mews et al., 2014). Indeed, intracellular acetyl-CoA levels increase substantially upon entry into growth and consequently induce the Gcn5p/SAGA-catalyzed acetylation of histones at genes important for growth (Cai et al., 2011).

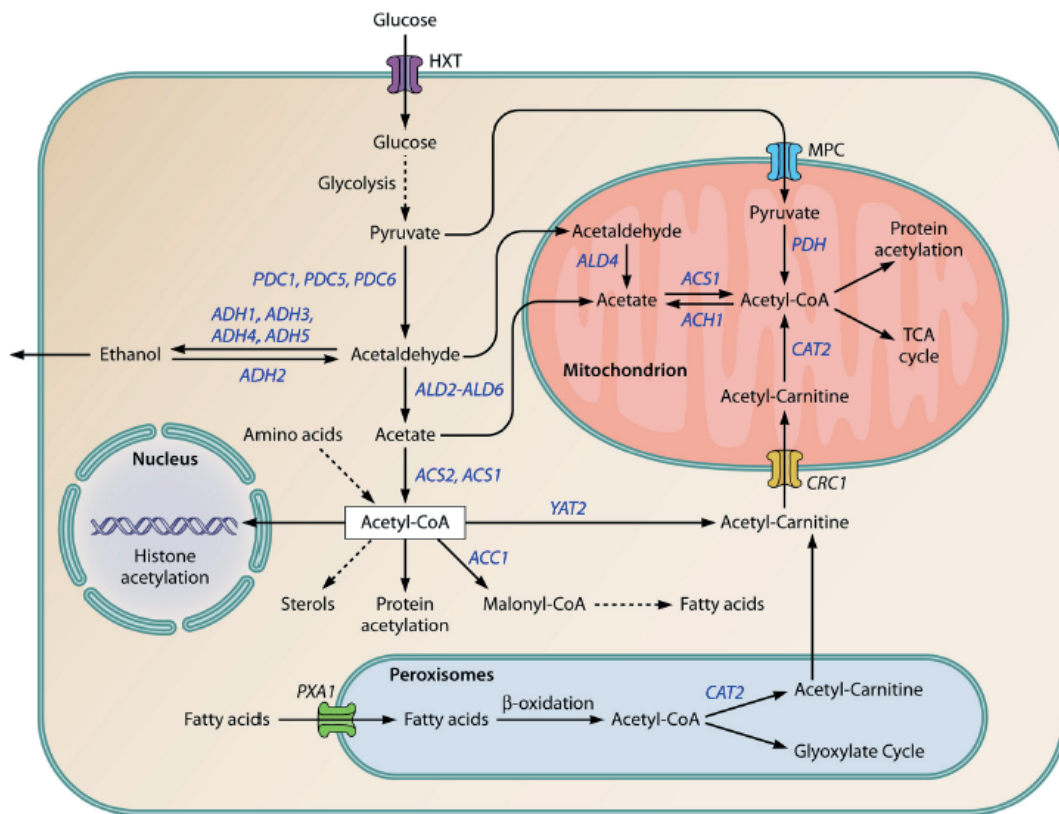


Figure 17: Acetyl CoA in budding yeast.

Multistep pathways of glycolysis and fatty acid synthesis are indicated by dashed lines. Enzymes are shown in blue. Adapted from (Galdieri et al., 2014)

In agreement with these studies, recent work published by Moussaieff and colleagues showed that glycolytic production of acetyl-CoA drives histone acetylation in pluripotent stem cell. Moreover, the metabolic regulation of this metabolite appears to control the early differentiation of human embryonic stem cells in culture, suggesting that a glycolytic switch controlling histone acetylation can release cells from pluripotency (Moussaieff et al., 2015).

Although acetylation constitutes the most frequent and studied acylation histone mark, recent works demonstrated that other acyl moieties, such as crotonylation (Tan et al., 2011), can be added to histone tail (Rousseaux and Khochbin, 2015). Like acetylation, also crotonylation positively correlates with gene expression (Rousseaux and Khochbin, 2015; Sabari et al., 2015). However, the latter appear more resistant than acetylation to gene repressive mechanisms, a characteristic that could be particularly important for expression of genes surrounded by a repressive environment (Rousseaux and Khochbin,

2015). While acetyl-CoA is mainly produced by glycolysis, other acyl-CoA derives from fatty acid oxidation (Grevengoed et al., 2014) and from still unknown metabolic processes. As a consequence, a metabolic shift increasing the ratio acyl-CoA/acetyl-CoA would favour histone “non-acetyl” acylation.

To summarize, several evidences underline that life-style and diet could affect different cellular and nuclear processes. Among all, metabolites used by nuclear enzymes to perform histone PTM, such as NAD⁺ and Acetyl-CoA for histone (de)acetylation, appear to have key roles for nuclear functions. It is thus tempting to speculate that a “nutritional control of epigenetic processes” exists in yeast as well as in human cells (Sadhu et al., 2013).

2.4 The yeast response to the external environment

While in metazoans the regulation of metabolic activity, cell growth or developmental progression at the cellular level is mainly dictated by growth factors, hormones and modulators, budding yeast responds primarily to nutrients. Nutrients indeed not only supply energy and induce cell growth, but also function as signals to dictate the best metabolic, transcriptional and developmental programs under the particular environment of the cell (Broach, 2012). For instance, in rich media yeast cells undergo rapid mitotic growth, but under certain limiting nutrient conditions yeast develops a filamentous growth that favours food foraging while other kinds of starvation reversibly stop cell growth or can induce sporulation (Broach, 2012).

In this last part of the introduction chapter, I will describe how different environments impact on a population of *S. cerevisiae*, focusing on factors that could influence cell ability to survive under the absence of nutrients.

2.4.1 Gene expression changes in response to different nutrients

Yeast cells finely tune their gene expression and behaviour adapting to different environments (Broach, 2012; Gasch et al., 2000; Smets et al., 2010). Here below I will report some examples of how the availability of different nutrients impact on yeast behaviour.

The “make-accumulate-consume (ethanol)” strategy

One of the most prominent features of *S. cerevisiae* is its ability to rapidly convert sugars to ethanol and carbon dioxide in both anaerobic and aerobic conditions. When oxygen is present, respiration is possible but *S. cerevisiae* prefers to use its favourite carbon source - glucose- through alcoholic fermentation (glycolysis) until the sugar reaches low levels – Crabtree effect (De Deken, 1966). One of the main problems of glycolysis is that it leads to low levels of energy, in the form of ATP and NADH/NAD⁺ redox. However, this life strategy represents in the wild a strong tool to outcompete other microorganisms. Indeed, yeast can consume very fast more sugar than other species and convert it into ethanol to inhibit the growth of other organisms -especially bacteria. Once they have established competitive dominance in their micro-environment, also named “niche”, yeast cells can efficiently catabolize non fermentable carbon source in presence of oxygen by performing ethanol respiration (Dashko et al., 2014). For this reason, the Crabtree effect is also known as the “make-accumulate-consume” ethanol strategy (Piskur et al., 2006; Rozpedowska et al., 2011; Thomson et al., 2005).

However, it is possible to induce respiratory utilization of glucose by keeping glucose levels very low using continuous culture operating below a “critical” glucose level (Postma et al., 1989).

Yeast metabolic cycles in chemostat

To keep yeast cells under continuous mode, low glucose levels have to be added at a constant dilution rate to cells that have previously grown to high OD and experienced few hours of starvation (Postma et al., 1989).

More than 60 years ago researchers demonstrated that during continuous cultures, yeast cells spontaneously began yeast metabolic cycles (YMC), in the form of glycolytic and

respiratory oscillations (Chance et al., 1964). Successively, other studies revealed that over half of the yeast genome is expressed periodically during these cycles, underlying a temporal compartmentalization of cellular processes (Tu et al., 2005; Tu and McKnight, 2007). Three “superclusters” of gene expression were found: Ox (oxidative), R/B (reductive/building) and R/C (reductive/charging), each of which contains distinct subclasses of genes periodically expressed. Based on these results, respiration, mitochondria biogenesis ribosome biogenesis, DNA replication, cell division, fatty acid oxidation, glycolysis and vacuole-mediated catabolism are all predicted to be precisely compartmentalized in time.

This particular yeast behaviour should allow a fine coordination of anabolic and catabolic processes thus minimizing the occurrence of futile reactions.

Growth curve in glucose based liquid medium (batch culture)

On the other hand, when batch cultures are kept growing until cells stop dividing (stationary phase), other metabolic changes, corresponding to different gene expression programs, occur. Yeast cells harvested on YPD medium first pass through a “lag phase” during which they “adapt” to the new environment (Ginovart et al., 2011) and then divide in an exponential way predominantly metabolizing glucose and releasing ethanol (see below). When glucose levels become limiting, yeast cell enter the “diauxic shift” (DS) (Figure 18), reprogramming their global gene expression and protein translation to switch metabolism from glycolysis to aerobic respiration of ethanol (Fuge et al., 1994; Galdieri et al., 2014; Kalhor et al., 2012). The cellular responses initiated at the diauxic shift transition include the transcriptional induction of genes important for respiration, fatty acid metabolism, glyoxylate cycle reactions and likely of genes encoding antioxidant defences that allow scavenging and/or destruction of reactive oxygen species (ROS) (De Virgilio, 2012). Once the respiration phase starts, growth rate is decreased and yeasts exhibit thick cell walls and accumulate storage molecules, acquiring characteristics of resistance to different kinds of stress (Lillie and Pringle, 1980; Werner-Washburne et al., 1993). When no carbon source is available anymore, the culture reached the stationary phase and all yeast cells stop dividing (Gray et al., 2004). The stationary phase culture is a heterogeneous population composed of different kinds of cells (Allen et al., 2006), (Figure 18). Each of these subpopulations exhibits a specific gene and protein expression pattern (Aragon et al., 2008; Davidson et al., 2011; McKnight et al., 2015) (see next

paragraph). However, the majority of the cells found in a stationary phase culture undergo a drastic transcriptional shutoff (McKnight et al., 2015). Nevertheless, refeeding of the stationary phase culture results in extremely rapid and global changes in transcript abundance (more than half occurring within the first 5 minutes) (Martinez et al., 2004).

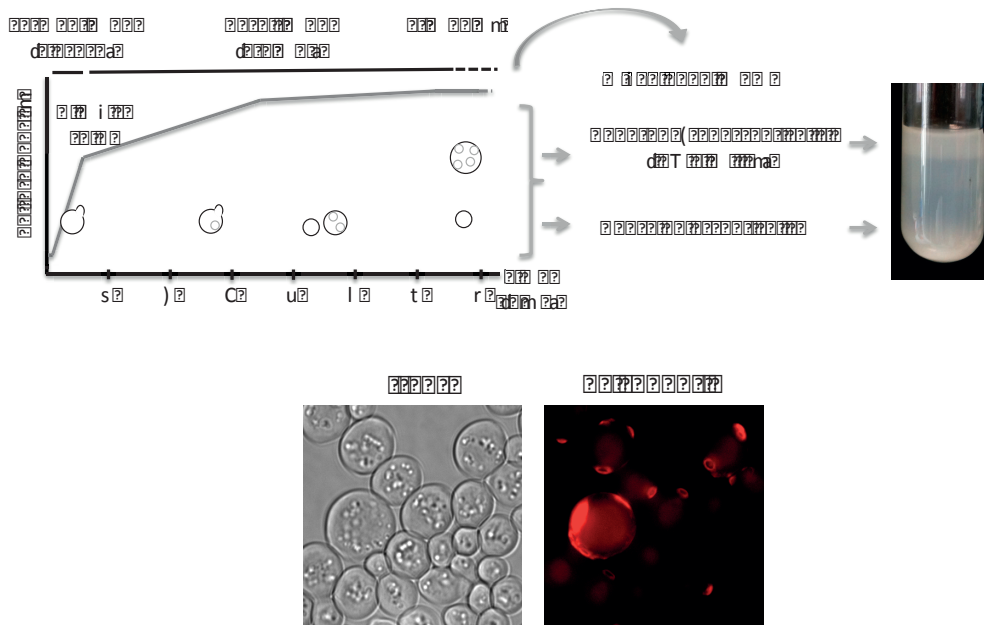


Figure 18: The stationary phase culture in budding yeast.

Top: Representative scheme of the growth curve of a liquid YPD culture upon carbon source exhaustion. When cells reach the stationary phase, they can be separated by density gradient in two subpopulations. The less dense population show low viability; on the contrary, the dense population is long-lived and defined by Allen and colleagues as “the quiescent fraction” (Allen et al., 2006). Bottom: Microscope images of a typical stationary phase population. On the transmitted light image (left) one can distinguish cells with different sizes and morphology. On the right, the same cells visualized with calcofluor staining to count the number of bud scars on each cell’s membrane (index of the number of division performed by each cell).

2.4.2 Concept of “differentiation” in yeast:

Despite the fact that budding yeast is a unicellular organism, yeast cells organize themselves into communities that, to some extent, behave as primitive multicellular organisms. These communities, which occurs both in liquid and in solid cultures, are composed of at least two groups of cells that become specialized as a result of changes in the external environment (Figure 19) (Allen et al., 2006; Palkova et al., 2014; Vachova et al., 2009a). These cells, which differ in longevity, stress resistance, cell metabolism,

respiration, ROS production and other phenotypes, are normally non-growing stationary-phase cells that differentiated in response to external stimuli.

In this paragraph I will summarize the works of few laboratories that contributed to our knowledge on yeast differentiation in solid and liquid communities.

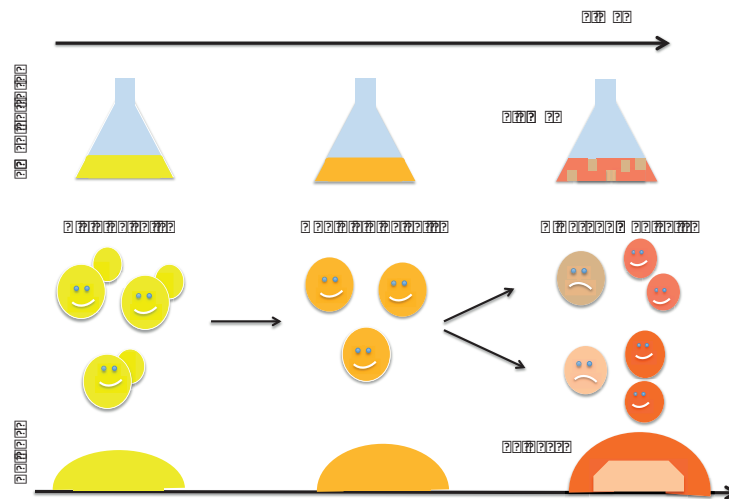


Figure 19: yeast haploid cells undergo differentiation upon time both in liquid cultures and within colonies.

Top: *S. cerevisiae* cells grown on rich YPD medium initially undergo exponential growth metabolizing glucose, then when the carbon sources become limiting drastically reduce their growing rate favouring the acquisition of resistance features and finally enter the stationary phase. At this last step, occurring around 7 days after the initial inoculation, senescent, necrotic, apoptotic (visualized in grey) and quiescent (rose-red) cells are found. Bottom: budding yeast cells grown on solid synthetic medium also undergo a similar process during time, with cells initially dividing and successively differentiate. After 15 days, two populations of cells are found: healthy and viable cells at the margin of the colony, and more sensitive and senescent cells in the middle. However, the characteristics of differentiated cells in liquid and solid cultures are not the same, probably because of the differences in medium compositions and in the external stimuli inducing the differentiation process. Reviewed in (Palkova et al., 2014).

Yeast differentiation within a colony

Yeast populations developing within colonies have been reported to change their behaviour several time over a period of 20-30 days or even longer by the Palkova laboratory (Palkova et al., 2014). After the first 2 days of colony development, during which all cells grow exponentially, the number of budding cells within the population drops to about 15%. The majority of the cells stop dividing and become “elders”

(Meunier and Choder, 1999). Colonies continue to slowly grow over the next 16-18 days; after that, this linear growth significantly decreases but does not completely cease for at least another week (Palkova et al., 2002).

Both *S. cerevisiae* micro-colonies (4 days old) (Vachova et al., 2013) and giant colonies (15 days old) (Vachova et al., 2009b) of BY4247 strain growing on complex glycerol medium have been reported to differentiate and to form two major layers of upper and lower cells in response to ammonia signalling. Elder cells induce the alkalization of the surrounding medium, which is accompanied by the production of volatile ammonia that functions as signal able to induce the other surrounding colonies to initiate their own ammonia production and transit to the alkali phase. This acid-to-alkali transition is accompanied by extensive metabolic reprogramming of the colony population, with the differentiation of a population of elders in the central part of the colonies during the acidic phase into two major elder subpopulations. In giant colonies, these subpopulations correspond to U cells, localized to the upper regions of alkali-phase colonies and characterized by increased stress resistance and longevity phenotype, and L cells, which are found in the interior and lower part of the colonies and are more sensitive to stress and to the aging process (Cap et al., 2012). Interestingly, L cells are thought to decrease their cell content over time to provide compounds important for the feeding of U cells. Thus, the two populations somehow seem to mutually interact, affecting each other over the course of long-term colony development (Palkova et al., 2014).

On the other hand, the spatiotemporal development of smooth colonies formed by *S. cerevisiae* laboratory haploid strains significantly differs from the development of structured biofilms colonies of *S. cerevisiae* natural diploid strains (Palkova et al., 2014), further indicating that yeast cells specifically respond to different kinds of environmental conditions.

Yeast differentiation in liquid cultures

Evidences of yeast cell differentiation during a liquid culture are mainly due to the work of the laboratory of Margaret Werner-Washburne, focused on stationary phase culture grown in YPD medium.

In a liquid culture, the sub-populations of yeast cells are mixed together. However, density gradient separation of SP cultures allows the isolation of two cell sub-

populations. The more dense and homogeneous one is composed mainly of daughter cells or mothers with few bud scars, while the other -less dense and heterogeneous- mainly consists of mother cells undergoing apoptosis, senescence and necrosis but includes also few cells blocked into quiescence (Allen et al., 2006). The dense population has been named the “quiescent fraction” (Q): cells found within this fraction are particularly resistant to different kinds of stress, are highly viable, show high genomic stability and high respiration rates. On the contrary, cells from the “non quiescent fraction” (NQ) rapidly lose the reproductive capacity, show higher genomic instability and are thought to provide nutrients and a regular source of genetic diversity to the rest of the culture (Allen et al., 2006; Aragon et al., 2008; Davidson et al., 2011). Interestingly, the dense population start to form around 20-24h after inoculation of the culture. At the state of the art, the molecular mechanisms leading to this form of differentiation are still not completely known. However, Davidson et al proposed a model where the decision to become Q or NQ occurs just before or around the diauxic shift. This is in agreement with the fact that G_1 arrest initiates before the diauxic shift (Miles et al., 2013). After this moment, this model predicts that NQ mother cells will give rise to NQ daughter cell, while Q cells will stop dividing or produce Q daughter cells. However, the majority of Q cells that divide will eventually become NQ (Davidson et al., 2011).

Sporulation as another way to differentiate

S. cerevisiae diploid cells dispose of an alternative possibility to cope with nutrient starvation: they can activate the meiotic division program and form resistant spores.

Interestingly, while in liquid cultures cells sporulate “randomly”, when harvested on sporulation acetate agar medium yeast diploid cells located at specific positions within the colony initiate the sporulation program. Indeed, it has been shown that the cells localized in the most internal part of a diploid colony (occupied by L cells in haploid colonies) do not sporulate, while the ones close to the agar and in the upper part of the colony do (Piccirillo et al., 2010). It seems thus that U cells in haploid colonies and sporulating cells in diploid colonies occupy the same position. Moreover, the boundary between external zones containing sporulating cells and more internal compartments where cells do not sporulate are quite sharp (Palkova et al., 2014; Piccirillo et al., 2010).

In summary, yeast survival in the wild may have taken advantage of the ability of yeast to cope with huge changes in nutrient availability, including fluctuations of carbon and nitrogen sources. Cell differentiation may have been an important adaptive mechanism to ensure the survival of some members of the clonal population, consistent with the existence of an “altruistic” aging program (Fabrizio et al., 2004).

2.4.3 The quiescent state

Like most living cells, budding yeast cells spend the majority of their lifetime in a quiescent, non-growing state (Broach, 2012; Fabrizio and Longo, 2003; Gray et al., 2004). Budding yeast haploid or diploid cells enter quiescence when they lack carbon, nitrogen, phosphate or sulphur sources. These forms of “natural” starvation lead to arrest of cell cycle progression prior to “start”, inducing the cell to enter the poorly defined G_0 state. Cells that entered the G_0 state because of the lack of one or more of the previously mentioned nutrients and that keep their ability to re-enter the cell cycle when the missing nutrient is restored are defined quiescent cells. It is important to note that the quiescent state can not be reached when the induced starvation is “not natural”, as in the case of auxotrophic cells deprived of the required amino acid: in this case, cells rapidly lose viability even if they arrest uniformly as unbudded cells (Broach, 2012).

However, the literature is quite controversial concerning the definition of quiescence. Indeed, quiescence has been also simply defined as a “reversible non-proliferative state”, thus independent of the G_0 state. In line with this definition, Laporte and colleagues reported that not only unbudded cells but also budded cells micromanipulated from a 7 days culture were able to re-enter the cell cycle and give rise to a colony after refeeding, yet with a lower percentage than the unbudded ones (Laporte et al., 2011). The same authors also claimed that quiescence exit can be triggered independently of re-entry into the proliferation cycle, showing that the sole addition of glucose was leading to the fast (5-15 minutes) mobilization of specific structures, namely actin bodies and PSGs (proteasome storage granules), found in these quiescent cells (Laporte et al., 2011). However, this last concept of exit from quiescence is in contradiction with the definition itself of the quiescent state, which is about the ability to proliferate again.

On the other hand, confusion in the literature on this field is also due to the tendency to define “quiescent” only certain cell populations which have gained some stress resistance

and longevity features and not others that indeed also retain the ability to give a progeny upon re-feeding. This other “abusive” use of the quiescent terminology became common after the work of Allen and colleagues about SP populations (Allen et al., 2006). After this paper, even whether the authors underlined that also the less dense fraction of the SP population contained a certain percentage of cells able to re-enter the cell cycle – although in a non-synchronous way-, cells isolated from the upper fraction of the density gradient of a SP culture are globally considered “non quiescent”.

These inconsistencies are likely due to the fact that researchers try to unify together different typologies of cells that indeed have in common only the need to cope with an unfavourable external environment but react through very different ways. Below I will describe different ways to induce a reversible cell cycle arrest, underlying that not all these conditions are necessarily associated with a good survival (Figure 20).

Different ways to induce quiescence lead to different quiescent cells.

Cell cycle arrest and entry into quiescence appear to be tightly regulated by programmed responses following lack of essential nutrients and are not just simple consequences of growth arrest. Yeast cells can sense signals from the environment, and the appropriate perception of nutrient limitation is critical for a cell to mount an appropriate quiescent program. Moreover, the role of signalling pathways in cell survival is much more critical: it does not only indicate the need to enter into quiescence, but it also controls the maintenance of the quiescent state until the missing nutrient is back. Nutrient signalling is thus fundamental for both entering and exiting quiescence (Broach, 2012; Gray et al., 2004).

By comparing transcriptional, metabolic and genetic analysis of quiescent cells induced by glucose, nitrogen or phosphate starvation, Klosinska and colleagues showed that all of them had in common a transcriptional program that also occurs during slow growth, while the metabolic changes and the genetic requirements for cell survival under each condition depend on the nutrient for which the cell was starved. The authors thus concluded that cells do not access a unique and discrete G_0 state but rather are programmed, thanks to the signalling pathway, to be prepared for a range of possible future sources of stress (Klosinska et al., 2011a).

Nitrogen starvation

A well known way to induce cells entering the G₀ state is to block the nutrient sensitive and central controller of growth Target of Rapamycin (TOR) pathway (Loewith and Hall, 2011). This quiescence induction can be accomplished either by rapamycin treatment or by maintaining cells in media with limiting nitrogen levels (De Virgilio, 2012).

Nitrogen starved quiescent cells are characterized by resistance to several kind of stresses, including homeostatic stress, oxidative stress and heat shock, and by expression of genes mediating vacuolar function and autophagy. These quiescent cells show around 40-50% viability after 1 week of starvation (Klosinska et al., 2011a)

Carbon starvation

Another way to block the cell cycle is to starve exponentially growing cells for their carbon source, which is glucose. Glucose starved cells exhibit characteristics of resistance to heat shock and oxidative stress but are quite sensitive to zymolyase (Klosinska et al., 2011a) and they show very low viability after 1 week of starvation (below 10%) (Li et al., 2013).

Carbon exhaustion (stationary phase)

On the other hand, quiescent cells found in stationary phase (7 days) cultures have not been abruptly starved for glucose but gradually exhausted the available carbon sources. Importantly, these cells passed through an important gene expression reprogramming, the diauxic shift, and grow slowly upon the respiration phase, during which they increased their resistance to stress. SP quiescent cells keep levels of viability higher than 80-90% over several weeks (Allen et al., 2006; Li et al., 2013). These “long-lived” quiescent cells are mainly daughter cells (Allen et al., 2006) expressing genes involved in mitochondrial function and respiration, and show resistance to heat shock, zymolyase treatment and oxidative stress. It is important to note that respiratory deficient *petite* cells, which reach the stationary phase 2-3 days after inoculation because of their incapacity to metabolize ethanol as a carbon source, are very different than wild type stationary phase cells. Accordingly, *petite* cells rapidly lose their viability upon starvation (Broach, 2012).

What is the hallmark of quiescent cells?

Given that G₀ cells are the result of different starvations, it seems unlikely that a unique characteristic could label them all. On the other hand, it is possible that different G₀ cells

able to survive for weeks or maybe months outside of the cell cycle – “long-lived” quiescent cells – share a common feature. However, hallmarks of long-lived quiescent cells are not yet identified to our knowledge.

In the last decades, several features of quiescence have been proposed, such as low levels of mRNA and proteins, high resistance to different stresses, increased levels of storage carbohydrates, thickened cell wall and higher respiration rate. However, these characteristics are not unique of the quiescent state (see above) and seem more due to adapting events than to quiescence itself (Broach, 2012).

Other proposed features of quiescence have been found in carbon-starved cells. They include both cytoplasmic changes, such as the formation of “bodies” where specific proteins (or components) are stored (Narayanaswamy et al., 2009; Sagot et al., 2006), and nuclear reorganization events, in particular the formation of a “microtubule bundle” (Laporte et al., 2013) that enters the nucleus and correlates with decreased centromere clustering (Laporte et al., 2013; Rutledge et al., 2015) and slightly increased telomere grouping and chromatin condensation (Rutledge et al., 2015). However, these characteristics have not been confirmed in other types of quiescent cells, and in particular in the long-lived fraction of SP cells. On the other hand, an old paper from 1978 also reported an increased chromatin compaction on G_0 cells from SP or nitrogen starvation (Pinon, 1978) and this compaction has been later associated with an increased binding of the linker histone Hho1 (Schafer et al., 2008).

It seems thus not possible, at least until now, to be certain that a cell *is* quiescent until this cell is not allowed to enter into the cell cycle and demonstrates that indeed *was* quiescent. Moreover, it is not clear *for how long* a cell has to survive without dividing in order to be considered “quiescent”. Finally, different external environments induce specific gene expression programs and consequent acquisition of specific features.

While all kind of G_0 cells are of interest to better understand mechanisms of entry and exit from the cell cycle, the characteristic that intuitively seems more important for quiescent cells in the wild is to maintain viability as long as possible, waiting until the environment becomes favourable again. Indeed, quiescent cells of both prokaryotic and eukaryotic microorganisms can survive for long periods, sometimes years, without added nutrients (Gray et al., 2004).

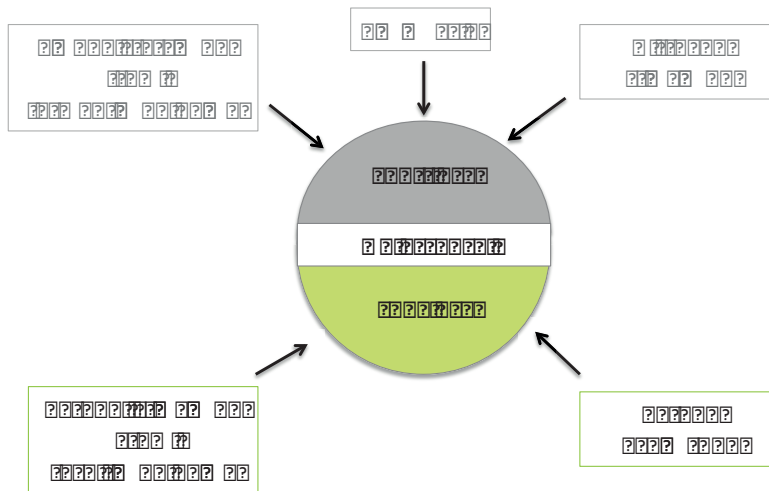


Figure 20: different kinds of quiescent cells show different survival under starvation. Quiescent cells induced by different means show specific feature, above all the ability to survive in the quiescent state. CLS correspond to the chronological longevity of a non dividing population of yeast (Fabrizio and Longo, 2003). Here, two groups of quiescent cell type are shown: in grey (top) quiescent cells with short CLS = viability lower than 50% after 1 week, and in green (bottom) quiescent cells with long CLS = viability higher than 90% at 1 week of starvation (data from J.Broach, L.Breeden and our laboratories).

Chromatin changes linked to the quiescent state in yeast

As I previously discussed, for several years the existence of a true quiescent state in yeast has been debated, mainly because of the heterogeneity of quiescent cells induced by different means. However, long-lived quiescent cells isolated from stationary phase culture appear highly different than any other cell type. Very recently McKnight and colleagues published a genome wide characterization of the transcriptome of these quiescent cells showing that a strong and global transcriptional shutoff -15 fold stronger than the one of the diauxic shift- occurs just after quiescence entry. This transcriptional reprogramming is associated with global nucleosome repositioning, increased histone occupancy and a global reduction in histone acetylation (McKnight et al., 2015; Mews et al., 2014; Schafer et al., 2008). Moreover, the deacetylation at promoters in quiescence, which appears dependent on the histone deacetylase Rpd3, has been reported of fundamental importance for quiescence entry or maintaining viability (McKnight et al., 2015).

2.3.4 How long a cell can be quiescent? The chronological life span

The amount of time that a cell can resist in the cell cycle arrested quiescent state is also defined “chronological life span” (CLS) (Longo and Fabrizio, 2012). The first method to study CLS in yeast was developed more than 20 years ago by the Longo laboratory, which proposed to use budding yeast as a simple model organism for the study of aging mechanisms in non-dividing cells (Fabrizio and Longo, 2003).

In the following paragraphs I will describe the concept of aging in *S. cerevisiae*, focusing on factors impacting on yeast chronological life span.

Aging in yeast: chronological life span versus replicative life span.

The study of aging in *S. cerevisiae* started more than 50 years ago with Mortimer and Johnson who first set up a method to monitor yeast life span. The assay was based on the concept that yeast cells divide by asymmetric budding a finite number of times: by removing with a micromanipulator daughter cells from their mother it was possible to count the number of daughters that an individual mother could generate before entering senescence. (Mortimer and Johnston, 1959). This method was named “replicative life span” (RLS) assay. However, whether the replicative life span of a yeast mother cell could be related to aging in multicellular organism is still under debate. On the other hand, aging in yeast is also assayed by measurement of chronological life span (CLS), which measures the survival of non-dividing cells (Longo and Fabrizio, 2012) (Figure 21). While both RLS and CLS have been in the forefront of discovery in the aging field, mechanisms that counteract replicative aging are in some cases in contradiction with mechanisms promoting CLS. Up to now, it is not clear whether one of the two yeast aging assays is more informative than the other (Longo et al., 2012); more likely, RLS and CLS are strictly linked in yeast and could be relevant for different cell types in humans (see discussion paragraph).

As RLS is linked to vegetative growth while CLS is associated with the quiescent state, I will not enter into details of mechanisms related to RLS but I will briefly discuss the budding yeast CLS.

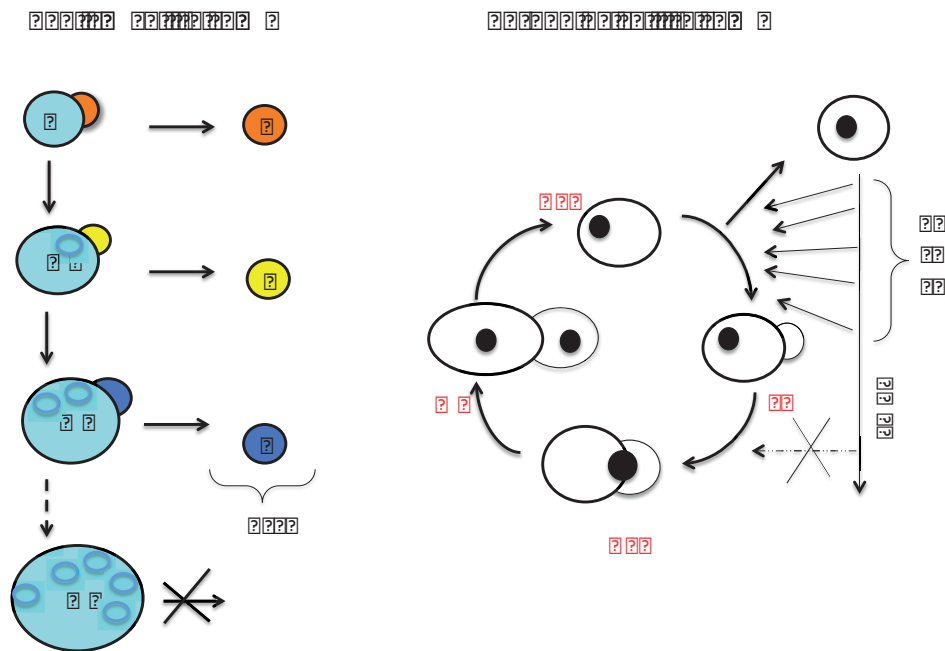


Figure 21: Replicative and chronological life span assays in yeast

Left: The total number of daughters (D, different colours) that a mother (M, light blue) can produce during her life in condition of nutrient availability can be counted and constitute the replicative life span (RLS) of a yeast cell. Right: The cell cycle is composed of the G₁ phase, during the while the cell increase in size, successively the cell will enter the S phase, during the while the DNA is replicated, continue growing in the G₂ phase and finally divide into two daughter during the M phase. The cell cycle is strictly regulated by checkpoints, found in G₁, G₂ and M, with the function to ensure that everything is ready for the next step. During conditions of limiting nutrients, cells do not pass the G₁ check-point, also called START, but exit the conventional cell cycle. The chronological life span (CLS) of a yeast cell is the time during the while this cell can resist in this non dividing state outside of the cell cycle, keeping the ability to proliferate again once the missing nutrient is restored. Reviewed in (Longo et al., 2012).

External factors known to have an impact on yeast CLS

The aging field is rapidly progressing, mainly thanks to genetics in model organisms such as *C. elegans*, *S. cerevisiae*, *D. melanogaster* and mice. However, we are still lacking a comprehensive view of how aging occurs at the cellular and organismal level in order to understand how this process could be delayed.

Briefly, there are two major pro chronological aging pathway which have been found in yeast and then confirmed in mammals: the TOR/S6K pathway (Fabrizio et al., 2001) and the Ras/adenylate cyclase/PKA pathway (Fabrizio and Longo, 2003; Longo, 1999). Both the TOR pathway, mainly linked to amino acid and other nutrient availability, and the

Ras pathway, which sense glucose but is also influenced by other nutrients, converge on the same kinase -Rim15- and on the transcription factors Msn2/4 and Gis1. These transcription factors control both stress responsive genes and balance between intracellular and extracellular carbon sources. Thus, metabolic regulation by Msn2/4 is thought to play a pivotal role in the regulation of longevity (Longo et al., 2012; Mirisola et al., 2014), mainly inducing a “protection program” from macromolecular damage and cellular stresses.

What are the external components that do influence the complex and multifactorial nature of chronological aging?

In general, oxidative stress, mitochondrial dysfunction and ROS, reduced autophagy, nuclear DNA damage, mutagenesis, high levels of ethanol and acetic acid and different other kinds of stress favour the aging process (Fabrizio et al., 2005; Longo et al., 2012). On the contrary, slow growth (Klosinska et al., 2011a; Lu et al., 2009a), caloric restriction (Fontana et al., 2010; Szafranski and Mekhail, 2014), respiration and mitochondrial adaptive signals (Mesquita et al., 2010; Piper et al., 2006; Schroeder et al., 2013) have been shown to positively regulate chronological lifespan.

In the chronological aging paradigm, the histone deacetylase Sir2 plays a pro-aging role (Casatta et al., 2013; Fabrizio et al., 2005; Lin et al., 2009). Yet *SIR2* deletion favours CLS by mechanisms not completely known and mainly in conditions of caloric restriction and/or in mutants of the Sch9 or Ras/PKA pathways (Fabrizio et al., 2005). It has been shown that Sir2 does not deacetylate only histones but has also other targets. Among all, the phosphoenolpyruvate carboxykinase Pck1, whose enzymatic activity is important for yeast cell ability to grow on nonfermentable carbon sources, lose its ability when deacetylated by Sir2 (Lin et al., 2009). In agreement with this, when growth relies on a respiratory metabolism, Sir2 inactivation favours growth and reduces pro-aging extracellular signals (Casatta et al., 2013). These data suggest that Sir2 negative role on CLS is due to a deregulation of metabolic pathway instead of a direct effect on chromatin organization.

It is important to note that the pro-chronological aging role of Sir2 is one of the main differences found between CLS and RLS, as eukaryotic sirtuins have been initially studied thanks to the yeast Sir2 positive effects on replicative lifespan (Wierman and Smith, 2014).

Interestingly, Sir3 has also been associated with regulation of longevity even though the mechanisms by which this could occur are still unknown. More than 10 years ago, the Runge lab proposed that nutrient dependent changes in Sir3 phosphorylation could affect yeast replicative lifespan (Ray et al., 2003). More recently, the Shadel lab proposed the existence of a conserved mitochondria-to-nucleus stress-signaling pathway that regulates chronological aging in a Sir3 dependent manner (Schroeder et al., 2013). Given that Sir3 has been shown to regulate telomere grouping (Ruault et al., 2011), it is tempting to speculate that telomere organization and CLS are strictly associated. However, the model proposed by the Shadel study only partially fits with the data shown (see below). Nevertheless, as it opened interesting possibilities, I think it deserve a detailed analysis.

Schroeder and colleagues showed that treating cells with mild concentration of menadione –which increase intracellular levels of the ROS superoxide (O_2^-), increased chronological life span in a Tel1 and Rad53 chekpoint kinases dependent manner. Moreover, they demonstrated that menadione treatment induced (i) the phosphorylation of the H3K36me3 histone demethylase Rph1, an already known Rad53 target, (ii) an increased H3K36me3 at two analysed subtelomeric genes and (iii) a different expression pattern of several subtelomeric genes, in a Rph1 dependent way. These data suggest that Rph1 detaches from subtelomeric regions following ROS signal thus favouring Sir3 dependent silencing. Consistently, menadione did not increase CLS on *sir3*Δ strains. However, *sir3*Δ cells were not deleted for the *HM* locus. As a consequence, these mutant cells were pseudodiploid, which could *per se* lead to short viability upon starvation (unpublished data from our laboratory). It would be thus important to confirm that the menadione induced increase in viability is Sir3 dependent in *HM* deleted strains. Second, the author model is that loss of Rph1 from subtelomeric chromatin elevates H3K36me3 levels thus enhancing binding of Sir3 to repress subtelomeric regions and increasing CLS. However, the Sir3 has high affinity for unmodified histones (Armache et al., 2011) (discussed in paragraph 1.3.2), and the H3K36me3 mark was instead proposed as a barrier for SIRs spreading as it antagonizes silencing (Tomba and Madhani, 2007; Verzijlbergen et al., 2009). In addition, the authors model predict that *RPH1* deletion should rescue both *TEL1* and *RAD53* deletions but the authors don't show this experiment and instead found that deletion of *RPH1* did not improve the CLS, nor in absence neither in presence of menadione treatment.

All together, these data indicate that SIR proteins could be possibly implicated on the regulation of yeast lifespan upon quiescence, but clearly further studies are needed to gain insight on the role of chromatin organization in yeast longevity.

To summarize, yeast cells respond to changes in the external environment by activating specific gene expression programs. In case of nutrient limitation, the long-term survival of a selected subpopulation is favoured. Quiescence is one of the strategies used by yeast cells to cope with nutrient limitation, and the chronological life span indicates for how long a cell survived in the quiescent state. Among the numerous factors involved in the regulation of the complex aging process in yeast, two members of the SIR complex are found. However, which are their roles and how these two proteins fulfil these functions are yet unsolved questions.

AIM OF THE THESIS

The aim of this work was first to describe the chromatin dynamics within the nucleus of *S. cerevisiae* upon changes in the external environment, especially upon carbon source exhaustion. Second, I aimed to gain some insights into the mechanisms leading to these chromatin dynamics. And third, I wanted to investigate the link between one particular chromatin architecture and the nuclear function in *S. cerevisiae*.

RESULTS

In this section, I will first report our study on silent chromatin in long-lived quiescent cell, which has been recently published on the journal Genome Biology and has been the subject of a Nature highlight (Result part I).

I will next report other unpublished results about:

- i) the events linking mitochondrial activity and commitment to the nuclear re-organization found upon quiescence (Result part II);
- ii) the release of telomeres upon re-entry into the cell cycle (Result part III);
- iii) the role of Sir2 on telomere grouping in long-lived quiescent cells (Result part IV).

Result part I

Spatial reorganization of telomeres in long-lived quiescent cells

M. Guidi, M. Ruault, M. Marbouty, I. Loiodice, A. Cournac, C. Billaudeau, A. Hocher, J. Mozziconacci, R. Koszul and A. Taddei

Nuclear architecture can vary between cell types and states, but the biological consequences of distinct genome organizations are less clear. Here, by combining live microscopy, DNA FISH and chromosome conformation capture (HiC) techniques, we report that the metabolic state of the cell regulates the architecture of the yeast genome. Following carbon source exhaustion and entry into stationary phase, the genome of long-lived quiescent cells undergoes a spatial reorganization driven by the grouping of telomeres into a “hypercluster”. This increased telomere grouping requires the silencing factors Sir3 and Sir4 and initiates after the transition from fermentation to respiration. However, artificially increasing the levels of reactive oxygen species (ROS) during fermentation is sufficient to commit cells to form telomere hyperclusters upon starvation. Moreover, we show that deletion of the *SIR3* gene abolishes telomere grouping and decreases longevity, and this last defect is rescued by expressing the silencing defective *Sir3-A2Q* allele, which is competent for telomere grouping.

RESEARCH

Open Access



Spatial reorganization of telomeres in long-lived quiescent cells

Micol Guidi^{1,2,6}, Myriam Ruault^{1,2,6}, Martial Marbouty^{3,4}, Isabelle Lo odice^{1,2,6}, Axel Cournac^{3,4}, Cyrille Billaudeau^{1,2,6}, Antoine Hocher^{1,2,6}, Julien Mozziconacci⁵, Romain Koszul^{3,4} and Angela Taddei^{1,2,6*} 

Abstract

Background: The spatiotemporal behavior of chromatin is an important control mechanism of genomic function. Studies in *Saccharomyces cerevisiae* have broadly contributed to demonstrate the functional importance of nuclear organization. Although in the wild yeast survival depends on their ability to withstand adverse conditions, most of these studies were conducted on cells undergoing exponential growth. In these conditions, as in most eukaryotic cells, silent chromatin that is mainly found at the 32 telomeres accumulates at the nuclear envelope, forming three to five foci.

Results: Here, combining live microscopy, DNA FISH and chromosome conformation capture (HiC) techniques, we report that chromosomes adopt distinct organizations according to the metabolic status of the cell. In particular, following carbon source exhaustion the genome of long-lived quiescent cells undergoes a major spatial re-organization driven by the grouping of telomeres into a unique focus or hypercluster localized in the center of the nucleus. This change in genome conformation is specific to quiescent cells able to sustain long-term viability. We further show that reactive oxygen species produced by mitochondrial activity during respiration commit the cell to form a hypercluster upon starvation. Importantly, deleting the gene encoding telomere associated silencing factor *SIR3* abolishes telomere grouping and decreases longevity, a defect that is rescued by expressing a silencing defective *SIR3* allele competent for hypercluster formation.

Conclusions: Our data show that mitochondrial activity primes cells to group their telomeres into a hypercluster upon starvation, reshaping the genome architecture into a conformation that may contribute to maintain longevity of quiescent cells.

Background

The spatiotemporal behavior of genomes and their regulatory proteins is an important control mechanism of genomic function. One of the most pervasive features of nuclear organization is the existence of subnuclear compartments, which are thought to create microenvironments that favor or impede specific DNA- or RNA-related processes [1]. Deciphering how the dynamics of this subnuclear compartmentalization are regulated in relation to changes in genome activity is a key step in understanding how nuclear organization participates in nuclear function.

Well-characterized examples of subnuclear compartments include clusters of specific genes or repetitive DNA sequences [2], such as telomeric repeats (in budding yeast) or centromeric satellites (in fission yeast, fly and mammals) and retrotransposons (in fission yeast, Tn2/Ku70-mediated clustering) [3]. These repetitive sequences generally nucleate patterns of histone modifications that are recognized by histone-binding repressors, and their clustering results in the sequestration of these general repressors into subcompartments. Besides its role in concentrating silencing factors, this evolutionarily conserved phenomenon has a dominant impact on chromosome folding and positioning. In metazoans, a cell type-specific nuclear distribution of heterochromatin is established upon cell differentiation, and is often compromised in cancer cells [4]. In budding yeast, the clustering of silent chromatin provides an excellent model of a subnuclear compartment.

* Correspondence: angela.taddei@curie.fr

Equal contributors

¹Institut Curie, PSL Research University, Paris F-75248, France

²CNRS, UMR 3664, Paris F-75248, France

Full list of author information is available at the end of the article



Most *Saccharomyces cerevisiae* functional and structural studies have been conducted on exponentially growing cell cultures. In these conditions, silent chromatin is mainly found at telomeres and at the cryptic mating type loci (*HM* loci), where it is generated by the recruitment of the SIR complex comprising Sir2, Sir3, and Sir4. At telomeres, this nucleation event is achieved by the transcription factor Rap1, which binds the telomere TG repeats and interacts with Sir3 and Sir4. Sir4 heterodimerizes with the NAD⁺-dependent histone deacetylase Sir2, which deacetylates H4 histone tails from neighboring nucleosomes, thus generating binding sites for Sir3. The SIR complex thus spreads over a 2–3-kb subtelomeric region leading to the transcriptional repression of subtelomeric regions.

The clustering of telomeres into perinuclear foci generates a zone that favors SIR-mediated repression at the nuclear periphery [5, 6] and ensures that SIR proteins do not bind promiscuously to repress other sites in the genome [7, 8]. Furthermore, telomere anchorage in S phase contributes to proper telomerase control and suppresses recombination among telomere repeats [9, 10].

The average large-scale organization of budding yeast chromosomes during exponential growth has been described through genome-wide capture of chromosome conformation (3C) experiments [11]. This analysis unveiled a polarized configuration with chromosome arms extending away from the centromeres that are held by the spindle-pole body, in agreement with microscopy data [12]. This so called Rabl organization — initially observed by Carl Rabl in rapidly dividing nuclei of salamanders [13] — can be mimicked to some extent by polymer models using a limited number of assumptions [11, 14–16]. However, it remains unclear how specific biological processes could affect this robust average organization.

As mentioned above, most of the studies characterizing genome organization and its functional consequences in budding yeast have been conducted in nutrient-replete conditions with cells undergoing exponential growth. However, yeast cells rarely experience such a lush environment and their survival in the wild depends on their ability to withstand adverse conditions.

It is well known that yeast cells finely tune their growth and behavior to their environment, adapting to nutritional depletion or stresses by engaging specific developmental programs [17]. When grown in rich media containing glucose, they progress through distinct metabolic programs (Fig. 1a), with each transition being accompanied by widespread transcriptional reprogramming [18, 19]. In the first phase (exponential phase), cells metabolize glucose predominantly by glycolysis, releasing ethanol in the medium. When glucose becomes limiting, the culture enters diauxic shift, a transition characterized by a decreased growth

rate and a metabolic switch from glycolysis to aerobic utilization of ethanol. Finally, when no other carbon source is available cells enter stationary phase (SP). During that stage most cells are in quiescence, a non-proliferative state that maintains the ability to resume growth following restoration of missing nutrients.

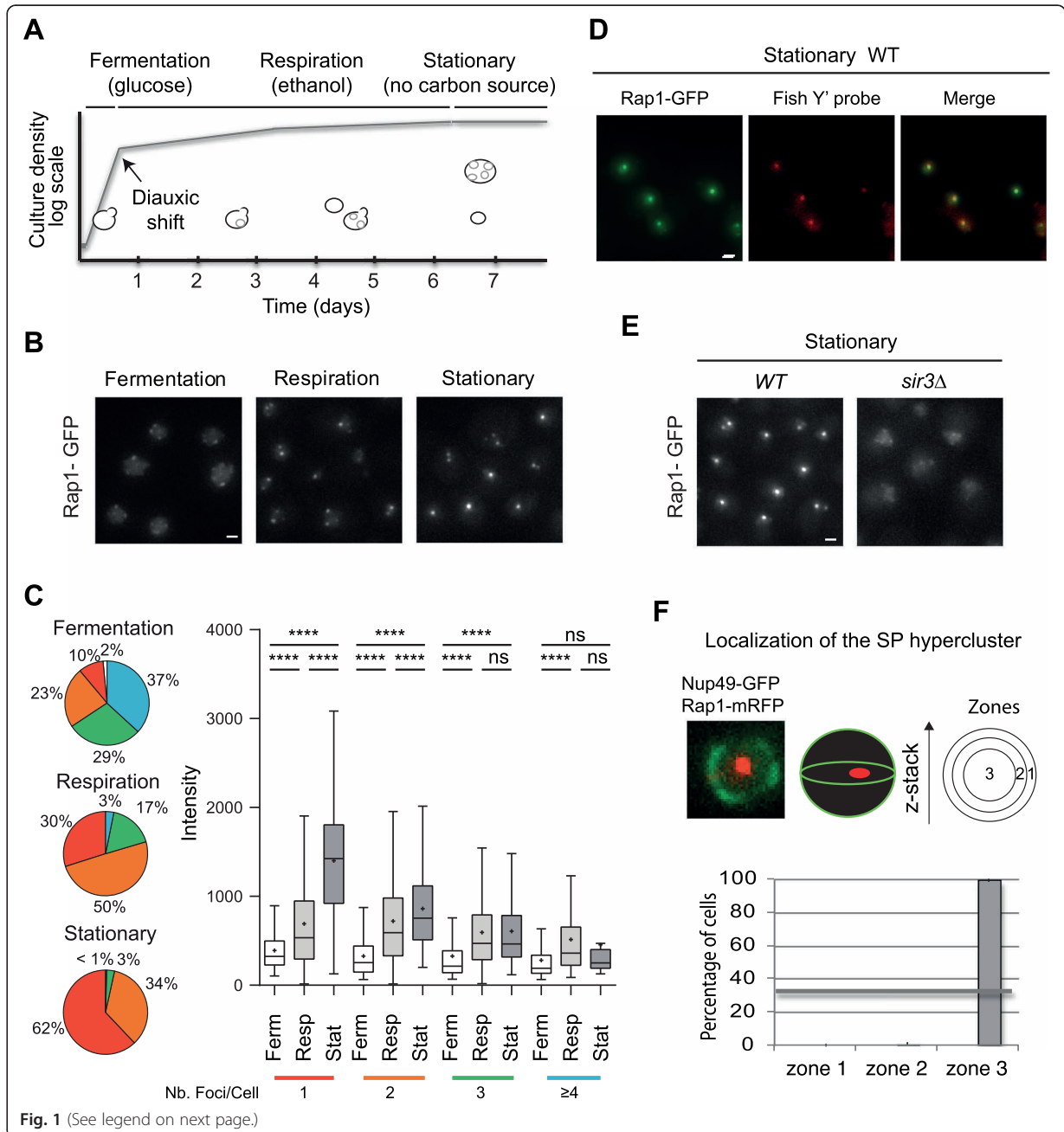
Recent studies in different species demonstrated that a hostile environment (i.e., caloric restriction or the presence of mild oxygen stresses) can trigger a “vaccination-like” adaptive response leading to the acquisition of anti-aging functions [20]. Following the same principle, budding yeast can reach different quiescent states depending on the conditions that induce the cell cycle exit, each of them leading to different outcome in terms of chronological lifespan (CLS) [21]. Deciphering the key features that differentiate each metabolic state is essential to understand mechanisms that extend lifespan in yeast.

Here we show that, following carbon source exhaustion, the silencing factor Sir3 drives the telomeres of quiescent cells to group together, forming a discrete, large cluster (hypercluster) at the center of the nucleus. This organization is specific to quiescent cells able to sustain long-term viability. Our data strongly support a model in which mitochondrial activity, through the production of reactive oxygen species (ROS) during cell respiration, commits cells to form a telomere hypercluster upon starvation. Importantly, *sir3Δ* cultures, which are defective in forming telomere hyperclusters in SP, show reduced CLS. Furthermore, expressing a silencing-defective *SIR3* allele rescues both telomere distribution and the CLS of a *sir3* null strain, strongly arguing that telomere clustering directly contributes to cell survival during quiescence.

Results

Massive telomere reorganization upon carbon source exhaustion

To investigate telomere organization in live cells, we monitored the subnuclear distribution of the telomeric protein Rap1 fused to green fluorescent protein (GFP) [22] at different stages of a liquid culture, from glycolysis to late respiration to SP. We observed dramatic changes in the distribution of the Rap1-GFP signal during this time course (Fig. 1a, b). In agreement with previous reports [6, 22], Rap1-GFP formed three to five foci during the logarithmic phase, quantified using our custom-made software (Fig. 1c; adapted from [22]). In cells undergoing respiration (after 2 days in culture), Rap1-GFP foci were fewer and brighter, with 50 % of the cells showing two foci and 30 % of the cells having only one focus (versus 23 % and 10 %, respectively, during fermentation). In SP 62 % of the cells exhibited a unique focus with a median intensity that was fivefold higher than in the exponential phase. Moreover, we noticed that



(See figure on previous page.)

Fig. 1 Massive telomere reorganization upon carbon source exhaustion. **a** Growth curve for *S. cerevisiae* grown in rich glucose-based liquid medium. Yeast cells grown in medium containing glucose divide exponentially, mainly perform glycolysis, and release ethanol into the medium. When glucose becomes limiting (roughly after 12 hours in the conditions used in this study; see “Materials and methods”) the cells undergo a major metabolic transition called “diauxic shift”, during which they stop fermentation and start aerobic utilization of ethanol (respiration phase). After this transition, cells divide slowly and become more resistant to different stresses. Once ethanol is exhausted and no other carbon source is available, around 7 days, the culture enters the stationary phase (SP). At this stage, the majority of the cells are in a quiescent state. **b** Representative fluorescent images of the telomere-associated protein Rap1 tagged with green fluorescent protein (*GFP*). Overnight wild-type (WT) “yAT1684” liquid cultures were diluted to 0.2 OD_{600nm}/ml and images were acquired after 5 hours (1 OD_{600nm}/ml, fermentation phase), 2 days (28 OD_{600nm}/ml, respiration phase) and 7 days (40 OD_{600nm}/ml, stationary phase). **c** Quantification of the distribution of intensity and number of foci of Rap1-GFP images from experiment shown in (b) with our in-house software. Pie charts represent percentages of cells with 0 (white), 1 (red), 2 (orange), 3 (green) and 4 (blue) foci. Box plots: white = fermentation (*Ferm*), light gray = respiration (*Resp*), dark grey = stationary (*Stat*). Median (line) and mean (cross) are indicated. For each condition, more than 1000 cells were analyzed. Statistical tests were carried out using the Mann-Whitney non-parametric test (**** $p < 0.0001$; *** $p < 0.001$; ** $0.001 < p < 0.01$; * $0.01 < p < 0.05$; $ns = p > 0$). **d** Colocalization of telomeres with Rap1 foci. ImmunoFISH with Y’ probes was performed on a WT strain yAT1684 at SP. **e** Representative fluorescent images of the telomere-associated protein Rap1 tagged with GFP in SP WT and *sir3Δ* cells. **f** Rap1-GFP hypercluster localization relative to the nuclear pore. Two-color z-stack images were acquired on a WT strain yAT2407 expressing Rap1-yemRFP and the GFP tagged nucleoporin 49 (Nup49-GFP) during SP. The localization of the Rap1-yemRFP hypercluster in one of the three equal concentric zones of the nucleus was scored in the focal plane. This experiment was repeated twice and for each experiment >100 nuclei with a hyper-cluster were analyzed

when the number of foci per cell decreases, the intensities of the remaining foci increase (Fig. 1c), suggesting that smaller foci group into larger ones. Importantly, we verified that the brightness of the Rap1-GFP clusters observed in SP was not due to an overall increase in Rap1-GFP levels (Additional file 1: Figure S1a). Furthermore, we observed a similar clustering with SIR complex proteins fused to GFP (*Sir2/3/4*; Additional file 1: Figure S1b). We confirmed that Rap1-GFP foci coincided with the Y’ telomeric clusters and *Sir3* foci in SP cells by combined immunostaining and fluorescence in situ hybridization (immuno-FISH; Fig. 1d) and in vivo imaging (Additional file 1: Figure S1c). Thus, telomere-associated silent chromatin groups into “hyperclusters” in SP cells.

As in exponentially growing cells, telomere hyperclustering requires *SIR3* and *SIR4* in SP cells (Fig. 1e; Additional file 1: Figure S1d). Although the brightest Rap1-GFP focus was mainly found adjacent to the nuclear envelope in exponentially growing cells [6, 22], telomere hyperclusters were overwhelmingly found in the innermost area in SP cells (>90 % in zone 3; Fig. 1f).

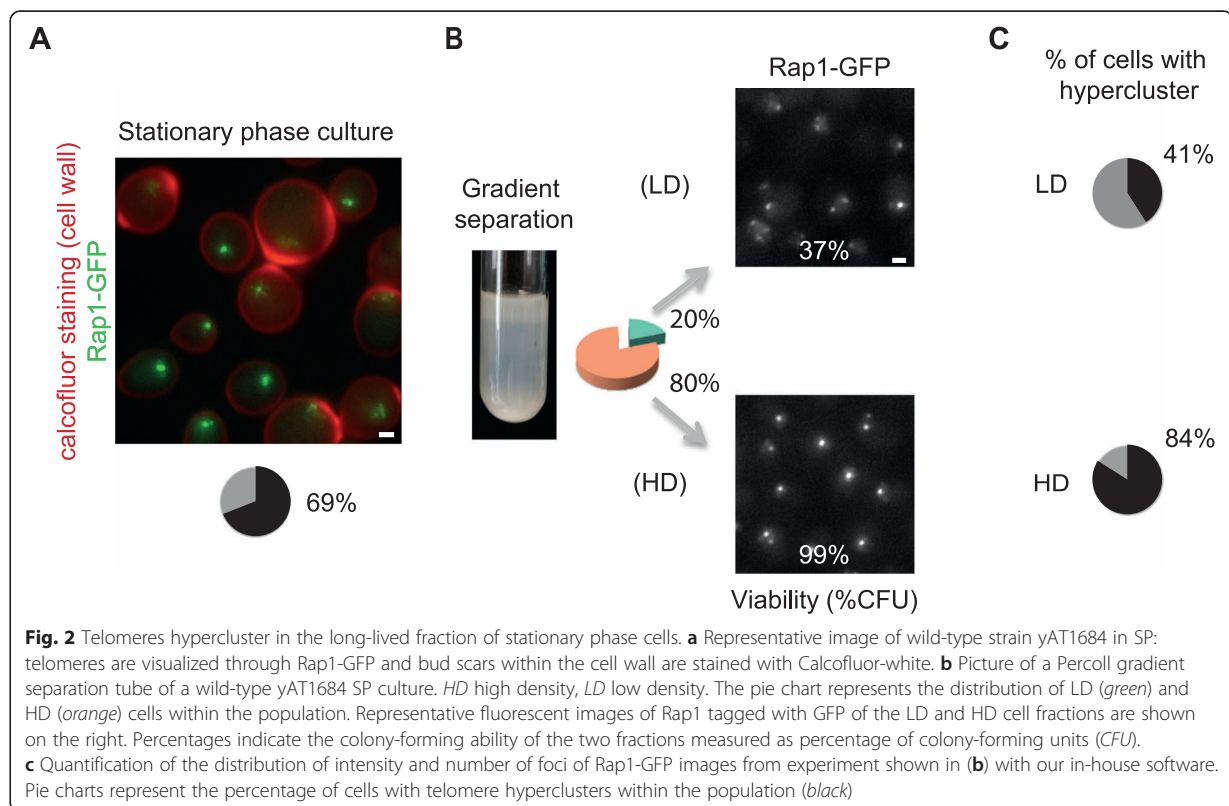
We next evaluated whether other nuclear landmarks were also altered in SP. In agreement with previous reports, we found that the nuclear diameter (data not shown, inferred from experiment Fig. 1f) was smaller and the nucleolus more compact in cells after the diauxic shift (Additional file 1: Figure S1e) [23]. Consistent with [24], we noticed that kinetochore proteins formed a “bundle” in a subpopulation of cells; however, this structure did not correlate with telomere hyperclusters (Additional file 1: Figure S1f). Furthermore, we did not observe major changes in the distribution of the centromere-associated protein *Cse4* in SP cells containing telomere hyperclusters (Additional file 1: Figure S1g). Thus, a specific SIR-dependent re-organization of telomeres occurs in a subpopulation of SP cells.

Hyperclustering of telomeres occurs only in the long-lived fraction of SP cells

As previously reported [25], SP cultures consist of different types of cells. Equilibrium density-gradient centrifugation enables the separation of a dense fraction mainly composed of small unbudded daughter cells that are able to sustain long-term viability, and a lighter fraction that includes both budded and unbudded cells that rapidly lose the ability to perpetuate over time. Calcofluor staining revealed that cells with hyperclusters (defined as cells containing one or two foci and at least one Rap1-GFP focus with intensity levels above 95 % of foci in exponentially growing cells) are essentially small unbudded cells (Fig. 2a). Sorting SP cells by density gradient enriched the population of cells showing hyperclusters from 69 % to 84 % in the densest fraction (HD) while most cells from the less dense fraction (LD) showed a distribution of Rap1-GFP foci similar to the post-diauxic shift cells (Figs. 1b, c and 2b, c). Moreover, we confirmed that the viability is significantly lower for the lighter cells than for the denser ones that show hyperclusters (37 % versus 99 %, respectively). We thus conclude that telomere hyperclustering occurs specifically in quiescent SP cells.

The global chromosome organization in long-lived SP cells is constrained by centromere and telomere clustering

To decipher the three-dimensional (3D) organization of the entire genome in long-lived SP cells, we turned to 3C [26]. We used an untagged strain to avoid any possible artifact related to the expression of tagged telomere proteins. As cells from the dense fraction of SP are small unbudded cells (Fig. 2a), we compared the genomic contact maps of these cells with G1 daughter cells elutriated from an exponential culture to avoid the contribution of

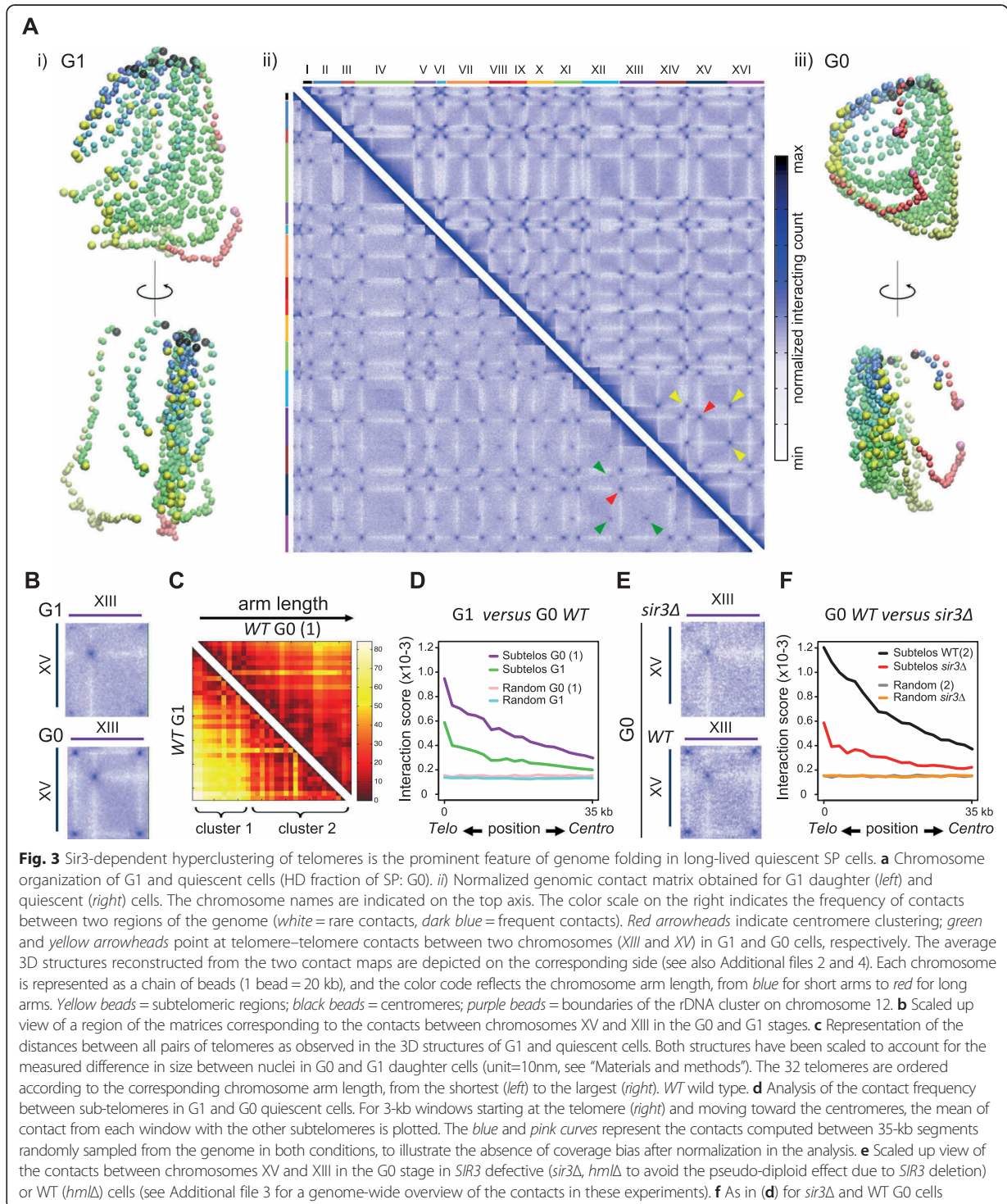


the cell cycle in this latter case. In order to facilitate the interpretation of the contact map [Fig. 3a(ii)], the matrix was converted into a 3D map in which the distance between each pair of genome segments was optimized to reach the inverse of their measured contact frequency [Fig. 3a(i); Additional file 2] [27]. This 3D reconstruction of the entire contact map provided a remarkable overview of the average yeast genome organization in a population of G1 cells, with the rDNA clearly isolated from the rest of the genome, a dense centromere cluster, and a tendency for subtelomeres to co-localize, consistent with the well-documented perinuclear clustering of telomeres [6].

In excellent agreement with our microscopy data, contacts between telomeres became prominent in quiescent cells, generating a remarkable hypercluster. The influence of chromosome arm length on the subtelomere contacts — which in exponentially growing cells discriminates two groups of telomeres exhibiting preferential contacts with each other's — is alleviated by the formation of the hypercluster, suggesting the formation of a grid-like/homogeneous disposition of telomeres (Fig. 3b, c) [11, 28]. In addition, regions closer to the telomeres exhibited an increased number of contacts in SP, whereas the number of contacts between centromeres decreased slightly (Fig. 3d; Additional file 3:

Figure S2a). Thus, the frequency of contacts increases specifically between telomeres, imposing a general constraint on the whole genome organization, with each chromosome arm now being tethered at two points of the nuclear space (Fig. 3a(iii); Additional file 4). As a result, the average contacts between chromosome arms, which are primarily constrained by their sizes and centromere clustering in G1 (Fig. 3a(i), c), appear distorted due to subtelomere interactions in G0 (Fig. 3a(iii), d). Importantly, these observations were confirmed in two different genetic backgrounds (BY and W303; Additional file 3: Figure S2c, d).

To test whether this reorganization is driven by increased telomere–telomere interactions, we compared the genomic contact map of cells in which *SIR3* had been deleted and wild-type cells from the dense fraction of a SP culture. In agreement with our microscopy data (Fig. 1e) we observed that *sir3Δ* cells were not able to generate a hypercluster upon entry into quiescence (Fig. 3e, f; Additional file 3: Figure S2b) and that the general organization of chromosomes in *sir3Δ* quiescent cells resembles the organization of wild-type G1 cells, with similar levels of contacts between subtelomeric regions (Fig. 3d, f; Additional file 3: Figure S2b). We thus conclude that the main changes in chromosome organization that occur as cells enter quiescence are driven by an increase in Sir3-dependent telomere clustering.



Telomeres form hyperclusters specifically in conditions inducing long-lived quiescent cells

To test whether telomere hyperclusters were a general feature of quiescence we compared telomere subnuclear distribution in quiescent cells induced by different means. As mentioned above, although quiescent cells are by definition viable, their CLS properties depend on the method/metabolic changes used to induce the cell cycle exit [21] (Fig. 4a). At day 7 of CLS 61 % of quiescent cells arising from progressive carbon source exhaustion (SP) had formed telomere hyperclusters and these retained >90 % viability (Fig. 4a, b). In contrast, quiescent cells induced by nitrogen starvation formed hyperclusters at a much lower rate (18 % had done so) and lost viability more rapidly, as previously reported [21]. Hence, the grouping of telomere foci into hyperclusters is not a consequence of cell cycle arrest but rather a specific feature of long-lived quiescent cells induced by carbon source exhaustion.

The ability to form telomere hyperclusters upon starvation is acquired during respiration

Interestingly, when abruptly starved from carbon source, cells respond differently depending on their initial metabolic status: few cells previously undergoing glucose fermentation formed telomere hyperclusters upon starvation (7 %) and showed a strong decrease in viability at day 7 (≈ 40 %), in agreement with previous reports [21, 29]. In contrast, 73 % of cells previously undergoing respiration (post-diauxic shift) formed telomere hyperclusters upon starvation and these retained ≈ 90 % of viability at day 7. Thus, only cells that experienced respiration before entering quiescence had a long CLS (>90 % viability after 1 week of starvation) and formed telomere hyperclusters at rates of more than 60 % (Fig. 4a, b). These characteristics could be attributed either to their metabolic activity or to their growth rates, as cells undergoing respiration divide slower and slow growth confers resistance to various stresses [30]. However, slow growth was not sufficient to prime cells to form a hypercluster upon starvation, as cells grown slowly in glucose at 25 °C and starved after fermentation did not form hyperclusters (Additional file 5). To determine if respiration was an obligatory step to induce telomere hyperclustering upon starvation, we monitored telomere clustering in respiratory deficient cells (*rho*-) after glucose exhaustion (Fig. 4b) or upon abrupt starvation (data not shown). These conditions led to a very low rate of cells with bright Rap1-GFP foci (3 %; Fig. 4b) indicating that respiration, or at least mitochondrial metabolism, favors the formation of telomere hyperclusters upon abrupt starvation. It is noteworthy that *rho*- cells show very short chronological lifespan in SP (Fig. 4a), consistent with our observation that telomere hyperclusters are a feature of long-lived quiescent cells. These data indicate that

the ability to form hyperclusters is favored by mitochondrial activity.

Hormetic ROS during exponential phase prime cells to form hyperclusters upon starvation and to sustain long-term viability

We reasoned that ROS, as byproducts of the respiration process, could prime cells to form telomere hyperclusters upon starvation. Indeed, studies in model organisms show that a mild increase in ROS levels can positively influence health and lifespan, a process defined as mitochondrial hormesis or mitohormesis [20, 31]. Since hydrogen peroxide (H_2O_2) has emerged as a ROS signaling molecule able to induce an adaptive response [32], we tested the effect of increasing intracellular H_2O_2 on telomere hypercluster formation. This was achieved either by deleting the gene encoding the cytoplasmic catalase *Ctt1*, which scavenges H_2O_2 [33], or by overexpressing the superoxide dismutase *Sod2*, which converts O_2^- into H_2O_2 (Fig. 5a, b). In agreement with our hypothesis, we observed that telomere hyperclusters formed more efficiently in SP of *cct1* Δ cells, and appeared earlier in cells overexpressing *SOD2*, compared with wild-type cells (Fig. 5a, b). Importantly, these strains deleted for *CTT1* or overexpressing *SOD2* both show extended lifespan [33, 34].

We next tested whether increasing ROS levels in fermenting cells by treating them with H_2O_2 would bypass the requirement for the respiration phase and promote hypercluster formation upon starvation. As expected, untreated cells were unable to form telomere hyperclusters after starvation (Fig. 5c) and had a short CLS (Fig. 5d). In contrast, H_2O_2 pre-treated cells contained brighter and fewer Rap1-GFP foci (Fig. 5c). Importantly, like SP HD cells, H_2O_2 pre-treated cells had >90 % viability at day 7 of CLS (Fig. 5d). Combined, these data strongly suggest that ROS exposure prior to starvation promotes telomere grouping and long-term viability during starvation.

Sir3-dependent telomere clustering favors long term survival during quiescence

We previously demonstrated that telomere grouping in exponentially growing cells is dependent on Sir3 protein amount but independent of silencing [22]. We found that telomere hyperclustering in wild-type quiescent cells is not driven by an increase in Sir3 protein levels as revealed by western blot analysis (Additional file 6: Figure S4a). Furthermore, monitoring Sir3 occupancy genome-wide by chromatin immunoprecipitation (ChIP) revealed no significant changes in Sir3 spreading between exponentially growing cells and SP cells showing telomere hyperclusters (Additional file 6: Figure S4b).

To evaluate whether the silencing function of Sir3 is required for telomere hyperclustering and for longevity

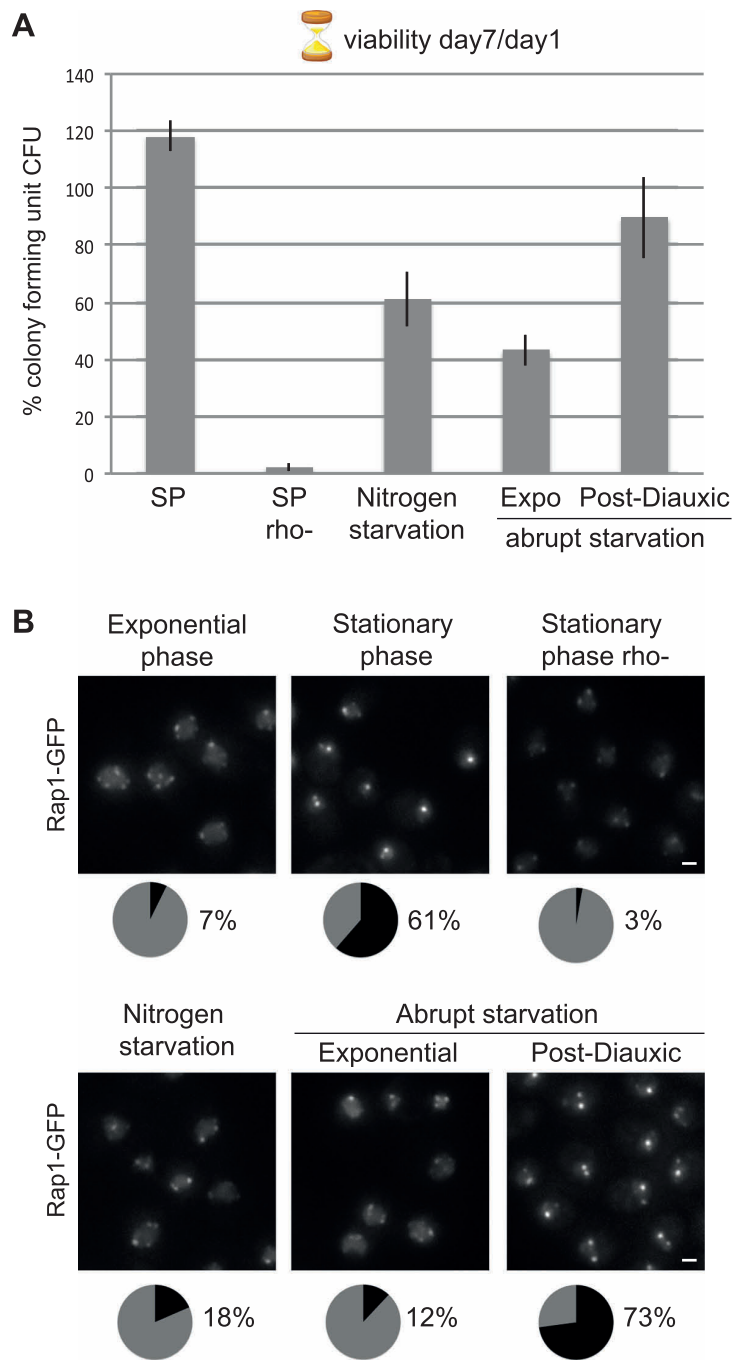
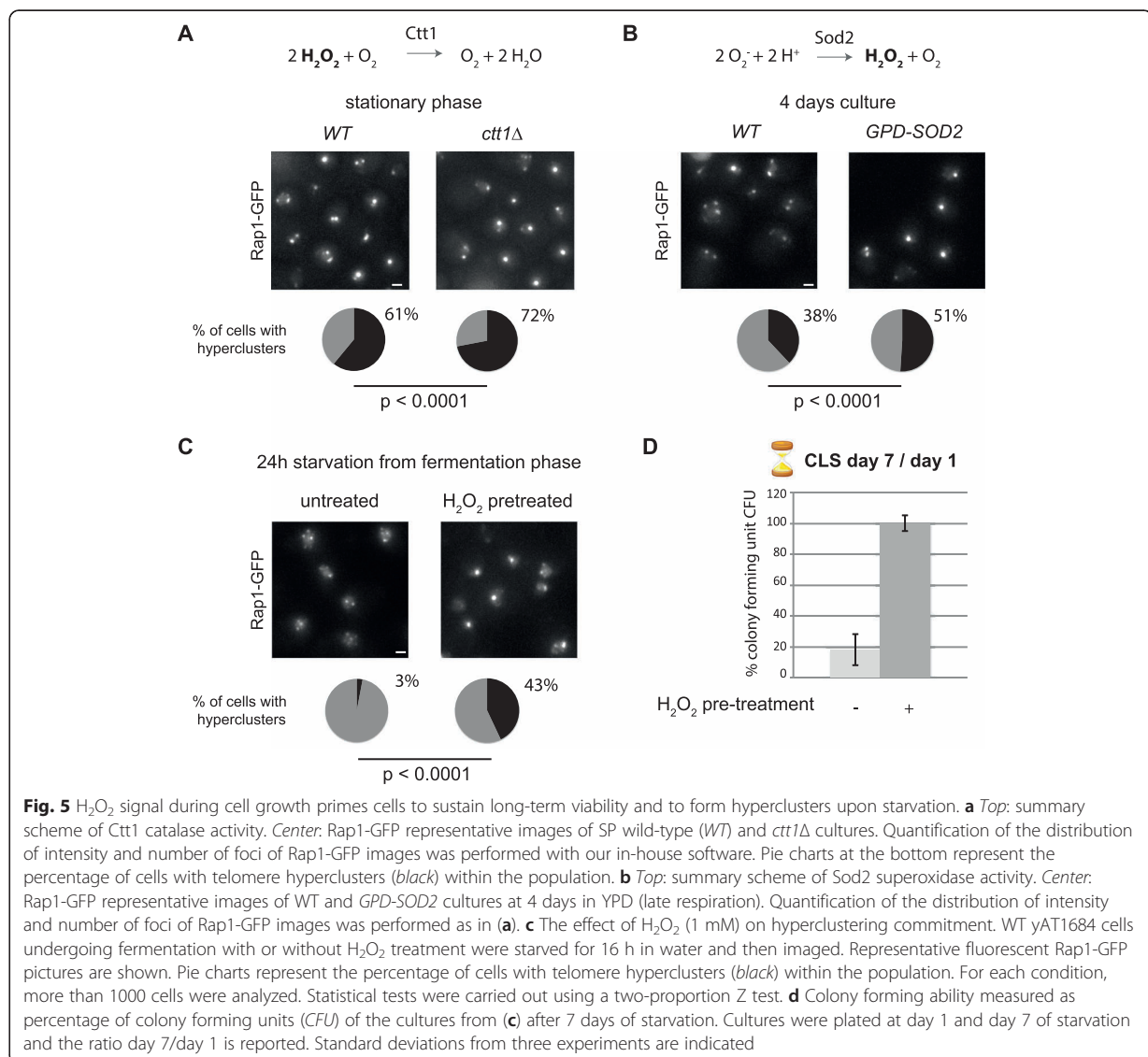


Fig. 4 Telomere hyperclusters are a feature of long-lived quiescent cells and require mitochondrial activity. **a** Colony forming ability measured as percentage of colony forming units (CFU) of WT strain yAT1684 after 7 days in quiescence induced by different methods: carbon exhaustion from YPD (SP); SP respiratory-deficient cells (SP rho-); nitrogen starvation; abrupt starvation of exponential and post-diauxic cells. Cells were plated at day 1 and day 7 after quiescence induction and the ratio day 7/day 1 was considered as the day 7 CLS. Standard deviations from three experiments are indicated. **b** Representative fluorescent Rap1-GFP images of cultures used for the CFU assay shown in (a). Cells were imaged at day 1 CLS. Pie charts represent the percentage of cells with telomere hyperclusters within the population (black)



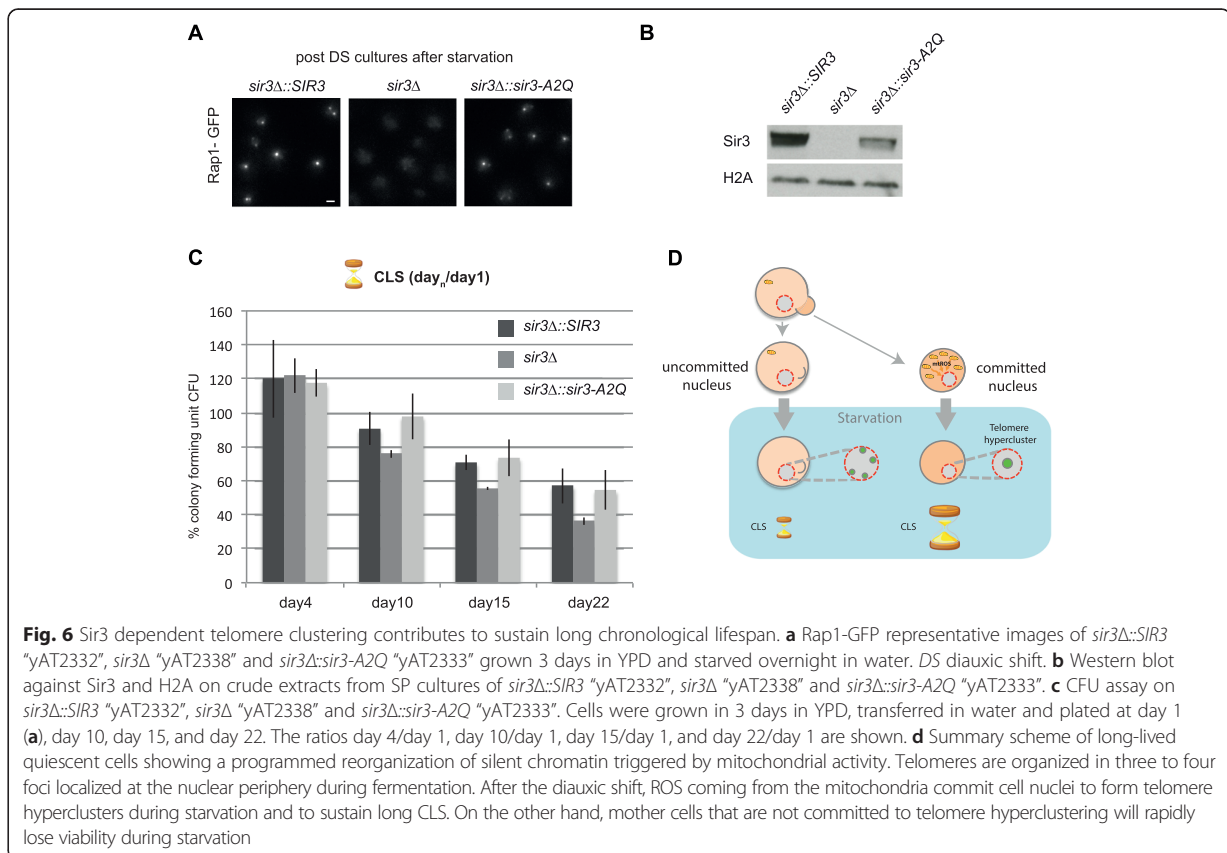
in quiescent cells, we transformed *sir3*Δ cells (defective for telomere clustering) with either a wild-type or a silencing dead copy of *SIR3* (*sir3-A2Q*) [22] and assessed their CLS. We found that the insertion of either *SIR3* or *sir3-A2Q* rescued the telomere hyperclustering in quiescent cells (Fig. 6a). We noticed that Rap1-GFP foci in the *sir3-A2Q* mutant were dimmer than in the *SIR3* strain, probably due to a lower stability of this mutant form of Sir3 in SP (Fig. 6b). Nevertheless, this establishes that the silencing function of Sir3 is not required for telomere clustering in quiescence.

The *sir3*Δ strain had viability similar to wild-type cells at days 4 and 7 (Fig. 6c and not shown), arguing that this mutant enters properly into quiescence upon carbon source exhaustion. In agreement with this, we observed that the

*sir3*Δ strain generates dense cells following the diauxic shift. Furthermore, these cells are as thermo-tolerant as their wild-type counterpart (Additional file 6: Figure S4c–e). In contrast, the *sir3*Δ strain shows a modest decrease in viability after day 10 compared with wild type, suggesting that while Sir3 is dispensable to enter into the quiescent state, it contributes to the maintenance of this specific cellular state. Importantly, expressing the *sir3-A2Q* mutant rescued the viability defect observed in the *sir3*Δ strain (Fig. 6c). Thus, Sir3-mediated telomere clustering but not silencing is required for the maintenance of the quiescent state.

Discussion

We report that the organization of the budding yeast genome changes drastically depending on the metabolic



status of the cell. In particular, quiescent cells that sustain long-term viability or increased CLS form a discrete subcompartment of telomeric silent chromatin in the most internal part of the nucleus (Fig. 6d).

Dynamics of nuclear organization upon carbon source exhaustion

We describe the dynamics of nuclear organization upon two major metabolic transitions: from fermentation to respiration and from respiration to SP. First, we show that telomere clusters, which are known to form three to five foci at the nuclear periphery in cells undergoing fermentation, form brighter and fewer foci after the diauxic shift. Furthermore, when cells exhaust the carbon source after respiration and enter the SP, these foci further group into a hypercluster located in the center of the nucleus in SP cells able to sustain long-term viability.

SIR-mediated telomere clustering drives chromosome conformation in long-lived quiescent cells

Genomic 3C analyses reveal that long-lived SP cells display increased constraints in their nuclear architecture, which appears to be driven by the clustering of telomeres. Because *S. cerevisiae* chromosomes exhibit such differences in size, mechanical constraints are likely to play significant roles on

the organization of chromosomes tethered at both their centromere and telomeric regions. The positioning of the cluster in the middle of the nuclear space may actually reflect this physical constraint imposed by the smallest chromosome arms. As *SIR3*-deleted cells are unable to form telomere hyperclusters in quiescence and show a global organization that is similar to that of G1 cells, we conclude that SIR-mediated telomere clustering drives the global reorganization of chromosomes in long-lived quiescent cells. Although both Sir3 and Sir4 are required for telomere hyperclustering, gene silencing is not necessary for this event, as demonstrated by expressing a silencing defective version of Sir3 [22]. Furthermore, telomere hyperclustering in quiescent cells is not driven by an increase in Sir3 protein or an increase of Sir3 spreading. As Sir3 may bind nucleosomes in more than one conformation [35], it is possible that telomere clustering after the diauxic shift is driven by specific post-translational modifications that increase Sir3 clustering function.

Mitochondrial ROS commit cells to form telomere hyperclusters upon starvation

Importantly, we show that increased telomere clustering is not a general feature of cell cycle arrest, as it is observed only in quiescent cells able to sustain long-term

viability. Furthermore, the ability to form telomere hyperclusters required mitochondrial activity and is acquired post-diauxic shift in the quiescent fraction of cells shown to have a six-fold higher respiration rate compared with the non-quiescent fraction of cells [36]. ROS, and more specifically H_2O_2 produced during respiration, are obvious candidates to trigger the commitment to form hyperclusters upon starvation [20]. Indeed, we show that mutants known to increase the cellular level of H_2O_2 form hyperclusters with a higher rate and faster kinetics than wild-type cells. Furthermore, treating pre-diauxic shift cells with a sub-lethal dose of H_2O_2 is sufficient to commit cells to form telomere hyperclusters upon starvation and to sustain long-term viability. This commitment could be mediated by the checkpoint kinase Rad53, which is activated at these levels of H_2O_2 [37], thus allowing crosstalk between mitochondria and the nucleus [38, 39].

Potential benefits of telomere hyperclustering for CLS

Although alterations of nuclear architecture have been reported upon differentiation [40] and in quiescent metazoan cells [41], the function of this reorganization remains elusive. Interestingly, dramatic changes in the distribution of silent chromatin are observed in mammalian senescent cells with the formation of senescence-associated heterochromatin foci, which are thought to contribute to the stability of the cell cycle arrest [42]. Another striking example of genome reorganization comes from rod photoreceptor cells of nocturnal rodents. In these cells, the nuclei exhibit an “inverted organization” — that is, reminiscent to the hypercluster observed in long live yeast cells — probably as an adaptation to limited light [43].

The large reorganization of budding yeast telomeres into a hypercluster concomitant with an important metabolic adaptation most likely provides a survival advantage in the long-term. Accordingly, *sir3Δ* strains, which cannot form telomere clusters, show a modest reduction in longevity compared with wild-type strains, when SP cultures (after 3 days in rich medium) were shifted to water. This is consistent with the findings of [38]. However, quiescent cells purified from 7-day cultures of prototroph W303 strains showed no difference in the lifespan of *sir3Δ* or *sir4Δ* and wild-type cells (Linda Breeden, personal communication), possibly due to strain or experimental procedure variations. Importantly, the viability defect that we observed is rescued by expressing a *SIR3* allele that is competent for telomere clustering but defective for silencing (*sir3-A2Q* mutant [22]), indicating that telomere clustering in quiescence has a positive effect on CLS independent of gene silencing under our conditions.

We propose that telomere hyperclusters could influence survival by protecting telomeres from degradation, fusion, and/or ectopic recombination events. Alternatively,

telomere hyperclustering in quiescence could also be a way to sequester multifunctional factors that could have deleterious effects if localized to nuclear subcompartments where they are not needed. Such a factor could be the sir-tuin Sir2, since it plays a pro-aging role by regulating cytoplasmic enzymes involved in carbon metabolism [44, 45].

Conclusions

By establishing that the nuclear organization of quiescent cells significantly differs from the well-described organization of cells grown in nutrient-replete conditions, our study sets the ground to (re)interpret studies on nuclear processes in the context of quiescence and aging. Moreover, our results unravel a novel connection between nuclear organization and aging, paving the way for future experiments analyzing the importance of nuclear organization for chronological lifespan.

Materials and methods

Media and growth conditions

All yeast strains used in this work are listed in Additional file 7 and are from the W303 background [46] except for the strains used for the HiC experiment (BY4741). Gene deletions and gene tagging were performed by PCR-based gene targeting [46, 47].

Yeast cells were grown in rich medium (YPD, yeast extract-peptone-dextrose) at 30 °C.

Induction of quiescence by carbon source exhaustion was performed as follows. Yeast cells were inoculated in YPD and grown overnight. The following day, cultures were diluted to an optical density of 0.2 (OD_{600nm}) and grown at 30 °C in agitation for 5–6 h (fermentation), 24–48 h (respiration) or more than 7 days (SP). Levels of glucose in the medium were determined by using the D-Glucose HK assay kit (Megazyme). Induction of quiescence by carbon source starvation was performed by growing the cells in YPD at 30 °C (before or after glucose exhaustion) and then transferring them to exhausted YPD or sterile water for at least 16 h. For nitrogen starvation experiments, cells were grown to an OD_{600nm} of 1 and transferred to a synthetic medium containing 0.17 % yeast nitrogen base (MP Biomedical) and 2 % glucose.

Density gradient fractionation

For density gradient fractionation, a solution of Percoll (Sigma-Aldrich) with a final NaCl concentration of 167 mM was added to a 30 ml Corex tube and centrifuged at 13,000 rpm for 20 min.

Approximately 2×10^9 cells were harvested, resuspended in 1 ml Tris buffer, added to the preformed gradient and centrifuged at 400 g_{av} for 60 min at 20 °C. Density gradient tubes were imaged, and fractions collected, washed once in water, and used directly for assays

or split into aliquots, pelleted, and frozen in liquid nitrogen. Cell number was determined for each fraction.

Viability (colony forming unit) assay

To test quiescent cells' colony forming ability, cultures were grown as indicated. After 24 h of quiescence induction (day 1 CLS), 50 μ l of each culture was collected, diluted 1:1.2 $\times 10^6$ and plated in YPD plates. Culture tubes were agitated at 30 °C for 7 days and plated. Colonies were counted after 3 days at 30 °C. Day 7 CLS was normalized to day 1 CLS. Plots represent the mean value obtained for at least three independent experiments; error bars correspond to standard error of the mean.

H₂O₂ treatment

To test whether direct addition of ROS in the medium of cultures undergoing fermentation could commit nuclei to form telomere hyperclusters during starvation, cells grown overnight were diluted to 0.002 OD_{600nm}/ml in fresh YPD containing no drugs or H₂O₂ 1 mM, grown until they reached 1 OD_{600nm}/ml, and then starved in water for at least 24 h.

Protein immunoblotting

For protein isolation, 200 μ l of trichloroacetic acid (TCA) 20 %, 200 μ l of TCA buffer [20 mM Tris-HCl pH 8, 50 mM ammonium acetate, 2 mM EDTA, 1 mM phenylmethylsulfonyl fluoride (PMSF)], 1 μ l of Protease inhibitor cocktail (Sigma-Aldrich), and 400 μ l of acid-washed glass beads (710–1180 μ m; Sigma-Aldrich) were added to 1 $\times 10^8$ pelleted cells. Cells were then disrupted by vigorous vortexing (1 min, two times). Resulting extracts were centrifuged for 30 min at 4 °C at 14,000 rpm, and pellets were resuspended in 200 μ l of TCA-Laemmli loading buffer (120 mM Tris base, 3.5 % sodium dodecyl sulfate (SDS), 8 mM EDTA, 5 % β -mercaptoethanol, 1 mM PMSF, 15 % glycerol, 0.01 % bromophenol blue). Samples were boiled for 10 min and centrifuged at 14,000 rpm for 10 min. Aliquots were immediately loaded or frozen. For immunoblotting, we used custom-made polyclonal antibodies against Rap1 (Agrobio, raised against Rap1[358–828] recombinant protein (a generous gift from M.H. LeDu, CEA Saclay) and Sir3 at 1:5000 [22]. Loading was normalized according to H2A at 1:5000 (Abcam).

Immuno-FISH

Immuno-FISH experiments were performed as in [22] with minor modifications. For quiescent cells, spheroplasting time was increased (20 min instead of 10 min).

Microscopy

Sets of images from any given figure panel were acquired the same day using identical acquisition parameters,

except for time course experiments where the same culture was imaged at different time points, using identical acquisition parameters and using a wild-type growing culture as control. Details are provided in Additional file 8.

Quantification of Rap1 foci

A dedicated tool has been designed to find and quantify the telomere cluster in the 3D images acquired with fluorescence microscopy. Details are provided in Additional file 8.

Construction of 3C libraries and sequencing

S. cerevisiae G1 daughter cells (strain BY4741) were recovered from an exponentially growing population through an elutriation procedure [48]. Long-lived quiescent cells were recovered as described above. 3C libraries were generated as described [49] with minor changes in the protocol. Briefly, the cells were cross-linked for 20 minutes with fresh formaldehyde (3 % final concentration), pooled as aliquots of 3 $\times 10^9$ cells, and stored at –80 °C until use. Aliquots were thawed on ice and resuspended in 6 ml 1 \times *DpnII* buffer (NEB). The cells were then split into four tubes and lysed using a Precellys grinder (3 cycles of 6500 rpm, 30 s ON/60 s OFF) and VK05 beads. The cells were incubated for 3 h with 50 units of restriction enzyme under agitation (*DpnII*; NEB). The digestion mix was then diluted into ligation buffer and a ligation was performed at 16 °C for 4 h followed by a decrosslinking step consisting of an overnight incubation at 65 °C in the presence of 250 μ g/ml proteinase K in 6.2 mM EDTA. DNA was then precipitated, resuspended in TE buffer, and treated with RNase.

The resulting 3C libraries were sheared and processed into Illumina libraries using custom-made versions of the Illumina paired-end adapters (Paired-End DNA Sample Prep Kit, Illumina PE-930-1001). Fragments of sizes between 400 and 800 bp were purified using a PippinPrep apparatus (SAGE Science), PCR amplified, and paired-end sequenced on an Illumina platform (HiSeq2000; 2 \times 100 bp).

Processing of paired-end reads

The raw data from each 3C experiment were processed as follows. First, PCR duplicates were collapsed using the six Ns present on each of the custom-made adapters. Reads were then aligned using Bowtie 2 in its most sensitive mode against the *S. cerevisiae* reference genome [50]. Paired-end reads were aligned as follows: for each read the length of the sequence mapped was increased gradually from 20 bp until the mapping became unambiguous (mapping quality >40). Paired reads were aligned independently.

Generation of contact maps

Each mapped read was assigned to a restriction fragment. Genome-wide contact matrices were built by binning the genome into units of 20 restriction fragments, resulting in 1797×1797 contact maps. The contact maps were subsequently filtered and normalized using the sequential component normalization procedure described in [51]. This procedure ensures that the sum over the column and lines of the matrix equals 1 and reduces the influence of biases inherent to the protocol. Full resolution contact maps binned at ten restriction fragments are available in the supplemental material section (Additional files 9, 10, 11 and 12). The 3D structures were directly computed from the normalized contact maps using ShRec3D [27]. The algorithm first computes a distance matrix from the contact map by assuming that the distance between each pair of beads is equal to the shortest path on the weighted graph associated with the inverse of the contact frequency between the two corresponding nodes. Multi-dimensional scaling is then applied to recover the optimal 3D coordinates from this distance matrix. To allow direct comparison between the structures obtained in different conditions we first re-scaled them to equalize the volume occupied by their associated convex hull. We then scaled the distances in each structure to account for the measured difference in size between nuclei in G0 and G1 daughter cells (1.5 and 1.7 μm , respectively; data not shown and [52]). Telomere pair distances were then directly computed from the structures to assess telomere re-organization.

Data availability

The sequences of the chromosome conformation capture experiments reported in this paper have been deposited in BioProject with accession number PRJNA291473 [53]. Microarray data are available from the Gene Expression Omnibus (GEO) under the accession number [GEO:GSE71273]. Microscopy data are available from Figshare [54].

Additional files

Additional file 1: Figure S1. Characterization of the SP silent chromatin hypercluster. **a** Western blot against Rap1 on crude extracts from exponential, respiratory, or stationary cultures of a WT strain (yAT1684). H2A antibody was used for the loading control. **b** Representative fluorescent images of wild-type (WT) strains tagged with Rap1-GFP “yAT1684”, GFP-Sir2 “yAT405”, Sir3-GFP “yAT779” and GFP-Sir4 “yAT431” strains. Overnight liquid cultures were diluted to 0.2 OD_{600nm}/ml and images were acquired after 5 h (1 OD_{600nm}/ml, fermentation phase) and 7 days (40 OD_{600nm}/ml, stationary phase). **c** Representative fluorescent image of a Rap1-GFP Sir3-mCherry-tagged strain “yAT194” from stationary phase cultures. We note that Sir3 associates with both telomeres and the rDNA in stationary phase cells. **d** Representative fluorescent images of Rap1-GFP in stationary cultures of WT “yAT1684” and *sir4Δ* “yAT2092” strains. **e** Representative fluorescent images of the nucleolar protein Sik1 tagged with mCherry during fermentation, respiration, and stationary phase

(“yAT340”). **f** Representative fluorescent image of Rap1-GFP Dad2-mRFP (Duo1 And Dam1 interacting, an essential component of the microtubule-kinetochore interface) tagged stationary phase cells (“yAT2279”).

g Representative fluorescent image of Sir3-mCherry Cse4-GFP-tagged strain “yAT2280” from stationary phase. Scale bar is 1 μm . (PDF 1343 kb)

Additional file 2: Movie S1. Related to Fig. 3. Animated 3D reconstruction of the entire contact map of G1 cells. Each chromosome is represented as a chain of beads (1 bead = 20 kb), and the color code reflects the chromosome arm length, from blue for short arms to red for long arms. Each chromosome carries a black bead that corresponds to the centromere position. Yellow beads = subtelomeric regions; black beads = centromeres; purple beads = boundaries of the rDNA cluster on chromosome XII (in pink/red). (GIF 15597 kb)

Additional file 3: Figure S2. SIR-mediated telomere clustering drives chromosome conformation in the dense fraction of SP cells. **a** Mean contacts frequencies between 100-kb centromeres windows in G1 (blue) and G0 quiescent cells (red). Black and green curves: contacts between 100-kb segments randomly sampled in both conditions, to illustrate the absence of coverage biases after normalization. **b** Chromosome organization of WT and *sir3Δ* quiescent cells (the cryptic mating type locus *HML* was deleted to prevent pseudo-diploid effect). ii) Normalized contact matrix obtained for *hmlΔ** (left) and *hmlΔ sir3Δ* (right) cells. Color scale: contact frequencies from rare (white) to frequent (dark blue). Red arrowheads: centromeres contacts; green and yellow arrowheads: telomere–telomere contacts in *hmlΔ* and *hmlΔ sir3Δ* G0 cells, respectively. The 3D representations of the *hmlΔ* and *hmlΔ sir3Δ* matrices are represented next to the contact maps. Each chromosome is represented as a chain of beads (1 bead = 20 kb), with color code reflecting the chromosome arm lengths, from short (blue) to long (red) arms. Yellow beads: subtelomeric regions; black beads: centromeres; purple beads: boundaries of the rDNA cluster. **c** Contact maps of W303 strain during exponentially growth (EXPO, left) and quiescence (G0, right). Red arrowheads: centromere clustering; green and yellow arrowheads: telomere–telomere contacts of two chromosomes (XIII and XV) in expo and G0 cells, respectively. Because of the low sequencing coverage and quality, the signal is not as strong as for data in Fig. 3 and the bins are larger (1 vector: 80 *Dpnl* RFs). **d** Quantification of colocalization of 30-kb telomeric regions (red dots) compared with the distribution of the colocalization scores (box plot, two standard deviations) computed for 1000 random sets of 32 windows of 30 kb in the genome (excluding centromeric regions). The colocalization score is normalized by the sequencing depth for each dataset.

Additional file 4: Movie S2. Related to Fig. 3. Animated 3D reconstruction of the entire contact map of long-lived SP cells (isolated from a SP culture by density gradient). Same annotations as in Additional file 2. (GIF 12057 kb)

Additional file 5: Figure S3. Telomere hyperclustering is not due to slow growth. **a** Representative fluorescent image of Rap1-GFP tagged strain grown either at 30 °C or 25 °C in exponential phase (top) and then starved for 16 h in water before imaging (bottom). **b** Calcofluor staining of LD and HD fractions of a post DS culture after gradient separation. **c** Heat shock (HS) assay on the LD and HD fractions used in **b**. (PDF 11591 kb)

Additional file 6: Figure S4. Mechanism driving telomere clustering in long-lived SP cells. **a** Western blot against Sir3 and H2A on crude extracts from exponential, respiratory, or stationary cultures of a wild-type (WT) strain (yAT1684). **b** Sir3 spreading at yeast subtelomeres in cells from an exponentially growing culture (Fermentation) or in cells isolated from the dense fraction of a SP culture (Stationary HD). ChIP-chip profiles (Sir3 enrichment Z score) correspond to the mean of two independent experiments. Pearson correlation between conditions is 0.95. Sir3 spreading at TELVIR was confirmed in independent experiments by ChIP-quantitative PCR for both conditions (not shown). Each panel spans the first 30 kb from each telomere and the heading color for each panel indicates the middle repeat element content of the corresponding telomere: Y' XCR XCS (beige), Y' XCS (green), XCS (red), or XCR XCS (blue). Each dot represents a data point and lines are drawn for visual purposes. **c** Quiescent *sir3Δ* cells are as thermotolerant as quiescent WT cells to heat shock (HS). Dilution assays are shown (starting at DO_{600nm} = 5 and diluted 1/5 each time). Left: growth control of exponential cells or 24 h LD cells. Middle: sensitivity to HS of WT exponential cells, 24 h LD cells or 24 h HD cells. Right: sensitivity to HS of WT or *sir3Δ* LD cells. **d** Stationary WT, *sir3Δ*, *sir3-Δ2Q* cells are resistant to HS like WT cells. Dilution

assays are shown (starting at $DO_{600nm} = 1$ and diluted 1/5 each time). *Left*: growth control. *Middle*: 30 min 52 °C HS. *Left*: 1 h 52 °C HS. **e** Stationary WT and *sir3Δ* cells that spent 14 days in water after glucose exhaustion show the same extent of thermotolerance to a 1 h 52 °C HS. Dilution assays are shown (starting at $DO_{600nm} = 1$ and diluted 1/5 each time). (PDF 12384 kb)

Additional file 7: Table S1. Strains used in this study. (DOCX 22 kb)

Additional file 8: Additional experimental procedures. (DOCX 32 kb).

Additional file 9: Full resolution contact map binned at 10 RF of G1 population presented in Fig. 3. (DAT 24.7 mb)

Additional file 10: Full resolution contact map binned at 10 RF of G0 population presented in Fig. 3. (DAT 16.3 mb)

Additional file 11: Full resolution contact map binned at 10 RF of G0 WT population presented in Additional file 3. (DAT 24.6 mb)

Additional file 12: Full resolution contact map binned at 10 RF of G0 *sir3Δ* population presented in Additional file 3. (DAT 24.6 mb)

Abbreviations

3C: capture of chromosome conformation; 3D: three-dimensional; bp: base pair; ChIP: chromatin immunoprecipitation; CLS: chronological lifespan; FISH: fluorescence in situ hybridization; GFP: green fluorescent protein; HD: high density; LD: low density; PMSF: phenylmethylsulfonyl fluoride; ROS: reactive oxygen species; SP: stationary phase; TCA: trichloroacetic acid.

Competing interests

All the authors declare that they have no competing interests.

Authors' contributions

MG generated strains and performed microscopy, lifespan, western blots and ROS treatment experiments. MR generated strains and contributed to microscopy experiments and writing/revising the manuscript. MM performed Hi-C experiments. IL contributed to lifespan experiments. AC conducted the bioinformatics analysis of the contact data. CB developed image analysis tools. AH performed and analyzed ChIP on ChIP experiments. JM built the 3D structures and performed bioinformatics analysis. AT, MG, MR and RK contributed to the design and interpretation of the study, drafting the figures and writing/revising the manuscript. All authors read and approved the final manuscript.

Acknowledgments

We thank Patricia Le Baccon for assistance with microscopy, M.H. LeDu for providing recombinant Rap1, and Sheldon Decombe for his help on Fig. 6b. We also thank Geneviève Almouzni for critical reading of the manuscript and the members of the Taddei laboratory. AT and MG thank Isabelle Sagot for discussion and sharing unpublished results. RK and MM thank Alain Jacquier and Gwenaél Badis-Breard for their constructive suggestions and comments and their help in the preparation of BY quiescent strains. M. Guidi was supported by a doctoral fellowship from the Association pour la Recherche sur le Cancer and the Institut Curie. M.M. is the recipient of an Association pour la Recherche sur le Cancer fellowship 20100600373. The research leading to these results has received funding from the European Research Council under the European Community's Seventh Framework Program (FP7/2007 2013/European Research Council grant agreement 210508 to AT and 260822 to RK) and the investissement d'avenir (Labex DEEP) Agence Nationale de la Recherche to A.T.

Author details

¹Institut Curie, PSL Research University, Paris F-75248, France. ²CNRS, UMR 3664, Paris F-75248, France. ³Institut Pasteur, Department Genomes and Genetics, Groupe Régulation Spatiale des Génomes, 75015 Paris, France. ⁴CNRS, UMR 3525, 75015 Paris, France. ⁵LPTMC, Université Pierre et Marie Curie, UMR 7600, Sorbonne Universités, 4 Place Jussieu, 75005 Paris, France. ⁶Sorbonne Universités, UPMC Univ, Paris 06, France.

Received: 2 April 2015 Accepted: 1 September 2015

Published online: 23 September 2015

References

1. Van Bortle K, Corces VG. Nuclear organization and genome function. *Annu Rev Cell Dev Biol.* 2012;28:163–87.

- Meister P, Taddei A. Building silent compartments at the nuclear periphery: a recurrent theme. *Curr Opin Genet Dev.* 2013;23:96–103.
- Tanaka A, Tanizawa H, Sriswasdi S, Iwasaki O, Chatterjee AG, Speicher DW, et al. Epigenetic regulation of condensin-mediated genome organization during the cell cycle and upon DNA damage through histone H3 lysine 56 acetylation. *Mol Cell.* 2012;48:532–46.
- Carone DM, Lawrence JB. Heterochromatin instability in cancer: from the Barr body to satellites and the nuclear periphery. *Semin Cancer Biol.* 2012;23:99.
- Andrulis ED, Neiman AM, Zappulla DC, Sternglanz R. Perinuclear localization of chromatin facilitates transcriptional silencing. *Nature.* 1998;394:592–5.
- Gotta M, Laroche T, Formenton A, Mailet L, Scherthan H, Gasser SM. The clustering of telomeres and colocalization with Rap1, Sir3, and Sir4 proteins in wild-type *Saccharomyces cerevisiae*. *J Cell Biol.* 1996;134:1349–63.
- Mailet L, Boscheron C, Gotta M, Marcand S, Gilson E, Gasser SM. Evidence for silencing compartments within the yeast nucleus: a role for telomere proximity and Sir protein concentration in silencer-mediated repression. *Genes Dev.* 1996;10:1796–811.
- Taddei A, Van Houwe G, Nagai S, Erb I, van Nimwegen E, Gasser SM. The functional importance of telomere clustering: Global changes in gene expression result from SIR factor dispersion. *Genome Res.* 2009;19:611–25.
- Ferreira HC, Luke B, Schober H, Kalck V, Lingner J, Gasser SM. The PIAS homologue Siz2 regulates perinuclear telomere position and telomerase activity in budding yeast. *Nat Cell Biol.* 2011;13:867–74.
- Schober H, Ferreira H, Kalck V, Gehlen LR, Gasser SM. Yeast telomerase and the SUN domain protein Mps3 anchor telomeres and repress subtelomeric recombination. *Genes Dev.* 2009;23:928–38.
- Duan Z, Andronescu M, Schutz K, Mcllwain S, Kim YJ, Lee C, et al. A three-dimensional model of the yeast genome. *Nature.* 2010;465:363–7.
- Taddei A, Gasser SM. Structure and function in the budding yeast nucleus. *Genetics.* 2012;192(1):107–29.
- Rabl C. über Zellteilung. *Morphol Jahrbuch.* 1885;10:214–330.
- Tjong H, Gong K, Chen L, Alber F. Physical tethering and volume exclusion determine higher-order genome organization in budding yeast. *Genome Res.* 2012;22:1295–305.
- Tokuda N, Terada TP, Sasai M. Dynamical modeling of three-dimensional genome organization in interphase budding yeast. *Biophys J.* 2012;102:296–304.
- Wong H, Marie-Nelly H, Herbert S, Carrivain P, Blanc H, Koszul R, et al. A predictive computational model of the dynamic 3D interphase yeast nucleus. *Curr Biol.* 2012;22:1881–90.
- Broach JR. Nutritional control of growth and development in yeast. *Genetics.* 2012;192:73–105.
- Martinez MJ, Roy S, Archuleta AB, Wentzell PD, Anna-Arriola SS, Rodriguez AL, et al. Genomic analysis of stationary-phase and exit in *Saccharomyces cerevisiae*: gene expression and identification of novel essential genes. *Mol Biol Cell.* 2004;15:5295–305.
- Gasch AP, Spellman PT, Kao CM, Carmel-Harel O, Eisen MB, Storz G, et al. Genomic expression programs in the response of yeast cells to environmental changes. *Mol Biol Cell.* 2000;11:4241–57.
- Ristow M, Schmeisser S. Extending life span by increasing oxidative stress. *Free Radic Biol Med.* 2011;51:327–36.
- Klosinska MM, Crutchfield CA, Bradley PH, Rabinowitz JD, Broach JR. Yeast cells can access distinct quiescent states. *Genes Dev.* 2011;25:336–49.
- Ruault M, De Meyer A, Loidice I, Taddei A. Clustering heterochromatin: Sir3 promotes telomere clustering independently of silencing in yeast. *J Cell Biol.* 2011;192:417–31.
- Fuge EK, Braun EL, Werner-Washburne M. Protein synthesis in long-term stationary-phase cultures of *Saccharomyces cerevisiae*. *J Bacteriol.* 1994;176:5802–13.
- Laporte D, Courtout F, Salin B, Ceschin J, Sagot I. An array of nuclear microtubules reorganizes the budding yeast nucleus during quiescence. *J Cell Biol.* 2013;203:585–94.
- Allen C, Butner S, Aragon AD, Thomas JA, Meirelles O, Jaetao JE, et al. Isolation of quiescent and nonquiescent cells from yeast stationary-phase cultures. *J Cell Biol.* 2006;174:89–100.
- Dekker J, Rippe K, Dekker M, Kleckner N. Capturing chromosome conformation. *Science.* 2002;295:1306–11.
- Lesne A, Riposo J, Cournac A, Mozziconacci J. A fast algorithm to reconstruct 3D genome structures from chromosomal contact maps. *Nat Methods.* 2014;11:1141–3.

28. Therizols P, Duong T, Dujon B, Zimmer C, Fabre E. Chromosome arm length and nuclear constraints determine the dynamic relationship of yeast subtelomeres. *Proc Natl Acad Sci U S A*. 2010;107:2025–30.
29. Li L, Miles S, Melville Z, Prasad A, Bradley G, Breeden LL. Key events during the transition from rapid growth to quiescence in budding yeast require posttranscriptional regulators. *Mol Biol Cell*. 2013;24:3697–709.
30. Lu C, Brauer MJ, Botstein D. Slow growth induces heat-shock resistance in normal and respiratory-deficient yeast. *Mol Biol Cell*. 2009;20:891–903.
31. Yun J, Finkel T. Mitohormesis. *Cell Metab*. 2014;19:757–66.
32. Veal EA, Day AM, Morgan BA. Hydrogen peroxide sensing and signaling. *Mol Cell*. 2007;26:1–14.
33. Mesquita A, Weinberger M, Silva A, Sampaio-Marques B, Almeida B, Leao C, et al. Caloric restriction or catalase inactivation extends yeast chronological lifespan by inducing H₂O₂ and superoxide dismutase activity. *Proc Natl Acad Sci U S A*. 2010;107:15123–8.
34. Fabrizio P, Liou LL, Moy VN, Diaspro A, Valentine JS, Gralla EB, et al. SOD2 functions downstream of Sch9 to extend longevity in yeast. *Genetics*. 2003;163:35–46.
35. Oppikofer M, Kueng S, Gasser SM. SIR-nucleosome interactions: structure-function relationships in yeast silent chromatin. *Gene*. 2013;527:10–25.
36. Davidson GS, Joe RM, Roy S, Meirelles O, Allen CP, Wilson MR, et al. The proteomics of quiescent and nonquiescent cell differentiation in yeast stationary-phase cultures. *Mol Biol Cell*. 2011;22:988–98.
37. Leroy C, Mann C, Marsolier MC. Silent repair accounts for cell cycle specificity in the signaling of oxidative DNA lesions. *EMBO J*. 2001;20:2896–906.
38. Schroeder EA, Raimundo N, Shadel GS. Epigenetic silencing mediates mitochondria stress-induced longevity. *Cell Metab*. 2013;17:954–64.
39. Tsang CK, Liu Y, Thomas J, Zhang Y, Zheng XF. Superoxide dismutase 1 acts as a nuclear transcription factor to regulate oxidative stress resistance. *Nat Commun*. 2014;5:3446.
40. Dixon JR, Jung I, Selvaraj S, Shen Y, Antosiewicz-Bourget JE, Lee AY, et al. Chromatin architecture reorganization during stem cell differentiation. *Nature*. 2015;518:331–6.
41. Bridger JM, Boyle S, Kill IR, Bickmore WA. Re-modelling of nuclear architecture in quiescent and senescent human fibroblasts. *Curr Biol*. 2000;10:149–52.
42. Corpet A, Stucki M. Chromatin maintenance and dynamics in senescence: a spotlight on SAHF formation and the epigenome of senescent cells. *Chromosoma*. 2014;123:423.
43. Solovei I, Kreysing M, Lanctot C, Kosem S, Peichl L, Cremer T, et al. Nuclear architecture of rod photoreceptor cells adapts to vision in mammalian evolution. *Cell*. 2009;137:356–68.
44. Fabrizio P, Gattazzo C, Battistella L, Wei M, Cheng C, McGrew K, et al. Sir2 blocks extreme life-span extension. *Cell*. 2005;123:655–67.
45. Casatta N, Porro A, Orlandi I, Brambilla L, Vai M. Lack of Sir2 increases acetate consumption and decreases extracellular pro-aging factors. *Biochim Biophys Acta*. 2013;1833:593–601.
46. Thomas BJ, Rothstein R. Elevated recombination rates in transcriptionally active DNA. *Cell*. 1989;56:619–30.
47. Longtine MS, McKenzie 3rd A, Demarini DJ, Shah NG, Wach A, Brachet A, et al. Additional modules for versatile and economical PCR-based gene deletion and modification in *Saccharomyces cerevisiae*. *Yeast*. 1998;14:953–61.
48. Marbouty M, Ermont C, Dujon B, Richard GF, Koszul R. Purification of G1 daughter cells from different *Saccharomyces* species through an optimized centrifugal elutriation procedure. *Yeast*. 2014;31:159–66.
49. Marie-Nelly H, Marbouty M, Courmac A, Liti G, Fischer G, Zimmer C, et al. Filling annotation gaps in yeast genomes using genome-wide contact maps. *Bioinformatics*. 2014;30:2105–13.
50. Langmead B, Salzberg SL. Fast gapped-read alignment with Bowtie 2. *Nat Methods*. 2012;9:357–9.
51. Cournac A, Marie-Nelly H, Marbouty M, Koszul R, Mozziconacci J. Normalization of a chromosomal contact map. *BMC Genomics*. 2012;13:436.
52. Heun P, Laroche T, Shimada K, Furrer P, Gasser SM. Chromosome dynamics in the yeast interphase nucleus. *Science*. 2001;294:2181–6.
53. BioProject: *Saccharomyces cerevisiae* strain:BY4741/W303 (baker's yeast). <http://www.ncbi.nlm.nih.gov/bioproject/291473>.
54. figshare: Guidi et al. 2015. <http://dx.doi.org/10.6084/m9.figshare.1505174>.

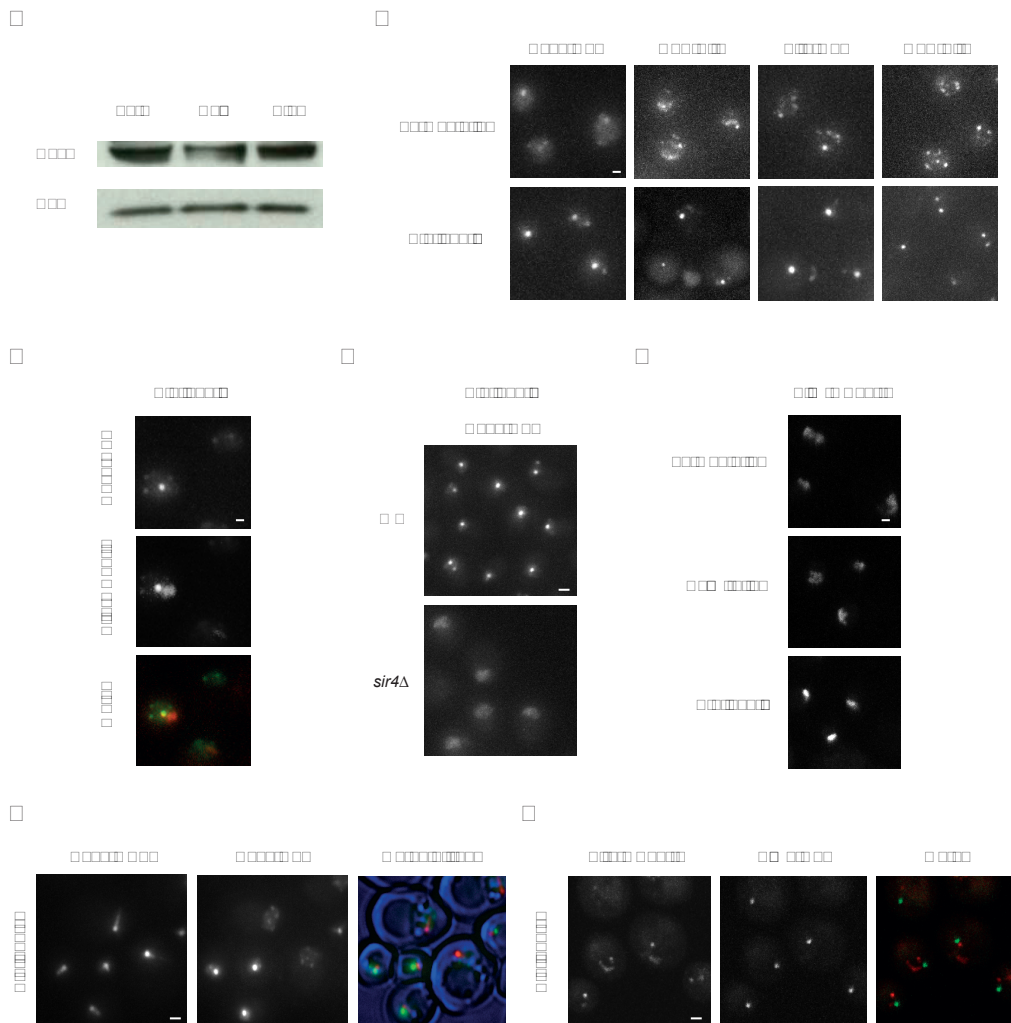
Submit your next manuscript to BioMed Central and take full advantage of:

- Convenient online submission
- Thorough peer review
- No space constraints or color figure charges
- Immediate publication on acceptance
- Inclusion in PubMed, CAS, Scopus and Google Scholar
- Research which is freely available for redistribution

Submit your manuscript at
www.biomedcentral.com/submit



??

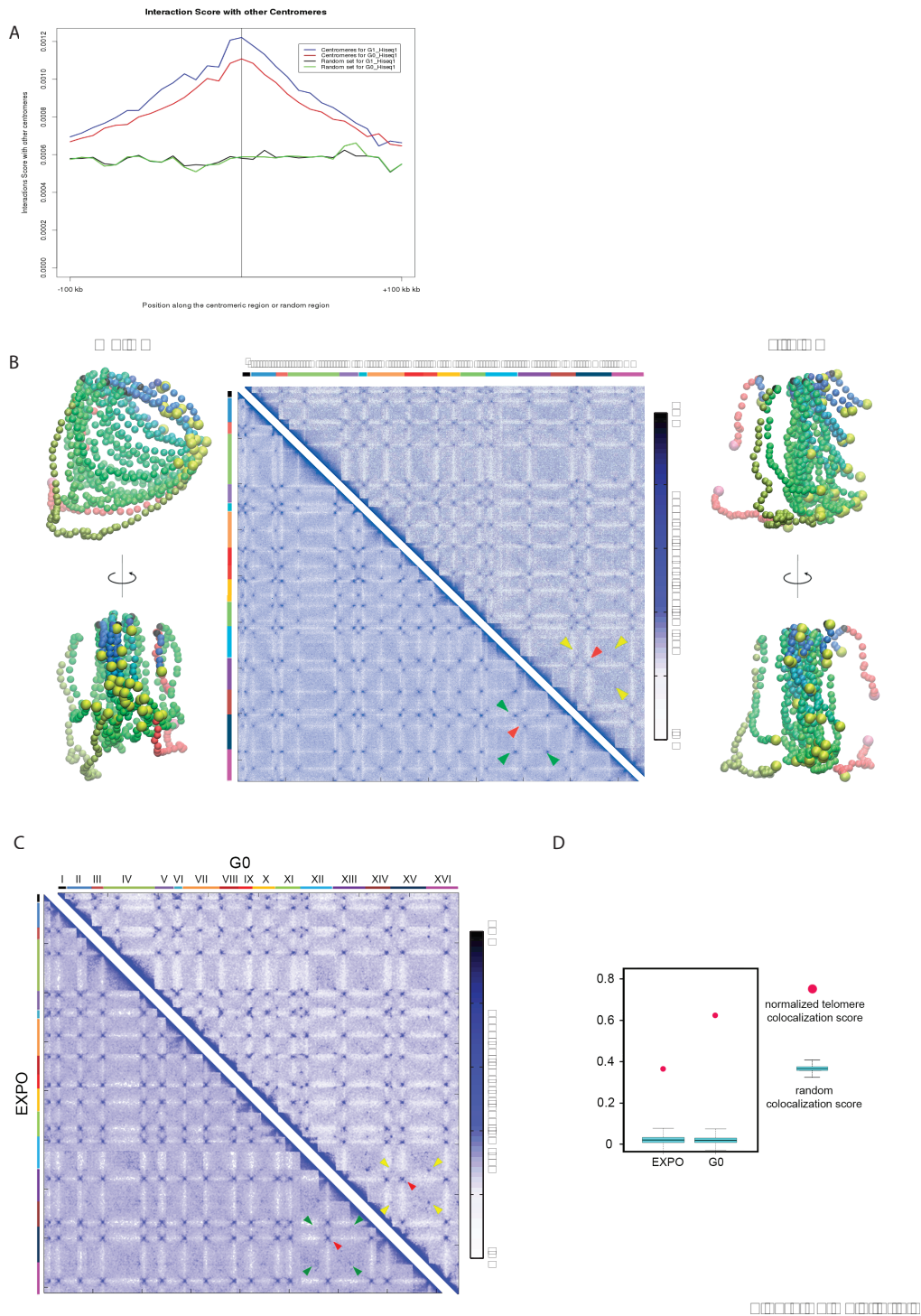


Additional File 1: Figure S1:

Characterization of the SP silent chromatin hypercluster. **a** Western blot against Rap1 on crude extracts from exponential, respiratory, or stationary cultures of a WT strain (yAT1684). H2A antibody was used for the loading control. **b** Representative fluorescent images of wild-type (WT) strains tagged with Rap1-GFP “yAT 1684”, GFP-Sir2 “yAT405”, Sir3-GFP “yAT779” and GFP-Sir4 “yAT431” strains. Overnight liquid cultures were diluted to 0.2 OD_{600nm} /ml and images were acquired after 5 h (1 OD_{600nm} /ml, fermentation phase) and 7 days (40 OD_{600nm} /ml, stationary phase). **c** Representative fluorescent image of a Rap1-GFP Sir3-mCherry-tagged strain “yAT194” from stationary phase cultures. We note that Sir3 associates with both telomeres and the rDNA in stationary phase cells. **d** Representative fluorescent images of Rap1-GFP in stationary cultures of WT “yAT1684” and *sir4Δ* “yAT2092” strains. **e** Representative fluorescent images of the nucleolar protein Sik1 tagged with mCherry during fermentation, respiration, and stationary phase (“yAT340”). **f** Representative fluorescent image of Rap1-GFP Dad2-mRFP (Duo1 And Dam1 interacting, an essential component of the microtubule–kinetochore interface) tagged stationary phase cells (“yAT2279”). **g** Representative fluorescent image of Sir3-mCherry Cse4-GFP-tagged strain “yAT2280” from stationary phase. Scale bar is 1 μm.

?

??



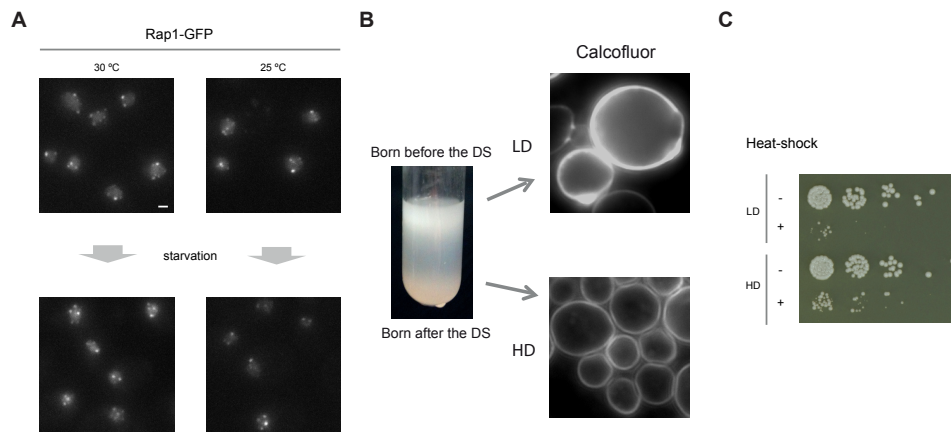
Additional file 3: Figure S2:??

SIR-mediated telomere clustering drives chromosome conformation in the dense fraction of SP cells. **a** Mean contacts frequencies between 100-kb centromeres windows in G1 (*blue*) and G0 quiescent cells (*red*). Black and green curves: contacts between 100-kb segments randomly sampled in both conditions, to illustrate the absence of coverage biases after normalization. **b** Chromosome organization of WT and *sir3Δ* quiescent cells (the cryptic mating type locus *HML* was deleted to prevent pseudo-diploid effect). ii) Normalized contact matrix obtained for *hmlΔ** (*left*) and *hmlΔ sir3Δ* (*right*) cells. Colour scale: contact frequencies from rare (*white*) to frequent

?

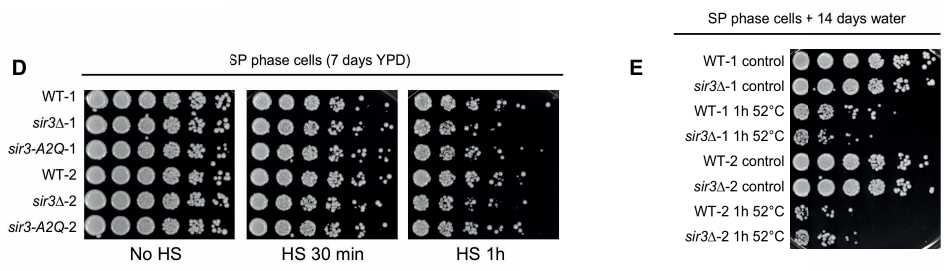
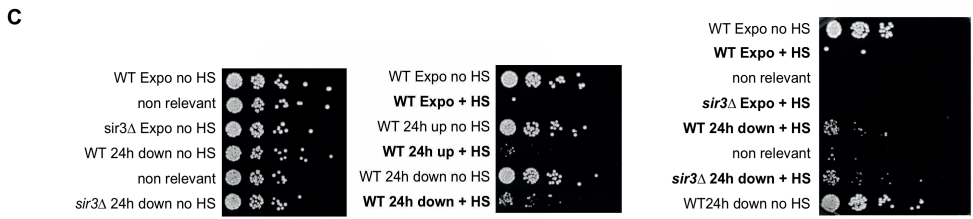
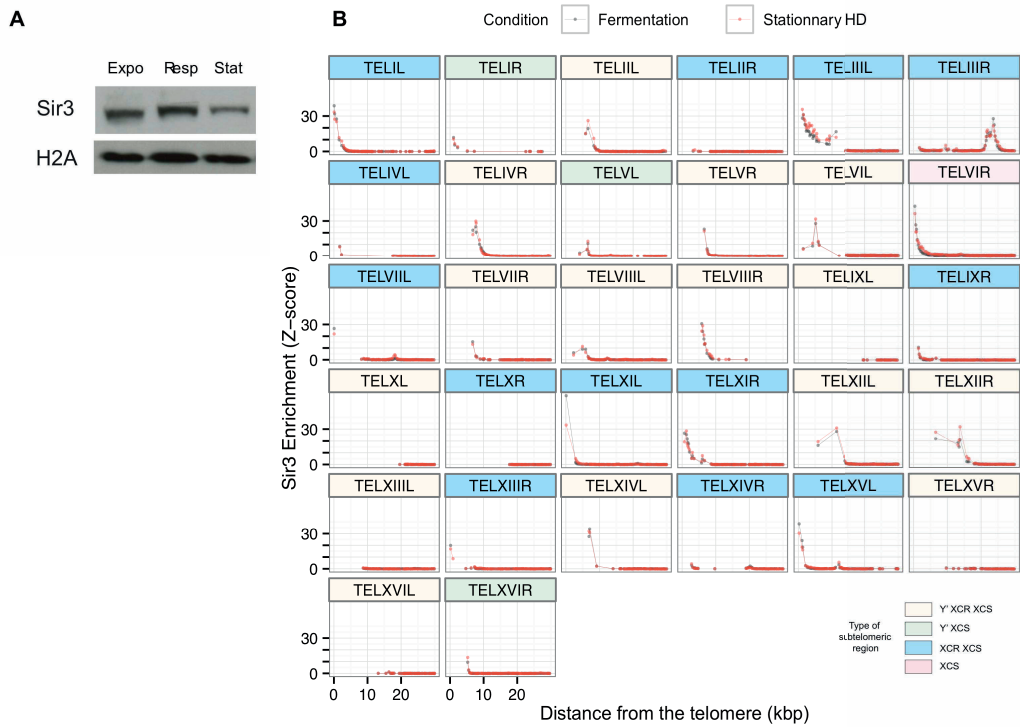
xB

(dark blue). Red arrowheads: centromeres contacts; green and yellow arrowheads: telomere–telomere contacts in *hmlΔ* and *hmlΔ sir3Δ* G0 cells, respectively. The 3D representations of the *hmlΔ* and *hmlΔ sir3Δ* matrices are represented next to the contact maps. Each chromosome is represented as a chain of beads (1 bead = 20 kb), with colour code reflecting the chromosome arm lengths, from short (blue) to long (red) arms. Yellow beads: subtelomeric regions; black beads: centromeres; purple beads: boundaries of the rDNA cluster. **c** Contact maps of W303 strain during exponentially growth (EXPO, left) and quiescence (G0, right). Red arrowheads: centromere clustering; green and yellow arrowheads: telomere–telomere contacts of two chromosomes (XIII and XV) in expo and G0 cells, respectively. Because of the low sequencing coverage and quality, the signal is not as strong as for data in Fig. 3 and the bins are larger (1 vector: 80 *DpnII* RFs). **d** Quantification of colocalization of 30-kb telomeric regions (red dots) compared with the distribution of the colocalization scores (box plot, two standard deviations) computed for 1000 random sets of 32 windows of 30 kb in the genome (excluding centromeric regions). The colocalization score is normalized by the sequencing depth for each dataset.



Additional file 5: Figure S3

Telomere hyperclustering is not due to slow growth. **a** Representative fluorescent image of Rap1-GFP tagged strain grown either at 30 °C or 25 °C in exponential phase (*top*) and then starved for 16 h in water before imaging (*bottom*). **b** Calcofluor staining of LD and HD fractions of a post DS culture after gradient separation. **c** Heat shock (HS) assay on the LD and HD fractions used in **b**. (PDF 11591 kb)



Additional file 6: Figure S4

Mechanism driving telomere clustering in long-lived SP cells. **a** Western blot against Sir3 and H2A on crude extracts from exponential, respiratory, or stationary cultures of a wild-type (WT) strain (*yAT1684*). **b** Sir3 spreading at yeast subtelomeres in cells from an exponentially growing culture (*Fermentation*) or in cells isolated from the dense fraction of a SP culture (*Stationary HD*). ChIP-chip profiles (Sir3 enrichment Z score) correspond to the mean of two independent

experiments. Pearson correlation between conditions is 0.95. Sir3 spreading at TELVIR was confirmed in independent experiments by ChIP-quantitative PCR for both conditions (not shown). Each panel spans the first 30 kb from each telomere and the heading color for each panel indicates the middle repeat element content of the corresponding telomere: Y' XCR XCS (*beige*), Y' XCS (*green*), XCS (*red*), or XCR XCS (*blue*). Each dot represents a data point and lines are drawn for visual purposes. **c** Quiescent *sir3*Δ cells are as thermotolerant as quiescent WT cells to heat shock (HS). Dilution assays are shown (starting at DO_{600nm} = 5 and diluted 1/5 each time). *Left*: growth control of exponential cells or 24 h LD cells. *Middle*: sensitivity to HS of WT exponential cells, 24 h LD cells or 24 h HD cells. *Right*: sensitivity to HS of WT or *sir3*Δ LD cells. **d** Stationary WT, *sir3*Δ, *sir3-A2Q* cells are resistant to HS like WT cells. Dilution assays are shown (starting at DO_{600nm} = 1 and diluted 1/5 each time). *Left*: growth control. *Middle*: 30 min 52 °C HS. *Left*: 1 h 52 °C HS. **e** Stationary WT and *sir3*Δ cells that spent 14 days in water after glucose exhaustion show the same extent of thermotolerance to a 1 h 52 °C HS. Dilution assays are shown (starting at DO_{600nm} = 1 and diluted 1/5 each time).

Additional file 7: Table S1: Strains used in this study

<u>W303</u> :	ade2-1 can1-100 his3-11,15 leu2-3,112 rad5- trp1-1 ura3-1
yAT194	MATa adh4::URA3-4xUASG-(C1-3A)n ppr1Δ::HIS3 rap1::GFP-RAP1(LEU2) sir3::SIR3-mcherry::kan(ADE2)
<u>yAT340</u>	MATa ade2-1::ADE2 sik1::SIK1-mRFP(KanMX) rap1::GFP-RAP1(LEU2)
yAT405	MATa ade2-1::ADE2 sik1::SIK1-mRFP(KanMX) sir2::SIR2-yeGFP(HPH)
yAT431	MATa ade2-1::ADE2 sik1::SIK1-mRFP(KanMX) sir4::GFP-SIR4(URA3)
yAT779	MATa ade2-1::ADE2 sir3::SIR3-GFP(LEU2)
yAT1684	MATa hmlΔ::HPH RAD5 rap1::GFP-RAP1(LEU2) RDN1::ADE2
yAT2022	MATa hmlΔ::HPH RAD5 rap1::GFP-RAP1(LEU2) RDN1::ADE2 sir3Δ::KanMX
yAT2092	MATa hmlΔ::HPH RAD5 rap1::GFP-RAP1(LEU2) RDN1::ADE2 sir4Δ::HIS5
yAT2279	MATa dad2::DAD2-TagRFP-T(SpHIS5) hmlΔ::HPH rap1::GFP-RAP1(LEU2) RDN1::ADE2
yAT2280	MATa cse4::CSE4-GFP(S65T) RAD5 sir3::SIR3-mcherry::kan(ADE2)
yAT2332	MATa hmlΔ::HPH RAD5 rap1::GFP-RAP1(LEU2) RDN1::ADE2 sir3Δ::KanMX pSIR3::SIR3(HIS3)
yAT2333	MATa hmlΔ::HPH RAD5 rap1::GFP-RAP1(LEU2) RDN1::ADE2 sir3Δ::KanMX pSIR3::sir3-A2Q(HIS3)
yAT2338	MATa his3::HIS3 hmlΔ::HPH RAD5 rap1::GFP-RAP1(LEU2) RDN1::ADE2 sir3Δ::KanMX
yAT2407	MATa ade2-1::ADE2 hmlΔ::HPH nup49::GFP-NUP49 rap1::yemRFP-RAP1(LEU2)

yAT2543 MATa ctt1Δ::HPH hmlΔ::HPH RAD5 rap1::GFP-RAP1(LEU2) RDN1::ADE2
yAT2546 MATa hmlΔ::HPH RAD5 rap1::GFP-RAP1(LEU2) RDN1::ADE2 sod2::GPD-SOD2(NAT)

BY: his3Δ0 leu2Δ0 met15Δ0 ura3Δ0

BY4141 MATa

yAT2527 MATa hmlΔ::HPH

yAT2540 MATa hmlΔ::HPH sir3Δ::KanMX

Result part II:

Quiescent-specific telomere hyper-cluster is a Mec1/Rad53-dependent programmed event

It is nowadays clear that budding yeast cells can reach different quiescent states depending on the conditions inducing the cell cycle exit leading to different outcome in terms of chronological life span (Broach, 2012; Guidi et al., 2015; Klosinska et al., 2011a, b). Thus, deciphering the pathways leading to the different quiescent states is essential to understand mechanisms that extend lifespan.

Progressive exhaustion of the carbon source is known to lead to quiescent cells able to sustain viability over several weeks (Allen et al., 2006; Davidson et al., 2011; Li et al., 2013). It is well documented that within hours of scavenging all the glucose in the medium, budding yeast cells undergo highly asymmetric cell divisions and build protective cell walls on the daughters that will give rise to the dense quiescent cells able to sustain long-term viability in stationary phase. These SP dense cells exhibit high rates of respiration -6 fold higher than their less dense counterpart (Davidson et al., 2011). This is consistent with the finding that mitochondrial function is important for survival within the stationary phase (Aerts et al., 2009; Aragon et al., 2008; Broach, 2012; Fabrizio et al., 2010; Guidi et al., 2015; Martinez et al., 2004; Mesquita et al., 2010) .

Our recent data unveiled that following carbon source exhaustion, the telomeres of quiescent cells group into a unique focus or “hypercluster”, localized in the center of the nucleus, thus constraining the global organization of the genome. Importantly, hypercluster formation occurs specifically in quiescent cells able to sustain long-term viability and contribute to lifespan extension by a yet unknown mechanism (Guidi et al., 2015).

We further showed that the ability to form telomere hyperclusters required mitochondrial activity and is acquired by the quiescent fraction of SP cells. Although cells undergoing fermentation –before the diauxic shift- are unable to form hyperclusters in case of abrupt starvation, a mild H₂O₂ treatment during glucose fermentation was

sufficient to prime these cells to form a telomere hypercluster upon starvation. As H₂O₂ pretreated quiescent cells had almost 100% viability after 1 week of starvation, our data support the hypothesis that health and lifespan could be promoted by mtROS adaptive signaling – also known as mitohormesis (Ristow and Schmeisser, 2011; Yun and Finkel, 2014).

Our data suggest that, after the diauxic shift, mitochondrial activity -through the production of reactive oxygen species (mt-ROS) during cell respiration- commits a subpopulation of cells to respond to starvation by reorganizing their telomeres forming a hypercluster (Guidi et al., 2015).

Here, we further characterized the cascade of events leading to this commitment. Our results indicate that 12 hours after the diauxic shift, cells from the dense fraction of the culture are already committed to form hyperclusters upon starvation. We show that this commitment is linked to the respiration process, in particular to mtROS signaling, and involves the activation of the Mec1/Rad53/Rph1 check-point pathway.

Telomere hyperclustering is a programmed event

Around 10-12h after the diauxic shift, the cell population differentiates into a dense fraction containing mainly un-budded daughter cells that will become the long-lived quiescent cells upon carbon source exhaustion and a less dense fraction containing mother cells that will have a shorter lifespan, (Allen et al., 2006; Davidson et al., 2011). We ask whether these two populations show a different telomere distribution by monitoring the distribution of telomeric protein Rap1 fused to GFP. We did not observe any major differences in Rap1-GFP foci distribution between the low (LD) and high (HD) density fractions (Figure. 1A left and 1B). To test whether the ability to form the hypercluster is already present at this step, we abruptly starved the two fractions in water. Interestingly, these two fractions behaved differently upon the induction of quiescence by starvation (Figure 1A right and 1B): we observed bright Rap1-GFP foci (hyperclusters) in the middle of the nuclei of HD cells, whereas the foci did not reorganize in less dense cells. Cells containing hyperclusters had a longer CLS: although cells from both fractions displayed slight differences in viability before starvation (75% for the LD versus 95% for the HD, not shown), only 15% of cells from the LD

??

population, which did not contain hyperclusters, were able to form a colony at day 7, compared to 90% of the HD population, which contain hyperclusters (Figure 1C). These results indicate that 3-4 days before carbon source exhaustion and before the induction of quiescence, the HD subpopulation of cells is already committed to form telomere hyperclusters and to maintain long-term viability upon starvation (Figure 1 D).

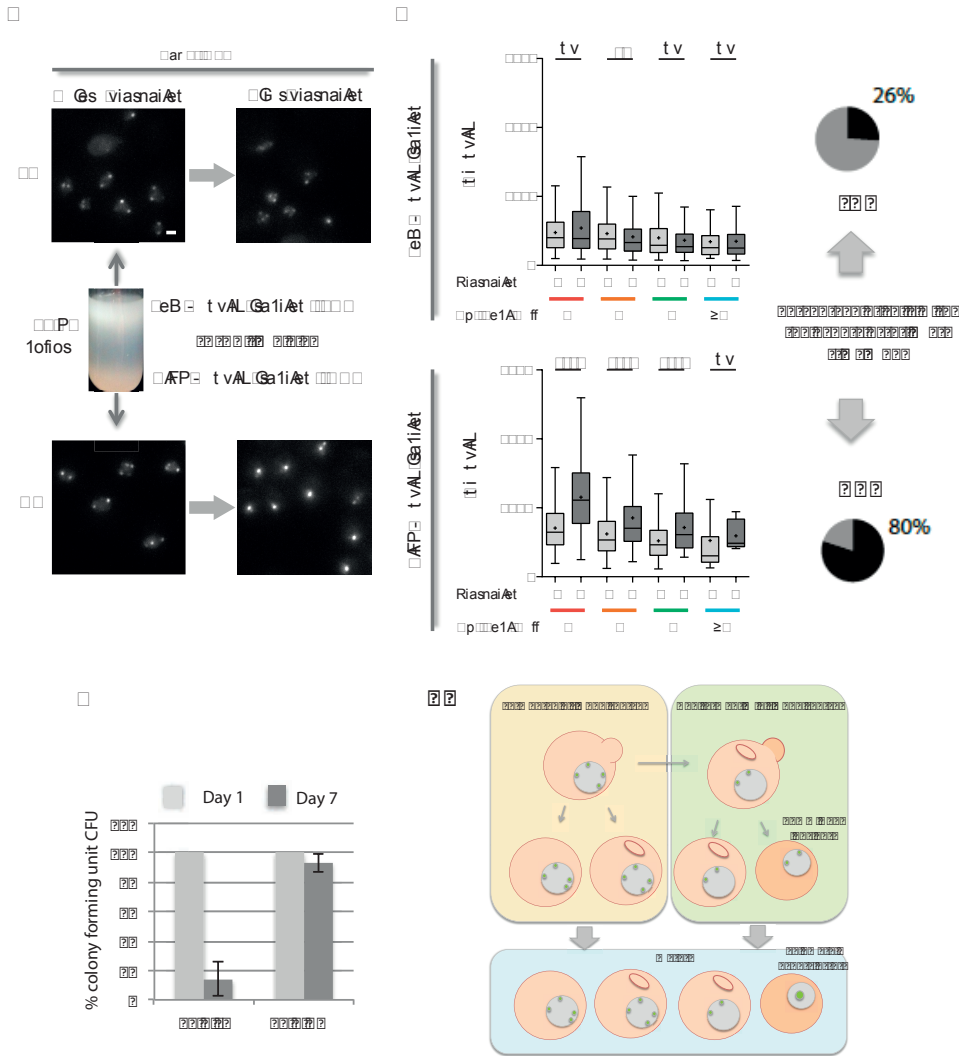


Figure1: the new-formed post diauxic shift HD cells are already committed to form telomere hypercluster in case of starvation.

A: Left, representative Rap1-GFP fluorescent images of LD (up) and HD (bottom) cells isolated by density gradient (center) from a WT culture 24 hours after inoculation in YPD medium. Right, representative Rap1-GFP fluorescent images of cells from the same LD and HD after overnight starvation in water. B: quantification of Rap1 foci from cells of the experiment showed in the panel A. Plots show the distribution of foci intensity in cells with 1 spot (red), 2 spots (orange), three spot (green) and 4 or more spots (blue). Light gray corresponds to foci in cells before starvation while dark grey corresponds to foci in

??

cells after starvation. Median (bars) and mean (stars) intensity are indicated. At the extreme right, pie chart represent a simplified summary of the quantification for post starvation LD (top) and HD (bottom) cultures. Black portion correspond to the percentage of cells with 1 or 2 spots considered as hyperclusters by our in house method (see material and methods). C: Colony forming unit assay of the cells shown in A at day 1 after starvation (considered as 100%) and after 7 days (shown as ratio day 7/day1). Standard deviations are indicated (error bars). D: Model of the physiology of hypercluster formation within a batch liquid culture. Non committed (light rose) and committed (darker rose) cells and telomere foci within their corresponding nuclei are drawn. Yellow indicate the presence of glucose within the medium, while green indicate the presence of non fermentable carbon sources and light blue indicate the absence of carbon source within the medium (starvation in water).

Rad53 checkpoint kinase activity is important for telomere cluster commitment

Our previous data showed that ROS exposure prior to starvation promotes telomere grouping and long-term viability during starvation (Guidi et al., 2015), in agreement with other studies supporting the mitohormesis concept (Mesquita et al., 2010; Ristow and Schmeisser, 2011; Schroeder et al., 2013; Veal et al., 2007; Yun and Finkel, 2014).

As sublethal doses of H₂O₂ are known to activate the checkpoint kinase Rad53 (Leroy et al., 2001), we tested whether Rad53 activation was involved in committing cells to form hyperclusters upon starvation. We found that, contrary to WT cells, exponentially growing Rad53 kinase-defective mutant cells treated with H₂O₂ were not able to form telomere hyperclusters upon starvation (Figure 2A). We next tested whether Rad53 was also involved in the commitment of post DS cells to form hypercluster upon starvation.

As Rad53 checkpoint activity has been shown to reinforce the G₁ arrest when glucose has been scavenged from the medium (Miles et al., 2013), we first checked whether Rad53 defective strain could form HD cells. We found that 24 h after culture inoculation both WT and *rad53K277A* formed LD and HD fraction with a similar ratio (around 1:1) (Figure 2B), ruling out that Rad53 deficient cells could not efficiently produce HD cells. Starving the HD fraction of both cultures, we observed that *rad53K277A* HD quiescent cells were deficient in forming telomere clustering (Fig. 2C).

Based on our results, we conclude that Rad53 activity is important for the commitment to telomere clustering in SP.

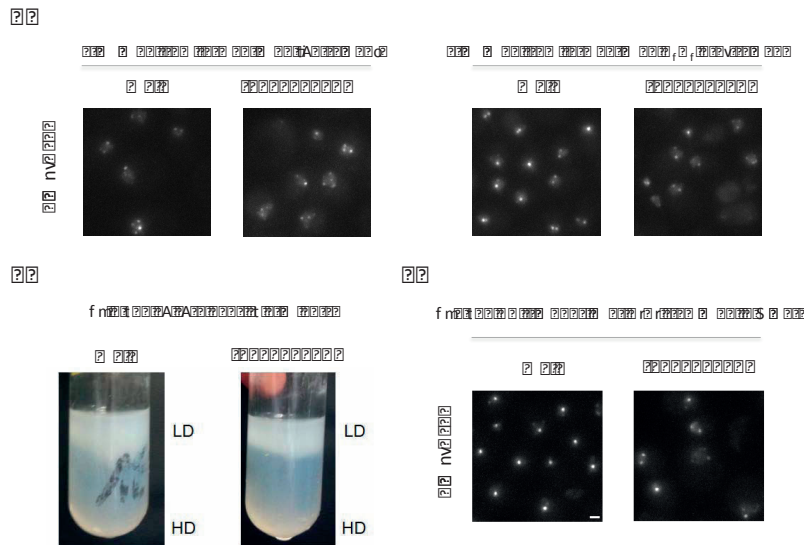


Figure 2: Rad53 kinase activity has a role in the formation of telomere hyperclusters upon starvation.

A: Representative Rap1-GFP images of WT and *rad53K277A* mutants after an overnight of starvation in water from (left) fermentating cultures untreated and (right) fermentating cultures pretreated with H_2O_2 1mM. B: Density gradients of WT and *rad53K277A* mutants at 24 h following the culture inoculation. C: Representative Rap1-GFP images of the HD fractions from panel A imaged after an overnight of starvation in water

SP hyperclusters are Mec1 and Rad53 dependent

We next tested which checkpoint kinase was involved in telomere hypercluster formation. In order to perform this experiment, we first deleted the Suppressor of Mec1 Lethality *SML1* (Zhao et al., 1998) and we found that *sml1* Δ cells were able to form telomere hyperclusters, although not as efficiently as wild type cells (Figure 3A). Consistent with the behavior of the *rad53* kinase dead mutant, the *rad53* Δ *sml1* Δ HD SP cells showed very weak telomere grouping (Figure 3A). Importantly, the HD:LD cell ratio was very similar with the one observed in the wild type (Figure 3B) indicating that *sml1 rad53* mutations did not interfere with the formation of a proper amount of SP dense cells but with telomere grouping. We observed that *tel1* Δ cells, but not *mec1* Δ cells, could efficiently form hyperclusters in SP (Figure 3A) consistent with the report that following 1mM H_2O_2 treatment, the checkpoint kinase Rad53 is activated by the ATM homolog Mec1 (Leroy et al., 2001).

These results suggest that oxidative stress induced Rad53 activation by Mec1 is important for telomere hypercluster formation in SP (Figure 3C).

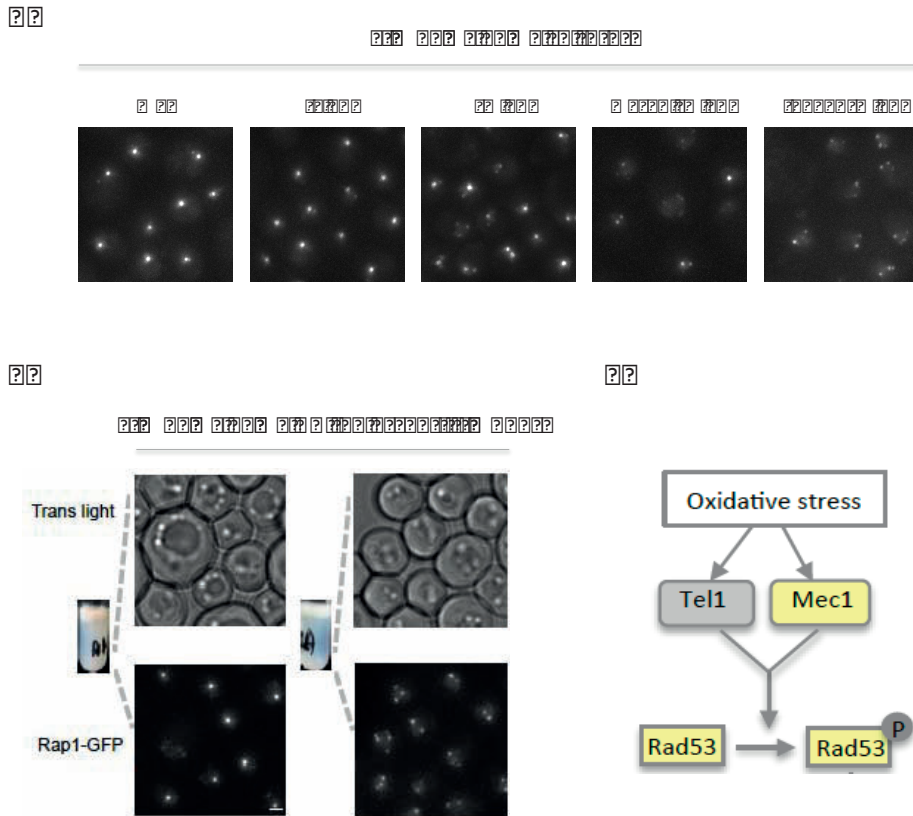


Figure 3: Stationary phase hyperclusters require the Mec1/Rad53 pathway.

A: Representative Rap1-GFP images of stationary phase culture from wild type, *tel1*, *sml1*, *mec1sml1* and *rad53sml1* mutants. B: Representative transmitted light (top) and corresponding Rap1-GFP fluorescent images of HD cells isolated by density gradients (shown on the left) from SP cultures of wild type and *rad53sml1* cultures. C: scheme of oxidative stress induction of Rad53 activation. Yellow indicate proteins important for telomere clustering.

Rph1 inactivation through the Mec1-Rad53 checkpoint pathway renders cells competent to form telomere hyperclusters

The Shadel lab published that Rad53-activation induced by hormetic oxidative stress ultimately imparts longevity by phosphorylating and thus inactivating the histone demethylase Rph1p (Schroeder et al., 2013). We thus checked whether Rph1 deletion could bypass the *rad53K277A* defect. Interestingly, we found that *rad53K277A rph1Δ* cells formed bright telomere hyperclusters in SP (Figure 4A), indicating that *RPH1* deletion rescues the Rad53 deficiency. Similarly, the *RPH1* deletion also rescued the *mec1Δ sml1Δ* defect (Figure 4B).

??

As both Mec1 and Rad53 deficient strains showed a decrease in viability at day 7 of CLS (Fig. 4C), we tested whether *RPH1* deletion could rescue not only telomere clustering but also chronological life span in these checkpoint defective strains. We found that the absence of Rph1 led to a 2-fold increase of viability at day 7 of CLS in both *mec1* and *rad53* mutants (Figure 4C).

We thus conclude that Rph1 inactivation in respiring yeast cells is the key event, driven by the Mec1/Rad53 checkpoint cascade, that primes cells to group telomeres into hyperclusters and increase viability during starvation (Figure 4D).

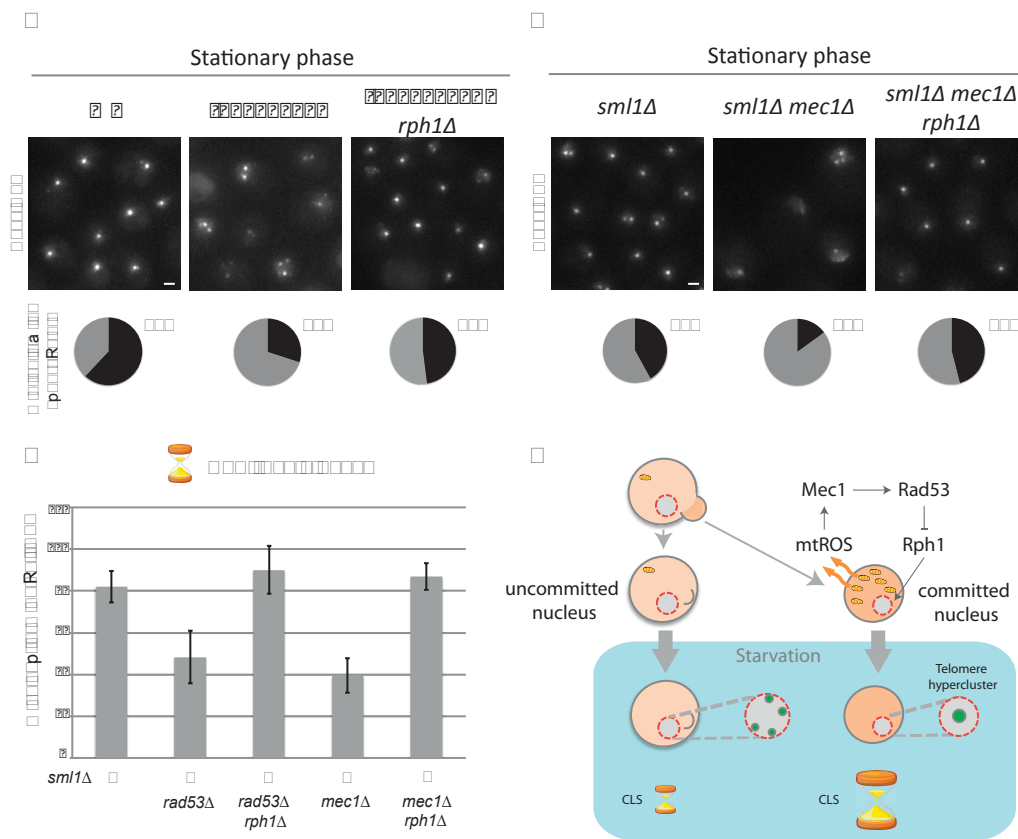


Figure 4: mtROS dependent Mec1/Rad53/Rph1 pathway activation is needed for proper telomere hypercluster formation upon starvation. A: Representative Rap1-GFP images of wild type, *rad53^{K277A}* and *rad53^{K277A} rpb1* stationary phase cultures. Pie charts represent the % of cells showing hyperclusters (black), quantified with our in house software. B: Representative Rap1-GFP images of *sml1*, *mec1sml1* and *mec1sml1 rpb1* stationary phase cultures. Pie charts represent the % of cells showing hyperclusters (black), quantified with our in house software. C: Colony forming unit assay of *sml1*, *rad53 sml1*, *rad53 sml1 rpb1*, *mec1sml1* and *mec1sml1 rpb1* cultures. The ratio of CFU formed at day 7 over day 1 of starvation is shown. Day 1 of starvation corresponded to the stationary phase (7 days in YPD medium), switched to water. Error bars indicate the standard error of the mean for each experiment. D: Schematic model for telomere clustering commitment and hypercluster correlation with high viability upon starvation (indicated as CLS).

??

Conclusions

We report that telomere hyperclusters found in quiescent cells able to sustain long-term viability are the result of a programmed event that starts upon respiration in a subpopulation of cells. Our finding will allow the study of both entry and exit from “long-lived quiescence” in a relatively fast and clean way, simply comparing HD cells found post diauxic shift before and after abrupt starvation in water.

Additional material and methods

Cell cultures, isolation of HD cells, CFU measurement and microscopy images were taken and quantified as in (Guidi et al., 2015).

Strains used in this study:

All the strains listed are W303 background: *ade2-1 can1-100 his3-11,15 leu2-3,112 rad5- trp1-1 ura3-1*

yAT1684 MATa *hml* Δ ::HPH RAD5 *rap1*::RAP1-GFP(LEU2) RDN1:ADE2

yAT2229 MAT α *ade2-1*::ADE2 *rap1*::RAP1-GFP(LEU2) *sml1* Δ ::HIS3

yAT2316 MATa *ade2-1*::ADE2 *mec1* Δ ::TRP1 *rap1*::RAP1-GFP(LEU2) *sml1* Δ ::HIS3

yAT2340 MATa *ade2-1*::ADE2 *rad53*::*rad53*K227A(KanMX) *rap1*::RAP1-GFP(LEU2) *sml1* Δ ::HIS3

yAT2369 MAT α *ade2-1*::ADE2 *rap1*::RAP1-GFP(LEU2) *rad53* Δ ::KanMX *sml1* Δ ::HIS3

yAT2372 MATa *ade2-1*::ADE2 *rad53*::*rad53*K227A(KanMX) *rap1*::RAP1-GFP(LEU2) *rph1* Δ ::NAT

yAT2373 MAT α *ade2-1*::ADE2 *rap1*::RAP1-GFP(LEU2) *rad53* Δ ::KanMX *sml1* Δ ::HIS3 *rph1* Δ ::NAT

yAT2436 MATa *ade2-1*::ADE2 *mec1* Δ ::TRP1 *rap1*::RAP1-GFP(LEU2) *rph1* Δ ::KanMX *sml1* Δ ::HIS3

Result part n III:

Memory of the hypercluster

We previously showed that telomere hyperclusters visualized in HD stationary phase cells are the result of a programmed event occurring during the respiration phase of a liquid culture (Figure 1A) (Guidi et al., 2015). Telomere hyperclusters are found only on cells able to sustain long-term viability upon starvation (long-lived quiescent cells). It is well known that quiescent cells re-enter the cell cycle around 1h30min after restoration of the missing nutrient (Sagot et al., 2006). Here we further characterized the dynamic of telomere organization upon re-entry into the cell cycle.

We asked how much time the cells need to reorganize their nuclear architecture in order to dissolve the telomere hypercluster and form perinuclear foci found during logarithmic growth.

We monitored cells expressing the telomere binding Rap1 tagged with GFP upon quiescence exit. We observed that 30 min after glucose addition the hypercluster was dissolved and Rap1-GFP foci had a peripheral distribution, indicating that telomere reorganization occurs roughly 1 hour before cells re-enter the cell cycle (Figure 1B). Moreover, if only glucose is added to the exhausted YPD medium, the hypercluster is dissolved although cells don't re-enter the cell cycle probably because they miss other nutrients (Figure 1C). We next checked whether only glucose or also non-fermentable carbon sources could lead to the dissolution of the hypercluster. We found that glucose was the only carbon source able to induce a rapid response; however, after roughly 5 hours from ethanol addition, the hypercluster was released (Figure 1D). We hypothesize that galactose and glycerol cannot enter the stationary phase cells while ethanol does. However, ethanol needs more time to dissolve the hypercluster.

??

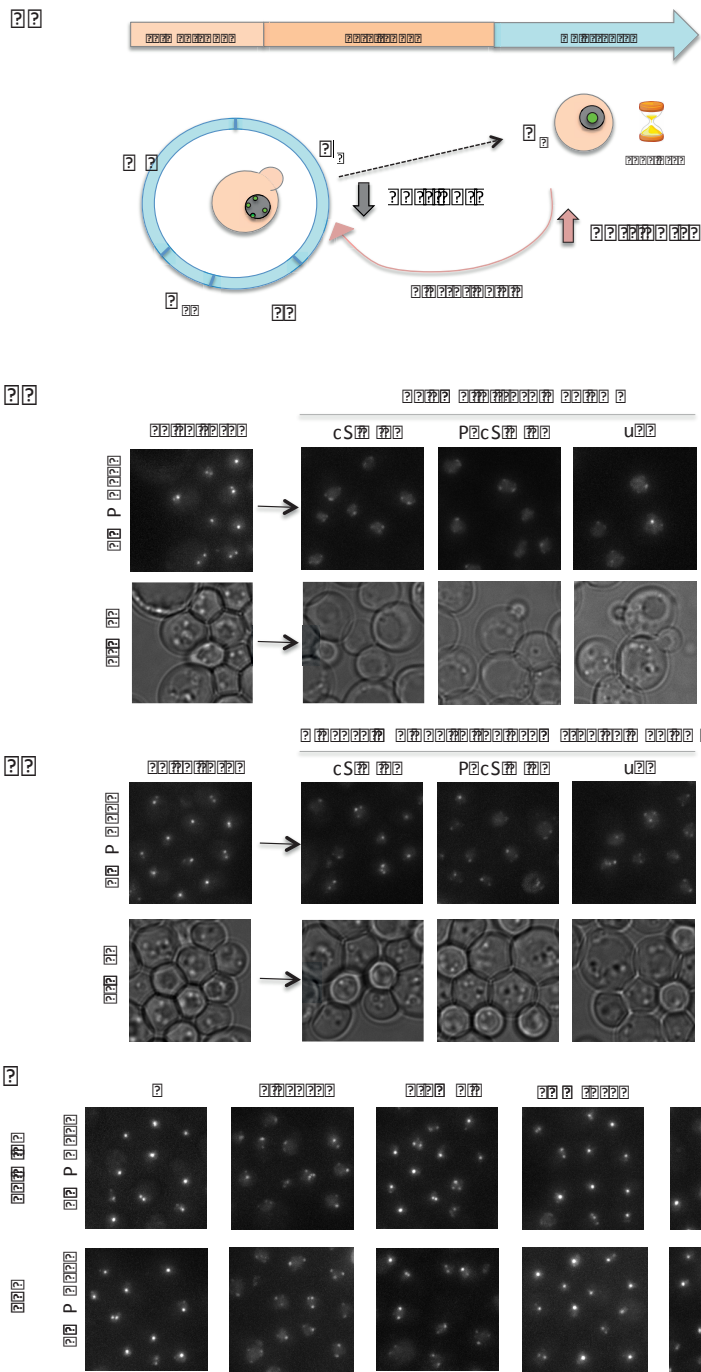


Figure 1: Telomere organization dynamic upon quiescent entry and exit.

A: Telomere organization dynamic upon exit from the cell cycle. Telomere foci, visualized as Rap1-foci, increase their grouping upon carbon source exhaustion and form a hypercluster in long-lived quiescent cells (> 90% after 1 week) (Guidi et al., 2015). SP quiescent cells are blocked in a poor described stage outside of the cell cycle, named G_0 . When nutrients are back, these cells re-enter the cell cycle and are able to form colonies if plated. B: Representative Rap1-GFP fluorescent images with the correspondent transmitted light images of WT stationary phase cells before (left) and after release in fresh YPD 2% glucose medium at different time points (30

?

- nZ

??

minutes, 1hour 30 minutes and 4 hours). C: Representative Rap1-GFP fluorescent images with the correspondent transmitted light images of WT stationary phase cells before (left) and after glucose addition to the exhausted SP medium at different time points (30 minutes, 1hour 30 minutes and 4 hours). D: Representative images of WT stationary phase cultures after 30 minutes (top) or 5 hours (bottom) of carbon source addition. The type of carbon source added is indicated in the top of the images. On the left, controls (no addition) are showed for both the time points.

Importantly, glucose metabolism appears essential for the release of telomere hyperclusters, as addition of the non-metabolizable glucose analogue 2DG didn't have any visible effect on the nuclear architecture of quiescent SP cells (Figure 2A). On the other hand, telomere ungrouping is independent from protein synthesis, as cycloheximide addition did not block the release of the hypercluster induced by fresh YPD medium (Figure 2B). Importantly, we confirmed that cycloheximide entered the cell by monitoring cell growth after the drug treatment: while control cultures started dividing after 1 hours and 30 minutes, cycloheximide treated cultures were not able to start cell division even after 5 hours (data not shown).

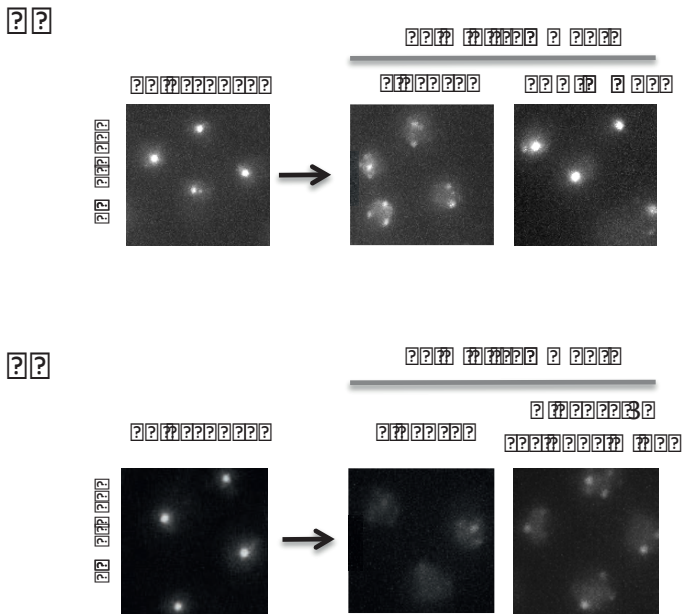


Figure 2: Hypercluster dissolution requires carbon source metabolism and is independent from protein synthesis.

A: representative Rap1-GFP fluorescent images of WT stationary phase quiescent cells before (left) and 30 minutes after glucose or 2DG treatment. 2DG is a non-fermentable glucose

?

- nD

??

analogue that blocks the glycolysis at the first step. B: A: representative Rap1-GFP fluorescent images of WT stationary phase quiescent cells before (left) and 30 minutes after glucose or glucose + cycloheximide treatment.

The “memory effect”

As telomere hyperclusters appear to be reversible, we asked whether the ability to group telomeres into one big focus could be associated to a memory event, in other words “remembered” by the cell. We thus asked whether stationary phase cells showing telomere hyperclusters, once released in fresh medium for 30 minutes, could respond to abrupt starvation forming a second hypercluster. As reported in Figure 3, these cells formed a second hypercluster when abruptly starved. This result indicated that cells could form a hypercluster even when starved from a glucose-containing medium.

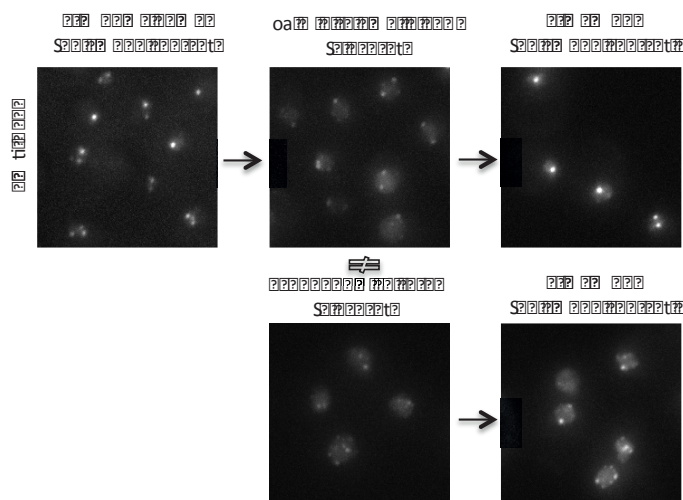


Figure 3: Memory of the hypercluster.

A: representative Rap1-GFP fluorescent images of WT stationary phase cells before (top left), after 30 minutes of glucose addition (top center) and following an overnight starvation in water after this glucose addition (top right). Below, representative Rap1-GFP fluorescent images of WT cells diluted at 0.2 OD and imaged after 5 hours of fermentation (center) successively starved overnight in water and imaged again (right).

It has been shown that within the first 5-10 minutes following nutrient addition to SP cultures gene expression undergoes global reprogramming (Martinez et al., 2004).

?

- nd

Moreover, certain bodies found in the cytoplasm of G_0 cells, such as actin bodies or proteasome storage granules (PSG), are dissolved within the first 5-15 minutes following nutrient addition (Laporte et al., 2008; Sagot et al., 2006). However, stationary phase released cells need to pass through a lag phase lasting more than 1 hour before starting their logarithmic growth. In order to test whether cells keep the ability to form hypercluster once they have re-entered the cell cycle, we released SP HD cells for 35 min, 2h30 and 5 hours before switching them into water to induce quiescence (Figure 4). Quantification of Rap1-GFP detected foci within the cultures indicates that telomere hyperclusters could be found both in cells released for 35 minutes and 2 hours and a half. However, after 5 hours and 30 minutes the number of cells with telomere hypercluster was strongly decreased (Figure 4).

We noticed that upon the second starvation, cells showing hyperclusters were not as small as the one from the first starvation. This was confirmed by measuring the area of calcofluor stained cells used in the experiment described above, both before release and after the second starvation step. As expected, we found that HD SP cells showing a unique bright Rap1-GFP spot were virgin cells (76/76) as indicated by the absence of bud scars and had an average cell area of $12 \mu^2$ (Figure 4, center left). In contrast, when released in fresh YPD medium for 2h and 30min and starved again, “second hyperclusters” were independent of the cell size (mean average $16 \mu^2$) and could be found also in budded cells (Figure 4, top right). Moreover, some of the cells showing the second hypercluster presented a bud scar, suggesting that the memory effect could last for at least the first cell division.

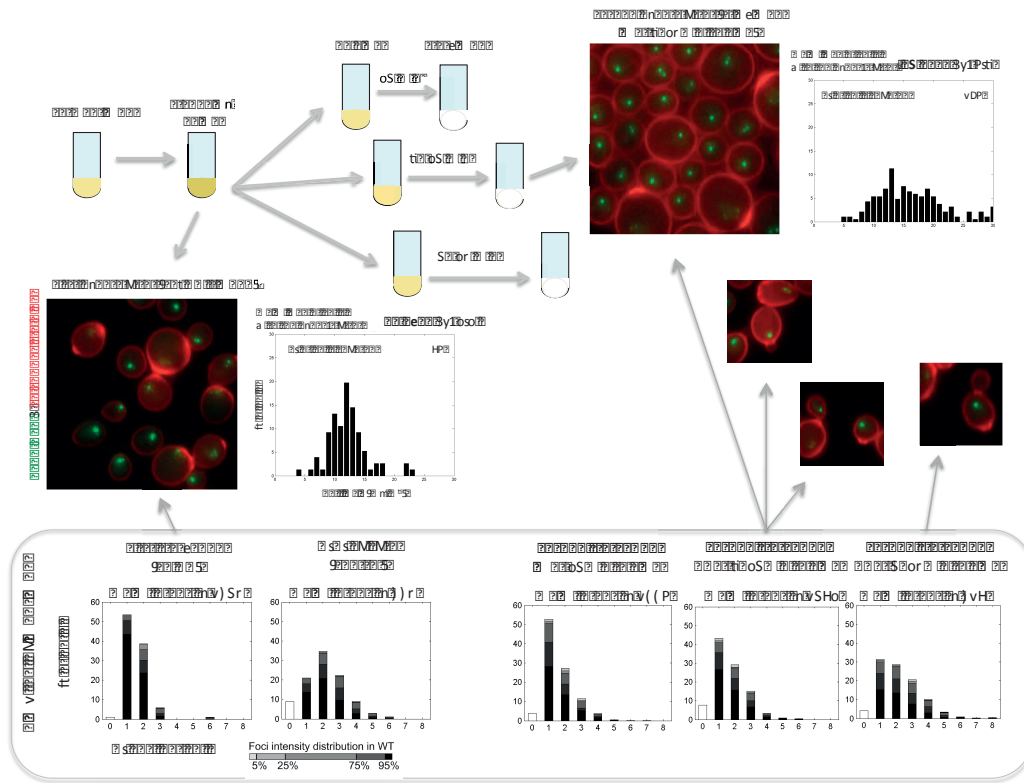


Figure 4: characterization of second hyperclusters

On the left corner, schematic draw of the experiment. Rap1-GFP tagged cells were grown in YPD for 7 days and the HD fraction was isolated and split into 4 tubes. Cells from the first tube were stained with calcofluor and imaged. A representative image is shown. On the right, the mean and the distribution of the areas of cells containing telomere hyperclusters (see material and method) are shown. Cells from the second tube were released in fresh medium for 35 minutes, starved overnight in water and successively stained with calcofluor and imaged. The same procedure was applied to the third and fourth tubes, but with longer release in fresh medium (2h35 min and 5h35 min respectively). A representative image of cells from the 3rd tube (2h35min release before starvation) is shown on the right corner, together with the quantification of the areas of cells containing a hypercluster. Three examples of cells showing second hyperclusters arrested in different stages of the cell cycle are shown below. On the bottom, quantification of Rap-1 foci (telomere clustering) with our in-house software of the cultures of the experiment. Quantification of an overnight culture is also shown as a control. The mean intensity of the foci is indicated on the top of each plot. Bars follow the color code indicated in the left corner, based on the foci intensity distribution in exponentially growing WT cultures.

Conclusion

To conclude, we found that telomere hypercluster formation upon quiescence is a reversible event. Hypercluster dissolution require carbon source metabolism and occurs

independently on the entry into the cell cycle. Moreover, our results show that cells committed to form telomere hyperclusters once can make another hypercluster if starved a second time. Importantly, our results indicate that telomere grouping is not unique of small cells, ruling out an indirect effect of the nuclear volume on the formation of the hypercluster.

Additional material and methods

Carbon source addition to the SP culture

The same culture was divided in 6 tubes with a volume of 500µl in each tube. On each tube, 50 µl of glucose 20%, ethanol 100%, galactose 20%, glycerol 50%, water were added. One tube was kept with no treatment.

2DG treatment

20 µl of a 20% solution of 2DG glucose analogue were added to each ml of culture for 30 minutes. Cells were then washed in water and imaged just after.

Cycloheximide treatment

5µl of a solution 94% cycloheximide were added to each ml of culture for 30 minutes. Cells were then washed in water and imaged just after.

Microscopy

Sets of images from each figure panel were acquired using identical acquisition parameters. A dedicated tool has been designed to find and to quantify Rap1-GFP foci, as in (Guidi et al., 2015).

In order to define the area of cells showing telomere hyperclusters, data from Rap1-GFP foci quantification were incorporated to their corresponding calcofluor stained images

using an ImageJ macro. This macro calculated the area of cells defined as “hyperclusters” by our in house software, as in (Guidi et al., 2015).

Strains used in this study:

W303 background: *ade2-1 can1-100 his3-11,15 leu2-3,112 rad5- trp1-1 ura3-1*

yAT1684 MATa hmlΔ::HPH RAD5 rap1::GFP-RAP1(LEU2) RDN1::ADE2

Result part n IV:

Sir2 increased activity counteracts telomere clustering and CLS in long lived quiescent cells

Our lab previously showed that telomere “hyperclustering” can be induced by overexpressing either Sir3 or its non-acetylatable N-terminal mutated form *sir3-A2Q*, which is dead for silencing (Ruault et al., 2011). Interestingly, in the latter case the increased telomere not only occurs independently of gene silencing but also does not need the presence of the other two members of the SIR complex, Sir2 and Sir4 (Ruault et al., 2011). However, wild type *SIR3* overexpression requires both Sir2 and Sir4 to cluster telomeres.

Here we report that the histone deacetylases Sir2 has an anti-clustering role in post diauxic shift strains overexpressing *sir3-A2Q*. In addition, we show that Sir2 counteracts both telomere clustering and chronological life span in long-lived quiescent cells.

The “adenine effect” on telomere clustering

By serendipity, we discovered that high levels of adenine - which leads to the deactivation of the expression of genes belonging to the *ADE* pathway (Daignan-Fornier and Fink, 1992; Zhang et al., 1997)- had an impact on telomere organization. In particular, adenine addition within the culture medium strongly counteracted telomere clustering in overnight *pGPD-sir3-A2Q* cultures (around 16 hours after inoculation), leading to the disappearing of telomere hyperclusters (Figure 1A). This “adenine effect” was not visible in exponentially growing cell cultures undergoing fermentation, but only

in cultures that had passed the diauxic shift. Moreover, glucose addition to *pGPD-sir3-A2Q* strains “affected” by high adenine levels led to the restoration of the hypercluster phenotype within 2 hours. Importantly, in this case glucose metabolism was not required, as also addition of the non-fermentable glucose analogue 2DG recapitulated the same result than glucose (Figure 1B). These results suggest that glucose is sensed by a signaling pathway linked to telomere organization.

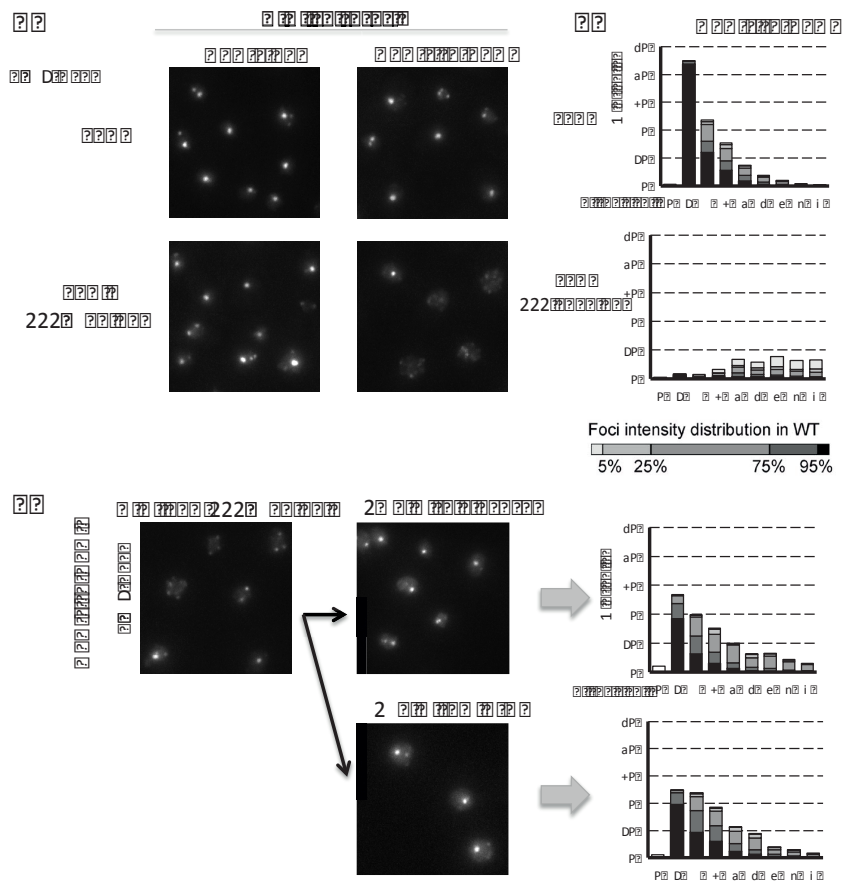


Figure 1: the adenine effect.

A: Representative Rap1-GFP images of strains overexpressing *SIR3* (*pGPD-SIR3*, left) or its mutated form *sir3-A2Q* (*pGPD-sir3-A2Q*, right) grown overnight (roughly 18 hours) in YPD or YPD enriched in adenine. B: quantification of Rap1-GFP foci of the *pGPD-sir3-A2Q* cultures grown overnight in YPD or YPD + adenine from panel A. Quantifications were performed with our in house software, as in (Ruault et al., 2011). The color code is showed below the plots, and it is based on the intensity of the foci distribution in wild type cells growing upon fermentation, as in (Ruault et al., 2011). C: Representative Rap1-GFP images of the *pGPD-sir3-A2Q* culture grown overnight in presence of high adenine levels from panel A, before and 2h after addition of glucose or glucose analogue 2DG. Quantifications of the experiment are shown on the right.

The adenine effect is Sir2-dependent

Interestingly, we found that the “adenine effect” is Sir2 dependent. As shown in Figure 2A, strains overexpressing *sir3-A2Q* but lacking Sir2 were not affected by adenine levels and kept their hyperclusters even after an overnight in presence of high adenine. On the contrary, strains overexpressing both *sir3-A2Q* and Sir2 were highly sensitive to adenine levels overnight, showing almost no hyperclusters. Importantly, *pGPD-sir3-A2Q* strains either with wild type levels, overexpressing or lacking Sir2 did not show evident differences when grown in synthetic medium lacking adenine (Figure 2A). These data indicate that adenine and Sir2, together with the exhaustion of glucose from the fermentation process, have an anti-clustering effect.

Sir2 hyper-activation counteract telomere clustering (after the diauxic shift)

These evidences suggested that adenine could burst Sir2 activity thus interfering with telomere clustering, even though the mechanism by which this could occur is not clear. We thus tried to use a drug shown to increase Sir2 activity both *in vitro* (Sauve et al., 2005) and *in vivo* (McClure et al., 2012), named isonicotinamide (INAM). In agreement with our hypothesis, INAM treatment on *pGPD-sir3-A2Q* overnight cultures leads to a decrease of telomere clustering comparable to the one provoked by adenine (Figure 2B).

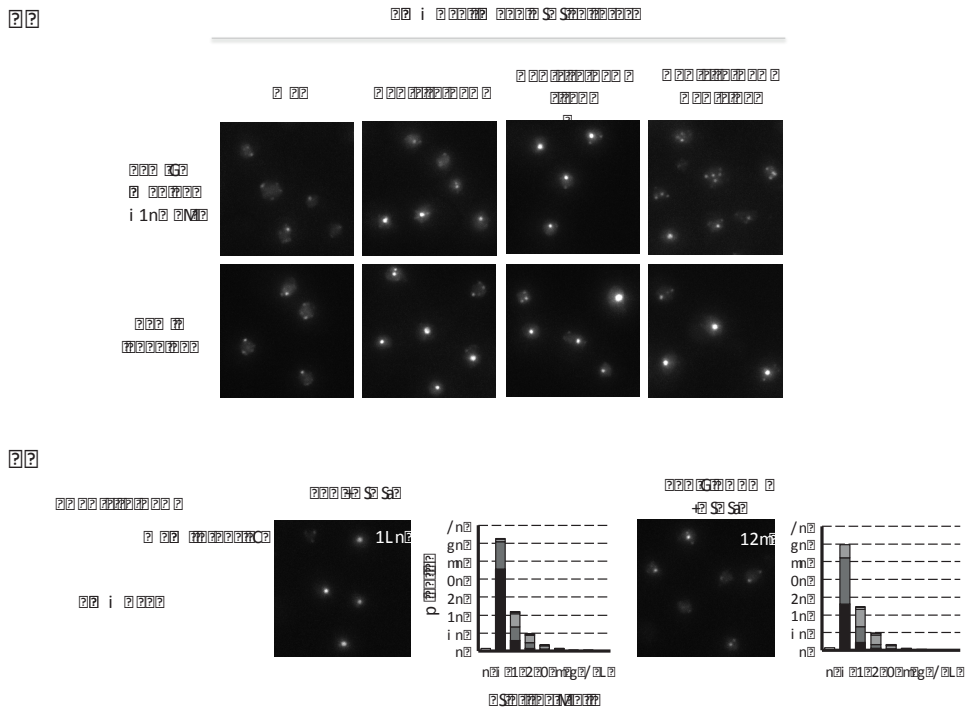


Figure 2: The adenine effect is Sir2 dependent

A: Representative Rap1-GFP cultures of wild type, *pGPD-sir3-A2Q*, *pGPD-sir3-A2Q sir2Δ* and *pGPD-sir3-A2Q pGPD-SIR2* grown overnight in CSM without adenine (top) or in CSM containing 120 mg/ml of adenine (bottom) (Matecic et al., 2010; Zhang et al., 1997). B: Representative Rap1-GFP and quantification of the number and intensity of Rap1-GFP foci of *pGPD-sir3-A2Q* cultures grown overnight in YPD medium in absence (left) or in presence (right) of 25mM INAM (Sir2 activator) (McClure et al., 2012).

Sir2 has an “anti-clustering” activity

These results suggested that, under certain conditions, adenine levels stimulate Sir2 to promote an “anti-clustering effect”. We thus checked whether the Sir2 protein could decrease telomere hyper-clustering in presence of adenine amount normally used in laboratory.

We thus compared Rap1-GFP foci in strains overexpressing *sir3-A2Q* in absence or presence of different amounts of Sir2, in post-diauxic shift synthetic medium cultures. We observed that indeed Sir2 overexpression slightly decreased telomere clustering and Sir2 absence lead to the formation of brighter and bigger hyperclusters (Fig 3).

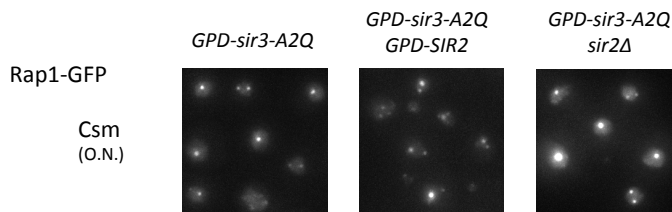


Figure 3: Sir2 anti-clustering activity on overnight cultures overexpressing sir3-A2Q. Representative Rap1-GFP images of *pGPD-sir3-A2Q* strains (left) in which *SIR2* was deleted (center) or overexpressed (right) grown overnight in conventional CSM medium.

Sir2 role in WT post diauxic shift clustering

Importantly, the adenine effect was found also on wild type *SIR3* cultures grown overnight. As shown in Figure 4A, wild type cells grown in YPD enriched in adenine had a slight defect in telomere clustering compared to the same strains grown on conventional YPD (whose adenine concentration is estimated roughly as 20 mg/L). Moreover, similar to adenine, also INAM induced a slight de-clustering on wild type strains (Figure 4B).

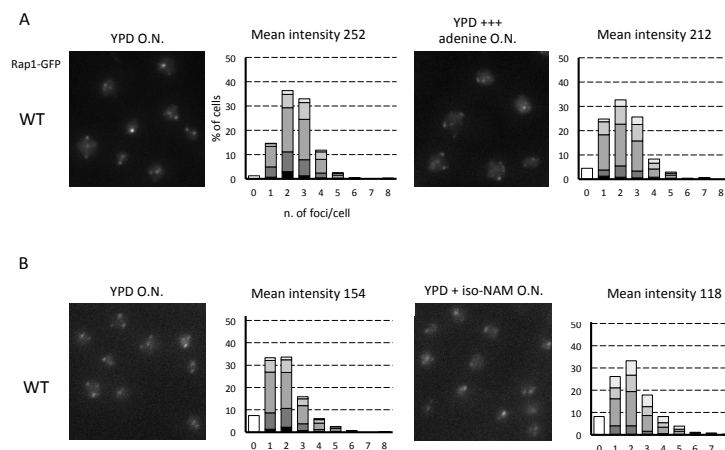


Figure 4: Sir2 hyper-activation counteracts telomere clustering also in WT post diauxic shift cultures.

A: Representative Rap1-GFP images and Rap1-GFP foci quantifications of wild type strains grown overnight in conventional YPD (left) or in YPD enriched in adenine (right). B: Representative Rap1-GFP images and Rap1-GFP foci quantifications of wild type strains grown overnight in conventional YPD (left) or in YPD containing isonicotinamide (Iso-NAM) 25 mg/ml (right).

SP telomere clustering requires Sir3 and Sir4 but not Sir2

As *SIR2* deletion improved telomere clustering in *pGPD-sir3-A2Q* strains and Sir2 hyperactivation appears to impair post diauxic shift telomere clustering, we wondered whether Sir2 was needed for the formation of telomere hyperclusters in stationary phase. We previously showed that the two structural proteins Sir3 and Sir4 are necessary for telomere hyperclusters in quiescence (Guidi et al., 2015), consistent with their requirement for telomere clustering under fermentation growth (Palladino et al., 1993). On the contrary, *SIR2* deleted strains show increased telomere clustering upon carbon source exhaustion, with the formation of hyperclusters in few cells (Figure 5). Interestingly, similarly to wild type culture, perinuclear telomere telomere foci can be visualized during the respiration phase (roughly 20 hours after inoculation) in *sir2* Δ cells, while in *sir3* Δ and *sir4* Δ strains almost no Rap1-GFP foci were visible (Figure 5 top). Similarly to the situation of wild type culture, hyperclusters were found only in SP cells isolated from the HD fraction of the *sir2* Δ culture (data not shown). Importantly, we confirmed that Rap1-GFP foci correspond to telomere foci in *sir2* Δ strains by immunofluorescence (data not shown). These results indicate that Sir2 is not required for quiescence-dependent telomere clustering, consistent with our previous report showing that stationary phase hyperclusters can occur in absence of SIR dependent gene silencing (Guidi et al., 2015). However, *sir2* Δ mutant quiescent cells show less and dimmer hyperclusters than wild type cells (Figure 5 bottom), suggesting that Sir2 levels should be well balanced in order to form proper telomere grouping upon quiescence.

??

Interestingly, we also noticed that Sir2 levels decreased in stationary phase (Figure 5B) thus changing the Sir3/Sir2 ratio. However, despite this decrease in Sir2 levels, we observed that H4K16 acetylation decreases in SP cells in agreement with (Mews et al., 2014)

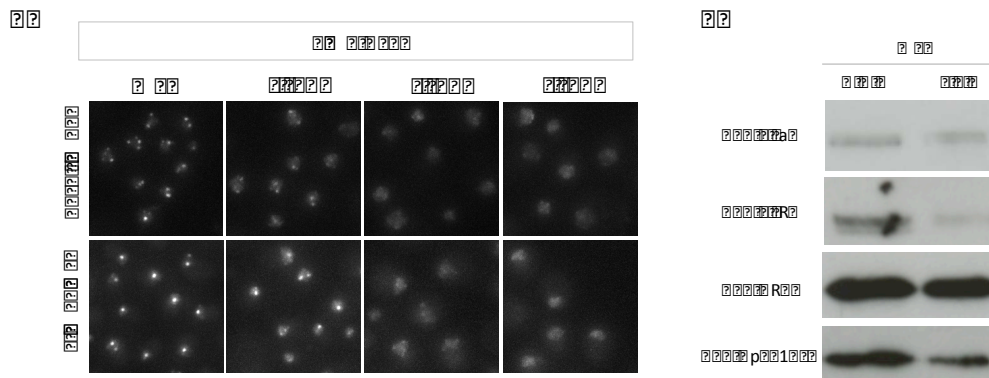


Fig 5: Sir3 and Sir4 are required for SP telomere hypercluster while Sir2 is not.

A: Representative Rap1-GFP images of wild type, *sir2Δ*, *sir3Δ* and *sir4Δ* strains undergoing respiration (top) and stationary phase (bottom). B: western blot analysis of Sir3, Sir2, H2A (loading control) and H4K16ac levels in wild type overnight and stationary phase cultures.

Link between medium composition, SIR2 activity, nuclear architecture and CLS

In order to check telomere organization in strains overexpressing Sir2, we induced quiescence by starving post diauxic shift cells in water to avoid indirect effects due to the toxic metabolites found in the medium of cells overexpressing Sir2 (Longo et al., 2012). Cells overexpressing Sir2 did not form telomere hyperclusters upon quiescence (Fig 6A) further supporting an anti-clustering activity of Sir2. In agreement with other reports about the negative effects of Sir2 on CLS (Casatta et al., 2013; Fabrizio et al., 2005) we observed that cells overexpressing *SIR2* are shorter-lived than wild-type cells upon quiescence (6B). Importantly, strains overexpressing *SIR2* but lacking *SIR3* had also low viability, indicating that Sir2 negative effect on life span is not due to an increase in telomere silencing (Figure 6B). We next asked if the decrease in telomere clustering of

?

- - F

??

this strain could contribute to its CLS defect. We constructed a double mutant overexpressing both Sir2 and sir3-A2Q (Figure 6B). Our preliminary results indicate that sir3-A2Q overexpression rescued not only telomere clustering but also the CLS defect in strains overexpressing Sir2 (Figure 6B).

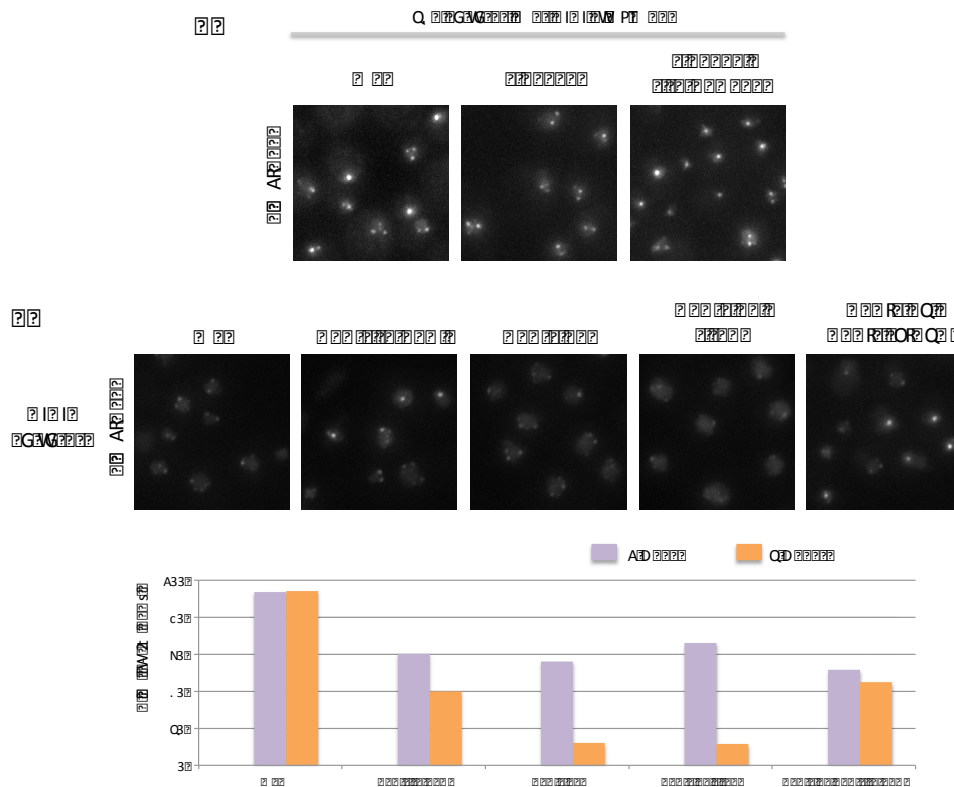


Figure 6: Rescuing telomere clustering could favor CLS of strains overexpressing SIR2.

A: representative Rap1-GFP images of wild type, *pGPD-SIR2* and *pGPD-SIR2 pGPD-sir3-A2Q* cultures grown 24 hours in YPD and then switched in water for an overnight (roughly 16 hours). B: top, representative Rap1-GFP images of wild type, *pGPD-sir3-A2Q*, *pGPD-SIR2*, *pGPD-SIR2 sir3* and *pGPD-SIR2 pGPD-sir3-A2Q* cultures grown overnight. Bottom: viability assay at 1 and 2 weeks of starvation in water of the cultures shown above. Cells were grown until stationary phase before being switched to water. The ratios week1/day1 CLS and week2/day1 CLS are shown. No error bars are shown, as the experiment needs to be repeated other times.

Conclusions

We conclude that while telomere clustering probably favors long chronological life-span, an excess of Sir2 counteracts both CLS and telomere clustering (Figure 7).

??

-- V

??

These data should be repeated and the result should be also confirmed with a different method, given the complexity of CLS assays (Longo et al., 2012). However, we speculate that induction of increased telomere clustering titrates Sir2 within the nucleus thus protecting the cell from Sir2-dependent effects on respiration and improving the viability of strains overexpressing Sir2 upon quiescence. Following Sir2 distribution by microscopy upon different metabolic conditions in these mutants should help us to confirm or reconsider our model.

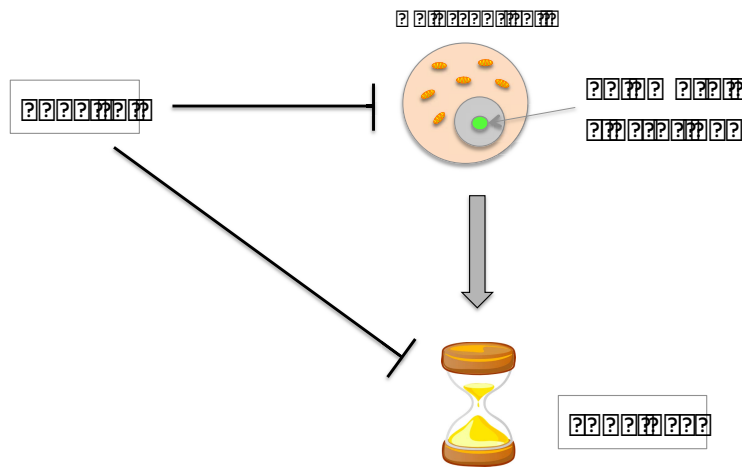


Figure 7: Sir2 counteracts both telomere clustering in quiescent cells and long CLS.

Scheme of Sir2 effects on telomere grouping and viability upon starvation. Mitochondria (in yellow-orange) and the nucleus (grey) containing the telomere hypercluster (green) are features of quiescent cell with good viability upon quiescence (hourglass).

Additional material and methods

Media compositions

YPD medium contains 2% glucose, 20% peptone and 10% yeast extract.

YPD +++ adenine contains 2% glucose, 20% peptone and 10% yeast extract plus an addition of 80 mg/ml of adenine, which was the minimum concentration of adenine leading to decrease clustering in strains with endogenous *SIR2*.

CSM medium contains yeast nitrogen base with ammonium sulfate, glucose 2% and synthetic complete media 2X.

??

-- X

CSM +++ adenine contained 120mg/ml of adenine, which are enough to deactivate the expression of genes belonging to the *ADE* pathway (Daignan-Fornier and Fink, 1992; Zhang et al., 1997).

Microscopy

Images belonging to the same panel were imaged the same day with same acquisition parameters. Rap1-GFP foci quantification was performed with our in house software as previously described in (Ruault et al., 2011).

Western blot

Proteins were extracted with TCA as previously reported in (Guidi et al., 2015) and loaded on precast 4-12% Bis-Tris gels or on 7.5% hand-made gels. When protein loading was effectuated on hand made 7.5 polyacrylamide gels, proteins run at 100V for 5 hours in order to resolve well any possible SIR post-translational modifications. As a consequence, smaller protein run out of the gel and the red ponceau staining of the membrane was imaged as a control for the loading. Antibodies used: polyclonal anti-Sir3 was used at 1:5000, polyclonal anti Sir2 at 1:5000, monoclonal anti H2A at 1:5000 (Active Motif) and monoclonal anti H4K16ac at 1:1000 (Millipore).

Viability assay

Cells were grown on YPD to stationary phase and successively switched in water for two weeks. The ratio of CFU found at 1 and 2 weeks over cfu found at day 1 in water is shown. The experiment was done only one time and has to be repeated.

Strains used in this study

W303 background: *ade2-1 can1-100 his3-11,15 leu2-3,112 rad5- trp1-1 ura3-1*

yAT1684 MATa *hml Δ::HPH RAD5 rap1::RAP1-GFP(LEU2) RDN1:ADE2*

yAT1559 MATa *hml Δ::HPH RAD5 rap1::RAP1-GFP(LEU2) RDN1:ADE2 sir3::GPD-SIR3(NAT)*

yAT1560 MATa *hml Δ::HPH RAD5 rap1::RAP1-GFP(LEU2) RDN1:ADE2 sir3::GPD-sir3-A2Q(NAT)*

yAT1667 MATa *hml Δ::HPH RAD5 rap1::RAP1-GFP(LEU2) RDN1:ADE2 sir2::GPD-SIR2(KanMX)*

yAT1669 MATa *hml Δ::HPH RAD5 rap1::RAP1-GFP(LEU2) RDN1:ADE2 sir2::GPD-SIR2(KanMX) sir3::GPD-sir3-A2Q(NAT)*

yAT1708 MATa *hml Δ::HPH RAD5 rap1::RAP1-GFP(LEU2) RDN1:ADE2 sir3::GPD-sir3-A2Q(NAT) sir2Δ::KanMX*

yAT1985 MATa *hml Δ::HPH RAD5 rap1::RAP1-GFP(LEU2) RDN1:ADE2 sir2::GPD-SIR2(KanMX) sir3Δ::HPH*

yAT2021 MATa *hml Δ::HPH RAD5 rap1::RAP1-GFP(LEU2) RDN1:ADE2 sir2Δ::TRP1*

yAT2022 MATa *hml Δ::HPH RAD5 rap1::RAP1-GFP(LEU2) RDN1:ADE2 sir3Δ::KanMX*

yAT2092 MATa *hml Δ::HPH RAD5 rap1::RAP1-GFP(LEU2) RDN1:ADE2 sir4Δ::HIS5*

Discussion

Massive telomere reorganization upon carbon source exhaustion

We reported that the 3D organization of *S. cerevisiae*'s nucleus responds to changes in the external environment, in particular to the fluctuations of carbon source availability. During logarithmic growth, the clustering of centromeres attached to the SPB constrains the whole genome organization, leading to a “Rabl conformation” that last for the whole cell cycle (Bystricky et al., 2005; Dekker et al., 2002; Schober et al., 2009). Redundant anchoring pathways keep telomeres close to the nuclear periphery, grouped in 3-5 foci per haploid cell (Taddei and Gasser, 2012). As a consequence, telomeres 3D position is strictly dependent on the length of the chromosome arm to which they belong (Schober et al., 2009; Therizols et al., 2010). We showed that after the diauxic shift, i.e. when cells perform respiration and decrease their division rate, telomeres tend to group more, forming fewer and brighter foci. Moreover, we report that when the available carbon source is exhausted from the medium, the dense SP daughter quiescent cells show an additional increase in telomere grouping that results in the formation of one bright focus of telomeres localized in the center of the nucleus (Guidi et al., 2015). The telomere “hypercluster” imposes a general constrain on the whole genome, as chromosomes become tethered at two points of the nuclear space, one driven by centromere interactions and the other by telomere interactions.

I will further discuss the physiology of this increased telomere grouping and the possible mechanisms involved in its formation. Finally, I will speculate on the hypothetical function of this specific chromatin organization.

Physiological relevance of telomere hypercluster formation

Quiescent specific telomere hyperclusters are the result of a programmed event starting upon cellular respiration

We demonstrate that telomere hyperclusters found in long-lived quiescent cells are the outcome of a process that initiates upon the respiration phase, when glucose has been scavenged.

Pre DS cultures subjected to abrupt carbon starvation (ie. switched to a medium without glucose, or more drastically to water) tend to slightly increase their telomere clustering still keeping their perinuclear telomere architecture (Rutledge et al., 2015). These starved cells won't survive long (Guidi et al., 2015; Li et al., 2013). In contrast, one doubling after the DS (roughly 12 hours) a subpopulation differentiates that is forming hypercluster upon abrupt starvation and survives several weeks in water. This population corresponds to the dense daughter cells suggesting that cells formed after DS.

Importantly, we confirmed that slow growth upon respiration induce the acquisition of characteristics of resistance to different stresses (Lu et al., 2009a) but, more importantly, we showed that only half of the population completely “differentiate”, developing the ability to form telomere hypercluster in case of the lack of nutrients.

To conclude, we showed that quiescence is not simply an extreme form of slow growth (Daignan-Fornier and Sagot, 2011; Klosinska et al., 2011a) and that a specific program leading to robust and long-term quiescence exists.

Do telomere hyperclusters occur also in the wild?

As in the wild yeast cells rarely experience logarithmic growth in presence of nutrient excess, our results suggest that in the “real life”, in other words outside of the laboratory, the Rabl conformation within the *S. cerevisiae* nucleus is not found so often.

However, wild type yeasts found in the wild are different than laboratory strains. First of all, they are diploids. One could think that in the wild, yeast cells show perinuclear telomere organization while growing in presence of carbon sources and start the sporulation program in case of nutrient scarcity. If this is true, telomere hyperclusters would probably not be found in nature, as we observed no hyperclusters in yeast spores. Albeit, as several yeast researchers know, the nutritional environment required to induce the developmental program leading to meiosis and sporulation is not an easy one. The conditions needed are: 1) the absence of one essential growth nutrient leading to the G₁ arrest; 2) the absence of glucose; 3) the presence of a non fermentable carbon source (Broach, 2012). As these three criteria together are not so evident to find, it is likely that

??

yeast diploid cells have developed a “B plan” to survive in case of nutrient scarcity. In agreement with this hypothesis, we observed increased telomere grouping (two bright Rap1-GFP foci) in diploid cells abruptly starved after glucose exhaustion (data not shown).

We think that, when meiosis is not possible, diploid cells enter into quiescence and we speculate that cells able to resist long time in this situation reorganize their nuclear architecture forming one or more likely two telomere hyperclusters (Figure A).

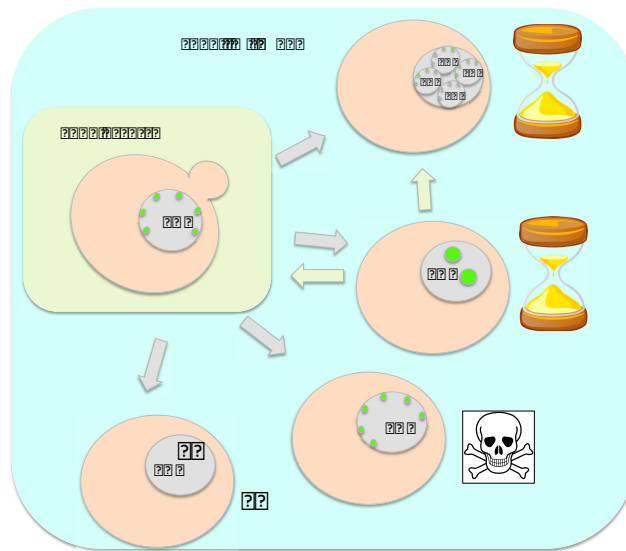


Figure A: Model for telomere organization in wild type diploid cells upon different external environments.

Diploid cells growing in condition of food excess divide logarithmically and present telomeres grouped at the nuclear periphery (Taddei and Gasser, 2012). When the environment becomes more hostile, cells will react in different ways. Right corner top: if the conditions allow the initiation of the meiosis program, diploid cells will sporulate. The new-formed spores can survive long term in absence of nutrients (Broach, 2012). Right corner bottom: if the environment pass from glucose excess to absence of carbon source, we hypothesize that cells are not able to start a program to cope with the change: they arrest to divide and wait for glucose to come back. These cells will not resist long time in this condition. Right center: if diploid cells had the time to perform respiration before exhausting the available carbon source, they will start the program to form telomere hyperclusters. These cells will keep viability for several weeks, and will re-enter the cell cycle when nutrients will be totally restored or will start the sporulation program if the external conditions will allow this option. Left corner bottom: cells could initiate other programs in order to cope with different combination of nutrients. 2N= diploid, 1N= haploid. Telomere foci are shown in green.

?

- uu

It would be interesting to collect several yeast strains in the wild and perform FISH and HiC analysis in order to define their nuclear architecture when living in their natural habitat.

Role of the asymmetric post DS cell division in the commitment process

Our data indicate that only cells born in conditions of increased respiration can be efficiently committed to form the hypercluster.

This effect could be simply linked to the replicative age of these cells, indicating that only young cells can sense certain signals and develop specific programs. Indeed, it is known that *S. cerevisiae* cell divisions are asymmetric and that the yeast mother cell devotes its energy to generate daughter cells, losing fitness with time (Barral et al., 2000; Hartwell et al., 1974; Pruyne and Bretscher, 2000; Shcheprova et al., 2008). Mother cells aim to produce a healthy progeny and retain damaged proteins during cell division (Zhou et al., 2014); on the contrary, daughter cells dedicate their energy to grow, at least before becoming new mothers (Hartwell et al., 1974). It is thus possible that the replicative age of one cell could impact on its chronological life span.

However, post-diauxic shift cell divisions appear different from the ones occurring upon fermentation, as these new born cells are smaller, dense, very resistant and present high levels of mitochondrial markers (Allen et al., 2006; Davidson et al., 2011). Moreover, we showed that, differently than their mothers, they do not start cell division although the medium still contain carbon sources (non fermentable) and are able to sustain long term viability and to form telomere hyperclusters upon quiescence.

Interestingly, mitochondria –which are fundamental for the hypercluster formation- are non randomly distributed between mother and daughter cells and their number within the bud is strictly regulated before cell division (Chernyakov et al., 2013; McFaline-Figueroa et al., 2011; Yang et al., 1999). Importantly, McFaline-Figueroa and colleagues found that during mitosis the mitochondria with a lower redox potential and higher superoxide levels are retained in mother cells, while the ones distributed to the buds are qualitatively better (McFaline-Figueroa et al., 2011). This could be particularly important and probably exacerbated in cell divisions occurring during or after the diauxic shift, in agreement with the fact that mitochondrial activity is needed for viability upon quiescence and for the formation of telomere grouping (Davidson et al., 2011; Guidi et al., 2015). Another option is that post DS daughter cells are born with limiting nutrients,

and this could impact on their chromatin, as discussed in the introduction chapter. This last option could be easily checked for example measuring the histone acetylation levels before and after starvation on HD cells isolated during respiration (see paragraph “fast protocol to study mechanisms linked to telomere grouping upon quiescence”).

It would be interesting to develop a system to monitor chromatin proteins or histones during the first cell division after the diauxic shift, in order to gain insights into this mysterious and asymmetric cell division from which cells committed to telomere hyperclusters originate. Once the key players are found, it would be interesting to follow their dynamic upon cells starvation, release and successive divisions to understand if they could be inherited by the next generation.

We think that at the diauxic shift the cells produced new and very active mitochondria to distribute to the daughter cells. Mitochondrial ROS produced by these cells signal to their nucleus to stop dividing and to “organize a plan” to cope with possible dangers instead of proliferating.

**Link between mitochondrial activity and nuclear organization:
the H₂O₂/Mec1/Rad53/Rph1 pathway commits cells to the hypercluster formation**

We showed that only wild type cells that experienced respiration and ROS signaling manage to form telomere hyperclusters in case of starvation and enter a stable quiescent state that can last for weeks.

Upon respiration, generation of energy within mitochondria leads to the production of reactive oxygen species (ROS), which cause cellular damage and promote the aging process in stationary phase cells but are thought to exert positive effects on the biological outcome on growing cells (Ristow, 2014). We show that mild levels of H₂O₂ prime cells to the hypercluster formation and to sustain viability upon starvation, thus bypassing the need to pass through the respiration phase (Guidi et al). This result indicates that the carbon-source dependent switch of gene expression occurring at the diauxic shift is not required for the commitment to the hypercluster. However, H₂O₂ treatment slows down the division time of the culture. Thus ROS signal together with slow growth likely mimic the situation found post diauxic shift that is necessary for the commitment.

Importantly, mtROS fail to prime cells in which the Rad53 checkpoint kinase is deactivated, indicating that mitochondrial messages must be picked up by the DNA checkpoint pathway in order to carry out their signaling function.

How could mtROS link mitochondria to telomere architecture?

The Shadel laboratory showed that treating yeast growing cells with menadione, which increases the generation of the ROS superoxide (Castro et al 2008), induces an adaptive mitochondrial signal that promotes longevity (Pan et al 211). The same lab successively showed that menadione activates a cascade pathway that lead to the detachment of Rph1 from subtelomeric regions (Schroeder et al., 2013). As Rph1 is not only a TF but also a histone H3K36 demethylase, Schroeder and colleagues proposed that its detachment induces an increase of H3K36me3 and favors chronological life span (CLS) in a Sir3-dependent way. However, as I discussed in the introduction chapter, their data do not completely fit with their model, as Rph1 deletion –which should also lead to more H3K36me3 at subtelomeric regions- did not increase CLS. Nevertheless, we also found that Rph1 links mitochondrial signaling to chromatin organization, although the mechanisms by which this occurs are not known yet.

It is well known that the H3K36me3 Rph1 is one of the targets of the check point kinase Rad53 (Liang et al., 2011; Liang et al., 2013) and is involved in nutrient signaling and oxidative stress (Nordberg et al., 2014; Zhu et al., 2009). Our data thus suggest that the Rad53/Mec1 pathway mediates the H₂O₂ signal necessary for the commitment. In agreement with this hypothesis a mild H₂O₂ treatment induces phosphorylation of Mec1 (Haghnazari and Heyer, 2004; Tsang et al., 2014).

The involvement of the Mec1/Rad53 pathway in the commitment step should be further confirmed by testing the level of the two checkpoint kinase phosphorylation before and after the diauxic shift both in cells able to form telomere hyperclusters and in cells “non committed”. However, the evidence that deleting *RPH1* rescues both clustering and viability defect of Rad53 and Mec1 mutants strongly argues that the Mec1/Rad53 checkpoint cascade leads to Rph1 inactivation. Rph1 inactivation might contribute to telomere hyperclustering and increased survival upon quiescence both through the activation of environmental stress response (ERS) gene expression (Liang et al., 2013; Nordberg et al., 2014) after the diauxic shift (DS), or through its enzymatic activity (Tu et al., 2007). Testing the ability to form telomere clustering in Rph1 mutants dead for demethylase activity but functional for gene repression (Nordberg et al., 2014) should help to understand its role on nuclear architecture upon quiescence.

We propose that mtROS activate a signaling cascade that involves Rad53, Mec1 and Rpb1 phosphorylation and that links external environment, mitochondrial activity and nuclear organization in cells born after the diauxic shift.

Mechanisms

Although we described the (or one of the) pathway leading to the commitment to form telomere hyperclusters upon starvation, the direct mechanism that induces telomere foci to group together is still unknown. We have several hypothesis, briefly described below.

H3K36me3 involvement in telomere clustering

(Schroeder et al., 2013) reported that menadione-induced Rph1 inactivation leads to an increase of Sir3 spreading in some subtelomeric regions possibly due to the higher amount of H3K36me3 in those regions. However, other studies showed that H3K36me3 together with other histone marks act as a barrier for the SIRs to protect euchromatin from ectopic silencing (Tompa and Madhani, 2007; Verzijlbergen et al., 2009). Based on our published and unpublished data we do not think that this histone modification could interfere with Sir3 spreading in stationary phase. However, we don't rule out that H3K36me3 could have a role in the commitment to telomere clustering, for example by inducing conformational changes in the chromatin structure. For example, H3K36 methylation in *S. pombe* has been reported as crucial for the formation of highly condensed chromatin structures, "knobs", found at subtelomeric regions (Matsuda et al., 2015).

It is well known that the H3K36me3 mark recruits the histone deacetylases Rpd3 that deacetylates histone tails thus repressing erroneous transcriptional initiation (Carrozza et al., 2005). As already discussed, the genome of long-lived quiescent cells is massively deacetylated by Rpd3 (McKnight et al., 2015). It is thus tempting to hypothesize that during early respiration mtROS induce a cascade of phosphorylation events culminating with an increased amount of the H3K36me3 mark genome wide. In case of abrupt starvation, H3K36me3 will massively recruit Rpd3 thus favoring the global shutoff of gene expression during quiescence. We speculate that H3K36me3 at subtelomeric regions favour telomere grouping by recruiting Rpd3 that could competes with the

HDACs usually found there, Sir2 (Robyr et al., 2002), that in quiescence appears to counteract telomere clustering (see paragraph “two faced role of Sir2 on telomere clustering”).

SIRs involvement on the formation of telomere hyperclusters

We know that the two structural components of the SIR complex (Sir3 and Sir4) are required for telomere clustering upon quiescence, while Sir2 presence is not absolutely needed and on the contrary an increased Sir2 activity has counteracting effect on telomere grouping.

Our laboratory showed that, upon logarithmic growth, Sir3 overexpression induces a drastic reorganization within the budding yeast nucleus, with telomeric silent chromatin concentrating in one or two “hyperclusters” localized far from the nuclear periphery (Ruault et al., 2011). Sir3 overexpression-induced hyperclusters are Sir2 and Sir4 dependent and correlates with an increased Sir3 spreading. However, upon overexpression of the N-term mutated Sir3 sir3A2Q, which does not spread at all along subtelomeric regions, telomere hyperclustering can occur also in the absence of the other two components of the SIR complex (Ruault et al., 2011). Successively, we showed that a similar structure is found also on quiescent cells able to sustain long-term starvation (Guidi et al., 2015). Interestingly, in long-lived quiescent cell, Sir3 is neither overexpressed nor differently distributed along the subtelomeric regions compared to the fermentation phase.

Our results suggest that telomeres could be kept together through interactions occurring at their extreme tips and rule out that an increased Sir3 spreading and silencing is required for telomere grouping. We speculate that the Sir3 protein could be post-translational modified and acquire an increased clustering function post diauxic shift. In support of this hypothesis, we observe a progressive shift in the migration of Sir3 upon carbon source exhaustion (Figure B).

We speculate that mtROS upon respiration lead to an increased H3K36me3 mark at subtelomeric region; the HDAC Rpd3 bind H3K36me3 nucleosomes thus counteracting Sir2 localization at subtelomeric regions and indirectly favoring telomere clustering. Indeed, an increased Sir2 activity counteracts the Sir3 glue function required for telomere grouping. We hypothesize that a decrease of the Sir2 protein is sufficient to increase Sir3 dependent clustering without changing the amount of Sir3, especially if Sir3 gained new “pro-clustering” PTMs.

Our hypothesis and speculations should be confirmed by performing ChIP experiments in order to study the distribution of Rph1, H3K36me3, Rpd3 and Sir2 upon the different metabolic states found within liquid cultures (see paragraph “Fast protocol to study mechanisms connected to telomere hyperclusters in long-lived quiescence”).

Other possible mechanisms leading to the increased telomere grouping

It is reported that during prolonged growth (100-400 generations) in non-fermentable media chromosome telomeres becomes longer (Romano et al., 2013). However, we rule out that an increase in telomere length induce telomere grouping as *TEL1* deleted strains, which have short telomeres, are very efficient in forming the hypercluster. Moreover, we do not see evident changes in telomere length between cells undergoing fermentation and long lived quiescent cells (data not shown).

Another possibility is that the chromatin fiber itself changes upon carbon source exhaustion and in particular in long lived quiescent cells, where histones deacetylation is drastically increased and the global mRNA levels are roughly 30-fold lower than during log phase (McKnight et al., 2015). Telomere clustering could also be favoured by a decrease in chromosome movements, which consequently changes the balance of aggregation/dissociation of telomeres (Hoze et al., 2013) and could lead to the formation of a unique cluster.

In order to gain insight into the physical structure of the hypercluster of telomeres, it would be interesting to establish collaborations with research groups expert in structural informatics/chromatin modelling. By combining knowledge from microscopy, molecular biology, genetics and biochemical assay with computational methods, it would be probably possible to predict the structure of the silent chromatin hypercluster found upon quiescence. Finally, super-resolution microscopy –whose establishment is on going

in our laboratory- should shed some light on chromatin organization within the hypercluster.

Mechanisms leading to telomeres detachment from the nuclear periphery

During fermentation, silent chromatin is localized attached to the nuclear periphery and close to nucleoli, like heterochromatin in the majority of metazoan cells.

One simple explanation for telomere detachment from the NE could be that the steric constraints imposed by 32 chromosome arms do not allow telomere interactions with the nuclear periphery. Moreover, as all centromeres are kept attached to the nuclear envelope by the SPB, an hypercluster containing all the telomeres should be not too far from the centromere cluster because of the limitation due to small chromosomes arms.

However, we believe that internal telomere clustering could be the consequence of both physical constrains and different protein-protein interactions.

For example, it is tempting to speculate that the C-terminal part of Sir4, which allow telomere anchoring and mediates Sir4 interactions with Sir3 and Rap1 (Kuong et al., 2013), could play a role in the hypercluster localization. In agreement with this hypothesis, the γ Ku complex and Sir4 C terminal can be sumoylated by the Siz2 enzyme *in vivo* and Siz2 have been shown to regulate perinuclear telomere position by specifically influencing the ability of yku70/80 and Sir4 to interact with elements of the nuclear envelope (Ferreira et al., 2011).

It is also legitimate to imagine that a new Sir3 PTM could be associated with a different chromatin-binding mode and could change the chromatin folding, thus excluding telomeres from interactions with other proteins, such as the nuclear envelope ones

We hope to find different proteins associated with the telomere hypercluster and/or specific SIRs PTM favoring telomere grouping in long-lived quiescent cells, by analysing Sir3 partners in native conditions and by purifying SIR proteins in denaturing conditions. The resulting data should next be used as a screening and successively confirmed and deepened by genetics and microscopy experiments.

To summarize, western blot experiments performed during my PhD opened several hypothesis regarding Sir3 modifications upon carbon source exhaustion. Mass Spectrometry analysis of is now in progress in order to better understand the mechanisms leading to telomere grouping occurring in this physiological condition.

Fast protocol to study mechanisms connected to telomere hyperclusters in long-lived quiescence

We found a fast and clean way to study the mechanisms linked to telomere clustering. We can study and compare four conditions belonging to the same liquid culture but showing different telomere organization: 1) G_1 cultures undergoing fermentation (uncommitted, no hypercluster, pre DS gene expression); 2) HD fraction of post diauxic shift cells before starvation (committed, post DS gene expression, no hyperclusters) 3) HD fraction of post diauxic shift cells after starvation (quiescence and hyperclusters) and 4) HD fraction of post diauxic shift starved cells 30-40 minutes following their release in fresh medium (commitment, glucose induced gene expression, no hyperclusters).

These conditions should be studied under different points of view, such as RNA levels (RNA seq), chromosomal interactions (HiC), genes or loci localization (microscopy), protein modifications or different interactions (mass spectrometry) and distribution of proteins and histone modifications within chromatin (microscopy and ChIP experiments).

The two-faced role of Sir2 on telomere clustering

Our data show that Sir2 has a non essential but positive role in telomere clustering upon logarithmic growth. On the other hand, our data indicate that Sir2 activity in cells that have passed the diauxic shift counteracts telomere clustering. Indeed, *SIR2* deletion has a positive effect on telomere clustering in strains overexpressing the *sir3-A2Q* gene grown after the DS, while both overexpression or increased activation of Sir2 counteract telomere clustering in *pGPD-sir3-A2Q* and in wild type *SIR3* post DS cultures. This anti-clustering effect becomes stronger upon quiescence. In fact, *pGPD-SIR2* SP cells don't show telomere hyperclusters and have a lower CLS than cells with endogenous levels of Sir2, in agreement with the hypothesis that telomere hyperclusters favour viability upon quiescence (Result chapter).

We showed that adding an excess of adenine in the growth medium negatively impacts on telomere grouping in a Sir2 dependent manner. Adenine levels impact on the expression of genes of the *de novo* purine biosynthesis *ADE* pathway, which eventually lead to the production of IMP and AMP (Rebora et al., 2001). Interestingly, strains in

which the *ADE* pathway is compromised are long-lived (Matecic et al., 2010). In agreement with this, we noticed that YPD enriched in adenine not only counteracted telomere clustering but also reduced CLS of wild type cells, with drastic effects on strains overexpressing Sir2 (data not shown). Intriguingly, the Smith lab showed that the effects of calorie restriction and of regulation of the *ADE* pathway on CLS are very similar and proposed that the two mechanisms partially overlap (Matecic et al., 2010). We thus speculate that Sir2 activity could link calorie restriction and *ADE* pathway effects on viability upon quiescence.

However, whether Sir2 activity directly impacts on telomere organization or the decreased telomere clustering is simply an indication of the suffering state of the cell is not clear yet.

The decreased telomere clustering in post DS cultures overexpressing *SIR2* could be indirect and dependent on the fact that Sir2 deacetylates –thus inactivates- an important enzyme for the TCA cycle named phosphoenolpyruvate carboxykinase Pck1 (Lin et al., 2009). Indeed, Pck1 acetylation is crucial for its enzymatic activity and Pck1 deacetylation has negative effect on chronological life span (Lin et al., 2009). Moreover, *SIR2* deletion correlates with a more efficient acetate utilization and with a consequent reduction of pro-aging extracellular metabolites such as acetic acid and ethanol (Casatta et al., 2013), both negatively impacting on CLS (Burtner et al., 2009; Fabrizio et al., 2004; Fabrizio et al., 2005; Kaeberlein, 2010; Mirisola and Longo, 2012; Orlandi et al., 2013). As previously mentioned, *SIR2* deletion is thought to extend CLS mainly when associated with caloric restriction (Fabrizio et al., 2005), a condition that *per se* already favors longevity (Smith et al., 2007). It is thus possible that Sir2 post-diauxic shift effects on ethanol metabolism impact on cell fitness and as a consequence indirectly interfere with the nuclear organization.

Nevertheless, these evidences do not rule out a direct anti-clustering activity of the Sir2 protein, which could for example sequester Sir4 protein levels far from telomeres. Another option could be that upon enhanced Sir2 activity, the local concentration of OOADPR increases (Tanner et al., 2000) and interferes with the binding of the SIR complex to chromatin, as Sir3 can change conformation in presence of this metabolite (Liou et al., 2005).

However, a certain amount of Sir2 is necessary for the proper formation of telomere hyperclusters upon quiescence, as strains lacking *SIR2* are less efficient than wild type

cells in telomere grouping. Moreover, as Sir2 has anti-aging effects in the replicative life span, it is possible that *sir2* cells have troubles upon quiescence because “born old” (Kennedy et al., 1994).

It would be interesting to induce Sir2 degradation upon quiescence, for example using a degron approach, to understand whether low levels of Sir2 are important for the maintenance of the hypercluster of telomeres. These cells, which should form wild type like hyperclusters upon carbon source exhaustion, would show (i) increased telomere grouping if Sir2 counteracts the quiescence specific hypercluster or (ii) decreased clustering if Sir2 low levels are important to maintain the hypercluster structure.

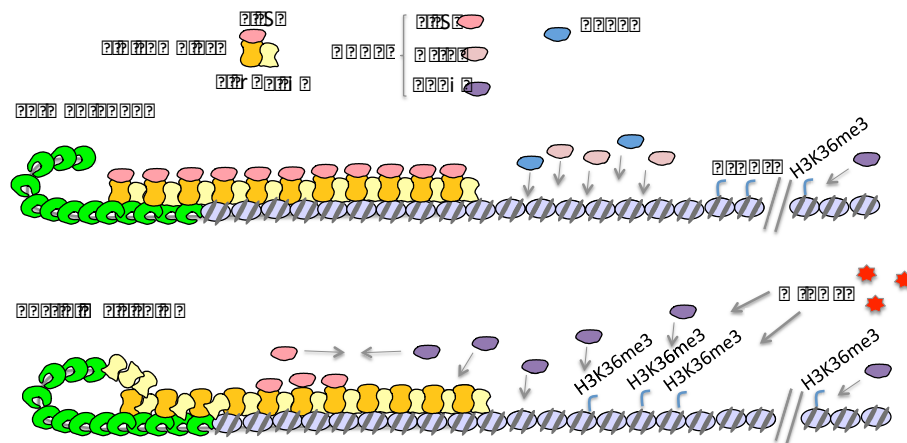


Figure C: Model of telomeric chromatin upon fermentation (up) and in HD cells born after the diauxic shift (bottom).

Mitochondrial ROS produced after the diauxic shift activate a signaling pathway that lead to the deactivation of the histone demethylase Rph1 and to the consequent increase of H3K36me3 genome wide. The histone deacetylases Rpd3 is successively recruited at H3K36 methylated histones to deacetylate them. At subtelomeric regions, Rpd3 competes with the other HDACs and partially substitutes Sir2. At the tip of telomeres, the Sir3 protein, post translational modified after mtROS signaling, binds nucleosomes and other proteins in different conformations.

Possible function of telomere hyperclusters

Upon quiescence, yeast cells drastically shut down gene expression and protein synthesis, reducing to minimal level the energy consumption. Up to now, there is a growing number of examples of cellular reorganization occurring when proliferation ceases upon

nutritional deprivation and likely others will be discovered soon (Daignan-Fornier and Sagot, 2011).

However, the clustering of telomere appears as a longer and more complex process occurring only in certain situations and seems to favour the maintenance of viability upon starvation.

Our data suggest that telomere hyperclusters favor survival upon quiescence: first, mutants completely (*sir3Δ*) or partially (*mec1Δsml1Δ*, *rad53Δsml1Δ*, *pGPD-SIR2*) defective for telomere clustering had lower CLS than wild type strains; and second, the viability of the latter strains was improved by rescuing their telomere grouping (*sir3Δ::sir3-A2Q*, *mec1Δsml1Δrpb1Δ*, *rad53Δsml1Δrpb1Δ*, *pGPD-SIR2-pGPD-sir3-A2Q*).

The aging process appears as a complex and multifactorial phenomenon.

Several factors have been found to slow down or favour yeast ageing, including the medium composition, internal carbon sources, slow growth and respiration process, as well as expression or deletion of several genes (Longo et al., 2012). To our knowledge, our results are the first to connect chronological life span with nuclear architecture and could pave the way for other studies relating ageing and chromatin organization.

It would be interesting to study the dynamics of chromatin in different long-lived yeast mutants (Fabrizio et al., 2005; Fabrizio et al., 2010; Fabrizio et al., 2003; Fabrizio et al., 2001) where the main nutrient signalling pathways are blocked (De Virgilio, 2012). As chromatin organization appears linked to cell longevity, these cells may show specific rearrangement of their nuclear architecture.

However, we don't know yet *how* telomere grouping does impact on yeast lifespan.

Given that telomere hyperclusters can occur also in absence of silencing, the main function of this structure is likely independent of gene repression. Moreover, telomere clustering seems not linked to different telomere sizes. Several options are possible:

- 1) Telomere hyperclusters could help maintaining the genome stability preserving chromosome end integrity by avoiding recombination between telomeres and the rest of the genome. This possibility could be checked by performing different experiments in order to compare the stability of subtelomeric and internal genes in quiescent cells showing or not able to form telomere hyperclusters upon quiescence. Moreover, telomere fusions could be analyzed in wild type cells versus mutant cells defective for the hypercluster (Pobiega and Marcand, 2010).

2) Telomere grouping could favour the expression of subtelomeric genes important for the survival upon carbon source starvation. Indeed, we noticed that HD quiescent cells are more “sticky” than exponentially growing cells; this could be due to a different expression of the telomeric *FLO* genes, which are involved in cell adhesion. On the other hand, we also noticed that in a specific background (YPH499), LD stationary phase highly flocculate while HD cells do not. This is probably an indication that some *FLO* genes involved in pseudo ifae formation are strongly expressed when telomeres are not grouped and repressed within the hypercluster. It would be interesting to compare RNA seq analysis of cells showing the hypercluster with the ones of cells defective for telomere grouping upon quiescence.

3) Telomere hyperclusters could be important for the re-entry into the cell cycle upon nutrient restoring by positioning genes in a configuration that favour their fast expression. This should be fundamental to compete for the nutrients with other organisms. We could first check on our HiC contact maps if these genes are localized in a particular zone upon quiescence in cells showing telomere hyperclusters while they are dispersed within the nucleus in *sir3* quiescent cells. If this is the case, it would be interesting to follow the expression of these genes upon exit from quiescence.

4) Telomere grouping could act as a sink to store factors that have deleterious effects during quiescence but are important upon return to growth. Upon fermentation, the redistribution of silencing proteins from one subcompartment to another has been associated with the regulation of genome stability and of replicative life span (Kennedy et al., 1997). Our results suggest that the telomere hypercluster could trap Sir2 thus preventing its localization outside of the nucleus, where it would interfere with ethanol metabolism thus counteracting the cell fitness. By following the distribution of the Sir2 protein by microscopy in cells overexpressing Sir2 in presence of wild type Sir3 and when the *sir3-A2Q* mutant is overexpressed (given that the latter rescues both telomere clustering and cell fitness, see result chapter) we could check this hypothesis.

However, at the state of the art we are not completely sure that telomere clustering directly impact on genome functions and we cannot rule out that telomere clustering is only a consequence of the healthy state of the cell. On the other hand, it would be interesting to follow telomere organization several weeks or months after quiescence entry, to determine whether chronological life span does affect the nuclear architecture.

Link with similar chromatin organization in other organisms?

The formation of a telomere hypercluster detached from the nuclear periphery upon quiescence constitutes a quite uncommon chromatin architecture. However, this chromatin reorganization does not appear so surprising if we think that upon quiescence the majority of the genome is silent and only few chromatin regions should be active. It could be that upon these conditions active genes are mainly found close to the nuclear periphery, likely in correspondence to the nuclear pores. Indeed, it has been already shown that the nuclear periphery *per se* does not have silencing effect but simply favour the clustering of silencing factors (Taddei et al., 2009), and we showed that upon quiescence SIR proteins are mainly localized within the hypercluster (Guidi et al., 2015). It would be interesting to analyse our HiC contact map in order to compare the localization of specific genes that are known to be activated or silenced in stationary phase, and to next confirm these results by FISH.

The telomere hypercluster resembles somehow other structures that are found on very specialized cells in metazoan, such as rod cells of nocturnal animals or mouse olfactory neurons (see introduction chapter). As already discussed, these cells undergo a specific differentiation program where their nuclei are drastically reorganized and eventually show heterochromatin grouped in one main locus far from the nuclear periphery. Interestingly, the “inverted organization” in mouse rod cells is thought to favour their particular nuclear function and has been proposed as an adaptation to limited light. As we also found that telomere hyperclusters are the outcome of a specific yeast cell differentiation programs, and that they are associated with a good survival upon quiescence, we speculate that also telomere hyperclusters provide a survival advantage in the long-term (Guidi et al., 2015).

References

- Aerts, A.M., Zabrocki, P., Govaert, G., Mathys, J., Carmona-Gutierrez, D., Madeo, F., Winderickx, J., Cammue, B.P., and Thevissen, K. (2009). Mitochondrial dysfunction leads to reduced chronological lifespan and increased apoptosis in yeast. *FEBS letters* *583*, 113-117.
- Ai, W., Bertram, P.G., Tsang, C.K., Chan, T.F., and Zheng, X.F. (2002). Regulation of subtelomeric silencing during stress response. *Mol Cell* *10*, 1295-1305.
- Akhtar, A., and Gasser, S.M. (2007). The nuclear envelope and transcriptional control. *Nature reviews Genetics* *8*, 507-517.
- Allen, C., Buttner, S., Aragon, A.D., Thomas, J.A., Meirelles, O., Jaetao, J.E., Benn, D., Ruby, S.W., Veenhuis, M., Madeo, F., *et al.* (2006). Isolation of quiescent and nonquiescent cells from yeast stationary-phase cultures. *The Journal of cell biology* *174*, 89-100.
- Allfrey, V.G., Faulkner, R., and Mirsky, A.E. (1964). Acetylation and Methylation of Histones and Their Possible Role in the Regulation of Rna Synthesis. *Proceedings of the National Academy of Sciences of the United States of America* *51*, 786-794.
- Andrulis, E.D., Neiman, A.M., Zappulla, D.C., and Sternglanz, R. (1998). Perinuclear localization of chromatin facilitates transcriptional silencing. *Nature* *394*, 592-595.
- Aoto, T., Saitoh, N., Ichimura, T., Niwa, H., and Nakao, M. (2006). Nuclear and chromatin reorganization in the MHC-Oct3/4 locus at developmental phases of embryonic stem cell differentiation. *Developmental biology* *298*, 354-367.
- Aragon, A.D., Rodriguez, A.L., Meirelles, O., Roy, S., Davidson, G.S., Tapia, P.H., Allen, C., Joe, R., Benn, D., and Werner-Washburne, M. (2008). Characterization of differentiated quiescent and nonquiescent cells in yeast stationary-phase cultures. *Molecular biology of the cell* *19*, 1271-1280.
- Armache, K.J., Garlick, J.D., Canzio, D., Narlikar, G.J., and Kingston, R.E. (2011). Structural basis of silencing: Sir3 BAH domain in complex with a nucleosome at 3.0 Å resolution. *Science* *334*, 977-982.
- Arnaudo, N., Fernandez, I.S., McLaughlin, S.H., Peak-Chew, S.Y., Rhodes, D., and Martino, F. (2013). The N-terminal acetylation of Sir3 stabilizes its binding to the nucleosome core particle. *Nature structural & molecular biology* *20*, 1119-1121.
- Barral, Y., Mermall, V., Mooseker, M.S., and Snyder, M. (2000). Compartmentalization of the cell cortex by septins is required for maintenance of cell polarity in yeast. *Molecular cell* *5*, 841-851.
- Bednar, J., Horowitz, R.A., Grigoryev, S.A., Carruthers, L.M., Hansen, J.C., Koster, A.J., and Woodcock, C.L. (1998). Nucleosomes, linker DNA, and linker histone form a unique structural motif that directs the higher-order folding and compaction of chromatin. *Proceedings of the National Academy of Sciences of the United States of America* *95*, 14173-14178.
- Belenky, P., Racette, F.G., Bogan, K.L., McClure, J.M., Smith, J.S., and Brenner, C. (2007). Nicotinamide riboside promotes Sir2 silencing and extends lifespan via Nrk and Urh1/Pnp1/Meu1 pathways to NAD⁺. *Cell* *129*, 473-484.
- Bickmore, W.A., and van Steensel, B. (2013). Genome architecture: domain organization of interphase chromosomes. *Cell* *152*, 1270-1284.

Bitterman, K.J., Anderson, R.M., Cohen, H.Y., Latorre-Esteves, M., and Sinclair, D.A. (2002). Inhibition of silencing and accelerated aging by nicotinamide, a putative negative regulator of yeast sir2 and human SIRT1. *The Journal of biological chemistry* 277, 45099-45107.

Blaze, J., and Roth, T.L. (2015). Evidence from clinical and animal model studies of the long-term and transgenerational impact of stress on DNA methylation. *Semin Cell Dev Biol*.

Bolzer, A., Kreth, G., Solovei, I., Koehler, D., Saracoglu, K., Fauth, C., Muller, S., Eils, R., Cremer, C., Speicher, M.R., *et al.* (2005). Three-dimensional maps of all chromosomes in human male fibroblast nuclei and prometaphase rosettes. *PLoS biology* 3, e157.

Boyle, S., Gilchrist, S., Bridger, J.M., Mahy, N.L., Ellis, J.A., and Bickmore, W.A. (2001). The spatial organization of human chromosomes within the nuclei of normal and emerin-mutant cells. *Human molecular genetics* 10, 211-219.

Branco, M.R., Branco, T., Ramirez, F., and Pombo, A. (2008). Changes in chromosome organization during PHA-activation of resting human lymphocytes measured by cryo-FISH. *Chromosome research : an international journal on the molecular, supramolecular and evolutionary aspects of chromosome biology* 16, 413-426.

Broach, J.R. (2012). Nutritional control of growth and development in yeast. *Genetics* 192, 73-105.

Bulger, M., and Groudine, M. (1999). Looping versus linking: toward a model for long-distance gene activation. *Genes & development* 13, 2465-2477.

Burke, B., and Stewart, C.L. (2013). The nuclear lamins: flexibility in function. *Nature reviews Molecular cell biology* 14, 13-24.

Burtner, C.R., Murakami, C.J., Kennedy, B.K., and Kaeberlein, M. (2009). A molecular mechanism of chronological aging in yeast. *Cell Cycle* 8, 1256-1270.

Bystricky, K., Laroche, T., van Houwe, G., Blaszczyk, M., and Gasser, S.M. (2005). Chromosome looping in yeast: telomere pairing and coordinated movement reflect anchoring efficiency and territorial organization. *The Journal of cell biology* 168, 375-387.

Cai, L., Sutter, B.M., Li, B., and Tu, B.P. (2011). Acetyl-CoA induces cell growth and proliferation by promoting the acetylation of histones at growth genes. *Molecular cell* 42, 426-437.

Canto, C., and Auwerx, J. (2011). NAD⁺ as a signaling molecule modulating metabolism. *Cold Spring Harbor symposia on quantitative biology* 76, 291-298.

Canto, C., Menzies, K.J., and Auwerx, J. (2015). NAD(+) Metabolism and the Control of Energy Homeostasis: A Balancing Act between Mitochondria and the Nucleus. *Cell metabolism* 22, 31-53.

Cap, M., Stepanek, L., Harant, K., Vachova, L., and Palkova, Z. (2012). Cell differentiation within a yeast colony: metabolic and regulatory parallels with a tumor-affected organism. *Molecular cell* 46, 436-448.

Carrozza, M.J., Li, B., Florens, L., Suganuma, T., Swanson, S.K., Lee, K.K., Shia, W.J., Anderson, S., Yates, J., Washburn, M.P., *et al.* (2005). Histone H3 methylation by Set2 directs deacetylation of coding regions by Rpd3S to suppress spurious intragenic transcription. *Cell* 123, 581-592.

Casatta, N., Porro, A., Orlandi, I., Brambilla, L., and Vai, M. (2013). Lack of Sir2 increases acetate consumption and decreases extracellular pro-aging factors. *Biochimica et biophysica acta* 1833, 593-601.

Chance, B., Estabrook, R.W., and Ghosh, A. (1964). Damped Sinusoidal Oscillations of Cytoplasmic Reduced Pyridine Nucleotide in Yeast Cells. *Proceedings of the National Academy of Sciences of the United States of America* *51*, 1244-1251.

Chernyakov, I., Santiago-Tirado, F., and Bretscher, A. (2013). Active segregation of yeast mitochondria by Myo2 is essential and mediated by Mmr1 and Ypt11. *Curr Biol* *23*, 1818-1824.

Ciabrelli, F., and Cavalli, G. (2015). Chromatin-driven behavior of topologically associating domains. *Journal of molecular biology* *427*, 608-625.

Clowney, E.J., LeGros, M.A., Mosley, C.P., Clowney, F.G., Markenskoff-Papadimitriou, E.C., Myllys, M., Barnea, G., Larabell, C.A., and Lomvardas, S. (2012). Nuclear aggregation of olfactory receptor genes governs their monogenic expression. *Cell* *151*, 724-737.

Comerford, S.A., Huang, Z., Du, X., Wang, Y., Cai, L., Witkiewicz, A.K., Walters, H., Tantawy, M.N., Fu, A., Manning, H.C., *et al.* (2014). Acetate dependence of tumors. *Cell* *159*, 1591-1602.

Connelly, J.J., Yuan, P., Hsu, H.C., Li, Z., Xu, R.M., and Sternglanz, R. (2006). Structure and function of the *Saccharomyces cerevisiae* Sir3 BAH domain. *Molecular and cellular biology* *26*, 3256-3265.

Corpet, A., and Stucki, M. (2014). Chromatin maintenance and dynamics in senescence: a spotlight on SAHF formation and the epigenome of senescent cells. *Chromosoma* *123*, 423-436.

Cremer, M., von Hase, J., Volm, T., Brero, A., Kreth, G., Walter, J., Fischer, C., Solovei, I., Cremer, C., and Cremer, T. (2001). Non-random radial higher-order chromatin arrangements in nuclei of diploid human cells. *Chromosome research : an international journal on the molecular, supramolecular and evolutionary aspects of chromosome biology* *9*, 541-567.

Cremer, T., Cremer, C., Baumann, H., Luedtke, E.K., Sperling, K., Teuber, V., and Zorn, C. (1982). Rabl's model of the interphase chromosome arrangement tested in Chinese hamster cells by premature chromosome condensation and laser-UV-microbeam experiments. *Human genetics* *60*, 46-56.

Cremer, T., and Cremer, M. (2010). Chromosome territories. *Cold Spring Harbor perspectives in biology* *2*, a003889.

Croft, J.A., Bridger, J.M., Boyle, S., Perry, P., Teague, P., and Bickmore, W.A. (1999). Differences in the localization and morphology of chromosomes in the human nucleus. *The Journal of cell biology* *145*, 1119-1131.

Cutter, A.R., and Hayes, J.J. (2015). A brief review of nucleosome structure. *FEBS letters* *589*, 2914-2922.

Daignan-Fornier, B., and Fink, G.R. (1992). Coregulation of purine and histidine biosynthesis by the transcriptional activators BAS1 and BAS2. *Proc Natl Acad Sci U S A* *89*, 6746-6750.

Daignan-Fornier, B., and Sagot, I. (2011). Proliferation/Quiescence: When to start? Where to stop? What to stock? *Cell Div* *6*, 20.

Dang, W., Steffen, K.K., Perry, R., Dorsey, J.A., Johnson, F.B., Shilatifard, A., Kaerberlein, M., Kennedy, B.K., and Berger, S.L. (2009). Histone H4 lysine 16 acetylation regulates cellular lifespan. *Nature* *459*, 802-807.

Dashko, S., Zhou, N., Compagno, C., and Piskur, J. (2014). Why, when, and how did yeast evolve alcoholic fermentation? *FEMS yeast research* *14*, 826-832.

Davidson, G.S., Joe, R.M., Roy, S., Meirelles, O., Allen, C.P., Wilson, M.R., Tapia, P.H., Manzanilla, E.E., Dodson, A.E., Chakraborty, S., *et al.* (2011). The proteomics of quiescent and nonquiescent cell differentiation in yeast stationary-phase cultures. *Molecular biology of the cell* 22, 988-998.

De Deken, R.H. (1966). The Crabtree effect: a regulatory system in yeast. *Journal of general microbiology* 44, 149-156.

de Laat, W., and Duboule, D. (2013). Topology of mammalian developmental enhancers and their regulatory landscapes. *Nature* 502, 499-506.

De Virgilio, C. (2012). The essence of yeast quiescence. *FEMS microbiology reviews* 36, 306-339.

de Wit, E., and de Laat, W. (2012). A decade of 3C technologies: insights into nuclear organization. *Genes & development* 26, 11-24.

Dekker, J., Rippe, K., Dekker, M., and Kleckner, N. (2002). Capturing chromosome conformation. *Science* 295, 1306-1311.

Dewar, J.M., and Lydall, D. (2012). Similarities and differences between "uncapped" telomeres and DNA double-strand breaks. *Chromosoma* 121, 117-130.

Dixon, J.R., Jung, I., Selvaraj, S., Shen, Y., Antosiewicz-Bourget, J.E., Lee, A.Y., Ye, Z., Kim, A., Rajagopal, N., Xie, W., *et al.* (2015). Chromatin architecture reorganization during stem cell differentiation. *Nature* 518, 331-336.

Dixon, J.R., Selvaraj, S., Yue, F., Kim, A., Li, Y., Shen, Y., Hu, M., Liu, J.S., and Ren, B. (2012). Topological domains in mammalian genomes identified by analysis of chromatin interactions. *Nature* 485, 376-380.

Dorigo, B., Schalch, T., Kulangara, A., Duda, S., Schroeder, R.R., and Richmond, T.J. (2004). Nucleosome arrays reveal the two-start organization of the chromatin fiber. *Science* 306, 1571-1573.

Edward J. Louis, M.M.B. (2014). *Subtelomeres* (Springer).

Ehrentraut, S., Hassler, M., Oppikofer, M., Kueng, S., Weber, J.M., Mueller, J.W., Gasser, S.M., Ladurner, A.G., and Ehrenhofer-Murray, A.E. (2011). Structural basis for the role of the Sir3 AAA+ domain in silencing: interaction with Sir4 and unmethylated histone H3K79. *Genes & development* 25, 1835-1846.

Elgin, S.C., and Reuter, G. (2013). Position-effect variegation, heterochromatin formation, and gene silencing in *Drosophila*. *Cold Spring Harbor perspectives in biology* 5, a017780.

Fabrizio, P., Battistella, L., Vardavas, R., Gattazzo, C., Liou, L.L., Diaspro, A., Dossen, J.W., Gralla, E.B., and Longo, V.D. (2004). Superoxide is a mediator of an altruistic aging program in *Saccharomyces cerevisiae*. *The Journal of cell biology* 166, 1055-1067.

Fabrizio, P., Gattazzo, C., Battistella, L., Wei, M., Cheng, C., McGrew, K., and Longo, V.D. (2005). Sir2 blocks extreme life-span extension. *Cell* 123, 655-667.

Fabrizio, P., Hoon, S., Shamalnasab, M., Galbani, A., Wei, M., Giaever, G., Nislow, C., and Longo, V.D. (2010). Genome-wide screen in *Saccharomyces cerevisiae* identifies vacuolar protein sorting, autophagy, biosynthetic, and tRNA methylation genes involved in life span regulation. *PLoS genetics* 6, e1001024.

Fabrizio, P., Liou, L.L., Moy, V.N., Diaspro, A., Valentine, J.S., Gralla, E.B., and Longo, V.D. (2003). SOD2 functions downstream of Sch9 to extend longevity in yeast. *Genetics* 163, 35-46.

Fabrizio, P., and Longo, V.D. (2003). The chronological life span of *Saccharomyces cerevisiae*. *Aging cell* 2, 73-81.

Fabrizio, P., Pozza, F., Pletcher, S.D., Gendron, C.M., and Longo, V.D. (2001). Regulation of longevity and stress resistance by Sch9 in yeast. *Science* 292, 288-290.

Fawcett (1966). *The Cell*.

Ferreira, H.C., Luke, B., Schober, H., Kalck, V., Lingner, J., and Gasser, S.M. (2011). The PIAS homologue Siz2 regulates perinuclear telomere position and telomerase activity in budding yeast. *Nature cell biology* 13, 867-874.

Filion, G.J., van Bommel, J.G., Braunschweig, U., Talhout, W., Kind, J., Ward, L.D., Brugman, W., de Castro, I.J., Kerkhoven, R.M., Bussemaker, H.J., *et al.* (2010). Systematic protein location mapping reveals five principal chromatin types in *Drosophila* cells. *Cell* 143, 212-224.

Fisher, C.L., and Fisher, A.G. (2011). Chromatin states in pluripotent, differentiated, and reprogrammed cells. *Curr Opin Genet Dev* 21, 140-146.

Fontana, L., Partridge, L., and Longo, V.D. (2010). Extending healthy life span--from yeast to humans. *Science* 328, 321-326.

Fourel, G., Revardel, E., Koering, C.E., and Gilson, E. (1999). Cohabitation of insulators and silencing elements in yeast subtelomeric regions. *The EMBO journal* 18, 2522-2537.

Fraser, J., Williamson, I., Bickmore, W.A., and Dostie, J. (2015). An Overview of Genome Organization and How We Got There: from FISH to Hi-C. *Microbiology and molecular biology reviews* : MMBR 79, 347-372.

Fraser, P., and Bickmore, W. (2007). Nuclear organization of the genome and the potential for gene regulation. *Nature* 447, 413-417.

Freitas-Junior, L.H., Bottius, E., Pirrit, L.A., Deitsch, K.W., Scheidig, C., Guinet, F., Nehrbass, U., Wellems, T.E., and Scherf, A. (2000). Frequent ectopic recombination of virulence factor genes in telomeric chromosome clusters of *P. falciparum*. *Nature* 407, 1018-1022.

Fuge, E.K., Braun, E.L., and Werner-Washburne, M. (1994). Protein synthesis in long-term stationary-phase cultures of *Saccharomyces cerevisiae*. *Journal of bacteriology* 176, 5802-5813.

Funabiki, H., Hagan, I., Uzawa, S., and Yanagida, M. (1993). Cell cycle-dependent specific positioning and clustering of centromeres and telomeres in fission yeast. *The Journal of cell biology* 121, 961-976.

Galdieri, L., Zhang, T., Rogerson, D., Lleshi, R., and Vancura, A. (2014). Protein acetylation and acetyl coenzyme a metabolism in budding yeast. *Eukaryotic cell* 13, 1472-1483.

Gallardo, F., Laterreur, N., Cusanelli, E., Ouenzar, F., Querido, E., Wellinger, R.J., and Chartrand, P. (2011). Live cell imaging of telomerase RNA dynamics reveals cell cycle-dependent clustering of telomerase at elongating telomeres. *Molecular cell* 44, 819-827.

Gallo, C.M., Smith, D.L., Jr., and Smith, J.S. (2004). Nicotinamide clearance by Pnc1 directly regulates Sir2-mediated silencing and longevity. *Molecular and cellular biology* 24, 1301-1312.

Gasch, A.P., Spellman, P.T., Kao, C.M., Carmel-Harel, O., Eisen, M.B., Storz, G., Botstein, D., and Brown, P.O. (2000). Genomic expression programs in the response of yeast cells to environmental changes. *Molecular biology of the cell* 11, 4241-4257.

Georgel, P.T., Palacios DeBeer, M.A., Pietz, G., Fox, C.A., and Hansen, J.C. (2001). Sir3-dependent assembly of supramolecular chromatin structures in vitro.

Proceedings of the National Academy of Sciences of the United States of America *98*, 8584-8589.

Giadrossi, S., Dvorkina, M., and Fisher, A.G. (2007). Chromatin organization and differentiation in embryonic stem cell models. *Current opinion in genetics & development* *17*, 132-138.

Ginovart, M., Prats, C., Portell, X., and Silbert, M. (2011). Exploring the lag phase and growth initiation of a yeast culture by means of an individual-based model. *Food microbiology* *28*, 810-817.

Gorkin, D.U., Leung, D., and Ren, B. (2014). The 3D genome in transcriptional regulation and pluripotency. *Cell Stem Cell* *14*, 762-775.

Gotta, M., Laroche, T., Formenton, A., Maillet, L., Scherthan, H., and Gasser, S.M. (1996). The clustering of telomeres and colocalization with Rap1, Sir3, and Sir4 proteins in wild-type *Saccharomyces cerevisiae*. *The Journal of cell biology* *134*, 1349-1363.

Gotta, M., Palladino, F., and Gasser, S.M. (1998). Functional characterization of the N terminus of Sir3p. *Molecular and cellular biology* *18*, 6110-6120.

Gottschling, D.E., Aparicio, O.M., Billington, B.L., and Zakian, V.A. (1990). Position effect at *S. cerevisiae* telomeres: reversible repression of Pol II transcription. *Cell* *63*, 751-762.

Govin, J., Escoffier, E., Rousseaux, S., Kuhn, L., Ferro, M., Thevenon, J., Catena, R., Davidson, I., Garin, J., Khochbin, S., *et al.* (2007). Pericentric heterochromatin reprogramming by new histone variants during mouse spermiogenesis. *The Journal of cell biology* *176*, 283-294.

Govin, J., and Khochbin, S. (2013). Histone variants and sensing of chromatin functional states. *Nucleus* *4*, 438-442.

Gray, J.V., Petsko, G.A., Johnston, G.C., Ringe, D., Singer, R.A., and Werner-Washburne, M. (2004). "Sleeping beauty": quiescence in *Saccharomyces cerevisiae*. *Microbiology and molecular biology reviews : MMBR* *68*, 187-206.

Greil, F., Moorman, C., and van Steensel, B. (2006). DamID: mapping of in vivo protein-genome interactions using tethered DNA adenine methyltransferase. *Methods in enzymology* *410*, 342-359.

Grevengoed, T.J., Klett, E.L., and Coleman, R.A. (2014). Acyl-CoA metabolism and partitioning. *Annual review of nutrition* *34*, 1-30.

Grunstein, M., and Gasser, S.M. (2013). Epigenetics in *Saccharomyces cerevisiae*. *Cold Spring Harbor perspectives in biology* *5*.

Guarente, L. (2011). The logic linking protein acetylation and metabolism. *Cell metabolism* *14*, 151-153.

Guidi, M., Ruault, M., Marbouty, M., Loiodice, I., Cournac, A., Billaudeau, C., Hocher, A., Mozziconacci, J., Koszul, R., and Taddei, A. (2015). Spatial reorganization of telomeres in long-lived quiescent cells. *Genome biology* *16*, 206.

Gurard-Levin, Z.A., and Almouzni, G. (2014). Histone modifications and a choice of variant: a language that helps the genome express itself. *F1000prime reports* *6*, 76.

Gut, P., and Verdin, E. (2013). The nexus of chromatin regulation and intermediary metabolism. *Nature* *502*, 489-498.

Haghnazari, E., and Heyer, W.D. (2004). The Hog1 MAP kinase pathway and the Mec1 DNA damage checkpoint pathway independently control the cellular responses to hydrogen peroxide. *DNA Repair (Amst)* *3*, 769-776.

Haldar, S., Saini, A., Nanda, J.S., Saini, S., and Singh, J. (2011). Role of Swi6/HP1 self-association-mediated recruitment of Clr4/Suv39 in establishment and maintenance of heterochromatin in fission yeast. *The Journal of biological chemistry* *286*, 9308-9320.

Halme, A., Bumgarner, S., Styles, C., and Fink, G.R. (2004). Genetic and epigenetic regulation of the FLO gene family generates cell-surface variation in yeast. *Cell* *116*, 405-415.

Hannan, A., Abraham, N.M., Goyal, S., Jamir, I., Priyakumar, U.D., and Mishra, K. (2015). Sumoylation of Sir2 differentially regulates transcriptional silencing in yeast. *Nucleic acids research*.

Hardie, D.G. (2015). AMPK: positive and negative regulation, and its role in whole-body energy homeostasis. *Current opinion in cell biology* *33*, 1-7.

Hartwell, L.H., Culotti, J., Pringle, J.R., and Reid, B.J. (1974). Genetic control of the cell division cycle in yeast. *Science* *183*, 46-51.

Hawkins, R.D., Hon, G.C., Lee, L.K., Ngo, Q., Lister, R., Pelizzola, M., Edsall, L.E., Kuan, S., Luu, Y., Klugman, S., *et al.* (2010). Distinct epigenomic landscapes of pluripotent and lineage-committed human cells. *Cell Stem Cell* *6*, 479-491.

Hecht, A., Strahl-Bolsinger, S., and Grunstein, M. (1996). Spreading of transcriptional repressor SIR3 from telomeric heterochromatin. *Nature* *383*, 92-96.

Hirano, Y., Fukunaga, K., and Sugimoto, K. (2009). Rif1 and rif2 inhibit localization of tel1 to DNA ends. *Molecular cell* *33*, 312-322.

Hoze, N., Ruault, M., Amoroso, C., Taddei, A., and Holcman, D. (2013). Spatial telomere organization and clustering in yeast *Saccharomyces cerevisiae* nucleus is generated by a random dynamics of aggregation-dissociation. *Molecular biology of the cell* *24*, 1791-1800, S1791-1710.

Hsieh, T.H., Weiner, A., Lajoie, B., Dekker, J., Friedman, N., and Rando, O.J. (2015). Mapping Nucleosome Resolution Chromosome Folding in Yeast by Micro-C. *Cell* *162*, 108-119.

Huang, Z., Cai, L., and Tu, B.P. (2015). Dietary control of chromatin. *Current opinion in cell biology* *34*, 69-74.

Ikeda, A., Muneoka, T., Murakami, S., Hirota, A., Yabuki, Y., Karashima, T., Nakazono, K., Tsuruno, M., Pichler, H., Shirahige, K., *et al.* (2015). Sphingolipids regulate telomere clustering by affecting the transcription of genes involved in telomere homeostasis. *Journal of cell science* *128*, 2454-2467.

Izzo, A., Kamieniarz, K., and Schneider, R. (2008). The histone H1 family: specific members, specific functions? *Biological chemistry* *389*, 333-343.

Joffe, B., Leonhardt, H., and Solovei, I. (2010). Differentiation and large scale spatial organization of the genome. *Curr Opin Genet Dev* *20*, 562-569.

Jost, K.L., Bertulat, B., and Cardoso, M.C. (2012). Heterochromatin and gene positioning: inside, outside, any side? *Chromosoma* *121*, 555-563.

Kaeberlein, M. (2010). Lessons on longevity from budding yeast. *Nature* *464*, 513-519.

Kalhor, R., Tjong, H., Jayathilaka, N., Alber, F., and Chen, L. (2012). Genome architectures revealed by tethered chromosome conformation capture and population-based modeling. *Nature biotechnology* *30*, 90-98.

Kaochar, S., and Tu, B.P. (2012). Gatekeepers of chromatin: Small metabolites elicit big changes in gene expression. *Trends in biochemical sciences* *37*, 477-483.

Kato, M., and Lin, S.J. (2014). Regulation of NAD⁺ metabolism, signaling and compartmentalization in the yeast *Saccharomyces cerevisiae*. *DNA repair* 23, 49-58.

Keating, S.T., and El-Osta, A. (2015). Epigenetics and metabolism. *Circulation research* 116, 715-736.

Kellermann, N.P. (2013). Epigenetic transmission of Holocaust trauma: can nightmares be inherited? *Isr J Psychiatry Relat Sci* 50, 33-39.

Kennedy, B.K., Austriaco, N.R., Jr., and Guarente, L. (1994). Daughter cells of *Saccharomyces cerevisiae* from old mothers display a reduced life span. *J Cell Biol* 127, 1985-1993.

Kennedy, B.K., Gotta, M., Sinclair, D.A., Mills, K., McNabb, D.S., Murthy, M., Pak, S.M., Laroche, T., Gasser, S.M., and Guarente, L. (1997). Redistribution of silencing proteins from telomeres to the nucleolus is associated with extension of life span in *S. cerevisiae*. *Cell* 89, 381-391.

Klosinska, M.M., Crutchfield, C.A., Bradley, P.H., Rabinowitz, J.D., and Broach, J.R. (2011a). Yeast cells can access distinct quiescent states. *Genes & development* 25, 336-349.

Klosinska, M.M., Crutchfield, C.A., Bradley, P.H., Rabinowitz, J.D., and Broach, J.R. (2011b). Yeast cells can access distinct quiescent states. *Genes Dev* 25, 336-349.

Kueng, S., Oppikofer, M., and Gasser, S.M. (2013). SIR proteins and the assembly of silent chromatin in budding yeast. *Annual review of genetics* 47, 275-306.

Kupiec, M. (2014). Biology of telomeres: lessons from budding yeast. *FEMS microbiology reviews* 38, 144-171.

Kupper, K., Kolbl, A., Biener, D., Dittrich, S., von Hase, J., Thormeyer, T., Fiegler, H., Carter, N.P., Speicher, M.R., Cremer, T., *et al.* (2007). Radial chromatin positioning is shaped by local gene density, not by gene expression. *Chromosoma* 116, 285-306.

Lakadamyali, M., and Cosma, M.P. (2015). Advanced microscopy methods for visualizing chromatin structure. *FEBS letters* 589, 3023-3030.

Landry, J., Sutton, A., Tafrov, S.T., Heller, R.C., Stebbins, J., Pillus, L., and Sternglanz, R. (2000). The silencing protein SIR2 and its homologs are NAD-dependent protein deacetylases. *Proceedings of the National Academy of Sciences of the United States of America* 97, 5807-5811.

Laporte, D., Courtout, F., Salin, B., Ceschin, J., and Sagot, I. (2013). An array of nuclear microtubules reorganizes the budding yeast nucleus during quiescence. *The Journal of cell biology* 203, 585-594.

Laporte, D., Lebaudy, A., Sahin, A., Pinson, B., Ceschin, J., Daignan-Fornier, B., and Sagot, I. (2011). Metabolic status rather than cell cycle signals control quiescence entry and exit. *The Journal of cell biology* 192, 949-957.

Laporte, D., Salin, B., Daignan-Fornier, B., and Sagot, I. (2008). Reversible cytoplasmic localization of the proteasome in quiescent yeast cells. *The Journal of cell biology* 181, 737-745.

Le, T.B., Imakaev, M.V., Mirny, L.A., and Laub, M.T. (2013). High-resolution mapping of the spatial organization of a bacterial chromosome. *Science* 342, 731-734.

Lemaitre, C., and Bickmore, W.A. (2015). Chromatin at the nuclear periphery and the regulation of genome functions. *Histochemistry and cell biology* 144, 111-122.

Leroy, C., Mann, C., and Marsolier, M.C. (2001). Silent repair accounts for cell cycle specificity in the signaling of oxidative DNA lesions. *Embo J* 20, 2896-2906.

Lewis, E.B. (1978). A gene complex controlling segmentation in *Drosophila*. *Nature* 276, 565-570.

Li, G., and Zhu, P. (2015). Structure and organization of chromatin fiber in the nucleus. *FEBS letters* 589, 2893-2904.

Li, L., Miles, S., Melville, Z., Prasad, A., Bradley, G., and Breeden, L.L. (2013). Key events during the transition from rapid growth to quiescence in budding yeast require posttranscriptional regulators. *Molecular biology of the cell* 24, 3697-3709.

Liang, C.Y., Hsu, P.H., Chou, D.F., Pan, C.Y., Wang, L.C., Huang, W.C., Tsai, M.D., and Lo, W.S. (2011). The histone H3K36 demethylase Rph1/KDM4 regulates the expression of the photoreactivation gene PHR1. *Nucleic Acids Res* 39, 4151-4165.

Liang, C.Y., Wang, L.C., and Lo, W.S. (2013). Dissociation of the H3K36 demethylase Rph1 from chromatin mediates derepression of environmental stress-response genes under genotoxic stress in *Saccharomyces cerevisiae*. *Mol Biol Cell* 24, 3251-3262.

Lillie, S.H., and Pringle, J.R. (1980). Reserve carbohydrate metabolism in *Saccharomyces cerevisiae*: responses to nutrient limitation. *Journal of bacteriology* 143, 1384-1394.

Lin, S.J., Ford, E., Haigis, M., Liszt, G., and Guarente, L. (2004). Calorie restriction extends yeast life span by lowering the level of NADH. *Genes & development* 18, 12-16.

Lin, S.J., and Guarente, L. (2003). Nicotinamide adenine dinucleotide, a metabolic regulator of transcription, longevity and disease. *Curr Opin Cell Biol* 15, 241-246.

Lin, Y.Y., Lu, J.Y., Zhang, J., Walter, W., Dang, W., Wan, J., Tao, S.C., Qian, J., Zhao, Y., Boeke, J.D., *et al.* (2009). Protein acetylation microarray reveals that NuA4 controls key metabolic target regulating gluconeogenesis. *Cell* 136, 1073-1084.

Liou, G.G., Tanny, J.C., Kruger, R.G., Walz, T., and Moazed, D. (2005). Assembly of the SIR complex and its regulation by O-acetyl-ADP-ribose, a product of NAD-dependent histone deacetylation. *Cell* 121, 515-527.

Liti, G., Carter, D.M., Moses, A.M., Warringer, J., Parts, L., James, S.A., Davey, R.P., Roberts, I.N., Burt, A., Koufopanou, V., *et al.* (2009). Population genomics of domestic and wild yeasts. *Nature* 458, 337-341.

Liu, T., Rechtsteiner, A., Egelhofer, T.A., Vielle, A., Latorre, I., Cheung, M.S., Ercan, S., Ikegami, K., Jensen, M., Kolasinska-Zwiercz, P., *et al.* (2011). Broad chromosomal domains of histone modification patterns in *C. elegans*. *Genome research* 21, 227-236.

Loewith, R., and Hall, M.N. (2011). Target of rapamycin (TOR) in nutrient signaling and growth control. *Genetics* 189, 1177-1201.

Loiodice, I., Dubarry, M., and Taddei, A. (2014). Scoring and manipulating gene position and dynamics using FROS in budding yeast. *Current protocols in cell biology / editorial board, Juan S Bonifacino [et al]* 62, Unit 22 17 21-14.

Longo, V.D. (1999). Mutations in signal transduction proteins increase stress resistance and longevity in yeast, nematodes, fruit flies, and mammalian neuronal cells. *Neurobiology of aging* 20, 479-486.

Longo, V.D., and Fabrizio, P. (2012). Chronological aging in *Saccharomyces cerevisiae*. *Sub-cellular biochemistry* 57, 101-121.

Longo, V.D., Shadel, G.S., Kaeberlein, M., and Kennedy, B. (2012). Replicative and chronological aging in *Saccharomyces cerevisiae*. *Cell metabolism* *16*, 18-31.

Lu, C., Brauer, M.J., and Botstein, D. (2009a). Slow growth induces heat-shock resistance in normal and respiratory-deficient yeast. *Molecular biology of the cell* *20*, 891-903.

Lu, S.P., Kato, M., and Lin, S.J. (2009b). Assimilation of endogenous nicotinamide riboside is essential for calorie restriction-mediated life span extension in *Saccharomyces cerevisiae*. *The Journal of biological chemistry* *284*, 17110-17119.

Lu, S.P., and Lin, S.J. (2010). Regulation of yeast sirtuins by NAD(+) metabolism and calorie restriction. *Biochimica et biophysica acta* *1804*, 1567-1575.

Lu, S.P., and Lin, S.J. (2011). Phosphate-responsive signaling pathway is a novel component of NAD+ metabolism in *Saccharomyces cerevisiae*. *The Journal of biological chemistry* *286*, 14271-14281.

Luger, K., Dechassa, M.L., and Tremethick, D.J. (2012). New insights into nucleosome and chromatin structure: an ordered state or a disordered affair? *Nature reviews Molecular cell biology* *13*, 436-447.

Luger, K., Mader, A.W., Richmond, R.K., Sargent, D.F., and Richmond, T.J. (1997). Crystal structure of the nucleosome core particle at 2.8 Å resolution. *Nature* *389*, 251-260.

Luke, B., Panza, A., Redon, S., Iglesias, N., Li, Z., and Lingner, J. (2008). The Rat1p 5' to 3' exonuclease degrades telomeric repeat-containing RNA and promotes telomere elongation in *Saccharomyces cerevisiae*. *Molecular cell* *32*, 465-477.

Lupianez, D.G., Kraft, K., Heinrich, V., Krawitz, P., Brancati, F., Klopocki, E., Horn, D., Kayserili, H., Opitz, J.M., Laxova, R., *et al.* (2015). Disruptions of topological chromatin domains cause pathogenic rewiring of gene-enhancer interactions. *Cell* *161*, 1012-1025.

Ma, J., Goryaynov, A., Sarma, A., and Yang, W. (2012). Self-regulated viscous channel in the nuclear pore complex. *Proceedings of the National Academy of Sciences of the United States of America* *109*, 7326-7331.

Maicher, A., Kastner, L., Dees, M., and Luke, B. (2012). Deregulated telomere transcription causes replication-dependent telomere shortening and promotes cellular senescence. *Nucleic acids research* *40*, 6649-6659.

Maillet, L., Boscheron, C., Gotta, M., Marcand, S., Gilson, E., and Gasser, S.M. (1996). Evidence for silencing compartments within the yeast nucleus: a role for telomere proximity and Sir protein concentration in silencer-mediated repression. *Genes & development* *10*, 1796-1811.

Maillet, L., Gaden, F., Brevet, V., Fourel, G., Martin, S.G., Dubrana, K., Gasser, S.M., and Gilson, E. (2001). Ku-deficient yeast strains exhibit alternative states of silencing competence. *EMBO reports* *2*, 203-210.

Malyavko, A.N., Parfenova, Y.Y., Zvereva, M.I., and Dontsova, O.A. (2014). Telomere length regulation in budding yeasts. *FEBS letters* *588*, 2530-2536.

Marcand, S., Brevet, V., and Gilson, E. (1999). Progressive cis-inhibition of telomerase upon telomere elongation. *The EMBO journal* *18*, 3509-3519.

Marcand, S., Buck, S.W., Moretti, P., Gilson, E., and Shore, D. (1996). Silencing of genes at nontelomeric sites in yeast is controlled by sequestration of silencing factors at telomeres by Rap 1 protein. *Genes & development* *10*, 1297-1309.

Marcand, S., Gilson, E., and Shore, D. (1997). A protein-counting mechanism for telomere length regulation in yeast. *Science* *275*, 986-990.

Marcand, S., Pardo, B., Gratias, A., Cahun, S., and Callebaut, I. (2008). Multiple pathways inhibit NHEJ at telomeres. *Genes & development* 22, 1153-1158.

Martinez, M.J., Roy, S., Archuletta, A.B., Wentzell, P.D., Anna-Arriola, S.S., Rodriguez, A.L., Aragon, A.D., Quinones, G.A., Allen, C., and Werner-Washburne, M. (2004). Genomic analysis of stationary-phase and exit in *Saccharomyces cerevisiae*: gene expression and identification of novel essential genes. *Molecular biology of the cell* 15, 5295-5305.

Martino, F., Kueng, S., Robinson, P., Tsai-Pflugfelder, M., van Leeuwen, F., Ziegler, M., Cubizolles, F., Cockell, M.M., Rhodes, D., and Gasser, S.M. (2009). Reconstitution of yeast silent chromatin: multiple contact sites and O-AADPR binding load SIR complexes onto nucleosomes in vitro. *Molecular cell* 33, 323-334.

Matecic, M., Smith, D.L., Pan, X., Maqani, N., Bekiranov, S., Boeke, J.D., and Smith, J.S. (2010). A microarray-based genetic screen for yeast chronological aging factors. *PLoS Genet* 6, e1000921.

Matsuda, A., Chikashige, Y., Ding, D.Q., Ohtsuki, C., Mori, C., Asakawa, H., Kimura, H., Haraguchi, T., and Hiraoka, Y. (2015). Highly condensed chromatin is formed adjacent to subtelomeric and decondensed silent chromatin in fission yeast. *Nature communications* 6, 7753.

Mattout, A., Cabianca, D.S., and Gasser, S.M. (2015). Chromatin states and nuclear organization in development--a view from the nuclear lamina. *Genome Biol* 16, 174.

Maze, I., Noh, K.M., Soshnev, A.A., and Allis, C.D. (2014). Every amino acid matters: essential contributions of histone variants to mammalian development and disease. *Nature reviews Genetics* 15, 259-271.

McBrian, M.A., Behbahan, I.S., Ferrari, R., Su, T., Huang, T.W., Li, K., Hong, C.S., Christofk, H.R., Vogelauer, M., Seligson, D.B., *et al.* (2013). Histone acetylation regulates intracellular pH. *Molecular cell* 49, 310-321.

McBryant, S.J., Krause, C., Woodcock, C.L., and Hansen, J.C. (2008). The silent information regulator 3 protein, SIR3p, binds to chromatin fibers and assembles a hypercondensed chromatin architecture in the presence of salt. *Molecular and cellular biology* 28, 3563-3572.

McClure, J.M., Wierman, M.B., Maqani, N., and Smith, J.S. (2012). Isonicotinamide enhances Sir2 protein-mediated silencing and longevity in yeast by raising intracellular NAD⁺ concentration. *The Journal of biological chemistry* 287, 20957-20966.

McFaline-Figueroa, J.R., Vevea, J., Swayne, T.C., Zhou, C., Liu, C., Leung, G., Boldogh, I.R., and Pon, L.A. (2011). Mitochondrial quality control during inheritance is associated with lifespan and mother-daughter age asymmetry in budding yeast. *Aging Cell* 10, 885-895.

McKnight, J.N., Boerma, J.W., Breeden, L.L., and Tsukiyama, T. (2015). Global Promoter Targeting of a Conserved Lysine Deacetylase for Transcriptional Shutoff during Quiescence Entry. *Molecular cell* 59, 732-743.

Meister, P., and Taddei, A. (2013). Building silent compartments at the nuclear periphery: a recurrent theme. *Current opinion in genetics & development* 23, 96-103.

Mekhail, K., and Moazed, D. (2010). The nuclear envelope in genome organization, expression and stability. *Nature reviews Molecular cell biology* 11, 317-328.

Melters, D.P., Nye, J., Zhao, H., and Dalal, Y. (2015). Chromatin Dynamics in Vivo: A Game of Musical Chairs. *Genes* 6, 751-776.

Mesquita, A., Weinberger, M., Silva, A., Sampaio-Marques, B., Almeida, B., Leao, C., Costa, V., Rodrigues, F., Burhans, W.C., and Ludovico, P. (2010). Caloric restriction or catalase inactivation extends yeast chronological lifespan by inducing H₂O₂ and superoxide dismutase activity. *Proceedings of the National Academy of Sciences of the United States of America* 107, 15123-15128.

Meunier, J.R., and Choder, M. (1999). *Saccharomyces cerevisiae* colony growth and ageing: biphasic growth accompanied by changes in gene expression. *Yeast* 15, 1159-1169.

Mews, P., Zee, B.M., Liu, S., Donahue, G., Garcia, B.A., and Berger, S.L. (2014). Histone methylation has dynamics distinct from those of histone acetylation in cell cycle reentry from quiescence. *Molecular and cellular biology* 34, 3968-3980.

Miles, S., Li, L., Davison, J., and Breeden, L.L. (2013). Xbp1 directs global repression of budding yeast transcription during the transition to quiescence and is important for the longevity and reversibility of the quiescent state. *PLoS genetics* 9, e1003854.

Mirisola, M.G., Braun, R.J., and Petranovic, D. (2014). Approaches to study yeast cell aging and death. *FEMS yeast research* 14, 109-118.

Mirisola, M.G., and Longo, V.D. (2012). Acetic acid and acidification accelerate chronological and replicative aging in yeast. *Cell cycle* 11, 3532-3533.

Mizuguchi, T., Fudenberg, G., Mehta, S., Belton, J.M., Taneja, N., Folco, H.D., FitzGerald, P., Dekker, J., Mirny, L., Barrowman, J., *et al.* (2014). Cohesin-dependent globules and heterochromatin shape 3D genome architecture in *S. pombe*. *Nature* 516, 432-435.

Moazed, D. (2001). Enzymatic activities of Sir2 and chromatin silencing. *Current opinion in cell biology* 13, 232-238.

Mortimer, R.K., and Johnston, J.R. (1959). Life span of individual yeast cells. *Nature* 183, 1751-1752.

Mosser, D.M., and Edwards, J.P. (2008). Exploring the full spectrum of macrophage activation. *Nature reviews Immunology* 8, 958-969.

Moussaieff, A., Rouleau, M., Kitsberg, D., Cohen, M., Levy, G., Barasch, D., Nemirovski, A., Shen-Orr, S., Laevsky, I., Amit, M., *et al.* (2015). Glycolysis-mediated changes in acetyl-CoA and histone acetylation control the early differentiation of embryonic stem cells. *Cell metabolism* 21, 392-402.

Nagai, S., Dubrana, K., Tsai-Pflugfelder, M., Davidson, M.B., Roberts, T.M., Brown, G.W., Varela, E., Hediger, F., Gasser, S.M., and Krogan, N.J. (2008). Functional targeting of DNA damage to a nuclear pore-associated SUMO-dependent ubiquitin ligase. *Science* 322, 597-602.

Narayanaswamy, R., Levy, M., Tsechansky, M., Stovall, G.M., O'Connell, J.D., Mirrieles, J., Ellington, A.D., and Marcotte, E.M. (2009). Widespread reorganization of metabolic enzymes into reversible assemblies upon nutrient starvation. *Proceedings of the National Academy of Sciences of the United States of America* 106, 10147-10152.

Nemeth, A., Conesa, A., Santoyo-Lopez, J., Medina, I., Montaner, D., Peterfia, B., Solovei, I., Cremer, T., Dopazo, J., and Langst, G. (2010). Initial genomics of the human nucleolus. *PLoS genetics* 6, e1000889.

Nishikawa, K., Iwamoto, Y., Kobayashi, Y., Katsuoka, F., Kawaguchi, S., Tsujita, T., Nakamura, T., Kato, S., Yamamoto, M., Takayanagi, H., *et al.* (2015). DNA

methyltransferase 3a regulates osteoclast differentiation by coupling to an S-adenosylmethionine-producing metabolic pathway. *Nature medicine* 21, 281-287.

Nora, E.P., Lajoie, B.R., Schulz, E.G., Giorgetti, L., Okamoto, I., Servant, N., Piolot, T., van Berkum, N.L., Meisig, J., Sedat, J., *et al.* (2012). Spatial partitioning of the regulatory landscape of the X-inactivation centre. *Nature* 485, 381-385.

Nordberg, N., Olsson, I., Carlsson, M., Hu, G.Z., Orzechowski Westholm, J., and Ronne, H. (2014). The histone demethylase activity of Rph1 is not essential for its role in the transcriptional response to nutrient signaling. *PLoS One* 9, e95078.

Norris, A., and Boeke, J.D. (2010). Silent information regulator 3: the Goldilocks of the silencing complex. *Genes & development* 24, 115-122.

Olins, A.L., and Olins, D.E. (1974). Spheroid chromatin units (v bodies). *Science* 183, 330-332.

Oppikofer, M., Kueng, S., and Gasser, S.M. (2013a). SIR-nucleosome interactions: structure-function relationships in yeast silent chromatin. *Gene* 527, 10-25.

Oppikofer, M., Kueng, S., Keusch, J.J., Hassler, M., Ladurner, A.G., Gut, H., and Gasser, S.M. (2013b). Dimerization of Sir3 via its C-terminal winged helix domain is essential for yeast heterochromatin formation. *The EMBO journal* 32, 437-449.

Orlandi, I., Ronzulli, R., Casatta, N., and Vai, M. (2013). Ethanol and acetate acting as carbon/energy sources negatively affect yeast chronological aging. *Oxid Med Cell Longev* 2013, 802870.

Padeken, J., and Heun, P. (2014). Nucleolus and nuclear periphery: velcro for heterochromatin. *Current opinion in cell biology* 28, 54-60.

Palazzo, A.F., and Gregory, T.R. (2014). The case for junk DNA. *PLoS genetics* 10, e1004351.

Palkova, Z., Devaux, F., Icovova, M., Minarikova, L., Le Crom, S., and Jacq, C. (2002). Ammonia pulses and metabolic oscillations guide yeast colony development. *Molecular biology of the cell* 13, 3901-3914.

Palkova, Z., Wilkinson, D., and Vachova, L. (2014). Aging and differentiation in yeast populations: elders with different properties and functions. *FEMS yeast research* 14, 96-108.

Palladino, F., Laroche, T., Gilson, E., Axelrod, A., Pillus, L., and Gasser, S.M. (1993). SIR3 and SIR4 proteins are required for the positioning and integrity of yeast telomeres. *Cell* 75, 543-555.

Peric-Hupkes, D., Meuleman, W., Pagie, L., Bruggeman, S.W., Solovei, I., Brugman, W., Graf, S., Flicek, P., Kerkhoven, R.M., van Lohuizen, M., *et al.* (2010). Molecular maps of the reorganization of genome-nuclear lamina interactions during differentiation. *Mol Cell* 38, 603-613.

Perrod, S., Cockell, M.M., Laroche, T., Renauld, H., Ducrest, A.L., Bonnard, C., and Gasser, S.M. (2001). A cytosolic NAD-dependent deacetylase, Hst2p, can modulate nucleolar and telomeric silencing in yeast. *The EMBO journal* 20, 197-209.

Perrod, S., and Gasser, S.M. (2003). Long-range silencing and position effects at telomeres and centromeres: parallels and differences. *Cellular and molecular life sciences : CMLS* 60, 2303-2318.

Phillips, D.M. (1963). The presence of acetyl groups of histones. *The Biochemical journal* 87, 258-263.

Phillips-Cremins, J.E., Sauria, M.E., Sanyal, A., Gerasimova, T.I., Lajoie, B.R., Bell, J.S., Ong, C.T., Hookway, T.A., Guo, C., Sun, Y., *et al.* (2013). Architectural protein

subclasses shape 3D organization of genomes during lineage commitment. *Cell* *153*, 1281-1295.

Piccirillo, S., White, M.G., Murphy, J.C., Law, D.J., and Honigberg, S.M. (2010). The Rim101p/PacC pathway and alkaline pH regulate pattern formation in yeast colonies. *Genetics* *184*, 707-716.

Pinon, R. (1978). Folded chromosomes in non-cycling yeast cells: evidence for a characteristic g0 form. *Chromosoma* *67*, 263-274.

Piper, P.W., Harris, N.L., and MacLean, M. (2006). Preadaptation to efficient respiratory maintenance is essential both for maximal longevity and the retention of replicative potential in chronologically ageing yeast. *Mechanisms of ageing and development* *127*, 733-740.

Piskur, J., Rozpedowska, E., Polakova, S., Merico, A., and Compagno, C. (2006). How did *Saccharomyces* evolve to become a good brewer? *Trends in genetics* : TIG *22*, 183-186.

Pobiega, S., and Marcand, S. (2010). Dicentric breakage at telomere fusions. *Genes Dev* *24*, 720-733.

Polak, P., Karlic, R., Koren, A., Thurman, R., Sandstrom, R., Lawrence, M.S., Reynolds, A., Rynes, E., Vlahovicek, K., Stamatoyannopoulos, J.A., *et al.* (2015). Cell-of-origin chromatin organization shapes the mutational landscape of cancer. *Nature* *518*, 360-364.

Pombo, A., and Dillon, N. (2015). Three-dimensional genome architecture: players and mechanisms. *Nature reviews Molecular cell biology* *16*, 245-257.

Postma, E., Scheffers, W.A., and van Dijken, J.P. (1989). Kinetics of growth and glucose transport in glucose-limited chemostat cultures of *Saccharomyces cerevisiae* CBS 8066. *Yeast* *5*, 159-165.

Power, P., Jeffery, D., Rehman, M.A., Chatterji, A., and Yankulov, K. (2011). Sub-telomeric core X and Y' elements in *S. cerevisiae* suppress extreme variations in gene silencing. *PloS one* *6*, e17523.

Pruyne, D., and Bretscher, A. (2000). Polarization of cell growth in yeast. I. Establishment and maintenance of polarity states. *Journal of cell science* *113 (Pt 3)*, 365-375.

Ptashne, M., and Gann, A. (1997). Transcriptional activation by recruitment. *Nature* *386*, 569-577.

Radman-Livaja, M., Ruben, G., Weiner, A., Friedman, N., Kamakaka, R., and Rando, O.J. (2011). Dynamics of Sir3 spreading in budding yeast: secondary recruitment sites and euchromatic localization. *The EMBO journal* *30*, 1012-1026.

Rathke, C., Baarends, W.M., Awe, S., and Renkawitz-Pohl, R. (2014). Chromatin dynamics during spermiogenesis. *Biochimica et biophysica acta* *1839*, 155-168.

Ray, A., Hector, R.E., Roy, N., Song, J.H., Berkner, K.L., and Runge, K.W. (2003). Sir3p phosphorylation by the Slt2p pathway effects redistribution of silencing function and shortened lifespan. *Nat Genet* *33*, 522-526.

Rebora, K., Desmoucelles, C., Borne, F., Pinson, B., and Daignan-Fornier, B. (2001). Yeast AMP pathway genes respond to adenine through regulated synthesis of a metabolic intermediate. *Mol Cell Biol* *21*, 7901-7912.

Reddy, K.L., and Feinberg, A.P. (2013). Higher order chromatin organization in cancer. *Seminars in cancer biology* *23*, 109-115.

Renauld, H., Aparicio, O.M., Zierath, P.D., Billington, B.L., Chhablani, S.K., and Gottschling, D.E. (1993). Silent domains are assembled continuously from the

telomere and are defined by promoter distance and strength, and by SIR3 dosage. *Genes & development* *7*, 1133-1145.

Ristow, M. (2014). Unraveling the truth about antioxidants: mitohormesis explains ROS-induced health benefits. *Nat Med* *20*, 709-711.

Ristow, M., and Schmeisser, S. (2011). Extending life span by increasing oxidative stress. *Free Radic Biol Med* *51*, 327-336.

Robinson, P.J., Fairall, L., Huynh, V.A., and Rhodes, D. (2006). EM measurements define the dimensions of the "30-nm" chromatin fiber: evidence for a compact, interdigitated structure. *Proceedings of the National Academy of Sciences of the United States of America* *103*, 6506-6511.

Robyr, D., Suka, Y., Xenarios, I., Kurdistani, S.K., Wang, A., Suka, N., and Grunstein, M. (2002). Microarray deacetylation maps determine genome-wide functions for yeast histone deacetylases. *Cell* *109*, 437-446.

Romano, G.H., Harari, Y., Yehuda, T., Podhorzer, A., Rubinstein, L., Shamir, R., Gottlieb, A., Silberberg, Y., Pe'er, D., Ruppin, E., *et al.* (2013). Environmental stresses disrupt telomere length homeostasis. *PLoS Genet* *9*, e1003721.

Rousseaux, S., and Khochbin, S. (2015). Histone Acylation beyond Acetylation: Terra Incognita in Chromatin Biology. *Cell journal* *17*, 1-6.

Rousseaux, S., Reynoird, N., Escoffier, E., Thevenon, J., Caron, C., and Khochbin, S. (2008). Epigenetic reprogramming of the male genome during gametogenesis and in the zygote. *Reproductive biomedicine online* *16*, 492-503.

Rozpedowska, E., Hellborg, L., Ishchuk, O.P., Orhan, F., Galafassi, S., Merico, A., Woolfit, M., Compagno, C., and Piskur, J. (2011). Parallel evolution of the make-accumulate-consume strategy in *Saccharomyces* and *Dekkera* yeasts. *Nature communications* *2*, 302.

Ruault, M., De Meyer, A., Liodice, I., and Taddei, A. (2011). Clustering heterochromatin: Sir3 promotes telomere clustering independently of silencing in yeast. *The Journal of cell biology* *192*, 417-431.

Rutledge, M.T., Russo, M., Belton, J.M., Dekker, J., and Broach, J.R. (2015). The yeast genome undergoes significant topological reorganization in quiescence. *Nucleic acids research* *43*, 8299-8313.

Sabari, B.R., Tang, Z., Huang, H., Yong-Gonzalez, V., Molina, H., Kong, H.E., Dai, L., Shimada, M., Cross, J.R., Zhao, Y., *et al.* (2015). Intracellular crotonyl-CoA stimulates transcription through p300-catalyzed histone crotonylation. *Molecular cell* *58*, 203-215.

Sadhu, M.J., Guan, Q., Li, F., Sales-Lee, J., Iavarone, A.T., Hammond, M.C., Cande, W.Z., and Rine, J. (2013). Nutritional control of epigenetic processes in yeast and human cells. *Genetics* *195*, 831-844.

Sagot, I., Pinson, B., Salin, B., and Daignan-Fornier, B. (2006). Actin bodies in yeast quiescent cells: an immediately available actin reserve? *Molecular biology of the cell* *17*, 4645-4655.

Salvi, J.S., Chan, J.N., Pettigrew, C., Liu, T.T., Wu, J.D., and Mekhail, K. (2013). Enforcement of a lifespan-sustaining distribution of Sir2 between telomeres, mating-type loci, and rDNA repeats by Rif1. *Aging cell* *12*, 67-75.

Sauve, A.A., Moir, R.D., Schramm, V.L., and Willis, I.M. (2005). Chemical activation of Sir2-dependent silencing by relief of nicotinamide inhibition. *Mol Cell* *17*, 595-601.

Schafer, G., McEvoy, C.R., and Patterton, H.G. (2008). The *Saccharomyces cerevisiae* linker histone Hho1p is essential for chromatin compaction in

stationary phase and is displaced by transcription. *Proceedings of the National Academy of Sciences of the United States of America* *105*, 14838-14843.

Schober, H., Ferreira, H., Kalck, V., Gehlen, L.R., and Gasser, S.M. (2009). Yeast telomerase and the SUN domain protein Mps3 anchor telomeres and repress subtelomeric recombination. *Genes & development* *23*, 928-938.

Schroeder, E.A., Raimundo, N., and Shadel, G.S. (2013). Epigenetic silencing mediates mitochondria stress-induced longevity. *Cell metabolism* *17*, 954-964.

Sexton, T., and Cavalli, G. (2015). The role of chromosome domains in shaping the functional genome. *Cell* *160*, 1049-1059.

Sexton, T., Schober, H., Fraser, P., and Gasser, S.M. (2007). Gene regulation through nuclear organization. *Nature structural & molecular biology* *14*, 1049-1055.

Sexton, T., Yaffe, E., Kenigsberg, E., Bantignies, F., Leblanc, B., Hoichman, M., Parrinello, H., Tanay, A., and Cavalli, G. (2012). Three-dimensional folding and functional organization principles of the *Drosophila* genome. *Cell* *148*, 458-472.

Shcheprova, Z., Baldi, S., Frei, S.B., Gonnet, G., and Barral, Y. (2008). A mechanism for asymmetric segregation of age during yeast budding. *Nature* *454*, 728-734.

Shchuka, V.M., Malek-Gilani, N., Singh, G., Langroudi, L., Dhaliwal, N.K., Moorthy, S.D., Davidson, S., Macpherson, N.N., and Mitchell, J.A. (2015). Chromatin Dynamics in Lineage Commitment and Cellular Reprogramming. *Genes* *6*, 641-661.

Shi, L., and Tu, B.P. (2014). Protein acetylation as a means to regulate protein function in tune with metabolic state. *Biochemical Society transactions* *42*, 1037-1042.

Shi, L., and Tu, B.P. (2015). Acetyl-CoA and the regulation of metabolism: mechanisms and consequences. *Current opinion in cell biology* *33*, 125-131.

Shlyueva, D., Stampfel, G., and Stark, A. (2014). Transcriptional enhancers: from properties to genome-wide predictions. *Nature reviews Genetics* *15*, 272-286.

Smets, B., Ghillebert, R., De Snijder, P., Binda, M., Swinnen, E., De Virgilio, C., and Winderickx, J. (2010). Life in the midst of scarcity: adaptations to nutrient availability in *Saccharomyces cerevisiae*. *Current genetics* *56*, 1-32.

Smith, D.L., Jr., McClure, J.M., Matecic, M., and Smith, J.S. (2007). Calorie restriction extends the chronological lifespan of *Saccharomyces cerevisiae* independently of the Sirtuins. *Aging Cell* *6*, 649-662.

Smith, J.S., Brachmann, C.B., Celic, I., Kenna, M.A., Muhammad, S., Starai, V.J., Avalos, J.L., Escalante-Semerena, J.C., Grubmeyer, C., Wolberger, C., *et al.* (2000). A phylogenetically conserved NAD⁺-dependent protein deacetylase activity in the Sir2 protein family. *Proceedings of the National Academy of Sciences of the United States of America* *97*, 6658-6663.

Smith, J.S., Brachmann, C.B., Pillus, L., and Boeke, J.D. (1998). Distribution of a limited Sir2 protein pool regulates the strength of yeast rDNA silencing and is modulated by Sir4p. *Genetics* *149*, 1205-1219.

Solovei, I., Kreysing, M., Lanctot, C., Kosem, S., Peichl, L., Cremer, T., Guck, J., and Joffe, B. (2009). Nuclear architecture of rod photoreceptor cells adapts to vision in mammalian evolution. *Cell* *137*, 356-368.

Solovei, I., Wang, A.S., Thanisch, K., Schmidt, C.S., Krebs, S., Zwerger, M., Cohen, T.V., Devys, D., Foisner, R., Peichl, L., *et al.* (2013). LBR and lamin A/C sequentially tether peripheral heterochromatin and inversely regulate differentiation. *Cell* *152*, 584-598.

Stone, E.M., and Pillus, L. (1996). Activation of an MAP kinase cascade leads to Sir3p hyperphosphorylation and strengthens transcriptional silencing. *J Cell Biol* *135*, 571-583.

Strahl, B.D., and Allis, C.D. (2000). The language of covalent histone modifications. *Nature* *403*, 41-45.

Suka, N., Luo, K., and Grunstein, M. (2002). Sir2p and Sas2p opposingly regulate acetylation of yeast histone H4 lysine16 and spreading of heterochromatin. *Nature genetics* *32*, 378-383.

Szafranski, K., and Mekhail, K. (2014). The fine line between lifespan extension and shortening in response to caloric restriction. *Nucleus* *5*, 56-65.

Taddei, A., and Gasser, S.M. (2012). Structure and function in the budding yeast nucleus. *Genetics* *192*, 107-129.

Taddei, A., Hediger, F., Neumann, F.R., and Gasser, S.M. (2004). The function of nuclear architecture: a genetic approach. *Annual review of genetics* *38*, 305-345.

Taddei, A., Maison, C., Roche, D., and Almouzni, G. (2001). Reversible disruption of pericentric heterochromatin and centromere function by inhibiting deacetylases. *Nature cell biology* *3*, 114-120.

Taddei, A., Schober, H., and Gasser, S.M. (2010). The budding yeast nucleus. *Cold Spring Harbor perspectives in biology* *2*, a000612.

Taddei, A., Van Houwe, G., Nagai, S., Erb, I., van Nimwegen, E., and Gasser, S.M. (2009). The functional importance of telomere clustering: global changes in gene expression result from SIR factor dispersion. *Genome research* *19*, 611-625.

Takahashi, H., McCaffery, J.M., Irizarry, R.A., and Boeke, J.D. (2006). Nucleocytoplasmic acetyl-coenzyme A synthetase is required for histone acetylation and global transcription. *Molecular cell* *23*, 207-217.

Tan, M., Luo, H., Lee, S., Jin, F., Yang, J.S., Montellier, E., Buchou, T., Cheng, Z., Rousseaux, S., Rajagopal, N., *et al.* (2011). Identification of 67 histone marks and histone lysine crotonylation as a new type of histone modification. *Cell* *146*, 1016-1028.

Tanner, K.G., Landry, J., Sternglanz, R., and Denu, J.M. (2000). Silent information regulator 2 family of NAD- dependent histone/protein deacetylases generates a unique product, 1-O-acetyl-ADP-ribose. *Proc Natl Acad Sci U S A* *97*, 14178-14182.

Tanny, J.C., and Moazed, D. (2001). Coupling of histone deacetylation to NAD breakdown by the yeast silencing protein Sir2: Evidence for acetyl transfer from substrate to an NAD breakdown product. *Proceedings of the National Academy of Sciences of the United States of America* *98*, 415-420.

Teixeira, M.T., Arneric, M., Sperisen, P., and Lingner, J. (2004). Telomere length homeostasis is achieved via a switch between telomerase- extendible and - nonextendible states. *Cell* *117*, 323-335.

Therizols, P., Duong, T., Dujon, B., Zimmer, C., and Fabre, E. (2010). Chromosome arm length and nuclear constraints determine the dynamic relationship of yeast subtelomeres. *Proceedings of the National Academy of Sciences of the United States of America* *107*, 2025-2030.

Thomson, J.M., Gaucher, E.A., Burgan, M.F., De Kee, D.W., Li, T., Aris, J.P., and Benner, S.A. (2005). Resurrecting ancestral alcohol dehydrogenases from yeast. *Nature genetics* *37*, 630-635.

Tolhuis, B., Palstra, R.J., Splinter, E., Grosveld, F., and de Laat, W. (2002). Looping and interaction between hypersensitive sites in the active beta-globin locus. *Molecular cell* *10*, 1453-1465.

Tompa, R., and Madhani, H.D. (2007). Histone H3 lysine 36 methylation antagonizes silencing in *Saccharomyces cerevisiae* independently of the Rpd3S histone deacetylase complex. *Genetics* *175*, 585-593.

Tong, L., and Denu, J.M. (2010). Function and metabolism of sirtuin metabolite O-acetyl-ADP-ribose. *Biochimica et biophysica acta* *1804*, 1617-1625.

Tonna, S., El-Osta, A., Cooper, M.E., and Tikellis, C. (2010). Metabolic memory and diabetic nephropathy: potential role for epigenetic mechanisms. *Nature reviews Nephrology* *6*, 332-341.

Tremethick, D.J. (2007). Higher-order structures of chromatin: the elusive 30 nm fiber. *Cell* *128*, 651-654.

Trojer, P., and Reinberg, D. (2007). Facultative heterochromatin: is there a distinctive molecular signature? *Molecular cell* *28*, 1-13.

Tsang, C.K., Liu, Y., Thomas, J., Zhang, Y., and Zheng, X.F. (2014). Superoxide dismutase 1 acts as a nuclear transcription factor to regulate oxidative stress resistance. *Nat Commun* *5*, 3446.

Tu, B.P., Kudlicki, A., Rowicka, M., and McKnight, S.L. (2005). Logic of the yeast metabolic cycle: temporal compartmentalization of cellular processes. *Science* *310*, 1152-1158.

Tu, B.P., and McKnight, S.L. (2007). The yeast metabolic cycle: insights into the life of a eukaryotic cell. *Cold Spring Harbor symposia on quantitative biology* *72*, 339-343.

Tu, S., Bulloch, E.M., Yang, L., Ren, C., Huang, W.C., Hsu, P.H., Chen, C.H., Liao, C.L., Yu, H.M., Lo, W.S., *et al.* (2007). Identification of histone demethylases in *Saccharomyces cerevisiae*. *J Biol Chem* *282*, 14262-14271.

Vachova, L., Chernyavskiy, O., Strachotova, D., Bianchini, P., Burdikova, Z., Fercikova, I., Kubinova, L., and Palkova, Z. (2009a). Architecture of developing multicellular yeast colony: spatio-temporal expression of Ato1p ammonium exporter. *Environmental microbiology* *11*, 1866-1877.

Vachova, L., Hatakova, L., Cap, M., Pokorna, M., and Palkova, Z. (2013). Rapidly developing yeast microcolonies differentiate in a similar way to aging giant colonies. *Oxidative medicine and cellular longevity* *2013*, 102485.

Vachova, L., Kucerova, H., Devaux, F., Ulehlova, M., and Palkova, Z. (2009b). Metabolic diversification of cells during the development of yeast colonies. *Environmental microbiology* *11*, 494-504.

van Koningsbruggen, S., Gierlinski, M., Schofield, P., Martin, D., Barton, G.J., Ariyurek, Y., den Dunnen, J.T., and Lamond, A.I. (2010). High-resolution whole-genome sequencing reveals that specific chromatin domains from most human chromosomes associate with nucleoli. *Molecular biology of the cell* *21*, 3735-3748.

van Steensel, B. (2011). Chromatin: constructing the big picture. *The EMBO journal* *30*, 1885-1895.

Veal, E.A., Day, A.M., and Morgan, B.A. (2007). Hydrogen peroxide sensing and signaling. *Mol Cell* *26*, 1-14.

Verstrepen, K.J., and Fink, G.R. (2009). Genetic and epigenetic mechanisms underlying cell-surface variability in protozoa and fungi. *Annual review of genetics* *43*, 1-24.

Verstrepen, K.J., Reynolds, T.B., and Fink, G.R. (2004). Origins of variation in the fungal cell surface. *Nature reviews Microbiology* 2, 533-540.

Verzijlbergen, K.F., Faber, A.W., Stulemeijer, I.J., and van Leeuwen, F. (2009). Multiple histone modifications in euchromatin promote heterochromatin formation by redundant mechanisms in *Saccharomyces cerevisiae*. *BMC molecular biology* 10, 76.

Wakimoto, B.T. (1998). Beyond the nucleosome: epigenetic aspects of position-effect variegation in *Drosophila*. *Cell* 93, 321-324.

Wang, X., Connelly, J.J., Wang, C.L., and Sternglanz, R. (2004). Importance of the Sir3 N terminus and its acetylation for yeast transcriptional silencing. *Genetics* 168, 547-551.

Weiden, M., Osheim, Y.N., Beyer, A.L., and Van der Ploeg, L.H. (1991). Chromosome structure: DNA nucleotide sequence elements of a subset of the minichromosomes of the protozoan *Trypanosoma brucei*. *Molecular and cellular biology* 11, 3823-3834.

Werner-Washburne, M., Braun, E., Johnston, G.C., and Singer, R.A. (1993). Stationary phase in the yeast *Saccharomyces cerevisiae*. *Microbiological reviews* 57, 383-401.

White, C.L., Suto, R.K., and Luger, K. (2001). Structure of the yeast nucleosome core particle reveals fundamental changes in internucleosome interactions. *The EMBO journal* 20, 5207-5218.

Wierman, M.B., and Smith, J.S. (2014). Yeast sirtuins and the regulation of aging. *FEMS yeast research* 14, 73-88.

Wong, H., Marie-Nelly, H., Herbert, S., Carrivain, P., Blanc, H., Koszul, R., Fabre, E., and Zimmer, C. (2012). A predictive computational model of the dynamic 3D interphase yeast nucleus. *Curr Biol* 22, 1881-1890.

Worman, H.J., and Bonne, G. (2007). "Laminopathies": a wide spectrum of human diseases. *Experimental cell research* 313, 2121-2133.

Xie, W., Schultz, M.D., Lister, R., Hou, Z., Rajagopal, N., Ray, P., Whitaker, J.W., Tian, S., Hawkins, R.D., Leung, D., *et al.* (2013). Epigenomic analysis of multilineage differentiation of human embryonic stem cells. *Cell* 153, 1134-1148.

Yang, D., Fang, Q., Wang, M., Ren, R., Wang, H., He, M., Sun, Y., Yang, N., and Xu, R.M. (2013). Nalpha-acetylated Sir3 stabilizes the conformation of a nucleosome-binding loop in the BAH domain. *Nature structural & molecular biology* 20, 1116-1118.

Yang, H.C., Palazzo, A., Swayne, T.C., and Pon, L.A. (1999). A retention mechanism for distribution of mitochondria during cell division in budding yeast. *Curr Biol* 9, 1111-1114.

Yang, X.J., and Seto, E. (2008). The Rpd3/Hda1 family of lysine deacetylases: from bacteria and yeast to mice and men. *Nature reviews Molecular cell biology* 9, 206-218.

Yu, J., and Auwerx, J. (2009). The role of sirtuins in the control of metabolic homeostasis. *Annals of the New York Academy of Sciences* 1173 *Suppl* 1, E10-19.

Yun, J., and Finkel, T. (2014). Mitohormesis. *Cell Metab* 19, 757-766.

Zhang, F., Kirouac, M., Zhu, N., Hinnebusch, A.G., and Rolfes, R.J. (1997). Evidence that complex formation by Bas1p and Bas2p (Pho2p) unmasks the activation function of Bas1p in an adenine-repressible step of ADE gene transcription. *Mol Cell Biol* 17, 3272-3283.

- Zhao, X., Muller, E.G., and Rothstein, R. (1998). A suppressor of two essential checkpoint genes identifies a novel protein that negatively affects dNTP pools. *Molecular cell* 2, 329-340.
- Zhao, Y., and Garcia, B.A. (2015). Comprehensive Catalog of Currently Documented Histone Modifications. *Cold Spring Harbor perspectives in biology* 7.
- Zhou, C., Slaughter, B.D., Unruh, J.R., Guo, F., Yu, Z., Mickey, K., Narkar, A., Ross, R.T., McClain, M., and Li, R. (2014). Organelle-based aggregation and retention of damaged proteins in asymmetrically dividing cells. *Cell* 159, 530-542.
- Zhu, C., Byers, K.J., McCord, R.P., Shi, Z., Berger, M.F., Newburger, D.E., Saulrieta, K., Smith, Z., Shah, M.V., Radhakrishnan, M., *et al.* (2009). High-resolution DNA-binding specificity analysis of yeast transcription factors. *Genome Res* 19, 556-566.
- Zimmer, C., and Fabre, E. (2011). Principles of chromosomal organization: lessons from yeast. *The Journal of cell biology* 192, 723-733.
- Zink, D., Fischer, A.H., and Nickerson, J.A. (2004). Nuclear structure in cancer cells. *Nature reviews Cancer* 4, 677-687.

List of the major abbreviations used in this manuscript

Abbreviation	Description
ATP	adenosine triphosphate
3C	chromosome conformation capture
ChIP	chromatin immuno precipitation
CFU	colony forming unit
CID	chromosomally interacting domain
CLS	chronological life span
2DG	2-deoxy-D-glucose
DamID	DNA Adenine Methyltransferase Identification
DNA	deoxyribonucleic acid
DS	diauxic shift
EM	electron microscope
ERS	environmental stress response
ESC	embryonic stem cell
FISH	fluorescence <i>in situ</i> hybridization
GFP	green fluorescent protein
HATs	histone acetyltransferases
HC	hypercluster
HD	high density
HEZ	heterochromatin exclusion zones
YMC	yeast metabolic cycle
YPD	yeast extract peptone dextrose
KATs	lysine acetyltransferases
LADs	lamina associated domains
LD	low density
Mec1	mitosis entry checkpoint 1
NA	nicotinic acid
NAD ⁺ /NADH	nicotinamide adenine dinucleotide (oxidized or reduced form)
NADs	nucleolus-associated domains
Nam	nicotinamide
NaMN	nicotinic acid mononucleotide
NaR	nicotinic acid riboside
NE	nuclear envelope
NMN	nicotinamide mononucleotide
NPC	nuclear pore channel
NQ	non quiescent non dense fraction of SP culture
NR	nicotinamide riboside
O-AADPR	O-acetyl-ADP-ribose
OD	optical density
Ox	oxidative

PEV	position variegation effect
pGPD	promoter of Triose-phosphate dehydrogenase (TDH3)
PMN	post-mitotic neurons
PTM	post translational modification
PSG	proteasome storage granules
QA	quinolinic acid
Q	quiescent dense fraction of SP culture
Rap1	repressor activator protein 1
Rad53	radiation sensitive 53
R/B	reductive/building
R/C	reductive/charging
Rph1	regulator of PHR1
rDNA	ribosomal DNA
RLS	replicative life span
ROS	reactive oxygen species
SAHF	senescence associated heterochromatic foci
SIR	silent regulator factor
Sml1	suppressor of Mec1 lethality
SP	stationary phase
TAD	topologically associated domain
TCA	tricarboxylic acid cycle
TOR	target of rapamycin
TPE	telomere position effect
Trans	transmitted light
Trp	tryptophan

The tri-dimensional organization of the genome emerges as an important, still poorly understood, control mechanism in genomic function. Studies in *S. cerevisiae* have broadly contributed to demonstrate the functional importance of nuclear organization.

Although in the wild yeast cell survival depends on their ability to withstand adverse conditions, most of these studies were conducted on cells undergoing exponential growth. In this condition, as in most eukaryotic cells, silent chromatin that is mainly found at the 32 telomeres accumulates at the nuclear envelope, forming three to five foci.

The aim of my doctorate work was to study budding yeast telomeric silent chromatin dynamics upon major metabolic transitions.

We found that the genome of long-lived quiescent cells undergoes a major spatial reorganization following carbon source exhaustion. This change in nuclear architecture is driven by the grouping of telomeres into a unique focus (hypercluster) localized in the center of the nucleus. We also show that this reorganization is a programmed event triggered by reactive oxygen species (ROS) produced upon early respiration and involves the DNA damage checkpoint pathway. Finally, we report that excess of Sir2 activity counteracts telomere clustering upon quiescence and has a negative role on chronological life span.

Our work suggests that the drastic genome reorganization due to telomere grouping favors survival upon quiescence, and unravels a novel connection between metabolism, nuclear organization and aging.